



PEOPLE'S DEMOCRATIC REPUBLIC OF ALGERIA
 MINISTRY OF HIGHER EDUCATION AND SCIENTIFIC RESEARCH
HASSIBA BENBOUALI UNIVERSITY OF CHLEF
FACULTY OF TECHNOLOGY

IN COLLABORATION WITH THE



LABORATORY FOR
 THEORETICAL PHYSICS
 AND MATERIALS PHYSICS
 (LPTPM)

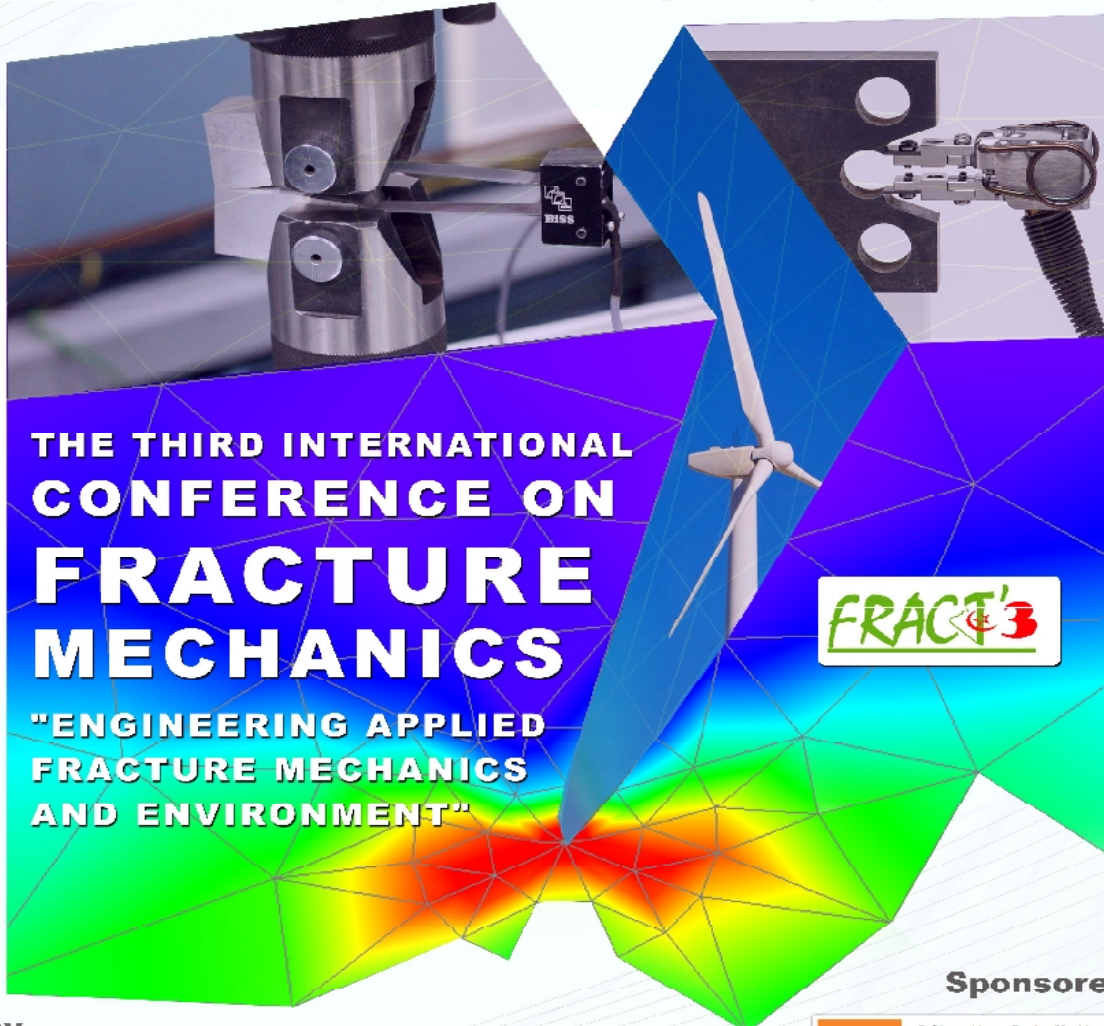
& THE



LABORATORY OF CONTROL,
 TESTING, MEASUREMENT
 AND SIMULATION IN MECHANICS
 (LCEMSM)

ORGANIZE

Book of abstracts



THE THIRD INTERNATIONAL
 CONFERENCE ON
**FRACTURE
 MECHANICS**

"ENGINEERING APPLIED
 FRACTURE MECHANICS
 AND ENVIRONMENT"



Supported by



Sponsored by



SCAN TO DISCOVER !



CHLEF, NOVEMBER 27-30, 2016

Technical Program Fract'3 Conference

Central Bibliotheque, UHBchlef

Monday, November 28th, 2016
Central Bibliotheque, UHBChef

08:00 – 09:00 Registration

9:00 – 9:25 Opening Ceremony

Represented of the Organizing Committee, Dr.
Represented of the Scientific Committee, Dr. Mohammed Hadj Meliani
Dean of the Faculty of Technology, Dr. Abedi Bouabdellah
Dean of the Faculty of Sciences, Dr. El-Miloudi Khaled
Vice Rector of the exterior relations and animations, Prof. Hassen Mahmoudi.
Rector of the Hassiba Benbouali university of Chlef, Prof. Abdelkader Hocine.

9:25 – 9:30 Eulogy words

In Memoriam of Hassiba Benbouali Martir
Represented of the university.

9:30 – 10:30 Opening Honor Lectures, Chairman's : Prof. Hocine Abdelkader & Dr. M. Hadj Meliani

Gear Failures: A Case Study of Premature Failure of an Industrial Mixer Gearset

Prof. Merah Ammar Nacer,

Mechanical Engineering. Director: Center of Excellence for Scientific Collaboration
with MIT. King Fahd University of Petroleum & Minerals. KSA.
nesar@kfupm.edu.sa



Multiscale Thermal Mechanics beyond Navier-Stokes Approach: Modeling, Simulation
and Applications".

Prof. Naji Hassane

Univ. Artois and Lille University Northern France, LGCGE
(EA 4515), France.
hassane.naji@univ-artois.fr



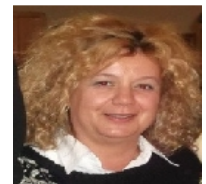
10:30 – 11:00 Coffee Break

Plenary Lectures Chairs : Prof. Naji Hassane, France

11:00–11:30 Behaviour of 9%cr steel and simulated HAZ at 600°C

Pr. Ijubica MILOVIC,

University of Belgrade, Faculty of Technology
and Metallurgy, Karnegijeva 4, 11120 Belgrade, Serbia
acibulj@tmf.bg.ac.rs.



11:30–12:00 Fracture Modelling and Analysis of Plates with Multiple Site
Cracks under Lateral Pressure

Pr. Željko Božić

Department of Aeronautical Engineering. Faculty of Mechanical
Engineering and Naval Architecture. University of Zagreb.
Croatia.
zeljko.bozic@fsb.hr



12:00 – 14:00 Lunch Time , Faculty of Economic Sciences

Oral Presentation TOPIC (A+B) : Fatigue, Failure Analysis, Criteria of Fracture and Failure, Damage and Micromechanics, Microstructurally Short Cracks, Fracture and Fatigue in Applied Biomechanics, Reliability and Integrity of Engineering Structures, Residual Stresses, Corrosion, Environmentally Assisted Cracking and Corrosion Fatigue, Extended Finite Elements Methods and their Application, Simulation and Testing of Crack Propagation on all Length Scales

Plenary Lectures, Chairs : Professor Y.G. Matvienko, Russia

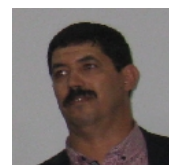
Central Bibliotheque, UHBChlef.

14:00 – 14:30

New concepts of modelling and elaboration of materials in order to develop negative Poisson's ratios

Pr : Abderezek Bezzazi,

Laboratoire de Mécanique & Structures (LMS),BP. 401 Université 08 Mai 1945
Guelma 24000 Algeria
ar_bezazi@yahoo.com



Oral Presentation, Session (A+B) List 1A and 1B

14:30–14 :40

Com 1 : **“HEAT TREATMENTS EFFECT ON THE FRACTURE TOUGHNESS OF AISI M2 TOOL STEEL”**
M. Benaissa, F. Benkhenafou, S. Belhenini, H. Lebbal, A. Ziadi , F.J.Belzunce
Abou Bakr Belkaid University , Tlemcen, Algeria.

14:40–14 :50

Com 2 : **Elastio-plastic modeling incorporating static strain aging (SSA) effect on the behavior of X5CrNi18-10 stainless steel and C-Mn steel coupled with the damage**
Nardjes DJAOUI, Aghilas HANNOU, Marzek ZEROUKI and Mohand OULD OUALI
Université Mouloud MAMMERI de Tizi-Ouzou, Algeria

14:50–15 :00

Com 3 : **WEAR BEHZVIOR OF ALUMINA COATING OBTAINED BY PLASMA ON AN ALUMINUM SUBSTRACTE**
N. Kennafi-Benghalem, S. Aounallah*, M. Hamidouche, A. Zahri, L. Louucif.
Unité de recherche de matériaux émergents, Sétif, Algeria

15:00–15 :10

Com 4 : **INFLUENCE OF RECYCLED SAND ON MECHANICAL PROPERTIES AND THE DURABILITY OF CEMENT MORTARS**
L. Berredjem1, N. Arabi1 and L. Molez
Badji Mokhtar University, Annaba, Algeria.

Oral Participants of the Section (A+B) List 2A and 2B

15 :30– 15 :40

Com 5 : **EXPERIMENTAL STUDY FOR CORROSION INHIBITION OF CARBON STEEL IN ACIDIC MEDIUM**
R. Mehdaoui, O. Aaboubi, K. Chouchane, A. Khadraoui , A. Khelifa , O. Aaboubi
Laboratoire de Génie Chimique (LGC), Blida, Algeria.

15 :40– 15 :50

Com 6 : **Effect of slag in the mechanical behavior of the alkali-silica reaction affected concrete beams**
Z. Douaissia, M.F.Habita
Badji Mokhtar University, Annaba, Algeria.

15 :50– 16 :00

Com 7 : **Effect of welding current on mechanical behavior of resistance spot welding of stainless steel 304 L sheets**
M. Benachour, M. Larbi Cherif
University of Tlemcen, Tlemcen, Algeria.

16 :00– 16 :10

Com 8 : **Mechanical and numerical characterization of the mild steel (E235) tube under uniaxial compression in quasi-static regime**
M.Zerouki, M. Haouchine, A. Ahmed Ali, M.Ould Ouali
Université Mouloud MAMMERI de Tizi-Ouzou, Algeria.

Oral Presentation TOPIC C : Mechanics, Materials domain and Rheology, Domain , CFD, Heat transfert, Renewable energy

Plenary Lectures, Chairs : Professor Najji Hassen, France

Place : Faculty of Economic Sciences

14:00 – 14:30

Numerical investigation of the geometry influence on the aerodynamic fields of the free turbulent jets

Assoc. Prof. Ali Khelil.

Controls, Testing, Measurement and Simulation Mechanical laboratory ,
University of Chlef, Chlef, Algeria
khelila@yahoo.fr



Oral Participants of the Session (C) List 1C

14 :30– 14 :40

Com 1 : **On the fouling of ultra-filtration membrane in the pretreatment process of seawater desalination**

Asma Adda, Mohamed Abbas, salah Hanini

University, Medea, Algeria.

14 :40– 14 :50

Com 2 : **COMPUTATIONAL STUDY OF FE-DOPED TiO₂ NANOPARTICLES**

B. Bezzina¹, , c.e. ramoul, k.e. slimani, o. Ghelloudj, m.t. abed ghars, m. Kahalerras,h.bendjama, d.e. khatmi

Research Centre in Industrial Technology (CRTI), P.O.BOX 64, Cheraga 16014, Algiers

14 :50– 15 :00

Com 3 : **EFFECTS OF OXYGEN FLOW RATE ON THE PROPERTIES OF ZNO THIN FILMS PREPARED BY DC REACTIVE MAGNETRON SPUTTERING**

F. Bouarabaa, S. Lamri, N. Ziani, O.Boussoum, M.S.Belkaid

Université Mouloud Mammeri, Laboratoire Des Technologies Avancées Du Génie Electrique, Tizi-Ouzou, Algérie

15 :00– 15 :10

Com 4 : **Study on the parameters influencing length interface in multiproduct pipelines**

D. Bennacer, R. Saim, B. Benameur, F. Benkhenafou

Université de Tlemcen, Energétique et Thermique Appliquée (ETAP), B.P 109, 13000, Tlemcen, Algérie

15 :10– 15 :20

Com 5 : **Numerical and experimental investigation of dynamic behavior of laminate composite under flexural vibration**

Abdelhafid Rahmane , Toufik. Benmansour

University, Road of ,Ain El Bey, Constantine,Algeria

15 :20– 15 :30

Com 6 : **Optical Simulations Of P3ht/Pcbm Bulk- Heterojunction Organic Photovoltaic For Improving Absorption**

F. Brioua, C. Daoudi, H. Bourouina, M.Remram

Laboratoire LEMEAMED , Département d'électronique, Université des Frères Mentouri Constantine ,Algerie

15 :30– 15 :40

Com 7 : **Study of dynamics of carriers in InSb/GaAs Quantum Dot Solar cell**

F.Benyettou, A.Aissat

University of Blida, LASICOM, Route de Soumaa, 09000, Blida, Algeria

15 :40– 15 :50

Com 8 : **Heat transfer enhancement inside a solar chimney**

M.T.Bouzaher, M. Lebbi, L. Boutina, H. Boualit

1 Unité de Recherche Appliqué en Energies Renouvelables, URAER, Centre de Développement des Energies Renouvelables, CDER, 47133, Ghardaïa, Algeria

16 :00– 16 :10

Com 8 : **Investigation Of Aisi 316l Cardiovascular Stent Behaviour Under Bloodpressure And**

Restenosis Loadings

M. Benhaddou, M. Abbadi, M. Ghammouri

ENSA, University of Oujda, Morocco.

15:10– 16:20 Coffee Break

16:20–16:50 Poster session C : Responsable : Prof. Naji Hassen, Prof. Loukarfi Larbi, Dr. Ali Khelil

- Post :1 **THEORETICAL STUDY OF inasxsbl-x /gaasquantum WELL SOLAR CELL**
S.Taleb, I.Lagraa
University of Sidi Bel Abbes, Sidi Bel Abbes, Algeria
- Post :2 **Experimental thermal study of turbulent jet swirling: Application in the HVAC systems**
Abderazak BENNIA, Larbi LOUKARFI, Ali KHELIL Hachimi FELLOUAH, Mohamed BRAIKIA, Youcef BOUHAMIDI
Université Hassiba Benbouali of Chlef, Algeria
- Post :3 **Numerical investigation of Heat Transfer Enhancement inside a Parabolic Trough Solar Collector using Geometrical Modification and Hybrid Nanofluid**
Amina Benabderrahmane*, Abdelylah Benazza, Miloud Aminallah, Samir Laouedj
University, Sidi Belabbes. Algeria
- Post :4 **Simulation study of the surface aerator power for the Chlef sewage station**
Aoumeur Djelloul, Madjid Meriem-Benziane
University Hassiba Benbouali of Chlef
- Post :5 **Glass forming ability and crystallization behavior of nickel-based amorphous alloy membranes for hydrogen separation by electronic and calorimetric measurements**
Billel SMILI, Moussa Mayoufi, Ivan KABAN, Jean-Georges GASSER
University Badji Mokhtar of Annaba, Algeria
- Post :6 **Etude comparative entre les corrélations d'identification du transfert de chaleur HTC à l'extérieur d'un tube lisse horizontal.**
Dj. AMGHAR, M. TEBBAL, B. TOUHAMI, H. LAIDOUDI, F. KEBIR
University of El -Menaouer, Oran, Algeria
- Post :7 **L'effet de taux d'injection et l'angle d'inclinaison sur l'efficacité du refroidissement par film**
F. Kebir, A. Azzi, H. Laidoudi, D. Amghar
University of El -Menaouer, Oran, Algeria
- Post :8 **L'Effet d'un Chargement Thermique sur la Variation des Contraintes Résiduelles d'un Assemblage Metal-Ceramique**
K. Messaoudi, F. Bouafia, F. Benkhenafou
Université of Tlemcen, Algérie
- Post :9 **Étude numérique tridimensionnelle de l'écoulement généré par un agitateur de type ANCRE**
KAMLA Youcef, AMEUR Houari, SAHEL Djamel
Unisversity Hassiba Ben Bouali of Chlef, Algeria
- Post :10 **The collector radius effects on the mass flow rate in a small-scale solar chimney**
M. Lebbi, A. Bouabdallah, T. Chergui, H. Boualit, L. Boutina, M.T. Bouzaher, S. Laouar, M. Lounici
Unité de Recherche Appliquée en Energies Renouvelables, URAER, Centre de Développement des Energies Renouvelables, Ghardaïa, Algeria
- Post :11 **Effect stresses induced by ion exchange in the case of a glass subjected to soft thermal shock**
Z. Malou, T. Benouioua, O. Gridi, M. Hamidouche, G. Fantozzi
Optical and mechanical precision Institute, University of Setif 1, 19000 Algeria
- Post :12 **NATURAL CONVECTION IN A CAVITY SIMULATING A THERMOSYPHON**
Abderazak BENNIA, Samir RAHAL, Ali KHELIL, Ghazali MEBARKI, Larbi LOUKARFI
Université Hassiba Benbouali de Chlef, Algérie
- Post :13 **Solar driven air-conditioning system based on desiccant materials**
L. Merabti, M. Merzouk, N.Kasbadji Merzouk, W. Taane, M. Abbas
Unité de Développement des Equipements Solaires, UDES/Centre de Développement des Energies

- Renouvelables, CDER, 42415, W. Tipaza, Algérie
- Post :14 **Thermal and dynamic characterization of air jet issued from a diffuser provided with lobes.**
M. Braikia *, **A. Khelil**, **L. Loukarfi**, **A. Bennis**,
 Université Hassiba Benbouali of Chlef,, Algérie
- Post :15 **Thermoelectric properties of skutterudite materials**
C.Bouhafs, **M.Chitroub**
 Laboratoire de Science et Génie des Matériaux, Département de Métallurgie, Ecole
 Nationale Polytechnique
 El-Harrach, Alger, Algeria
- Post :16 **Adsorption of anionic dye by zeolite commercial and equilibrium study**
F.lasnami1, **a.labbaci**, **m.douani**
 Université Hassiba Benbouali de Chlef, Algérie
- Post :17 **Aerodynamic Shape Optimization of NACA0012 Profile using Adjoint Solver**
Abd Ellatif AMOR; Ramzi MDOUKI; Ahmed BETTAHAR
 University of Chlef, Algeria.
- Post :18 **Water irrigation in the Chlef region using photovoltaic solar energy**
T. Tahri, **H. Zahloul**, **K. E. Meddah**, **H. Lazergue**
 Université Hassiba Benbouali de Chlef, Algérie
- Post :19 **The Distance Effect between the Tubes on Horizontal Ground Heat Exchange**
M. Ben Maachou, **A. Benazza**
 University of Sidi Bel Abbes, Algérie
- Post :20 **Poly-silicon for heterojunction solar cells based on numerical simulations**
ZIANI Nora
 Université Mouloud MAMMARI of , TiziOuzou, Algeria
- Post :21 **Étude de stabilité de phase de AIN dans les conditions à haut pression**
N. BOUTELDJA, **S. DAHMANE**, **M. TRAICHE**, **A. CHENOUNE**, **A. ALIBENAMARA**
 University of Chlef, Algeria
- Post :22 **AB INITIO STUDY OF STRUCTURAL , ELECTRONIC ,OPTICAL AND THERMAL PROPERTIES OF aginte2**
H.BENDJEDDOU, **A.GASSMI**, **H.MERADJI**, **S.GHEMID**
 Université Badji Mokhtar, Annaba , Algeria
- Post :23 **MECHANICAL CHARACTERIZATION OF THE BEAD Welding of High-Density Polyethylene (HDPE)**
M.BELHOUARI, **A. Belaziz**, **M. Mazari**, **M.Belhouari**
 University Djillali Liabes, Sidi Bel Abbes, Algeria.
- Post :24 **Study of a new geometry of beam welded reconstituted (composite bridges)**
A. Houda, **H. Zedira**, **B. Redjel**
 University, Abbas Laghrou, khenchela, Algeria
- Post :25 **A Simple Quasi-3D Theory With Five Unknowns For The Static Analysis Of FGM Sandwich Plates**
A. Hamidi, **M. Zidour**, **A. Tounsi**, **E. A. Adda Bedia**
 A. Hamidi, M. Zidour, A. Tounsi, E. A. Adda Bedia
- Post :26 **Comportement dynamique des poutres sandwiches fonctionnellement graduées (FGM)**
L. Hadji, **N. Zouatnia**, **Y. Tlidji1**, **A. Kassoul**
 Université Ibn Khaldoun, Tiaret, Algérie
- Post :27 **Design and Analysis of Two Gantries in Steel Structures**
O. Belaidi, **F. Taouche-kheloui**, **Kh. Iftene**, **M. Almansba**, **N.E Hannachi**
 University of Tizi Tizi-Ouzou Algeria.
- Post :28 **Flexion statique des poutres composite type 'FGM'**
N. Zouatnia, **L. Hadji2**, **A. Kassoul**
 Université Hassiba Benbouali de Chlef, Algérie
- Post :29 **Interfacial Stress Analysis in Multimaterial Metal / ceramic / metal by the method of finite element**
W. Bensmain, **B. Serier**, **H.Fekirini**
 Université Djilali Liabes de Sidi Bel Abbes
- Post :30 **Analyze of interfacial cracks in a composite material subjected to different loads**

Y. Chahraoui, L. Zouambi, F. Bouafia, B. Serier
University of, SidiBel Abbes, Algeria,

- Post :31 **The effect of cutting parameters on the state of the surfaces of work-pieces (Case Bronze and Aluminum)**
M. Hachellaf kaddour, Oud Chikh el Bahri, Merdji Ali
University of Mustapha Stambouli Mascara, Algeria
- Post: 32 **The Influence of the Methods of Preparation on the Textural and Structural Properties of the Titanium Dioxide**
A.MENNAD, A.MAHIOUT
Unité de Développement des Equipements Solaires, UDES / Centre de Développement des Energies Renouvelables, CDER, Bou-Ismaïl, 42415 Tipaza, Algeria.
- Post: 33 **Failure analysis of a gas turbine blade using FEM**
S.Tahraoui, H. kourt, O. Bouledroua, A.Khelil, M.Hadj milaini
University of chlef, Algeria
- Post: 34 **THERMAL AND DYNAMIC CHARACTERIZATION OF A TURBULENT SWIRLING JET IMPACTING PLATE PLANNE (EXPERIMENTAL AND NUMERICAL STUDY)**
A. Zerrou, A. Khelil, L. Loukarfi
University of Chlef, Algeria
- Post: 35 **Simulation of Shunt active power filter controlled by SVPWM connected to a photovoltaic generator**
Omar.Maarouf, Ismail Bouyakoub, Benyounes Mazari
Université Hassiba ben bou ali de Chlef
- Post: 36 **Numerical Simulation of Dynamics Flows of Diffusion Flames in the Combustion Chamber**
S. Nechada*, A. Khelila, L. Loukarfia, M. Bouketitaa, A. Benniaa, Y. Bouhamidia
University Hassiba Benbouali, Chlef, Algeria
- Post: 37 **A Numerical Study of Building Configuration Impact on Airflow and Dispersion Processes of Traffic Emissions in Urban Street Canyons with Tree Planting**
Lakhdar BOUARBI, Bouabdellah ABED, Mohamed BOUZIT
University of sciences and technology of Oran (USTO), Oran, Algeria
- Post: 38 **EFFECT OF THE TYPE OF THE TURBINE IN AN AGITATED TANK**
M. Foukrach, M. Bouzit, Y. Kamla, H.Ameur
University Oran Algérie.

16:50 – 17:00	Selected the Best Poster Topic C
17:00--17:30	Exhibition in Chlef city
19:00--20:00	Meeting Cooperation
20:00-22:00	Lunch- Hotel La Vallée

08:00 – 08:30 Registration

8:30 – 09:30 Honor Lectures, Chairman's : Prof. Merah Naser, KFUPM, KSA

08:30–09:00 Two-parameter approaches in elastic-plastic fracture mechanics

Pr. Yury .G. Matvienko,

1 Mechanical Engineering Research Institute of the Russian Academy of Sciences, 4 M. Kharitonievsky Per., 101990 Moscow, Russia. e-mail: ygmatvienko@gmail.com



09:00–09:30 Some Application of the fatigue field on structures

Pr. Abdelkrim Aid

Laboratory of Mechanic Testing and fatigue,
University of Mascara
Algeria
aid_abdelkrim@yahoo.com



09:30– 10:00 Coffee Break ,

Plenary Lectures Chairs : Prof. Ljubica MILOVIC, Belgrade University, Serbia

10:00–10:30 The effect of plasma welding and carbides presence on the occurrence of cracks and micro-cracks

Pr. Simon Sedmak,

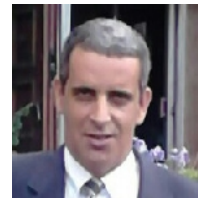
University of Belgrade, Serbia
simon.sedmak@yahoo.com



10:30–11:00 FATIGUE THRESHOLD COMPUTATION IN MODE I, MODE II AND MIXED MODE I-II BY SHAKEDOWN ANALYSIS

Pr. Med Amine Belouchrani

Ecole Militaire polytechnique-Bordj El Bahri
Alger, Algeria
belouchrani_ma@yahoo.fr



11:00–11:30 Mécanismes de Fissuration par Fatigue : Essais, Mesures & Interprétations micro-cracks

Pr. Taoufik Boukharouba

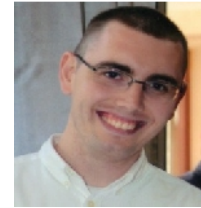
Laboratory of Advanced Mechanics, LMA,
"USTHB", Alger.
Algeria
t.boukha@gmail.com



11:30–12:00 Influence of exploitation conditions and welding on crack initiation and propagation in pressure vessels

Dr. Branislav Djordjevic,

University of Belgrade, Serbia
bane.beca@hotmail.com



12:00 – 14:00 Lunch Time , Faculty of Economic Sciences

14:00 -

Oral Presentation TOPIC A+B : Fatigue, Failure Analysis, Criteria of Fracture and Failure, Damage and Micromechanics, Microstructurally Short Cracks, Fracture and Fatigue in Applied Biomechanics, Reliability and Integrity of Engineering Structures, Residual Stresses, Corrosion, Environmentally Assisted Cracking and Corrosion Fatigue, Extended Finite Elements Methods and their Application, Simulation and Testing of Crack Propagation on all Length Scales

15:30

Oral Presentation Second day Session (A+B)+ List 2A

Chairman : Prof. Bozic Zeljco, Zegreb University, Croatia.

- 14:00-14:10 **Com 1 : corrosion and protection of crude gas production aerial facilities in hassi r'mel field**
K. Gharbi, K. Benyounes, S. Chouicha, O. Bouledroua
M'Hamed Bougara University, Boumerdes, Algeria
- 14:10--14:20 **Com 2 : Analysis of Location of defects near geometric discontinuities on the Mechanical Behaviour of Bone Cement**
L. Zouambi, S. Gouasmi, F. Bouafia, B. Serier
University of SidiBel-Abbes. Algeria
- 14:20-14:30 **Com 3 : The Monte Carlo Method for Structural Failure Prediction of Civil Engineering Infrastructures**
Nabil KAZI TANI, Tawfik TAMINE, Djamel NEDJAR and Mebrouk HAMANE
Superior School of Applied Sciences of Tlemcen, Algeria.

Oral Participant Topic (A +B) List 2B

- 14:30-14:40 **Com 4 : Identification of the damage in the bone cement of the total hip prostheses**
Mohammed El Nedhir, Belgherras, Benouis Ali, B. Serier, L. Hachemi
University of SidiBel-Abbes. Algeria
- 14:40-14:50 **Com 5 : Numerical analysis of the interaction crack-defect in the cement PMMA**
A. Benouis, A. Boulouar, M. Cherfi, M. E. Belgherras, A. Sahli, B. Serier
University of Saida, Algeria.
- 14:50-15:00 **Com 6 : Predicting of viscoelastic damaged behavior of a multilayer composite tubular structure under a creep loading**
A. Ghouaoula, A. Hocine, D. Chapelle, and M. L. Boubakar
Benbouali Hassiba University of Chlef, Algeria.
- 15:00-15:10 **Com 7 : Failure Behavior and load transfer in Concrete-Steel Plate connection of Hybrid Constructions**
L. Madouni, M. Ould Ouali, A. Kezmane and N.E. Hannachi
University Mouloud MAMMERI of Tizi-Ouzou.
- 15:10–15:20 **Com 8 : Experimental study of the mechanical behavior and kinetics of the martensitic transformation in 304L trip steel: application spot welding**
Z. Sidhoum, R. Ferhoum, M. Almansba , R. Bensaada
University of Tizi Ouzou, Algeria.
- 15:20–15:30 **Com 9 : corrosion and scale green inhibitors on corrosion effects on the fracture mechanics properties of gas pipelines**
M. Ould Mbereick, M. Hadj Meliani, El-Miloudi Khaled, C.Fares ,M.A.Benghalia
LPTPM, Hassiba Benbouali University of Chlef, Algeria.

15:30–15:40 **The Effect of Plastic Deformation on Structural Integrity of Austenite-Ferrite Welded Joint**

Ramo Bakić, Aleksandar Sedmak, Simon Sedmak, Branislav Đorđević, Nevena Topalović

Technical school in Tutin, Serbia

14:00 - **Oral Presentation Second day Session (C)+ List 2C**

TOPIC C : Mechanics, Materials and Rheology, Domain CFD, Heat transfert, Renewable energy

15:30

14:00-14:10 **Com 1 : Computational analysis of flow and heat transfer characteristics in a floating solar chimney power plant FSCPP**

A. M.T.Bouzaher, M. Lebbi, L. Boutina

Unité de Recherche Appliqué en Energies Renouvelables, URAER, Centre de Développement des Energies Renouvelables, CDER, 47133, Ghardaïa, Algeria

14:10-14:20 **Com 2 : Strain energy density prediction of mixed-mode crack propagation in functionally graded materials**

N. Benamara, A. Boulenouar, M. Aminallah and N. Benseddig

Laboratory of Materials and Reactive Systems, Mechanical Engineering Department, University of Sidi-Bel-Abbes, BP. 89, City Larbi Ben Mhidi, Sidi Bel Abbes 22000, Algeria

14:20-14:30 **Com 3 : The local Nusselt number a long square cylinder immersed in power-law fluids under aiding thermal buoyancy**

H. Laidoudi, M. Bouzit, O. Bouledroua

Laboratoire des Sciences et Ingénierie Maritime (LSIM), Faculty of Mechanical engineering, USTO-MB, BP 1505, El-Menaouer, Oran.

14:30-14:40 **Com 4 : Effect Of The Substitution Of The Calcined Bentonite On The Chemical Durability And Rheological Properties Of Cement Mortars**

N. MESBOUA , K. BENYOUNES, A. BENMOUNAH

Research Unit Materials, Processes and Environment (UR-MPE), University M'Hamed Bougara Boumerdes, Avenue of Independence, Boumerdes, 35000, Algeria

14:40-15:50 **Com 5 : Effects of welding parameters on FSSW: Experimental and numerical study**

M. Merzoug A. Boulenouar N. Benamara B. Bouchouicha M. Mazari

Laboratory of Materials and Reactive Systems, Mechanical Engineering Department, University of Sidi-Bel-Abbes, BP. 89, City Larbi Ben Mhidi, Sidi Bel Abbes 22000, Algeria

14:50-15:00 **Com 6 : MECHANICAL PROPERTIES AND ADHESION BEHAVIOUR OF THERMAL BARRIER COATING**

Fizi Yazid, Mebdoua Yamina, Lahmar Hadj

Centre de Développement des Technologies Avancées, Cité 20 août 1956, BP.17 Baba Hassen, Alger, Algérie

15:10-15:10 **Com 7 : Study the effect of adhesive and patch in the plug safety by the Finite element method**

Gadi Ibrahima, MadjidMeriem-Benziane, and BelAbbesBachir-Bouiadjra

LRM, Mechanical engineering department, University of chlef, chlef Algeria

15:10-15:20 **Com 8 : Investigation on the constraint effect for the stainlessAISI 304L thin sheets using an hybrid method**

R. Bensaada, M. Almansba,R. Ferhoum , Z. Sidhoum4, N.E. Hannachi

University of Tizi-Ouzou, LAMOMS Lab. Hasnaoua II, 15000, Tizi-Ouzou Algeria

15:20-15:30 **Com 9 : Plastic Instability During Stretching Solid Polymers**

Boudjellel Moulay Ali, Belabbes Bachir Bouiadjera, El Bahri Ould Chikh

Faculty Technology, Mechanical Engineering Department, University of Sidi Bel Abbes

15:30– 16:00 **Coffee Break,**

16:00 - 17:00

Poster session A

Post :1

Heat treatment of a particle injects into a plasma-producing medium

Aissa Abderahmane, M.sahnoun, Aid A

University of Mascara, Algeria

- Post :2 **Characterization and Thermomechanical Modelling of an Anisotropic Aluminum Alloy Sheet Under Bending Loading**
N. BENCHABNE, N. DJAOUI, K. AIMEN et M. OULD OUALI
University of Tizi-ouzou, Algeria
- Post :3 **Failure mode i composite medapoxy al / e glass**
Abdallah Lounis, MEDDAH HADJ MILOUD, OULD CHIKH EL BAHRI, LARBI Gueraiche.
UNIVERSITY OF MASCARA- ALGERIA
- Post: 4 **Modeling without re-meshing of crack propagation: open mode and mixed mode**
K. Bendahane, , Y. Abdelaziz, S. Benkheira, Y. Labbaci
University of El Bayadh, Algeria
- Post :5 **Thermomechanical bending analysis of functionally graded sandwich plates**
Ahmed Hamidi, Zidour Mohamed, Abdelouahed Tounsi and Adda Bedia El abbes
University of Tiaret, Algeria
- Post :6 **Theoretical and Numerical Analysis of Stress Intensity Factor in the first mode (Mode I); Case of a Composite Material**
H. Hamli Benzahar, M. Chabaat
University of Khemis Miliana, Algeria.
- Post: 7 **Comprehensive approach to fracture mechanics applied to polymers (HDPE case)**
Houari tarek, Benguediab Mohamed, Houari mohamed sidahmed
University Mascara, Algeria
- Post :8 **Valorization of natural polymers (lignin) in the formulation of mortars and self-compacting concrete**
I. Djefour, M. Saidi
University of Boumerdes, Algeria
- Post :9 **The influence of the scale coefficients and the mode number on non-locale critical bulking load of double-walled carbon nanotubes (DWCNTs)**
K. Rakrak, M Zidour, A. Chemi, H Heireche
University of Hassiba benbouali, Chlef, Algeria
- Post :10 **Analyse numérique de la nocivité du phénomène de coup de béliet dans les conduites de transport des hydrocarbures**
L. Aminallah, A. Benhamena, A. Merdji, S. Habibi, A. Daikh, B. Medjadji, A. Aid
University of Mascara, Algeria
- Post :11 **Analysis of Location of defects near geometric discontinuities on the Mechanical Behaviour of Bone Cement**
L. Zouambi, S. Gouasmi, F. Bouafia, B. Serier
University of Hassiba benbouali, SidiBel Abbes, Algeria
- Post :12 **Preheat effects on LiF: Mg, Ti at low dose**
M. Halimi, D. Kadri, A. Mokeddem, I. Missoum
University of Sciences and Technology of Oran (USTO-MB), Algeria
- Post: 13 **Free vibration analysis of armchair double-walled carbon nanotubes embedded in an elastic medium using nonlocal theory**
M. ZIDOUR, A. HAMIDI, T. BENSATTALAH, B. ADIM and K. RAKRAK
Université Ibn Khaldoun, Tiaret, Algeria
- Post :14 **Finite element analysis of the interface cracks in composites reinforced with natural fiber in the presence of interphase**
Mokhtar. KHALDI1, Noureddine Mahmoudi2, Alexandre. VIVET
University of Mascara, Algeria

- Post :15 **Analysis efforts of shock on the stresses level in the elements of a dental prosthesis**
N. DJEBBAR*, B.BACHIR BOUIADJRA, B.SERIER
University of Hassiba Benbouali
- Post :16 **Application of depth-sensing microindentation testing to study of interfacial fracture toughness in reinforced Concrete: effect of water to binder ratio and the type of concrete**
Said. Grairia, Yacine. Chrait, Alex. Montagne, Alain. Iost, Mohamed. Bentoumi, Didier. Chicot
Guelma University, Algeria
- Post: 17 **Nonlinear Dynamics of mechanical systems using time integration scheme "implicit"**
R. Koulli, S. Mamouri
University of Tahri Mohamed Bechar, Béchar, Algeria
- Post :18 **Numerical investigation of shape effect of composite patch on Inclined crack reparation**
E.H. Besseghier, A. Aid, A. Djebli, M. Bendouba, A. Benhamena
University of Mascara, Algeria
- Post: 19 **Elastic analyses of the Pipeline API X65 Repaired with Composite Overwrap**
D.Belhadri, W.Oudad, H.Fekirini
Univ Ctr of Ain Temouchent, Algeria
- Post :20 **Fatigue Behavior of Composite Material to Use Orthopaedic**
S. Achouri, B. Redjel
CRTI Algiers, Algeria
- Post :21 **Repaired crack in Al7075T6 structures subjected to uniaxial and equibiaxial loading**
H. Fekirini, F. Bouafia, M. Khodja, L. Zouambi
University of SidiBel Abbes, Algeria
- Post :22 **Experimental Analysis of Aging Poly-Methyl-Methacrylate PMMA**
A. Kaddouri, S. Ramdoun, N. Serier, k. Kaddouri, B. Serier
University of SidiBel Abbes, Algeria
- Post: 23 **Biomechanical study of the effects of the inlet wave forms on the hemodynamics inside a patient specific circle of Willis**
D. SEKHANE, K. MANSOUR
University of Constantine 1- Algeria, Algeria
- Post :24 **Prediction of Residual Fatigue Life in Repaired Cracked Al-alloy plate**
F.Z. Serriari, N. Benachour, M. Benachour, M. Benguediab
University of Tlemcen, Algeria
- Post :25 **Fracture behavior modeling of a 3D crack emanated from bony inclusion in the cement PMMA of total hip replacement**
M. Cherfi, S. Benbarek, A Sahli
University of Sidi Bel Abbes, Algeria
- Post :26 **Numerical study of low temperature combustion strategies**
A. BENDRISS, C. KEZRANE, Y. LASBET, M. MAKHLOUF
Sidi-Bel-Abbès University, Algeria
- Post :27 **Modelisation of the optical gain in GaN/Ga_{0.8}Al_{0.2}N/SiC quantum well lasers under stress**
B. Bouabdallah, A.OumSalem, Z.Nabil, Y. Bourezig, S.Kheris, B. Benichou, O.Benhelal, A.Ridah
University of Sidi-Bel-Abbès, Algeria
- Post :28 **Simulation analysis of mechanical properties and adhesion behavior of thermal barrier coatings**
Yazid Fizi, Yamina Mebdoua, Hadj Lahmar
Centre de Développement des Technologies Avancées, Alger, Algeria
- Post :29 **Virtual strain gage method for numerical evaluation of fracture parameters**
F. Khelil, A. Aid1, M. Hadj Meliani, A. Benhamna, F. Benaoum
University Mustapha Stambouli, Mascara, Algeria
- Post :30 **Study the Emergence of the Phenomenon of Von Karman behind a Cylindrical Obstacle**
Sidali Bensedira, A. Abdellah El-Hadj, Djaffar Semmar
University of Blida, Algeria

- Post :31 **T-stress effects on crack path trajectory in bi-material structures under pure mode-I loading**
A. Kabila, T. Tamine, M. Hadj Meliani And Z. Azari
 LABORATORY OF LCGE, UNIVERSITY USTO Oran, Algeria
- Post :32 **Quantification d'un chargement variable de l'endommagement en fatigue**
S.Zengah, A.Aid, M. Benguediab, F.khlil, A.benhamena
 Labo. LPQ3M, Université de Mascara, Algeria
- Post :33 **Microstructure evolution during friction welding for AISI 316**
F. Arzour, M. Hadj Meliani, A. Jabbar Hassan, T. Boukharouba
 University of Chlef, LPTPM, Algeria.

Poster session B

- Post :1 **Numerical analysis of corroded structures with ansys apdl**
H. BERREKIA, A. CHOUITER, D. BENZERGA
 University of Mohamed boudiaf Oran, Algeria
- Post :2 **Inhibitors corrosion effect on mechanical properties of api 5l x52 steel in acid hcl environment**
RAHMANI-KOUADRI Yassine, M. Ould Mbereick, M. HadjMeliani, El-MiloudiKhaled, C.Fares,
M.A.Benghalia,K. Gharbi
 University of HassibaBenBouali University of Chlef,, Algeria
- Post :3 **Influence of sandblasting on mechanical properties of pipeline API 5L X52 steel**
Saadi Abdelbasset Abdessamad, O. Bouledroua, M. Hadj Meliani, G. Pluvinage
 LPTPM, Faculty of sciences, Hassiba Benbouali University, Algeria
- Post :4 **CORROSION STUDY OF TERNARY ALLOYS CZT FOR cztse SOLAR CELLS**
MERIEM HANLA, MOHAMED BENAICHA, MAHDI ALLM
 University of Setif, Algeria
- Post :5 **Determination of residual stress in Al-Alloys thin films**
S. Lallouche, M. Y. Debili
 University of Setif, Algeria
- Post :6 **Lipolytic bacteria use as bio-decontaminating natural in the water purification stations**
L. Hachemi, M. E. Belgherras, , Z. Benattouche
 University of Mascara, Algeria
- Post :7 **Reduction Of Alkali Silica Reaction Risk In Concrete By Ground Granulated Blast-Furnace Slag**
Z. Douaissia, M.F.Habita
 Badji Mokhtar university, Annaba, Algeria
- Post :8 **The effect of the electrical field and the polarization temprature on piezoelectric proprieties in the poly (vinylidene fluoride) (pvdf)**
S.DEBILI, T. CHELOUFI and A.GASMI
 Badji Mokhtar university, Annaba, Algeria
- Post :9 **Parametric relation Between Tenacity and Impact Strength in the Zone of Ductile-brittle transition of a Welding Joint**
M. TIRENIFI, B. BOUCHOUICHA, B. OULD CHIKH, H.M. MEDDAH
 University of Sidi Belabbes, Algeria
- Post :10 **Numerical Analysis of Fracture Behavior of Pipe under internal Pressure based on Arc-shaped specimens: CTPB**
A. Benhamena, L. Aminallah, A. Aid , A. Amrouche, N. Benseddiq
 University of Mascara, Algérie
- Post :11 **Numerical modeling of crack propagation under mixed-mode loading**
A. Boulenuar N. Benamara and M. Merzoug
 University Of Sidi-Bel-Abbes, Algeria
- Post: 12 **Numerical Estimation of Stress Intensity Factors and Crack Propagation in Cement PMMA**

- A. Boulououar, B. Benouis, N. Benamara**
University Of Sidi-Bel-Abbes, Algeria
- Post :13 **The influence of geometric discontinuity on the fatigue behavior of aluminum alloy 7075-T6 and 6082-T6.**
- A. BRAHAMI, B. BOUCHOUICHA, S. ADIM**
University of Setif, Algeria
- Post :14 **Checking the resistance of a drinking water supply to cracking consideration with his actual behavior**
- D. Said Lhadj**
National high School of hydraulics, Blida, Algeria
- Post :15 **Numerical Analysis of the Interface Cracks in Continuous Fibre Reinforced Metal Matrix Composites**
- F. Bouafia, H. Fekirini L. Zouambi, B. Serier**
University of Sidi Bel Abbes, Algeria
- Post :16 **Comprehensive approach to fracture mechanics applied to polymers (HDPE case)**
- Houari tarek, Benguediab Mohamed, Houari mohamed sidahmed**
University Mascara, Mascara, Algeria
- Post :17 **Strain energy density prediction of mixed-mode crack propagation in functionally graded materials**
- N. Benamara, A. Boulououar, M. Aminallah and N. Benseddiq**
University of Sidi Bel-Abbes, Algeria.
- Post :18 **Numerical Analysis of the Damage of Composed Materials: Metal-Ceramic type**
- S. Ramdoun, A. Kaddouri, H. Fekirini, N. Serier, B. Serier**
University of Sidi Bel-Abbes, Algeria
- Post: 19 **Crack damage indicator detection using the first mode shape measured**
- S. Tiachacht, A. Bouazzouni, M. Almansba, M. Almansba**
University of Tizi-Ouzou, Algeria
- Post: 20 **Evaluation of the stress corrosion of 304L stainless steel welded by GTAW process**
- Belkacem Amine KESSAL, Chahinez FARES, Ljubica MILOVIC, Madjid OUCHÈNE**
University of Chlef, Algeria.
- Post: 21 **Adsorption study of a non-biodegradable herbicide by natural clay surface reactivity**
- M. Makhloufi, A. Zehhaf, A. Benyoucef**
Université de Mascara. Algeria

17:00 – 17:20

Selected the Best Poster Topic A+B.

19:00 – 22:00 Closing Ceremony (La Vallée Hotel)

Represented of the Organizing Committee, Dr.
Represented of the Scientific Committee, Dr. Mohammed Hadj Meliani
Dean of the Faculty of Technology, Dr. Abedi Bouabdellah
Dean of the Faculty of Sciences, Dr. El-Miloudi Khaled
Vice Rector of the exterior relations and animations, Prof. Hassen Mahmoudi.
Rector of the Hassiba Benbouali university of Chlef, Prof. Abdelkader Hocine.

Wednesday, November 30, 2016

09:00 – 18:00 Touristique Tour and Social Diner

Hassiba Benbouali University of Chlef, Chlef- Algeria

Faculty of Technology



In collaboration with

The Laboratory for Theoretical
Physics and Materials Physics
LTPM, UHChlef



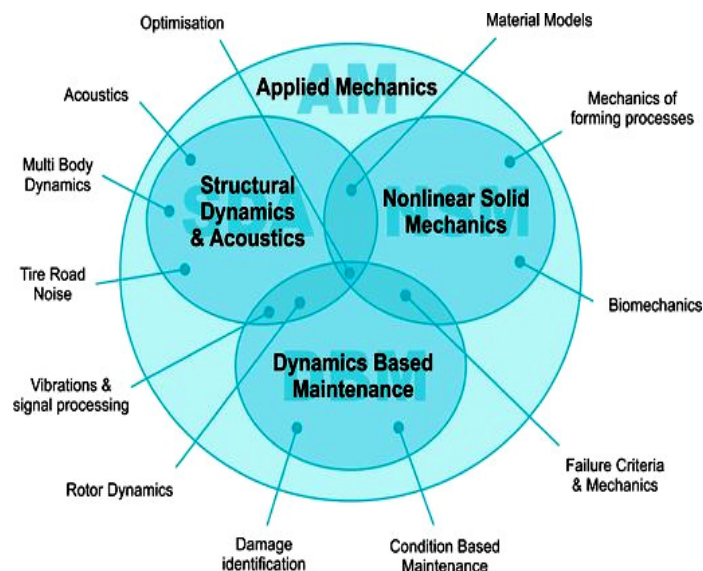
Laboratory of Control,
testing, Measurement and
Simulation in Mechanics.

Organize



The Third International Conference on **FRACTURE MECHANICS**

"Engineering Applied Fracture Mechanics and Environment"



FRACT'3 BOOK OF ABSTRACTS



Welcome to the HassibaBenbouali University
Welcome to Chlef, Algeria

Supported by



Laboratoire de Mécanique,
Biomécanique, Structure, Polymère et
Structures, Metz, France



Ecole Nationale d'Ingénieurs de Metz,
France



Mechanical Engineering Research, Academy
of Sciences, 101990 Moscow, Russia



University of Zagreb, Zagreb,
Croatia



University of Belgrade,
Serbia



جامعة الملك فهد للبترول والمعادن
King Fahd University of Petroleum & Minerals



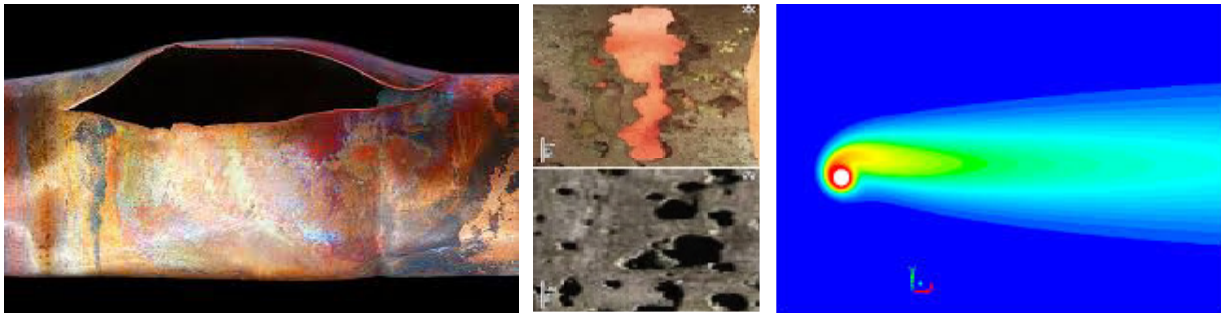
Faculty of Technology and Metallurgy,
University of Belgrade

Sponsoring



Aim & Objectives of the FRACT3

The objective of the Third International Conference on Fracture Mechanics "FRACT'3" will be focus on the "Engineering and Applied Fracture Mechanics and Environment" co-organized by the laboratory " Control Laboratory, testing, Measurement and Simulation in Mechanics", the " Laboratory for Theoretical Physics and Materials Physics and the University of HassibaBenbouali of Chlef, is to discuss the present status of the Applied mechanics based constitutive simulation, Rheology and modelling of materials and associated experimental observations methods. Such approaches allow a better understanding of how the material microstructure, environment and loadings affect degradation and failure mechanisms. Physics-based models are also necessary for extrapolation of data beyond operational experience and for correctly predicting the transferability between specimen tests and real components.



The structural integrity and functioning of Physical components is affected by initial defects as well as by time dependent degradation mechanisms such as creep, fatigue, stress-corrosion, irradiation embrittlement and thermal ageing. The modelling and understanding of degradation mechanisms and the predictability of failure loads is constantly evolving. Recently, we have seen a trend towards physics-based models that simulate the degradation and failure processes and mechanisms that operate at different length and time scales. Such approaches allow us to make better prediction of long-term performance and safety margins, transferability between specimens and components.



This event will give an overview of the different physics-based models, simulations and the experimental studies for theoretical phenomena and materials. The emphasis will be on the meso-scale, corresponding to grains, which is the relevant length-scale for many basic material properties and degradation mechanisms. Associated experimental studies and the multi-scale models from dislocation to phenomenological macro-scale studies are in the scope of the Conference. The Conference is also an opportunity for scientists and engineers from Algerians Master, Phd Students, Maghreb countries Communities and EU Member States to discuss research activities that could be a basis for future collaborations. Springer will be the supporting journal of the conference where all reviewed and accepted conference papers will be published in special issue "Engineering Applied Fracture Mechanics and Environment". Authors of selected papers will be invited to submit extended versions for publication.



Guy Pluinage
Emerite Professor

FM.C 57530 Silly Sur-Nied, France.
LaBPS – ENIM, France. Metz University,
ENIM-LaBPS, France.
pluinage@cegetel.net

Assessment of pipe defects using a constraint modified failure assessment diagram

Željko Božić
full Professor

Department of Aeronautical Engineering.
Faculty of Mechanical Engineering and Naval Architecture. University of Zagreb. Croatia. zeljko.bozic@fsb.hr



Fracture Modelling and Analysis of Plates with Multiple Site Cracks under Lateral Pressure



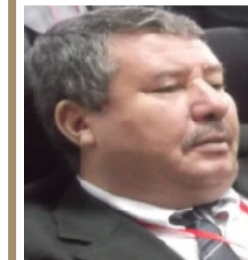
Ljubica Milovic
Professor

University of Belgrade, Faculty of Technology and Metallurgy, Karnegijeva 4, 11120 Belgrade, Serbia
acibulj@tmf.bg.ac.rs.

Behaviour of 9%Cr steel and simulated haz at 600°C

Merah Ammar Nacer,
Professor

Mechanical Engineering. Director: Center of Excellence for Scientific Collaboration with MIT King Fahd University of Petroleum & Minerals. KSA. nesar@kfupm.edu.sa ; nesarmerah@gmail.com



Gear Failures: A Case Study of Premature Failure of an Industrial Mixer Gearset



Naji Hassane
Professor

Univ. Artois and Lille University Northern France, LGCgE (EA4515), France
hassane.naji@univ-artois.fr

Multiscale Thermal Mechanics beyond Navier-Stokes Approach: Modeling, Simulation and Applications".

Simon Sedmak,
Ph.D.

University of Belgrade, Faculty of Technology and Metallurgy, Karnegijeva 4, 11120 Belgrade, Serbia



The effect of plasma welding and carbides presence on the occurrence of cracks and micro-cracks



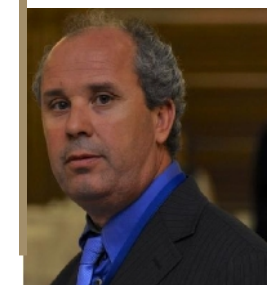
Abderezek Bezazi,
Professor

Laboratoire de Mécanique & Structures (LMS), BP. 401 Université 08 Mai 1945 Guelma 24000 Algeria.
e-mail: ar_bezazi@yahoo.com

New concepts of modelling and elaboration of materials in order to develop negative Poisson's ratios

Taoufik Boukharouba
Professor

Laboratoire de Mécanique Avancée "LMA" Université des Sciences et de la Technologie Houari Boumediene "USTHB", Alger - Algérie.
t.boukha@gmail.com



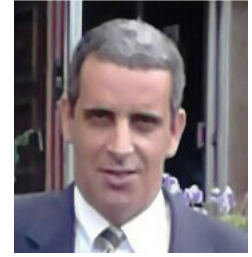
Mécanismes de Fissuration par Fatigue : Essais, Mesures & Interprétations micro-cracks



Yury .G. Matvienko,
Professor
1 Mechanical Engineering Research
Institute of the Russian Academy of
Sciences, 4 M. Kharitonievsky Per.,
101990 Moscow, Russia
e-mail: ygmatvienko@gmail.com

**Two-parameter approaches in elastic-plastic
fracture mechanics**

Med Amine Belouchrani,
Professor
Military Polytechnic School-Bordj El
Bahri Alger
Algeria
nbelouch@yahoo.fr



**FATIGUE THRESHOLD COMPUTATION IN MODE I,
MODE II AND MIXED MODE I-II BY SHAKEDOWN
ANALYSIS**



Abdelkrim Aid
Professor
Laboratory of Mechanic Testing and
fatigue, University of Mascara
Algeria
e-mail: abdelkrimaid@gmail.com

**Some Application of the fatigue field on
structures**

Ali Khelil,
Asso. Professor
Laboratory of Control, testing,
Measurement and Simulation in
Mechanics Algeria.
e-mail: khelila@yahoo.fr



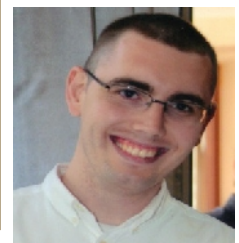
**Numerical investigation of the geometry
influence on the aerodynamic fields of the
free turbulent jets**



Hassen Mahmoudi,
Professor
Vice Rector of the Hassibabenbouali
University of Chlef,
Algeria,
email: h.mahmoudi@univhb-
chlef.dz


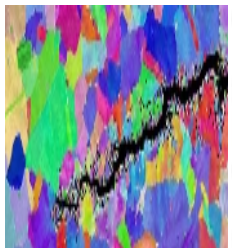

**How to Publish a Scientific Paper : A steps,
procedures and evaluations**

Branislav Djordjevic
Asso. Professor
University of Belgrade, Faculty of
Technology and Metallurgy,
Karnegijeva 4, 11120 Belgrade,
Serbia



**Influence of exploitation conditions and
welding on crack intitation and propagation
in pressure vessels**

CONFERENCE TOPICS

Topic A	<ul style="list-style-type: none"> -Fatigue -Failure Analysis -Criteria of Fracture and Failure -Damage and Micromechanics -Microstructurally Short Cracks -Fracture and Fatigue in Applied Biomechanics 	
Topic B	<ul style="list-style-type: none"> -Reliability and Integrity of Engineering Structures -Residual Stresses -Corrosion, Environmentally Assisted Cracking and Corrosion Fatigue -Extended Finite Elements Methods and their Application -Simulation and Testing of Crack Propagation on all Length Scales 	 
Topic C	<ul style="list-style-type: none"> - Fluids Mechanics - Materials domain and Rheology Domain - CFD, Heat transfert, Renewable energy 	

ABSTRACT SUBMISSION AND REGISTRATION

The Third International Conference on Fracture Mechanics "FRACT'3" "Engineering and Applied Fracture Mechanics and Environment" is open for registration now. Abstracts (in word format) not exceeding 400 words, for presentations and posters, are to be submitted to the Conference email address fract3@yahoo.com. After the Conference a local Commission scientific report with Workshop Proceedings will be published. The registration could be done by sending the [registration form](#) to the conference email address. The number of participants is limited and preference will be given participants who submit an abstract or PhD participants.

REGISTRATION FEE KEY DATES & FUNDING

Registration Fees are payable in advance of the conference, includes: Access to the Conference sessions, Poster area and Workshops, all conference documents and certificate of attendance, lunch and mid-session refreshments as scheduled in the Conference program.

Algerian Participants	12000 DA	Students	8000 DA
Exhibition	50000 DA or 500 Euros	Other Participants	350 Euros

Deadline for abstract submission, October 10, 2016 Extended October 25, 2016

Notification of abstract acceptance, October 20, 2016 Extended October 30, 2016

The Official language of the International Conference FRACT3 meeting is English. All the invited talks, oral and poster contributions must be done in English.

Abstract Submission

Participants, who would like to make an oral or poster presentation at the FRACT3 must submit an abstract for the consideration and approval of the Program Committee. All abstracts must be written, according to the Abstract Template, in English and submitted by e-mail, in format word at e-mail: fract3@yahoo.com

CONFERENCE FORMAT

The purpose of the Conference is to bring together scientists and researchers from the Maghreb member states and the target countries of E&IA (Enlargement & Interaction Action) of European Commission. The Conference will be a 4 days event based on the oral presentations from the invited international lecturers, presentations by participants and a poster session. In addition to the invited experts and the participants from the target countries, the Conference is open to the international community who are willing to attend or present their work. The target group of the workshop is the young scientists from both academia and industry.

LOCATION

Chlef, the capital of Chlef Province, is located in the north of Algeria 200 kilometres west of the capital Algiers. It is home to the Hassiba Ben Bouali university, and the basilica of Saint Reparatus, which is home to the oldest Christian labyrinth in the world and the site of the Roman citadel, CastellumTingitanum, was known as Al-Asnam (Arabic for "sculptures") for an area of 600 by 300 metres (2,000 by 980 feet) containing many statues.



During the Roman times, the chlef Province of Algeria was named CastellumTingitanum. For the French, the old Roman site was the ideal location to construct a military out post in 1843, which they named Orleanville. It was also the reason that one of the oldest churches in Africa came to be located here. No-one could predict that in 1954, the first earthquake would strike Orleanville, and that it was only a taste of what was to come. Together with celebrating the independence of Algeria in 1964, the city also celebrated the birth of a new name - El Asnam.



In 1980 disaster struck again, with a 8 earthquake hitting the city and surrounding areas, in which half the city was destroyed and approximately five thousand locals lost their lives. To distance the city and the province from this unthinkable tragedy, it was renamed for a last time to chlef in 1981. Today, visitors will still be able to visit what remains of the CastellumTingiranum (roman citadel), referred to as Al Asnam. It is a fascinating site as it contains a staggering number of statues. It is also home to the world's most ancient Christian labyrinths, Saint Reparatus. But mostly, visitors will see endless agricultural landscapes which include dairy farms, fruit orchards and fields filled with barley and wheat. The city is also known for its processing facilities and leather products. Chlef is easy to find and travel to, as it is a vital point on both the rail and road routes that run between Oran and Algiers.

History of FRACT Congress

The Congress FRACT3 was founded in 2011 by the " Laboratory for Theoretical Physics and Materials Physics in the University of HassibaBenbouali of Chlef," (Algeria) as a biannual meeting.



Fract'1.The Scientific Committee

Fract'1.Pleanary Lecture, Prof. G. Pluinage, France



Fract'2. Some pictures on the reception, opening ceremony and the Social Programme

Organizing Committee

Chairman's

Khelil Ali Chahinez Fares Abdellah Benarous

Members

Mohammed Hadjmeliani Ljubica Milovic Hebbal Brahim Omsalem Abdellah Ouagued Malik
Slimani Ahmed Bouledroua Omar Nasri Abdelaziz Braikia Mohamed Dehamni Salim
Nechad Said Guetarni Fatima Ghouaoula abdelhamid Hocine Bokortt kessal belkacem A. Kablia Aicha, attoui
Mohamed, Maarouf Omar, Kamla youcef
Elazzizi Abdellah Nateche Taher Oueld Mbeireik Mohamed Merym Bengalia Amel

Scientific Committee

Chairman's

Abdelkader Hocine, Professor, Rector, UHB Chlef, Algeria Abedi Bouabdellah, Dean of the Faculty of Technology, Algeria
Mohammed Hadjmeliani, Head of the LPTM, Algeria Guy Pluvinage, Emirite Professor, Metz, France
Ljubica Milovic, Faculty of Technology, Belgrade, Serbia

Members

Donka Angelova, Bulgaria	Zitouni Azari, France	Lajos Borbas, Hungary	Zijah Burzić, Serbia
Katia Casavola, Italy	Sveto Cvektovski, Macedonia	Ghabriout Boudjemaa, Algeria	Naser Merah, KSA
Dražan Kozak, Croatia	Paolo Lazzarin, Italy	Mersida Manjgo, Bosnia and Herzegovina	
Liviu Marsavina, Romania	Yury Matvienko, Russia	Carmine Pappalettere, Italy	Zeljko Bozic, Croatia
Zoran Radaković, Serbia	Marko Rakin, Serbia	Ivan Samardžić, Croatia	László Tóth, Hungary
Cetin Sonsino, Germany	Pruncu-catalin, UK	Sorin Vlase, Romania	omaž Vuherer, Slovenia
Milorad Zrilić, Serbia	Larbi Loukarfi, Algeria	Jesus Toribio, Spain	Taoufik Boukharouba, Algeria
Chaoui Kamel, Algeria	Madji M. Benziane, Algeria,	Ali Khelil, Algeria	Taoufik Tamine, Algeria
Ahmed Bettahar, Algeria	Aid Abdelkrim, Algeria	Abdelmoumen Guedri, Algeria	Hamou Zhloul, Algeria
Fares Chahinez, Algeria	Belouchrani M. Amine, Algeria	Fodil Hammadi, Algeria	Khaled El-Miloudi, Algeria
Abdelkader Oulhadj, Algeria	Adda Bedia El Abbas, Algeria	Abderezek Elhoud, Lybia	Mohamed Benarous, Algeria
Mustapha Allouti, Algeria	Mahmoudi Hacène, Algeria	Abdelah Ouagued, Algeria	Hamza Samir, Tunisia
Hadj Taieb Tunisia	Ahmed Abbadi, Morocco	Mohamed Abbadi, Morocco	Abderezek Bezazi, Algeria

Publication

All conference papers will be published in the FRACT3 Proceedings, with soft copies provided on a USB key. Selected papers presented at FRACT3congres will be compiled and published:

1- Aspecila issue “Engineering and Applied Fracture Mechanics and Environment” edited by Springer



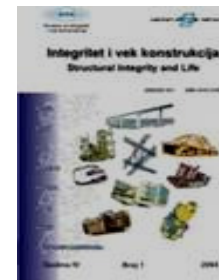
2- In the Journal “ Nature& Technologie” Classe A: Fundamental and Engineering Sciences edited by Hassiba Ben Bouali University Of Chlef-Algeria, under ISSN 1112-9778. www.univ-chlef.dz/revuenatec



3- Structural Integrity and Life (ISSN 1451-3749) will be the supporting journal of the conference where all reviewed and accepted conference papers will be published.

Editor-in-Chief: Aleksandar Sedmake-mail: asedmak@mas.bg.ac.rs

Office: University of Belgrade, Faculty of Mechanical Engineering, KraljiceMarije 16 (room 502), 11000 Belgrade, Serbia. Financially supported by the Ministry of Science and Technological Development, Republic of Serbia. Distributed to members of the Society and to the National Library of Serbia and to the Library of the University of Belgrade



divk.inovacionicentar.rs/ivk/home.html

4- In Journal of the Oil and Oil Products Pipeline Transportation: Science & Technology journal. The Oil and Oil Products Pipeline Transportation: Science & Technology is a specialized scientific periodical established as part of Transneft Research and Development Institute for Oil and Oil Products Transportation (Transneft R&D, LLC) for facilitating the innovation exchange and raising the professional level of national and foreign experts engaged in oil and petroleum products pipeline transportation.



Social Program

In the 30rd of novemberthe Organization committee Proposed a full funny day for our visitors. This will be a journey to many different traditional places in addition to a social traditional meal. The places we will visit are:



Cultural Program

During the Conference days the Organizing committee proposes a Cultural event. This will show the traditions and the variety of Algerian culture of different regions.



As you Know

The Registration Desk will be located at the Reception on La ValléeHotel****(lv-hotel.e-monsite.com) on Sunday, November 27th from 14h:00 -22h:00 , and will be open the Conference on the Center Bibliotheque on the Hassibabenbouali of Chlef, for:Monday,November 28that 08h:30

For informations, the registration fee cover only the admission to all conference session, workshops and commercial exhibition, the conference bag including relevant material, lunches (28,29) November 2016 and the Conference banquet on the 27 november at the La vallée Hotel. The Algerian PhD students and Othersparticipants how needed a reversion on the Vallée Hotel or El-Hadef Hotel, it's necessary to confirm the registartionformsende to eachparatcipants. For other participants, they should pay all the hotel nights of their staying in Chlef. As contribution, we made a deal with the La ValléeHotel and El-Hadef Hotel, near the Center of Chleffor special cost.Official Receipts (Invoices) will be given to delegates upon their arrival at the Conference on the Registration Desk. The Poster format should be A0.

• Travel and Weather

Can you make some horaire for train or transportation (Bejaia, Skikda, Tébessa, Annaba, ...) to Chlef

All the directions will coming soon on the final programme.

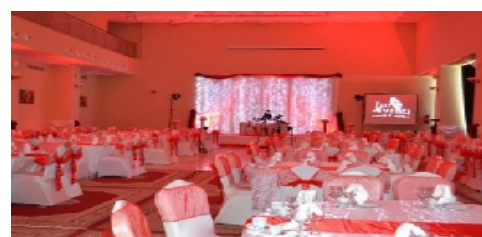
• Weather

November inChlefis cloudy and/or sometimes running. The average daily temperature is about 18°C, with lows of around 10°C. It is an ideal time for tourists to enjoy the beautiful sites of Chlef.



Recommended Hotels

There are a number of hotels of different categories, close to the Conference Venue. The reception and others accommodation will be in **La ValléeHotel******(single room :4000 DA, double room: 7500 DA) and **HadefHotel** (for PhD students, single Room : 3500 DA, double Room : 7000 DA). (Please find the Names of the hotel on the map below).





• **HADEF HOTEL**** +213 27798457 / (58) Hadef.hotel@gmail.com



Technical Program

Preliminary Program Schedule .All the Conferences will be take place at the Central Bibliotheque on the Hassibabenboualiuniversity of chlef.

	Saturday 26November r	Sunday 27November	Monday 28 November	Tuesday 29 November	Wednesday 30 November	
8 :30 - 9 :00	—	Pre-Social Programme for the International Delegation	Opening Ceremony & Opening Honor Lecture	Presidential Honor Lecture & Plenary Lectures	Open Touristique Tour In Chlef + Exhibition & Special Beach lunch	
9 :00 - 10 :10						Coffee Break
10:10 - 10:30			Plenary Lectures Session I + Plenary Lectures Session II	Plenary Lectures		Plenary Lectures
10:30 - 11 :10				&		&
11:30 - 13 :30			Coffee Break and Welcome Special Lunch	Topic A+B Session <small>List 2A</small>		Topic C session <small>List 2C</small>
12 :30 - 13 :30 13 :30 -14 :00				Lunch Time		
14 :00-14 :40 14 :40 15 :30			Reception of Internationa l Delegation	Reception Hotel La Vallée		Plenary Lectures (Session A+B)+ <small>List 1A+1B</small>
15 :40-16 :00	Coffee Break	Oral Presentation <small>List 2B</small>				
16 :00-16 :40	Poster Session C	Coffee Break				
16:40 - 17 :30		Exhibition in Chlef city			Poster Session A+B	
17 :00 -19 : 00	Registration &welcomeRec eption	Meeting Cooperation Lunch- Hotel La Vallée-			ClotureCeremony	
19 :00 – 20 :30						
The FRACT3 Secretariat reserves the right of changing any session in the final program Changes to the program will be published in the website on a regular basis.						

For the List 1A, 1B, 1C, 2A, 2B and 2C, please look about the table below.

List of the Plenary Lectures, Oral and Poster Presentations



Name/First Name	University	Country	
Plenary Lectures			
Guy Pluvinage	LaBPS-ENIM, Metz, France	France	
Ljubica Milovic	University of Belgrade,	Serbia	
Željko Božić	University of Zagreb	Croatia	
Merah Ammar Nacer	Center of Excellence for Scientific	KSA	
Naji Hassane	University of Artois and Lille	France	
Simon Sedmak	University of Belgrade	Serbia	
Abderezek Bezzari	University of 08 Mai 1945 Guelma	Algeria	
Taoufik Boukharouba	USTHB Houari Boumediene, Algiers	Algeria	
Yury .G. Matvienko	University of Sciences, Moscow,	Russia	
Med Amine Belouchrani	Military School Bordj El Bahri	Algeria	
Abdelkrim Aid	University of Mascara	Algeria	
Ali Khelil	Hassibabenbouali University Chlef	Algeria	
Hassen Mahmoudi	Hassibabenbouali University Chlef	Algeria	
Branislav Djordjevic	University of Belgrade	Serbia	
Hadj Meliani Mohammed	Hassibabenbouali University Chlef	Algeria	
Oral Presentation Topic A			
M. Benaissa	Tlemcen University	Algeria	1A
Nardjes Djaoui	Tizi-Ouzou University	Algeria	1A
Nafissa. Khennafi-Benghalem	Sétif1 University	Algeria	1A
L. Berredjem	Annaba University	Algeria	1A
M. El Nedhir Belgherras	Sidibel-Abbes University	Algeria	2A
L. Zouambi	Sidibel Abbes University	Algeria	2A
Nabil KaziTani	Tlemcen University	Algeria	2A
Poster Presentation Topic A			
Aissaabderahmane	Mascara	Algeria	
N. Benchabne	Tizi-ouzou	Algeria	
Abdallah Lounis	Mascara	Algeria	
Ahmed hamidi	Tiaret	Algeria	
Hamlibenzaharhamid	Khemismiliana	Algeria	
Houaritarek	Mascara	Algeria	
I. Djefour	Boumerdes	Algeria	
K. Rakrak	Chlef	Algeria	
L. Aminallah	Mascara	Algeria	
L. Zouambi	Sidibel abbes	Algeria	
M. Halimi	Oran	Algeria	
M. Zidour	Sidi bel abbés	Algeria	
Mokhtar KHALD	Mascara	Algeria	
N. Djebbar	Chlef	Algeria	
Said. Grairia	Guelma	Algeria	
Redouane koulli	Bachar	Algeria	
E.h. besseghier	Mascara	Algeria	

D.belhadri	Ain temouchent	Algeria
S. Achouri	Algiers	Algeria
H. Fekirini	Sidibel-abbes	Algeria
A. Kaddouri	Sidibel-abbes	Algeria
D. Sekhane	Constantine	Algeria
F.z. seriari	Tlemcen	Algeria
M. Cherfi	Sidibel abbes	Algeria
A. Bendriss	Djelfa	Algeria
B. Bouabdallah	Sidi-bel-abbès	Algeria
D.belhadri	Aintemouchent	Algeria
L. Hachemi	Mascara	Algeria

Oral Presentation Topic B			List
K. Gharbi	Boumerdes	Algeria	1B
M. Ould Mbereick	Chlef	Algeria	1B
R. Mehdaoui	Blida	Algeria	1B
Z. Douaissia	Annaba	Algeria	1B
M. Benachour	Tlemcen	Algeria	1B
M.Zerouki	Tizi-Ouzou	Algeria	1B
Z. Sidhoum	TiziOuzou	Algeria	2B
A. Benouis	Saïda	Algeria	2B
A. Ghouaoula	Chlef	Algeria	2B
L. Madouni	Tizi-Ouzou	Algeria	2B

Poster Presentation Topic B		
H. Berrekia	Oran	Algeria
Rahmani-K-Yassine	Chlef	Algeria
Saadi Abdel. Abdessamad	Chlef	Algeria
Meriem Hamla	Setif	Algeria
S. Lallouche	Chlef	Algeria
L. Hachemi	Mascara	Algeria
Z. Douaissia	Annaba	Algeria
S.DEBILI	Annaba	Algeria
M. Tirenifi	SidiBelabbes	Algeria
A. Benhamena	Mascara	Algeria
A. Boulouar	Sidi Bel Abbes	Algeria
A. Boulouar	Sidi-Bel-Abbes	Algeria
A. Brahami	Sidi Bel Abbes	Algeria
D. Said Lhadj	Blida	Algeria
F. Bouafia	Sidibel Abbes	Algeria
HouariTarek	Mascara	Algeria
N. Benamara	Sidi-Bel-Abbes	Algeria
S. Ramdoun	Sidi Bel Abbes	Algeria
S. Tiachacht	Tizi-Ouzou	Algeria
M.A. Benghalia	Chlef	Algeria

Oral Presentation Topic C			List
Asma Adda	Medea	Algeria	1C
B. Bezzina	Algiers	Algeria	1C
FaziaBouaraba	Tizi-Ouzou	Algeria	1C
D. Bennacer	Tlemcen	Algeria	1C
AbdelhafidRahmane	Constantine	Algeria	1C
F. Brioua	Constantine	Algeria	1C
F.Benyettou	Blida	Algeria	1C
M.T.Bouzaher	Ghardaïa	Algeria	1C
A. M.T.Bouzaher	Ghardaïa	Algeria	1C
N. Benamara	SidiBel Abbes	Algeria	1C

H. Laidoudi	Oran	Algeria	2C
N. Mesboua	Boumerdes	Algeria	2C
M. Merzoug	Sidi-Bel-Abbes	Algeria	2C
Fizi Yazid	Alger	Algeria	2C
Gadi Ibrahim	Chlef	Algeria	2C
R. Bensaada	Tizi-Ouzou	Algeria	2C
Boudjellel Moulay Ali	SidiBel Abbas	Algeria	2C
Poster presentation Topic C			
S.taleb	Sidibel abbes	Algeria	
Abderazak bennia	Chlef	Algeria	
Aminabenabderrahmane	Sidibelabbes	Algeria	
Aoumeurdjelloul	Chlef	Algeria	
Billelsmili	Annaba	Algeria	
Dj. Amghar	Oran	Algeria	
F. Kebir	Oran	Algeria	
K. Messaoudi	Tlemcen	Algeria	
Kamlayoucef	Chlef	Algeria	
M. Lebbi	Ghardaïa	Algeria	
Z. Malou	Setif	Algeria	
Abderazaak bennia	Chlef	Algeria	
L. Merabti	Tipaza	Algeria	
M. Braikia	Chlef	Algeria	
M. Benhaddou	Oujda	Morocco	
C.bouhafs	Alger	Algeria	
LASNAMI fadhilal	Chlef	Algeria	
Abdellatifamer	Chlef	Algeria	
Amar ZERROUT	Chlef	Algeria	
T. Tahri	Chlef	Algeria	
M.benmaachou	Sidi bel abbes	Algeria	
Nora ziani	Tizi-ouzou	Algeria	
N. Bouteldja	Chlef	Algeria	
H.bendjeddou	Annaba	Algeria	
A. Belaziz	Sidibel abbes	Algeria	
A. Houda	Khenchela	Algeria	
A. Hamidi	Bechar	Algeria	
L. Hadji	Tiaret	Algeria	
O. Belaidi	Tizi-ouzou	Algeria	
N. Zouatnia	Chlef	Algeria	
W. Bensmain	Sidi bel abbes	Algeria	
Y. Chahraoui	Sidi bel abbes	Algeria	
M. Hachellafkaddour	Mascara	Algeria	
A.Mennad	Tipaza	Algeria	

Two workshop will be organized on the marge of the conference. They provides an opportunity for young scientists, researchers and engineers from academy and industry to get acquainted with fundamental aspects of fracture mechanics, simulation and recent trends in practical applications of fatigue and fracture models, and advanced approaches such as multiscale materials modeling.

Workshop 1.Fatigue and Fracture Modeling and Analysis of Materials and Components (Dr. Mohammed HadjMeliani, LPTPM, Hassibabenbouali university of Chlef)

The Workshop provides an opportunity for young scientists, researchers and engineers from academy and industry to get acquainted with fundamental aspects of fracture mechanics, recent trends in practical applications of fatigue and fracture models, and advanced approaches such as multiscale materials modeling. Senior researchers and experts will give lectures on experimental and numerical techniques for modeling, analysis and assessment of damaged components and structures. Particular attention will be given to determining and analysis of crack extension in pipes, where the standard and new methods will be examined. Examples on multiscale modeling used in analyzing pipeline steel weldments, metal/ceramic interfaces and fatigue problems will be given. Models for fatigue crack growth prediction and remaining fatigue life assessment will be presented.

workshop 2.Mechanics Simulation and CFD applications. (Dr. AbdellahBenarous, Dr. Ali Khelil, LCTMSM, Hassibabenbouali university of Chlef).

Contact

e-mail: fract3@yahoo.com

<https://www.Univ-chlef.dz/lptpm>

<https://www.facebook.com/uahbc>.dzTél: (+213) 27 72 17 94 Mobile: (+213) 7 70709563 Fax: +213 27 72 17 94

Plenary

FATIGUE THRESHOLD COMPUTATION IN MODE I, MODE II AND MIXED MODE I-II BY SHAKEDOWN ANALYSIS

M. Bouchedjra, M.A. Belouchrani.*

Military Polytechnic school, Materials Laboratory, BP17C 16111 Bordj El Bahri Algiers, Algeria

Abstract: The fatigue thresholds remain very significant parameters, helping the designer and the manufacturer in their decision to reform a mechanical structure or its dimensioning. These last years, several models were advanced in order to propose a method of their determination or the study of their influence factors such as the microstructure or the load ratio. The established fatigue threshold models can be classified in two groups, the theoretical models and the models based on the experimentation. The majority of these models agree on the fact that the fatigue threshold increases with the size of the grain and depends strongly on the yield stress of the material. In this work, we will present determination of these parameters by the shakedown analysis. This analysis considers an elastic-plastic structure, subjected to variable loading in the three modes of fracture and uses the finite element method combined with an optimization procedure to determine the safety factor leading to the calculation of a fatigue threshold corresponding to the shakedown stress intensity factor.

Keywords: Fatigue Threshold, Shakedown, Stress Intensity Factor, Finite Elements, Optimization

1. Introduction

The majority of industrial parts are naturally subject to varying stresses over time (fatigue), this requires consideration of their fatigue resistance in the design rules; since it concerns the safety of structures in normal operation.

In practice, fatigue occurs in two steps: at first, there is the priming of one or more micro-cracks that will propagate irregularly, then one of them will dominate the propagation stably the sudden breakup of the part. One of the parameters characterizing the propagation of fatigue cracks is the fatigue threshold (K_{th}), this parameter allows us to know if a crack is able to propagate under such loads.

Determining the values of this parameter is based on a purely experimental procedure, according to ASTM E647 standard procedure. Note that a test piece used to provide a single value. Thus, the complete characterization of the behavior of cracking threshold of a material by this procedure is very costly in terms of material and time.

Based on the extension of the theorem MELAN [1], we present in this work a technical independent of cracking curve for determining the fatigue threshold. The results are presented for different loading modes (Mode I, Mode II and Mode mixed I + II).

2. Shakedown problem formulation for cracked body

It has been proposed [1, 2], that a cracked body shakes down under a given load, if we can find a time-independent residual stress field and satisfying the following conditions:

$$\left\{ \begin{array}{ll} \text{div} \rho = 0 & \text{dans } \Omega \\ \rho \cdot n = 0 & \text{dans } \Gamma_F \\ F(\alpha \sigma^{(e)}(x, t) + \rho(x), \sigma_y) \leq 0 \end{array} \right. \quad (1)$$

With supplementary condition on the limit crack length:

$$a_l \leq a_c \quad (2)$$

Where a_l is given by the following expression:

$$a_l = a_0 + \left[\frac{m+1}{m} \cdot \frac{1}{V} \cdot \frac{\alpha}{\alpha-1} \int_{\Omega} \frac{1}{2} \rho : S : \rho \, d\Omega \right]^{\frac{m}{m+1}} \quad (3)$$

Where a_0 : is the initial crack length,
 m et V : material constant representing the R-curve parameters;
 a_l : limit crack length reached at shakedown state.

3. Shakedown stress intensity factor

The stress intensity factor corresponding to the state of adaptation [2], noted KSD, was calculated for the three charging modes (Mode I and Mode II Mixed Mode I-II). The values obtained were compared with those of the corresponding fatigue threshold K_{th} in the case considered in this work [3-6]. This shows that the KSD determined by the shakedown analysis can be considered as fatigue thresholds.

In addition, the study of the influence of the microstructure through the grain size, and the load ratio shows that KSD has the same evolution then the K_{th} with respect to these parameters.

4. Conclusion

In this work, we presented a method for calculating fatigue threshold with the shakedown analysis for the three modes of loading: Mode I, Mode II and mixed mode I + II. Comparison of the shakedown stress intensity factor with the corresponding fatigue threshold for some materials shows that these two factors correlate well; this implies that the shakedown stress intensity factor may be considered the fatigue threshold.

The influence of the intrinsic parameters (Young's modulus and grain size) and extrinsic one (load ratio) on the shakedown stress intensity factor is similar to that the fatigue threshold. This reinforces the proposition that the shakedown stress intensity factor represent the fatigue threshold.

References

- [1] Belouchrani M. A., Weichert D., "An extension of the static shakedown theorem to inelastic cracked structures", *Int. J. Mech. Sci.*, 1999, 41, 163-177.
- [2] Belouchrani M. A., Weichert D., Hachemi A., "Fatigue threshold computation by shakedown theory", *Mech. Res. Commun.*, 2000, 27, 287-293.
- [3] Newman J.C., Robert.S., "Fatigue crack growth thresholds, endurance limits, and modulus and fracture surface roughness", *Int. J. Fatigue*, 1998, 20, 737-742.
- [4] Radhakrishnan V. M., Mutoh Y. "On fatigue crack growth in stage I, the behavior of short fatigue crack", *Cong. Mech. Eng.*, 1986, 87-99.
- [5] Otsuka A., Tohgo K. "Fatigue crack initiation and growth under mixed mode loading in aluminum alloys 2017-T3 and 7075-T6", *Eng. Frac. Mech.*, 1987, 128, 721-32.
- [6] Yongming L., Sankaran M., "Threshold stress intensity factor and crack growth rate prediction under mixed-mode loading", *Eng. Frac. Mech.*, 2007, 74, 332-345.

BEHAVIOUR OF 9% Cr STEEL AND SIMULATED HAZ AT 600°C

Ljubica MILOVIĆ*, Bojana ALEKSIĆ**, Abubakr M Hemer**, Vujadin Aleksić***

* University of Belgrade, Faculty of Technology and Metallurgy, Belgrade, Serbia

** Innovation Centre of the Faculty of Technology and Metallurgy, Belgrade, Serbia

*** Institute for testing of materials-IMS Institute, Belgrade, Serbia

Abstract: An investigation has been carried out into the behaviour of type IV cracks region in heat affected zone (HAZ) of P91 steel at 600°C. Microstructure zones where type IV failures may occur have been studied in details. Results are reported on the simulated specimens 11x11x70 mm tested at room and at operating temperature. The results of comparison of mechanical characteristics and microstructure have been analysed using two types of specimens: with post weld heat treatment (PWHT) and without PWHT. It has been found the presence of precipitates at the grain boundaries in simulated type IV zone of HAZ exposed to subsequent PWHT. It is further confirmed that the post weld heat treatment is necessary for 9%Cr (P91) steel.

Keywords: P91, Simulated HAZ, ICHAZ, PWHT.

Two-parameter approaches in elastic-plastic fracture mechanics

Yu.G. Matvienko^{1*}

1Mechanical Engineering Research Institute of the Russian Academy of Sciences, 4 M. Kharitonievsky Per., 101990 Moscow, Russia

Abstract: The three-term expansion describes crack-tip fields with two parameters, namely, J -integral and the second parameter A that can be treated as a constraint parameter. The two-parameter J - A approach in elastic-plastic fracture mechanics is discussed.

This approach is compared with other two-parameter approaches. Constraint parameter A and J -integral are computed by means of three-dimensional elastic-plastic stress analyses employing finite element method for various configurations of specimens and the hardening exponent. Values of J -integral and constraint parameter A are estimated for specimens with thickness variation. Influence of their distributions along the crack front on fracture process is discussed.

Keywords: three-term elastic-plastic asymptotic expansion, constraint parameter, J - A fracture criterion, finite element method.

1. Introduction

In many cases (for example, short and inner cracks) a one-parameter approach is not suitable for fracture prediction. Finite element modeling shows that the one-term asymptotic expansion is unable to produce satisfactory description of near-tip stress fields in the microstructurally significant region. Even for the small scale yielding conditions the deviation of actual stress field from HRR-field is noticeable.

A mathematical approach to the introduction of a second fracture parameter is based on higher order elastic-plastic asymptotic expansions of the stress field in the near crack tip region. Three-term asymptotic solutions have been reported by Yang, Chao and Sutton [1] and by Nikishkov [2]. It appeared that the three-term expansion (TTE) is controlled by just two parameters, namely, the J -integral and an additional amplitude parameter A . Amplitude can be used as a constraint parameter in elastic-plastic fracture.

2. Elastic-plastic asymptotic expansions of the stress field

The HRR field does not describe correctly stresses in the small region that is significant for fracture process. Better description of the stress field in this region can be achieved with the three-term asymptotic expansion proposed and further developed by Nikishkov [2]. The effective stress is defined as the average of the weighted stress inside the fracture process zone:

$$\frac{\sigma_{ij}}{\sigma_0} = A_0 \rho^s \tilde{\sigma}_{ij}^{(0)}(\theta) - A \rho^t \tilde{\sigma}_{ij}^{(1)}(\theta) + \frac{A^2}{A_0} \rho^{2t-s} \tilde{\sigma}_{ij}^{(2)}(\theta), \quad (1)$$

Here, A is the second fracture parameter that is usually called constraint parameter, σ_{ij} are stress components σ_r , σ_θ and $\sigma_{r\theta}$ in the polar coordinate system $r\theta$ with origin at the crack tip, $\tilde{\sigma}_{ij}^{(k)}$ are dimensionless angular stress functions obtained from the solution of asymptotic problems of order (0), (1) and (2). Angular stress functions $\tilde{\sigma}_{ij}^{(0)}$ and $\tilde{\sigma}_{ij}^{(1)}$ are scaled so as maximal equivalent Mises stress is equal to unity: $\max_\theta \tilde{\sigma}_e^{(0)} = \max_\theta \tilde{\sigma}_e^{(1)} = 1$. Amplitudes of stress functions for the problem (2) depend on the solutions of the problems (0) and (1). Power s has closed form expression $s = -1/(n+1)$, where n is the hardening exponent ($n > 1$) in

*Corresponding author

E-mail address: ygmavienko@gmail.com

Ramberg–Osgood power-law strain hardening curve. Power t is a numerically computed eigenvalue that depends on hardening exponent n . Coefficient A_0 is specified as $A_0 = (\alpha \varepsilon_0 I_n)^s$. Dimensionless radius ρ is defined by formula

$$\rho = \frac{r}{J / \sigma_0} \quad (2)$$

It is found that for Mode I plane strain crack the three terms of the asymptotic expansion are enough for representing the stresses in the crack tip region with sufficient accuracy (Fig. 1).

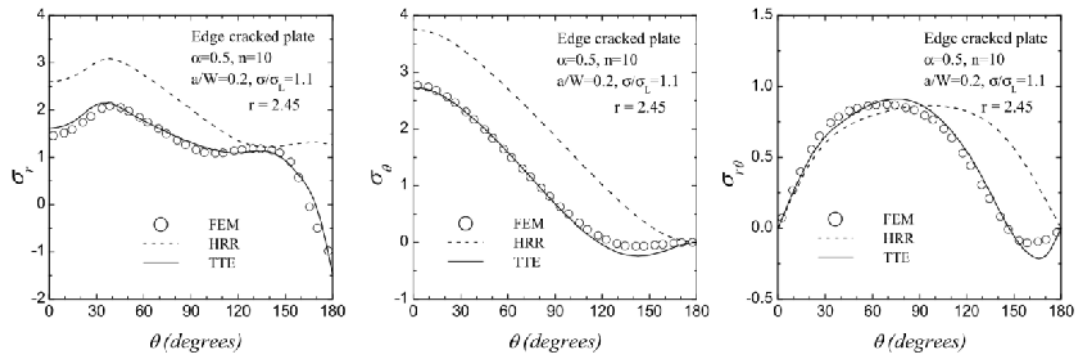


Fig. 1. Comparison of J - A field and FEM results.

Two-parameter fracture criterion implies comparison of computed J -integral for a cracked structure and the experimental fracture toughness J_C corresponding to computed value of constraint parameter A [3]

$$J(P)|_A = J_C(A) \quad (2)$$

Determination of the dependency $J_C(A)$ can be accomplished by testing cracked specimens with different constraint at fracture load.

Three-dimensional elastic-plastic stress analyses of four specimens - edge cracked plate, center cracked plate, three point bend and compact tension specimens were performed using the finite element method with variation of specimen thickness and crack depth [4]. Typical distribution of the constraint parameter A is characterized by two features: minimal A is at the specimen midplane, magnitude of A considerably increases to the specimen free surface. Comparison of different specimens show that the center cracked plate specimen has highest values of the constraint parameter A for all crack depths. The compact tension specimen demonstrates lowest values of A that are even less than its small scale yielding value.

3. Conclusions

Theoretical and numerical aspects of basic parameters J and A including in the three-term asymptotic expansion of the crack-tip stress field are discussed. The effect of specimen geometry and type of loading on the J -integral and the constraint parameter A is demonstrated. The two-parameter elastic-plastic fracture criterion J_C - A is described for structural integrity assessment.

References

- [1] Yang S., Chao Y.J., Sutton M.A.(1993). Higher-order asymptotic fields in a power-law hardening material. Eng. Fract. Mech., V. 45, pp. 1–20.
- [2] Nikishkov G.P.(1995). An algorithm and a computer program for the three-term asymptotic expansion of elastic–plastic crack tip stress and displacement fields. Eng. Fract.Mech., V. 50, pp.65–83.
- [3] Matvienko Yu.G., Nikishkov G.P. (2016) J - A elastic-plastic crack tip field and the two-parameter fracture criterion. Structural Integrity Procedia, V.2, pp. 26-33.
- [4] Nikishkov G.P., Matvienko Yu.G. (2016). Elastic–plastic constraint parameter A for test specimens with thickness variation, Fatig.Fract.Eng. Mater.Struct., V. 39, pp. 939-949.

The Effect of Plastic Deformation on Structural Integrity of Austenite-Ferrite Welded Joint

Ramo Bakić¹, Aleksandar Sedmak², Simon Sedmak^{3*}, Branislav Đorđević³, Nevena Topalović⁴

1 Technical school in Tutin, 7th July 18, Tutin, Serbia

2 University of Belgrade, Faculty of Mechanical Engineering, Kraljice Marije 16, Belgrade, Serbia

3 Innovation center of Faculty of Mechanical Engineering, Kraljice Marije 16, Belgrade, Serbia

4 University of Belgrade, Faculty of Philology, Students square 3, Belgrade, Serbia

Abstract: Structural integrity is the science and technology of the margin between safety and disaster. Catastrophic failure of any structure can be avoided if structural integrity is assessed and necessary precaution is taken. In this research structural integrity assessment of welded joints is studied both numerically and experimentally. The application of fracture mechanics depends on available data, material behavior, environmental effect and loading. In predominantly static loading material behavior can be described as elastic-plastic, with crack opening displacement (COD) or the J integral as parameters. The theoretical and experimental analyses cannot fully describe the behavior of the cracked welded joint and its heterogeneous microstructure. For that purpose, the numerical analysis can be helpful, if applied in a proper way. An example of the finite elements numerical analysis of welded joints is presented. It has been shown that previous plastic deformation of the base metal has detrimental effect on structural integrity of a pressure vessel.

Keywords: Structural integrity, elastic-plastic fracture mechanics, pressure vessels, J-R curve

1. Introduction

Structural integrity is the science and technology of the margin between safety and disaster. Catastrophic failure of any structure can be avoided if structural integrity is assessed and necessary precaution is taken. In this research structural integrity assessment of welded joints is studied both numerically and experimentally. The application of fracture mechanics depends on available data, material behavior, environmental effect and loading. In predominantly static loading material behavior can be described as elastic-plastic, with crack opening displacement (COD) or the J integral as parameters. Anyhow, the theoretical and experimental analyses cannot fully describe the behavior of the cracked welded joint and its heterogeneous microstructure.

Due to high ductility and strain hardening of stainless austenite steel, mechanical properties of welded joints made of it are typically not a problem. However, in the case of some processing equipment components, stainless steel is used in combination with structural steel, and they are connected by a heterogeneous welded joint. In this case, micro-structure and mechanical properties of welded joint constituents differ significantly, thus stress and strain distribution is non-uniform, as is the case with the structure investigated in this paper, made of stainless and normalised structural steel, micro-alloyed with vanadium. Due to the non-uniform micro-structure mentioned above, as well as stress and strain distribution in the welded joint, monitoring of crack behaviour and growth is of crucial significance for structural integrity assessments. For that purpose, the numerical analysis can be helpful, if applied in a proper way. An example of the finite elements numerical analysis of welded joints is presented. It has been shown that previous plastic deformation of the base metal has detrimental effect on structural integrity of a pressure vessel. The results presented here are extracted from the doctoral thesis of the first author, [1].

* Corresponding author

E-mail address: simon.sedmak@yahoo.com

2. Application of fracture mechanics in the evaluation of crack behaviour in structures

Application of fracture mechanics in determining of crack growth resistance nowadays represents the base for practical methods of ductile material testing. J integral was found to be the most suitable parameter for such applications, thus crack resistance curves, also known as J_R curves, have been developed for the purpose of determining the critical value, i.e. fracture toughness. Consideration of these curves has shown that J_{Ic} represents a conservative measure of fracture toughness for most structural materials. Application of J integral to crack growth analysis enables the use of fracture toughness before and after crack growth.

Dependence of J integral (as well as other fracture mechanics parameters) from crack growth can be expressed using the crack driving force, on one hand, and material strength (crack resistance curve – J_R), on the other. Based on the described material behaviour, a criteria for predicting failure in components and structures in plane stress and stable crack growth conditions can be established, by comparing the crack driving force and material strength curves. It is common practice to use \sqrt{J} instead of J (figure 1) for the purpose of determining the critical point. The procedure for determining the fracture criteria based on the resistance curve includes the following steps:

- determining of $\sqrt{J_R}$ values for the structure (prior to crack propagation) for various crack lengths and loads, using an adequate plasticity model;
- determining of $\sqrt{J_R}$ curves of the material of which the structure is made, using appropriate specimens;
- determining the intersection point A between the crack driving force and material strength curve (figure 1), which represents the initiation of unstable fracture. Representative fracture stress is given by σ_4 , whereas Δa represents crack length increment.

Determining of the intersection point for these curves is made significantly more complex due to slow stable crack growth (under quasi-static loading), which takes places before unstable growth and disastrous failure. Hence, instead of a single criteria for structures subjected to plane strain,

$$J \geq J_{Ic} \quad (1)$$

two criteria must be satisfied for structures with considerable slow stable growth,

$$J \geq J_r \quad (2)$$

and

$$\frac{\partial J}{\partial a} \geq \frac{\partial J_r}{\partial a} \quad (3)$$

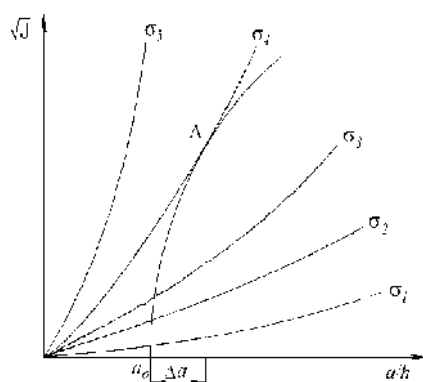


Fig. 1. Procedure for determining of fracture criteria based on resistance curves

3. Experimental Part

Four plates were welded for the purpose of cutting specimens. Each of these plates was obtained by welding micro-alloyed steel with a thickness of 14 mm to a high-alloyed steel, 12 mm thick.

Steel M corresponds to steel P460NL1 according to standard EN 10028 – 3 (ČRN 460 according to JUS C.B0.502) and is also known by its commercial name, NIOVAL 47. Steel V corresponds to steel X6CrNiMoTi 17 12 2, according to standard EN 10088 (Č.4574 according to JUS C.B0.600). These steels were selected for the experimental part of this paper since most tanks currently in use, for working temperatures down to -60°C , have connectors made of these materials, wherein the mantle and lid are made of steel P460NL1 and connector pipes are made of X6CrNiMoTi 17 12 2.

Given in table 1, 2 and 3 are the chemical composition and mechanical properties of these steels obtained by testing of plates used for welding, i.e. test specimens, as well as the micro-structure of the parent material (PM).

Table 1. Chemical composition of the PM

Steel	C	Si	Mn	P	S	Cr	Ni	Cu	Al	Mo	Ti	V	Nb
M	0,10	0,49	1,26	0,011	0,014	0,08	0,11	0,21	0,067	0,019	0,002	0,048	0,053
V	0,04	0,35	1,73	0,031	0,004	17,9	11,6	0,18	0,061	2,16	0,38	0,079	0,016

Table2. Mechanical properties of steel M

Spec. No	Upper yield stress R_{EH} , MPa		Lower yield stress R_{EL} , MPa		Tensile strength R_m MPa		Elongation A %		Contraction Z %	
	individual	average value	individual	average value	individual	average value	individual	average value	individual	average value
1	452	453	434	435	568	565	26	25	58	58
2	453		434		563		25		58	
3	453		438		564		25		59	

Table3. Mechanical properties steel V

Specimen number	Yield stress $R_{p0,2}$ MPa		Tensile strength R_m MPa		Elongation A %		Contraction Z %	
	individual	average value	individual	average value	individual	average value	individual	average value
4	321	324	592	595	37	37	53	53
5	321		596		37		53	
6	331		596		36		53	

Test plates were welded by manual arc procedure. Coated electrodes INOX R 29/9 were used as additional material, manufactured by Železarna Jesenice. Chemical composition of the pure weld metal made from this additional material is given in table 4. Electrodes have a rutile coating and are meant for welding high strength steel, steels with poor weldability, as well as for welding heterogeneous steels. This welding procedure and additional material were selected since they were also used during the manufacturing of welded joints in tanks.

Table 4. Chemical composition of pure weld metal, electrode INOX R 29/9

C	Si	Mn	Cr	Ni
0,15	≤ 0,9	0,9	29	9

4. Fracture Mechanics Tests

For the purpose of testing, Charpy specimens for three point bending (SENB) were used, and their geometry was defined in accordance with standard ASTM E1820 and is shown in figure 2. Crack opening displacement (COD) was measured using a special inductive transducer SD1, with an accuracy of ±0,01 mm. Notch and fatigue crack in these specimens were located in the part with the corresponding plastic strain in steel M (0, 10, 20, 30, 40 and 50%).

Testing procedure involved the obtaining of an R-curve, i.e. the J - Δa curve, which consists of J integral values for equal crack length increments, Δa. Experiments were performed by testing a single specimen by successive partial unloading, i.e. the single specimen yielding method, as defined according to ASTM E1152.

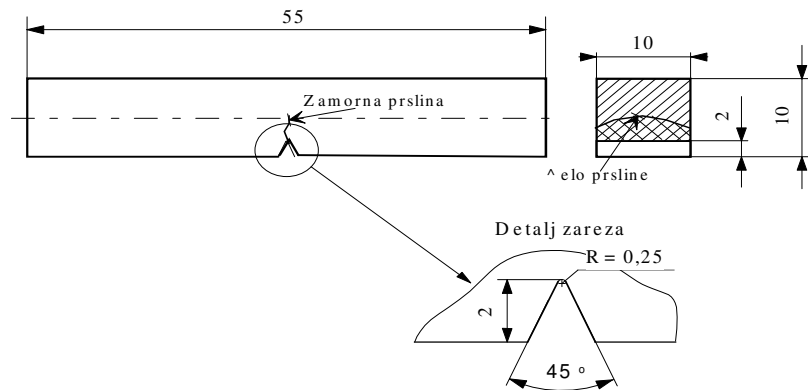


Fig. 2. Specimen used for fracture mechanics tests

Results for J - Δa curves are shown in figs. 5-10 for plastic strain of 0, 10, 20, 30, 40 and 50%, respectively. Based on the obtained regression line, critical J, J_{Ic} integral is determined, as shown in table 5.

Table 5. J_{Ic} values for various levels of plastic strain

Plastic strain	Critical J-integral, J_{Ic} , kJ/m ²
PM 0	28.6
PM 5	31.6
PM 10	25.4
PM 30	64.3
PM 50	46.2
PM 70	53.5

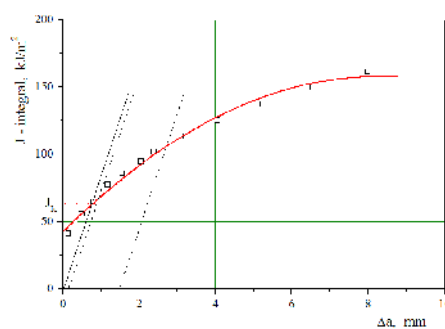
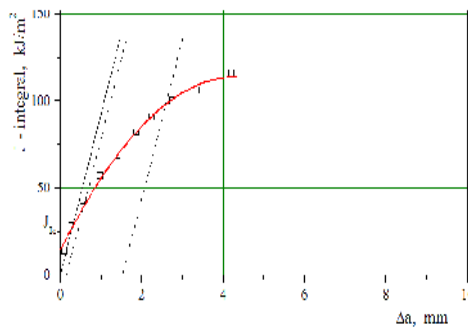


Fig. 5. J - Δa diagram for 0% plastic strain. Fig. 6. J - Δa diagram for 10% plastic strain

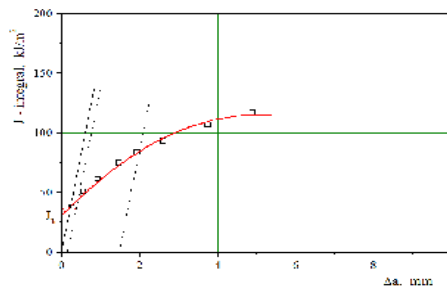
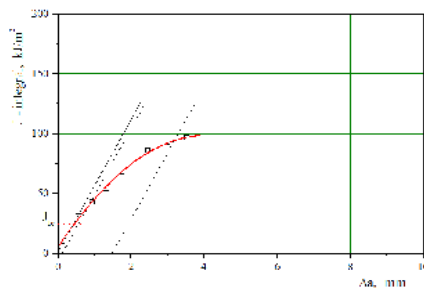


Fig. 7. J - Δa diagram for 20% plastic strain. Fig. 8. J - Δa diagram for 30% plastic strain

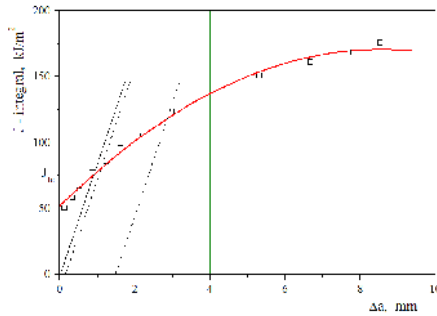


Fig. 9. J - Δa diagram for 40% plastic strain.

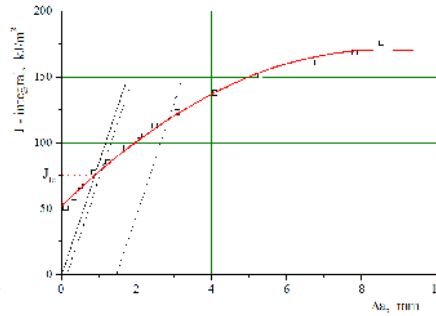


Fig. 10. J - Δa diagram for 0% plastic strain

5. Results and Discussion

Integrity assessment for tanks used for liquid carbon-dioxide storage, shown in paper [3], involved a series of complex tests, analysis of strain distribution and of mechanical properties of all zones within the welded ferrite-austenite steel, along with the application of analytical methods for determining of crack growth.

In this paper, integrity assessment of a tank used for liquid carbon-dioxide storage was based on the assumption the crack type defects will occur in the plastically deformed parent material, as opposed to the typical assumption about cracks forming in the HAZ and/or WM. Thus J-R curves have been determined for the PM with varying degrees of plastic strain, as described in chapter 6, whereas crack driving forces (J integral) were taken from paper (RJ), since they do not depend on the material properties.

Results for stress at which stable crack growth initiates (σ_{init}) and corresponding crack length (a_{unst}) are shown in table 6.

Table 6. Stress at which stable crack growth initiates (σ_{init}) and corresponding crack length (a_{unst}).

	PM 0	PM 10	PM 20	PM 30	PM 40	PM 50
σ_{init} (MPa)	264	319	298	306	264	285
σ_{init}/σ	0,62	0,74	0,70	0,72	0,62	0,67
(a_{unst}) mm	7,2	7,5	8,2	7,7	6,8	6,4

By comparing the results from table 7.1, it can be seen that plastic strain significantly reduces σ_{init} , as well as the critical crack length (a_{unst}), which confirms the assumption that structural integrity is important in case the PM suffers significant plastic strain. It should, however, be mentioned that the risk of unstable crack growth in the PM of the considered tank is still smaller than in the case of crack growth in HAZ and/or WM, which was analysed in (RJ).

6. Conclusions

Integrity of ferrite-austenite welded joints was not significantly jeopardized, not even due to considerable plastic strain in PM, since the parent metal maintains relatively high resistance to unstable crack growth at

high levels of plastic strain. Compared to problems related to crack initiation and growth in the WM and HAZ, the problem analysed in this paper (crack in the PM) is not as threatening to the structural integrity of a ferrite-austenite welded joint. Research presented in this paper has proven that by applying elastic-plastic fracture mechanics parameters, it is possible to assess pressure equipment integrity, taking into account all different zones and their mechanical properties, which is of crucial significance for heterogeneous welded joints.

References

- [1] RamoBakić, Assessment of pressure vessel integrity by using elastic-plastic fracture mechanics parameters (in Serbian), D.Sc. thesis, University of Belgrade, 2014

Influence of exploitation conditions and welding on crack initiation and propagation in pressure vessels

G.Bakić¹, B.Đorđević^{2,*}, L.Jeremić¹, M.Đukić¹, B. Rajičić¹, S.Sedmak², A.Sedmak¹
1University of Belgrade, Faculty of Mechanical Engineering, KraljiceMarije 16, Belgrade, Serbia
2University of Belgrade, Innovation center of Faculty of Mechanical Engineering, KraljiceMarije 16, Belgrade, Serbia

Abstract: Cracks in pressure vessels represent considerable and serious practical problem. These defects can be initiated and enhanced by various factors, such as manufacturing processes, development technology, welding, working conditions, and environment. Some of the factors are possible to monitor, thus gaining insight into how they can affect crack initiation and prevent it from occurring. However, some of them are not possible to predict since they represent a combination of several factors. Presented in this paper is the influence of exploitation conditions and welding on crack initiation and propagation on a specific example involving a starting vessel in thermal power plant. Crack was detected in the welded joint after a certain time in exploitation with relatively variable working conditions. Effects that could have led to crack initiation and propagation, as well as the potential solutions for avoiding them, were analysed. In addition, a short theoretical review of the demands which must be fulfilled by pressure vessels is given, with special focus on the effects of welding and the consequences of potential defects.

Keywords: pressure vessel, cracks, exploitation condition, welding

1. Introduction

Welding is one of the most important technological processes in modern industry, especially in mechanical engineering, civil engineering, shipbuilding and process industry. Welding is most commonly applied in manufacturing of load bearing metal structures by connecting parts, sheets and profiles, for manufacturing of processing equipment, pressure vessels and pipelines, and for repairing of broken, worn out metal parts. Welded structures occupy a very important position in modern day industrial manufacturing. Pressure vessels made by welding are among the most important equipment in many industry branches such as, process, chemical, oil industry, as part of refineries, nuclear and thermal power plants, etc.

Despite strict regulations regarding welded joint quality which were determined based on theoretical knowledge and practical experience, there are numerous examples of exploitation cracks occurrence and welded structure failure [1-3]. Pressure vessels should comply with regulations in terms of parent material used for their manufacturing, welded joint quality, manufacturing technology and exploitation safety. For this purpose, they are subjected to control during manufacturing and delivery, along with regular inspections during exploitation. Inspection of welded joints involves the application of non-destructive test methods such as ultrasound, magnets, x-rays, penetrant methods, acoustic emission, etc [4-6]. Experience up until now has indicated that the behaviour of a welded joint with a crack is unpredictable because of the influence of numerous factors such as residual stresses from welding, deviations in geometry, emphasised micro-structural heterogeneity of certain welded joint areas, and in relation to the previously mentioned factors, position of the crack tip, crack size and crack tip sharpness. Cracks in pressure vessels occur due to various damage mechanisms, typically including:

- creep
- fatigue
- corrosion fatigue

Failure of pressure vessels represents a significant practical problem even today, and cracks in welded joint in pressure vessels greatly jeopardize their exploitation safety [7, 8, 9]. With adequate control and inspection, cracks can be repaired, and prevent further crack growth which could lead to the final failure of machine or part. However, on the other hand, crack initiation during exploitation in welded joint cannot be excluded as a possibility, even if they were evaluated as acceptable in terms of quality

* Corresponding author

E-mail address: b.djordjevic88@gmail.com

when received [10]. More often than not, pressure vessels manufactured by welding are put in exploitation with cracks within acceptable limits.

In the following text, the effect of exploitation conditions on crack initiation in pressure vessels will be presented, on a specific example of a vessel used in a thermal power plant [11]. This example involves a starting vessel (vapour separator), made of steel 15 NiCuMoNb5, which has been in exploitation for 220 000 h. During exploitation, the vessel was subjected to variable internal pressure (from 150 to 220 bar) and temperature (from 350 to 400°C). After 220 000 hours, the starting bottle was inspected. Variable exploitation conditions enhance the possibility of crack initiation and/or growth, depending on whether the crack occurred during manufacturing or welding. The effect of previous welding technology was also analysed, along with oversights in control, as another possible cause of crack initiation.

2. The starting vessel and steel 15 NiCuMoNb5 (WB 36)

Basic elements of a boiler in thermal power plants are the ones where processes related to transformation and transfer of heat from the transmitter to the receiver take place, and they include the combustion chamber, water heaters, evaporators, vapour preheaters and air heaters. These elements are accompanied by auxiliary equipment, such as vapour coolers, separators, etc. Moist vapour exits the evaporator and is taken into the vertical vapour separator (starting vessel), wherein the remaining moisture is removed (Figure 1). Such a separator functions according to the Sulzer circulating boiler principle [11, 12].

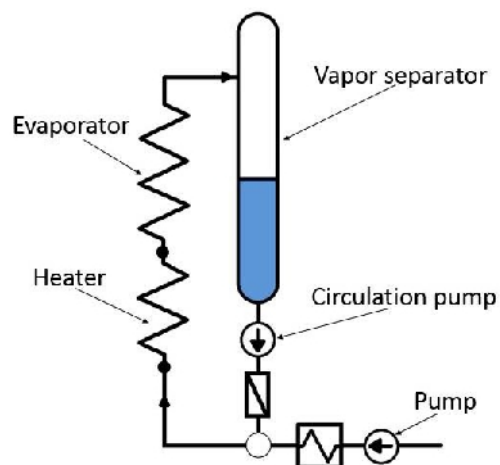


Fig. 1. Vapour separator (starting vessel) and other circulating boiler parts

Examined starting vessel was made of steel 15 NiCuMoNb5 (WB 36). This steel belongs to the category of low-alloyed high strength steels, i.e. micro-alloyed steels, and due to its high strength at elevated temperatures, it is used for manufacturing of pipelines and pressure vessels. These micro-alloyed steels are also widely used for manufacturing of parts in ships, vehicles, airplanes, guided missiles, weapons, railway, bridges, machine tools, mechanical components with a bigger cross-sectional size, etc. WB36 is a Ni-Mosteel whose main alloying elements are copper and niobium, which determine its properties. It is typically used in structures subjected to temperature up to 450°C and its basic micro-structure is ferrite-bainite. It is most often delivered in an enhanced state. Typically, it is manufactured by controlled rolling and normalisation, which results in a fine-grain material structure. Designation 15 NiCuMoNb 5 is in accordance with the DIN standard, whereas according to ASTM standard, the steel is denoted by WB36 [13]. Shown in tables 1 and 2 are the chemical composition and mechanical properties of steel 15 NiCuMoNb 5.

Table 1. Chemical composition of steel 15 NiCuMoNb 5

Element	C	Si	Mn	Cr	Mo	Ni	Nb	Cu	S	P
Percentage [%]	≤0.17	0.25-0.5	0.8-1.2	≤0.3	0.25-0.5	1-1.3	0.2	0.5-0.8	≤0.25	≤0.03

Table 2. Mechanical properties of steel 15 NiCuMoNb 5

Mechanical properties	Yield stress R_e (MPa)		Tensile strength R_m (MPa) - 22°C	Elongation (%)
	22 °C	350°C		
Values	≥430	≥353	610-760	≥16

Of all the alloying elements mentioned above, which are present in steel WB 36, copper is the most disruptive in terms of micro-structure [14].

Starting vessel was manufactured by welding, i.e. connecting branches were welded to the base. The appearance of a connecting branch and starting vessel is shown in Figure 2. In general, steel us for the starting vessel has good weldability and can be typically welded using any conventional welding technology. Welding was performed on connecting branches and the starting vessel, by making fillet welds between several connecting branches and the vessel itself. External diameter of the starting vessel was Ø585mm, whereas its thickness was 40 mm. Outer diameter of the connecting branch was Ø250mm, and its thickness was also 40 mm. Welding was performed using the manual arc procedure, i.e. MAW, whereas the root pass was made using TIG procedure. Before welding itself was performed, the surfaces to be welded were cleaned, and adequate thermal treatment was performed before and after the welding, as well. An electrode whose chemical composition is given in table 3 was used as the additional material.



Fig. 2. The welded joint between the connecting branch and strating vessel

Table 3. Chemical composition of the used electrode (values of matching filler material used nowadays [15])

Element	C	Si	Mn	Cr	Mo	Ni	Nb	Cu	V	S	P
---------	---	----	----	----	----	----	----	----	---	---	---

Percentage [%]	0,06	0,3	1,2	0,1	0,4	1	0,2	0,05	0,01	<0,01	<0,01
----------------	------	-----	-----	-----	-----	---	-----	------	------	-------	-------

3. Starting vessel inspection upon exploitation

Starting vessel was under exploitation for 220 000 h. During exploitation, it was subjected to variable internal pressure (from 150 to 220 bar) and temperature (from 350 to 400°C) [10]. Shown in Figure 3 is the distribution of exploitation time at certain pressure levels for the period of 220 000 hours. As can be seen, the starting vessel spent most of its exploitation subjected to pressure above 200 bar.

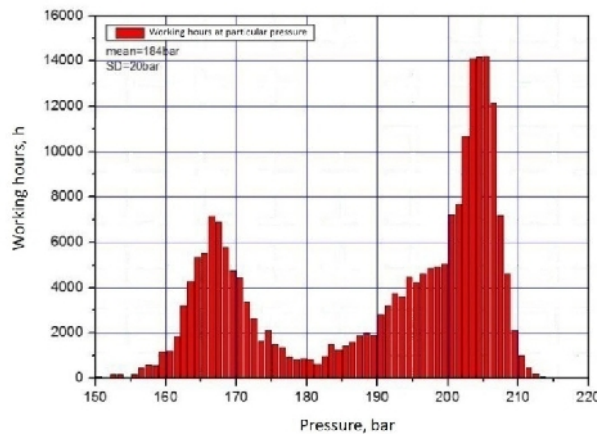


Fig. 3. Distribution of exploitation time for specific pressure levels of a starting vessel, for an exploitation period of 220 00 h

Shown in Figure 4 is the distribution of exploitation time for specific temperatures for the exploitation period of 220 000 hours. As can be seen, the starting vessels spent most of its exploitation subjected to temperatures of approximately 380 °C.

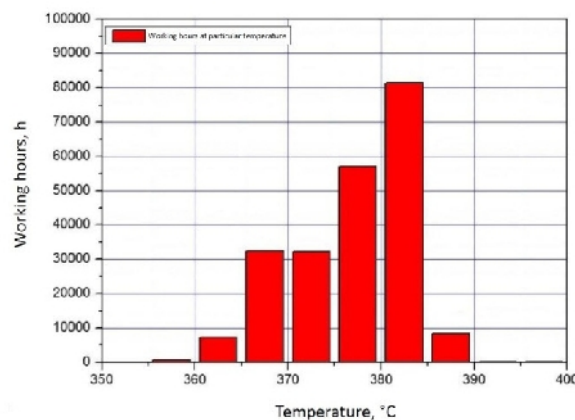


Fig. 4. Distribution of exploitation time for specific temperatures of a starting vessel, for an exploitation period of 220 00 h

After 220 000 hours of exploitation, starting vessel was inspected for the purpose of determining if there are cracks which need to be repaired. All locations where connectors were welded to the start vessel, i.e. welded joints were examined. The most typically encountered problem in the case of pressure vessels is crack initiation in the heat affected zone (HAZ), which can occur during its manufacturing or repair [1, 16]. In the case of pressure vessels, welded joints are the most likely locations for crack initiation, as well as structural changes. Inspection was performed using magnetic particles in accordance with standard SRPS EN ISO 17638:2012 on the outer side of the vessel. Examined surface did not undergo any special preparations. In the revision opening zone, a crack within the weld metal-heat affected zone area was detected in one of the connectors. Crack depth in the fillet weld zone in revision opening mantle joint was 35 mm, whereas its length was 250 mm. The cause of crack initiation was the change in WB 36 steel micro-structure due to exploitation conditions and welding.

Upon detecting the crack, repair welding of the starting vessel with accompanying procedures was performed so that it could be removed. Additional numerical tests were also performed, but will not be included in this paper.

4. Conclusions

One of the basic conditions that a structure must fulfil is the adequate material choice, which is of particular importance for pressure vessels. Factors which affect vessel integrity include the choice of parent material, additional materials, welding technology, the aggressiveness of the working fluid in the vessel and exploitation conditions (temperature, pressure, mechanical load, etc). In addition, failure is always preceded by crack initiation and propagation. Structures and welded joints can contain defects and micro-cracks from which cracks can initiate, as was the case in the aforementioned example. Exploitation conditions also further influence crack propagation.

A crack has occurred after a long exploitation period for a given temperature. Detailed analysis revealed that the crack most likely did not occur due to exploitation and excessive thermos-mechanical load, i.e. exploitation conditions, but was probably initiated due to residual stresses at the welded joint between the revision opening connector and the mantle, or due to a defect that was overseen during previous welding technology control. Thus, it can be concluded that residual stresses caused by the welding process and potential geometrical deviations affect crack initiation in starting vessels. Hence, a more thorough control of welded joints is recommended, before, during and after the welding process, especially in extreme exploitation conditions (high working pressures, high temperature, aggressive working fluid). The procedure for regular pressure vessel inspection after a certain exploitation period was also established. After non-tolerable cracks were detected, their repairing and removal took place, as was done in the example described above, in order to avoid catastrophic failure. In addition, it can be concluded that residual stresses after welding can also influence crack initiation.

References

- [1] [AlmarAlmarNaess, Per J. Haagenen, BjørnLian, Torgeir Moan, Tor Simonsen](#): Investigation of the Alexander L. Kielland Failure, Metallurgical and Fracture Analysis, Offshore Technology Conference, 3-6 May, Houston, Texas.
- [2] [Ali Farzadi](#), Gas Pipeline Failure Caused by In-service Welding, Journal of Pressure Vessel Technology 138(1), August 2015.
- [3] [MiodragArsić, Srđan M Bošnjak, NenadZrnic, A. Sedmak, NebojšaGnjatović](#), Bucket wheel failure caused by residual stresses in welded joints, Engineering Failure Analysis 18(2): 700-712, March 2011.
- [4] RadomirJovičić, Radica Prokić-Cvetković, OliveraPopović: Non-Destructive Testing Of Ferritic-Austenitic Welded Joints, Structural Integrity And Life Vol. 5, No 3 (2005), pp. 119-128
- [5] [F. M. Burdekin](#): Technical Note. Non-Destructive Testing Of Welded Structural Steelwork, Structures & Buildings 99(1):89-95, 1993
- [6] Igor Martić, AleksandarSedmak, RadoljubTomić, Izet Hot: Remaining Life Determination For Pressure Vessel In A Refinery, Structural Integrity And Life, Vol. 16, No. 1, 2016
- [7] R. Jovicic: Evaluation of exploitation safety of pressure vessels with a crack in the welded joint, Experimental and numerical methods for structure integrity evaluation, Belgrade 2000
- [8] A.Sedmak, S.Sedmak, Lj. Milovic. : Pressure equipment integrity assessment by elastic-plastic fracture mechanics methods, Monograph, Belgrade 2011
- [9] S. Sedmak: Exploitation cracks in welded joints in pressure vessels, Sixth summer school of Fracture Mechanics, 1991
- [10] SijackiZeravcic V, Bakic G, Djukic M et al (2010) Contemporary maintenance management of power plant life exhaustion components. Tech. Technol. Educ. Ma. 5:431-436
- [11] G.Bakic, V.Sijacki, et al.: Remaining life assessment of different pressure vessels and pipelines in Unit 1 TENT B, Report 12-03a-12.04/2015, Fac. of Mech. Engineering, University of Belgrade, 2015.
- [12] LjubišaBrkić, TitoslavŽivanović: Boilers, Faculty of Mechanical Engineering, Belgrade 2002
- [13] <http://www.basedosteel.com>

TopicA

HEAT TREATMENTS EFFECT ON THE FRACTURE TOUGHNESS OF AISI M2 TOOL STEEL

M. Benaissa¹, F. Benkhenafou¹, S. Belhenini², H. Lebbal³, A. Ziadi^{2,*}, F.J.Belzunce⁴
*1*Department of mechanical engineering, Abou Bakr Belkaid University, 13000, Tlemcen, Algeria.

*2*Smart Structures Laboratory/DGRSDT, Univ Ctr of Ain Temouchent, 46000, Ain Temouchent, Algeria.

*3*Department of mechanical engineering, University of Science and Technology, 31000, Oran, Algeria.

*4*University of Oviedo, Department of materials science, 33203, Gijon, Spain

Abstract: Fracture toughness tests of high and low chromium high speed steel type alloys containing high carbon was carried out by using the rupture weight on a 3 points bending specimens. AISI M2 tool steel roll manufactured with vertical centrifugal casting process. The shell is high harness high speed steels, and the core is nodular cast iron. M-2 roll materials contain high content alloy element, such as Mo,V,Cr, formed eutectic carbides, matrix is tempered martensite + second carbides. The rolls in the finishing stands must have good resistance to both wear and fire cracks. The use of M-2 roll at the finishing stands has shown satisfactory results. In addition, the resistance to roll surface roughing is also excellent. The addition of chromium to a certain level yielded microstructural modification, including the homogeneous distribution of primary carbides, thereby leading to enhancement of fracture toughness of the M-2 rolls. The influence of tempering temperatures on the mechanical properties of these products, determined using tensile and fracture toughness tests, was studied in this research work.

Keywords: fracture toughness, hollomon parameter, centrifugal casting, heat treatment.

1. Introduction

AISI M2 tool steel (M-2) rolls, characterized by enhanced thermal fatigue properties and excellent resistance to wear and abrasion, are replacing conventional high-chromium (Hi-Cr) rolls.[1] The high Chromium M-2 roll is characterized by a Chromium content in the range of 14 to 19 % . This grade has a martensitic matrix and contains about 25 to 30 % Chromium carbides (M₇C₃) which lead to its good wear resistance. The M-2 are important tool material due to the fact that they offer a wide spectrum of tailoring properties [2]. These materials have been developed to improve the quality and productivity of rolled goods in accordance with industrial demands. The fracture toughness of these products is generally used for evaluating structural stability of materials, and is considered to be one of the most important material properties. can be improved by promoting a large amount of hard carbides and plate-type tempered martensite in the matrix, fracture toughness can be deteriorated because of their brittleness.

2. Fracture toughness test

Tensile and fracture toughness tests were carried out on several products. Tensile tests were performed according to ASTM E8M-92 standard on cylindrical specimens with a diameter of 6 mm and a calibrated length of 60 mm, under a strain rate of 1 mm/min.

* Corresponding author

E-mail address: aezkiadi@cuniv-aintemouchent.dz, aezkiadi@yahoo.com

The tests for the determination of the fracture toughness were carried out according to ESIS P2-92 and ASTM E399-90 standards on SENB specimens with a cross section of 15x15 mm. Due to the high notch sensitivity of hard and brittle metallic materials, such as the AISI M2 tool steel, it is very difficult and sometimes almost impossible, to create a fatigue crack in the corresponding test specimens. However, a fatigue crack can be created on such test specimens if this is done before final heat treatment is performed.

All the specimens were precracked by fatigue, in accordance with the standards. Stress intensity factor K_I due to external load P was determined using the following equation:

$$K_I = K_Q = \frac{P_Q \cdot S}{B \cdot \sqrt{W^3}} \cdot f(a/w) \quad (1)$$

Thermal fatigue property of the roll materials is determined by the collective effect of their microstructures, mechanical and physical properties, therefore, the thermal fatigue test result is interpreted by focusing on these factors.

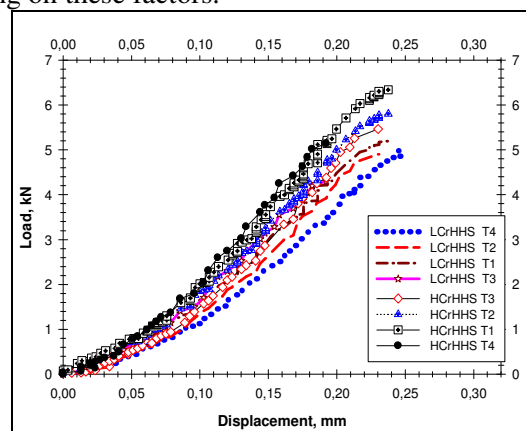


Fig. 1. Load – Displacement curves to determine fracture toughness

3. Conclusions

After an appropriate heat treatment, these M-2 are very hard products whose tensile strength decreases along with their hardness on increasing the tempering time and temperature.

The fracture toughness of these M-2steels is relatively high, especially when we compare it with that of conventional materials with similar microstructures. Moreover, this property is hardly modified in the course of normal heat treatments.

Failure of these products in tensile and fracture toughness tests is intergranular, since it preferentially takes place through the carbide network, due to their brittleness, and also as a result of the interphase decohesion between carbides and the dendritic tempered martensitic phase, which occurs under the strong local stresses, that developed ahead of the crack front.

References

- [1] Mingguì QU, Zhenhua WANG, Hui LI, Zhiqing LV, Shuhua SUN, Wantang FU, Effects of mischmetal addition on phase transformation and as-cast microstructure characteristics of M2 high-speed steel, *Journal of Rare Earths*, Volume 31, Issue 6, June 2013, Pages 628-633.
- [2] Yi Meng, Sumio Sugiyama, Jun Yanagimoto, Microstructural evolution during partial melting and semisolid forming behaviors of two hot-rolled Cr–V–Mo tool steels, *Journal of Materials Processing Technology*, Volume 225, November 2015, Pages 203-212.

ELASTO-PLASTIC MODELING INCORPORATING STATIC STRAIN AGING (SSA) EFFECT ON THE BEHAVIOR OF X5CRNI18-10 STAINLESS STEEL AND C-MN STEEL COUPLED WITH THE DAMAGE

N. Djaoui, A. Hannou, M. Zerouki, M. Ould Ouali

Université Mouloud MAMMERY de Tizi-Ouzou, Laboratoire Elaboration, Caractérisation des Matériaux et Modélisation, BP 17 RP, 15000. Algeria.

Abstract: The Cr -Mn steels are subject to the phenomenon of aging under strain, which is at the origin of the location of the plasticity under the form of Portevin-Lüders band's (Static Strain Ageing) or instability of Portevin and Chatelier (Dynamic Strain Ageing). This study propose take into account the effect of Static Strain Ageing (SSA) in the behavior law. To characterize the comporment of our materials, we realized tensile tests on specimens clipped in the three directions compared to the rolling direction in the raw state of X5CrNi18-10 stainless steel and for the C-Mn steel we used the experimental database of J. Belotteau extended by simple tensile testing by Huaidong Wang. These tests allowed to identify the principal mechanical properties of these materials. On the basis of previous results, we formulated a model of elastoplastic behavior including the effect of aging coupled with damage to this material. This model has been implemented in Abaqus finite element code using subroutine VUMAT (Vectorized User MATerial). A comparison of numerical predictions with experimental results showed the relevance of our approach.

Keywords: Modeling, Damage, Ageing, VUMAT, Abaqus.

1. Introduction

The physical origin of aging has been much studied in relation to the phenomena Portevin Le Chatelier (PLC) and Lüders effects. But its influence on the mechanical properties and in particular the breakdown of steel remains controversial. The mastery of predicting the behavior and failure of mechanical structures has become paramount. For this reason, numerical modeling is a powerful tool that figures prominently in the industry. In this work, we focus on numerical modeling of the behavior of a stainless steel X5CrNi18-10 in raw state and C-Mn steel in the aged condition coupled to the damage [1]. Once the numerical aspect is addressed, the model will be implemented in the Abaqus finite element code using the subroutine VUMAT (Vectorized User Material). Simulations on smooth specimens in simple tension are presented. These calculations are made on smooth cylindrical specimens in 3D. A comparison between the experimental results and those predicted numerically shows the relevance of our approach.

2. Experimental

The materials studied are unstable austenitic steel AISI 304 Family and C-Mn steel. Tensile tests were performed on standard specimens at raw and aged conditions. The specimens used were standardized according to NF A03-151 standard for stainless steel and according to NF A49-215 standard for C-Mn steel [2].

3. Results and discussions

The values adopted after calibrations are shown in Table 1 and 2 for each model.

Table 1. Parameters of elastoplastic model coupled with the damage.

Q_1 (MPa)	b	D_1	D_2	D_3	D_4	D_c	α	Q_2 (MPa)	(s^{-1})
430	2,789	0,159	0,95855	0,55998	0,2	0,529	2,15	100	0,001

Table 2. Parameters of elastoplastic aging model coupled to the damage.

Q_1 (MPa)	b	D_1	D_2	D_3	D_4	D_c	a
260	14.5	-0,09	0,48	0,6	0,014	0,97	1,185
Q_2 (MPa)	(s^{-1})	Ta_0 (s)	P_1 (MPa)	n	P_2 (s^{-n})	β	w
0	$1e^{-04}$	10000	120	0	0,00105	0,72	0,001

We performed a numerical simulation of the tensile test on stainless steel flat 304 in the raw state and C-Mn in the aged state using Abaqus finite element code.

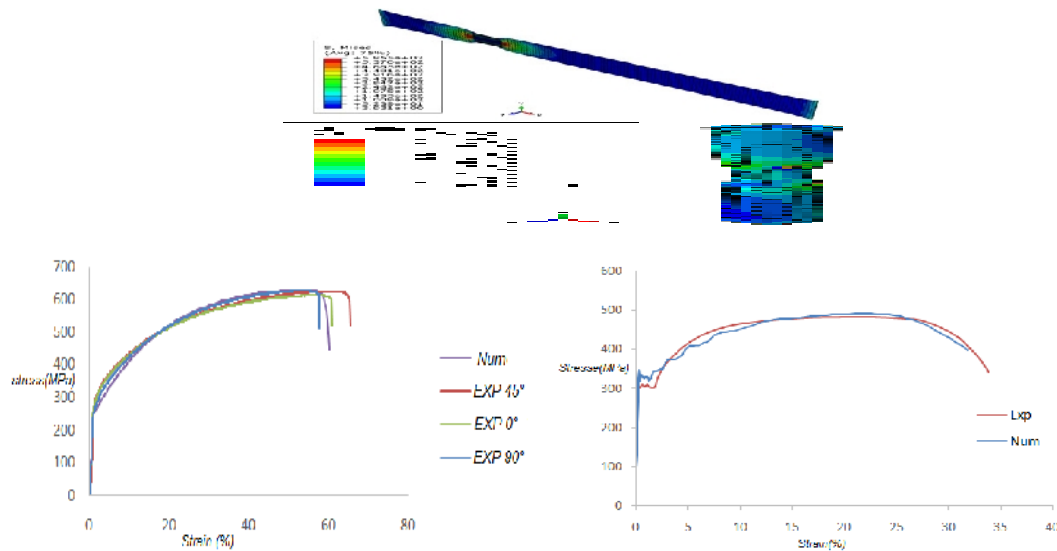


Fig.2. stress-strain curve obtained numerically and experimentally at raw and aged state.

6. Conclusion

The elastoplastic model coupled with the damage has been successfully used to predict the breaking of thin sheets during their formatting. This model has been extended to include the effect of aging using phenomenological laws and given satisfaction on all levels, for structures in 3D.

References

- [1] Belotteau. J. (2009) Comportement et rupture d'un acier au C-Mn en présence de vieillissement sous déformation. Laboratoire de Mécanique des Sols, Structures et Matériaux UMR CNRS 8579, Ecole Centrale, Paris.
- [2] Huaidong Wang (2012) Comportement mécanique et rupture des aciers au C-Mn en présence de vieillissement dynamique. Ecole Centrale Paris, French.
- [3] McCormick, P et al (1995) 'Numerical modeling of the Portevin-Le Chatelier effect'. Acta Metallurgica et Materialia, vol.43, pp.1969-1977.

Wear Behavior of Alumina Coating Obtained By Plasma on an Aluminum Substrate

N. Khennafi-Benghalem⁽¹⁾ *, S. Aounallah⁽¹⁾, M. Hamidouche⁽¹⁾, A. Zahri⁽¹⁾, K. Loucif⁽²⁾

⁽¹⁾Unité de recherche des matériaux émergents

⁽²⁾Laboratoire des Matériaux Non Métalliques

Institut d'optique et de mécanique de précision

Université Ferhat Abbas de Sétif1

Abstract: Knowledge of tribology has now become a necessity for many reasons, such as ensuring the proper functioning and reliability of the machines, reducing the cost of obtaining the friction surfaces and improving the performance and longevity machines. The friction phenomena, wear, and all those associated with them, were all time taken advantage and studied for various purposes. Wear is a progressive and irreversible phenomenon, each state of a system permanently destroyed the previous state, so it is very difficult, if not impossible, to reconstruct the past from the observation of degradation. The deposition of thin films is a technique used to minimize wear, among the most materials used in industrial we find aluminum because of its lightness, but this material does not support friction (wear is higher), especially for high speeds and high loads, because of this problem was thought to coat the aluminum by thin films on friction surfaces. The objective of the present work is to study the wear behavior layers deposited on an aluminum substrate; the substrate is first coated with a layer of stainless steel and the second by an alumina layer. The coating is performed at the Science Laboratory ceramic processes and surface treatment at the University of Limoges France. The wear tests were made in the laboratory of non-metallic materials of the optical department and precision mechanics. The device wear used is as a pin-disk type to study the effect of friction and wear, microhardness tests on worn tracks and some observations were made.

Keywords: wear, aluminum, alumina coating, plasma process, friction

1. Introduction

The surface treatment is a sector of the engineering industry where the environment must not be only considered as a constraint but as a source of innovation and development [1]. The surface modification techniques have become a fairly wide field of research [2-4]. The thermal spraying process is widely distributed for industrial applications in order to improve surface protection against the effects of corrosion and wear [5]. Among the many engineering techniques surface by spraying the plasma coating process that has had the greatest success. Currently it is widely used in engineering the surface of many materials [6]. The plasma process is used for certain applications where the areas are subject to high stress and wherein the mechanical strength of the substrate is low. Thick coatings (a few hundred microns) are required [7] and they adapt well to the substrates. Coated pieces are frequently used in tribological systems where the surfaces of two pieces are in contact and relative moving to each other as in the case of the automotive industry.

2. Results

The study parameter is the velocity v (32, 50, 88 mm / s) respectively corresponding to the radi R of tracks (5, 8, 14 mm) normal force applied is constant of the order of 30N for testing. The sample weight is performed before and after the wear test. Tables (1) summarize the main results and calculated readings.

* Corresponding author

E-mail address: n_khanafi@yahoo.fr

2.1 Effect of sliding velocity on the mass loss of alumina

We calculated the mass loss of each track according to formula $\Delta m = m_i - m_f$ at the end of each test. Fig. 1 is inserted to illustrate an image of the sample used for coating. Fig. 2 shows the variation of the loss mass of the alumina layer as a function of the sliding velocity. Generally the change in mass loss is minimal at low sliding velocity and high for large slip which may reflect an increase in weight loss as a function of the sliding velocity. Figure (2, 3) show the variation of loss mass and the track width for various velocity these two curves assuring that the two study parameters vary linearly with sliding velocity. This behavior is in good agreement with Archard's law of wear this is confirmed by calculating the wear coefficient k, which keeps its substantially constant value between 2, 5-3, 23 $10^{-6} \text{ mm}^3/\text{N.m}$. This value shows that the wear is mild.

Table 1: obtained results of the alumina layer

R (mm)/v (mm/s)	5/32	8/50	14/88
$\square m_e \square$ (mg)	6.7	8.7	14.3
$\square m_b \square$ (mg)	0.4	0.5	0.5
l (mm)	1.720	1.456	1.932
$V10^{-3}$ (mm^3)	1.71	3.23	3.66
K : 10^{-6} ($\text{mm}^3 \cdot \text{N}^{-1} \cdot \text{m}^{-1}$)	3.23	2,68	2,50



Fig.1.Tracks on alumina coated

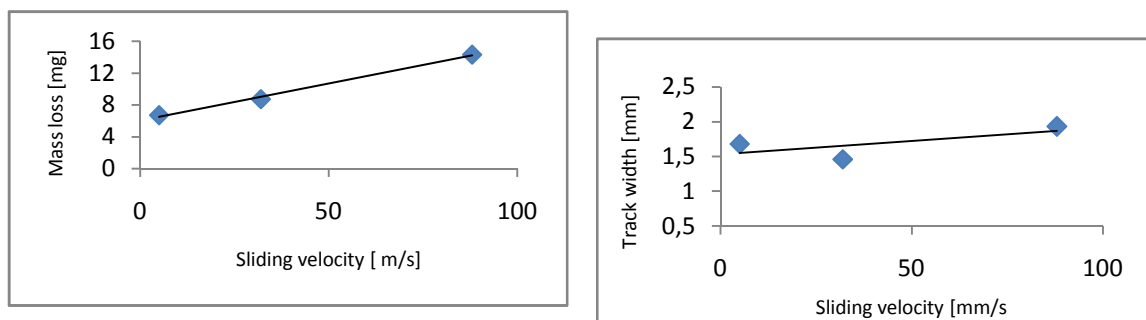


Fig. 2: Variation of loss mass and track width for various sliding velocity

3. Conclusion

In this work, the results revealed the following conclusions:

The substrate used is a ductile material, the Vickers hardness is about 187 HV and wear resistance is very low. The average wear rate coefficient $k = 1.25 \cdot 10^{-5} \text{ g} \cdot \text{N}^{-1} \cdot \text{m}^{-1}$. The layers deposited by plasma present inhomogeneities intense structures following the initial composition of the deposited powders or experimental deposition conditions. The improvement by plasma deposition primarily concerns the increase in hardness. It was reported that the hardness of the composite layer is de 356HV. The wear resistance of the alumina layer is of the order $k = 2, 5 \cdot 10^{-5} \text{ g m}^{-1} \text{N}^{-1}$.

References

- [1] Serres .N, Lawka. F.H, Cornet, Ostil. A, Langlade.C., Machi.F, Performances tribologiques de revêtements éco-conçus,"19ème Congrès Français de Mécanique Marseille, 24-28 août 2009

INFLUENCE OF RECYCLED SAND ON MECHANICAL PROPERTIES AND THE DURABILITY OF CEMENT MORTARS

L. Berredjem^{1,2}, N. Arabi¹ and L. Molez²

¹ Badji Mokhtar University, LMGE, BP N° 12, 2300, Annaba, Algeria.

² INSA de Rennes, LGCGM – EA 3913, 20 Avenue des Buttes de Coësmes, 35708, Rennes, Cedex7, France.

Abstract: Today, the recycling of construction and deconstruction as a source of aggregates is considered very important in the overall effort to protect the environment and to promote the principles of sustainable development. The use of recycled aggregates present new trends in construction as an alternative to natural aggregates. Most studies are oriented towards the use of recycled gravel in concrete, though many consider the use of recycled sand is harmful to the durability of concrete, against by other studies limit its use in the new concrete to a 30% threshold as a percentage of replacement of natural sand. However, when crushing debris constructs a large amount of fine fraction is inevitable and its spring is discharging. This work is performed on experimental contribution to the study of the sustainability of different compositions of cement mortars with and without adjuvants, replacing natural sand (SN) by the recycled sand (SR) with different volume percentages of 0, 15, 30, 50, 75 and 100%. After identification and physicochemical characterization of recycled sand in particular, it was determined the amounts of water and time of pre-wetting optimum required to have the same plasticity mortars. The experimental procedure consists of comparing the durability of the mortars indicators, namely: capillary absorption, the porosity accessible to water, gas permeability and leaching. The results obtained show that the recycled sand has a high water absorption, a high percentage of fillers (over 10%). The physicochemical properties quite low compared to natural sand, due to the heterogeneity and the large percentage of old mortar that contains recycled sand. The comparative study between the different compositions of recycled sand mortars showed acceptable mechanical properties relative to those of control mortar based on natural sand, however, mortars made of recycled sand with a percentage over 50% showed a significant resistance to acid attacks.

Keywords: Environment, recycled sand, porosity, durability.

1. Introduction

Very large quantities of construction and demolition wastes (CDW) are reproduced every year, nevertheless only a small fraction of them is recycled in the manufacture of concrete and mortar. The use of recycled aggregates present new trends in construction as an alternative to natural aggregates [1]. In Algeria, the extraction ban alluvial materials, the difficulties of implementation of new quarrying and saturation of landfills needed to seek new sources of aggregates for concrete to meet the needs of large sites implemented. In recent years, Most studies are oriented towards the use of recycled gravel (RG) in concrete, but few studies exist on the use of recycled sand (RS). However, when crushing old concrete inevitably results in a significant amount of RS, which contains major part of the hardened cement paste characterized by its high porosity. Though many consider the use of RS is harmful to the durability of concrete, against by other studies limit its use in the new concrete to a 30% threshold as a percentage of replacement of natural sand.

2. Mechanicals properties of cement mortars

²Corresponding author

E-mail address: berredjem2423@gmail.com

The mechanical behavior of mortars is evaluated using compression tests, according to the NF EN 196-1. Figure 1 shows the compressive strengths of mortars before and after leaching with sulfuric acid of high concentration (0,5 M/L).

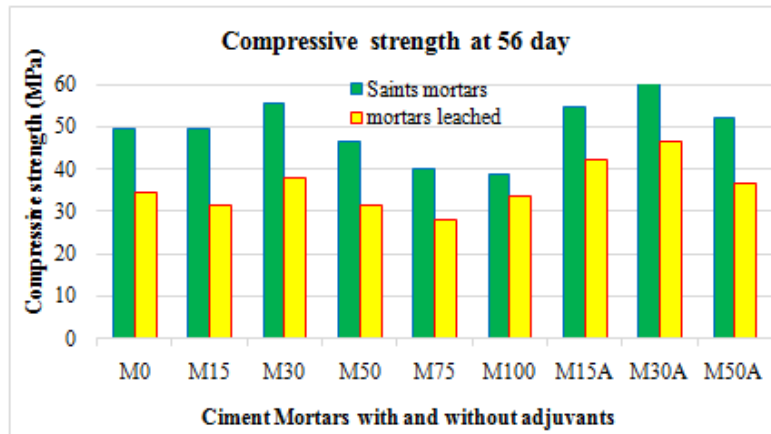


Fig. 1. Compressive strength comparison of different mortars before and after the attack of strong acid.

3. Conclusions

The resultant obtained show that the sand recycle has physicochemical properties quite low compared to natural sand, due to the heterogeneity and the large percentage of old mortar containing recycled sand. The comparative study between the different compositions of mortars made of recycled sand with and without adjuvant, showed acceptable mechanical properties and even better (M30) from the control mortar made of natural sand. However, mortars recycled with more than 50% RS 50% showed significant resistance to acid attack due to the creation of surface protective layer.

References

- [1] Zhao Z., Remond S., Damidot D. and Xu W. (2015), Influence of fine recycled concrete aggregates on the properties of mortars, *Construction and Building Materials*.
- [2] Neno C., de Brito J., and Veiga R. (2014), Using fine recycled concrete aggregate for mortar production, *Materials Research*.
- [3] Braga M., de Brito J., and Veiga R. (2012), Incorporation of fine concrete aggregates in mortars, *construction and building Materials*.

IDENTIFICATION OF THE DAMAGE IN THE BONE CEMENT OF THE TOTAL HIP PROSTHESES

M. E. N. Belgherras^{1*3}, A. Benouis¹, B. Serier¹, L. Hachemi².

¹ Mechanics and Physics of Materials Laboratory, Djillali Liabes University of Sidi Bel-Abbes, BP89 cité Larbi Ben M'hidi, Sidi Bel-Abbes, Algeria

² University of Mascara, Bioconversion laboratory Microbiological, Engineering and Safety (LBMSS), Mascara, Algeria. ³ University, School, Address, City, Country

Abstract: PMMA is the unique material used currently for fixing prosthesis in bone cemented arthroplasty. In this study, the finite element is used to analyze the level and the von Mises stress equivalent distribution induced in the component of the total hip prosthesis. Also the damage distribution induced between two cavities located in the bone cement polymethylmethacrylate (PMMA). The inter-porosity and the type of loading on the mechanical behavior of cement orthopedic were highlighted. We show that the breaking strain of the cement is largely taken when the cement left in its proximal part, containing cavities very close adjacent to each other is subjected to heel strike efforts.

Keywords: bone, cement, stress, damage, quasi-statics, total hip prosthesis.

1. Introduction

In orthopedic surgery and particularly in the total hip arthroplasty, the stem fixation is performed in general using surgical cement which consists essentially of polymer (PMMA). The mechanical strength of the THR largely depends on the type of cement used. The main role of the cement is to ensure good bone-implant adhesion and homogenize the load transfer from the implant [1, 2]

This study was realized in order to understand and explain the interconnecting cavities phenomena via defects observed experimentally Fig. 1 [3]

2. Methods and discussion

The finite element model is used to analyze the behavior of the pores supposed to exist in cement mantle. The model was defined in terms of geometric, loading and material definitions.

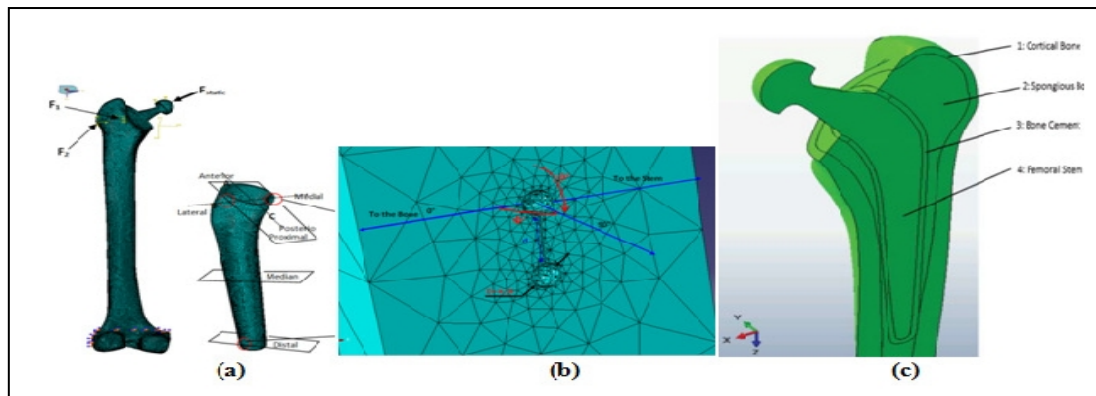


Fig. 1.(a) Model, mesh, boundary conditions and static loads applied to the structure analyzed, (b) Mesh cement around the cavity and (c) the artificial hip components.

The specific dimensions and the mechanical characteristics of the components of the CMK.3 model, a load of 80 kg was applied to the femoral head (3 times the average weight of a human being) [3,4]

3 Corresponding author

E-mail address: nadiringme@hotmail.fr

(Fig. 1a). The effort of the abductor muscle was simulated by a load applied to the anterior proximal part (Fabductor) and the VastusLateralis load applied to the lateral proximal part.

3. Identification of the damage in the cement mental

Figure.2 represents the damaged area in the in the cement in the vicinity of the interconnection distance cavity. We can notice that the presence of the damaged area (red). On the tip of this area we can notice a stress concentration .This figure shows a resemblance with that of a stress concentration around an adjacent micro-cavity. So we can approximate our damaged area to multi-cracks.

Conducting numerical calculations considering the damage process of model components' material structure as well as connections between them requires application of suitable numerical proceedings containing parameters describing the mechanism of damage formation and propagation. The XFEM a methods of damage process modeling. A basic constitutive law used for describing the damage process in ABAQUS/Standard software is Traction–Separation. In both cases elastic material with parameters characterizing material damage was defined as follows: Young's modulus $E = 2400$ MPa, Poisson's ratio $\nu = 0.3$, value of stress initiating damage of material fiber $\sigma_{max} = 25$ MPa.

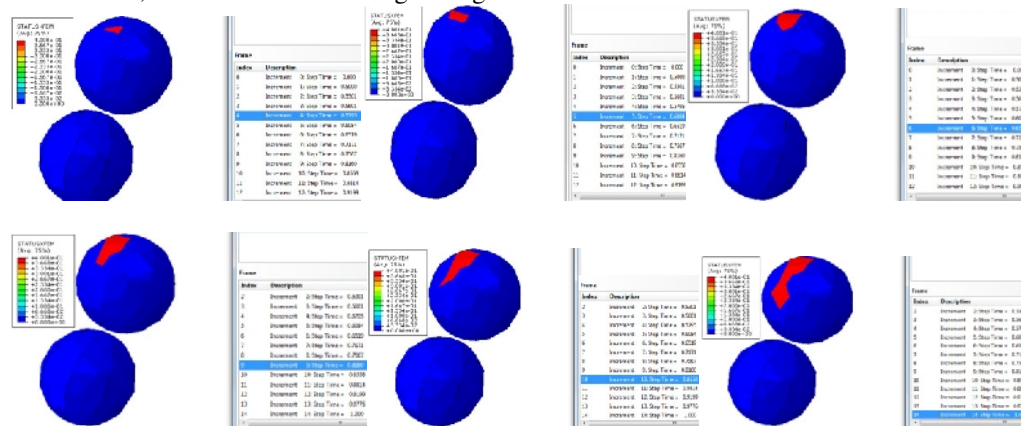


Fig.2. Stage of Simulation damage in the cement between tow cavities.

4. Conclusion

The results obtained in this work show that:

The micro-void situated in the proximal part presents the most important risk of the rupture of the cement mantle; the interaction between the edges affects the femoral stem and the micro-cavity is responsible for this behavior. Existence of micro-void in orthopedic cement rise angular stress and create tensile radial stresses.

The risk of crack initiation in orthopedic cement is in the radial direction.

The most important damage in the cement is located in the proximal lateral zone (compression stress) and with two cavities; it is caused by compression of the cement in the radial direction around the cavity. An implant inclination generates damage with different states and levels;

References

- A.Pustoch, "Elaboration d'un modèle mécanique de l'articulation de la hanche sous sollicitation dynamique", Thèse Université Claude Bernard - Lyon 1, 2007.
- S.Benbarek, B BachirBouiadjra, A. Mankour, T. Achour, B. Serier(2009),"Analysis of fracture behavior of the cement mantle of reconstructed acetabulum Original", Comp.Mater. Sci. 44 (4) 1291-1295.
- H.F. El-Sheikh, J.B. MacDonald, and M.S.J. Hashmi, //Material Selection in the Design of the Femoral Component of Cemented Total Hip Replacement. J. Mater. Process Technology 2002, vol. 122, pp. 309–317.
- G. Bergmann, F. Graichen, and A. Rohlmann, //Hip Joint Loading During Walking and Running, Measured in Two Patients. J.Biomech. 1993, vol. 26, pp. 969–990.

ANALYSIS OF LOCATION OF DEFECTS NEAR GEOMETRIC DISCONTINUITIES ON THE MECHANICAL BEHAVIOUR OF BONE CEMENT

L. Zouambi^{1,2*4}, S. Gouasmi¹, F. Bouafia^{1,3}, B. Serier¹

¹ILMPM, Mechanical Engineering Department, University of SidiBel Abbes, 22000, SidiBel Abbes, Algeria,

²University Center of Relizane, 48000, Relizane, Algeria

³University of Temouchent, 46000, Temouchent, Algeria.

Abstract: The objective of this study was to analyze, by the finite element method by the commercial code Abaqus 6.11 software, the stress level in the PMMA binder the prosthesis to the acetabulum and the inter-microvoids interaction effects on the mechanical behaviour bone cement. The interface and the free edges are stress concentration seats. At these sites, we assumed the location of microvoids. The interaction of the stress fields of these defects with the free edge and the cement-bone interface generates a significant concentration of shear stress priming generally to the free edges of the structure.

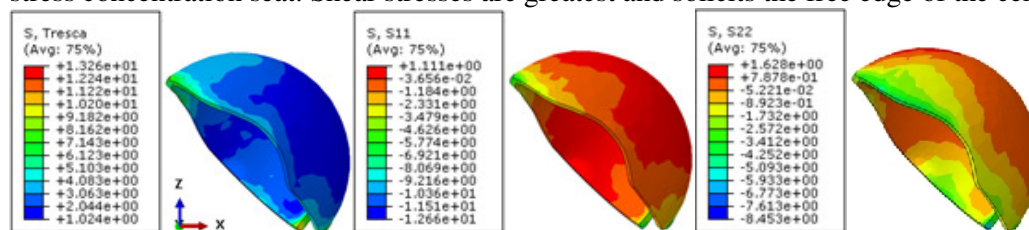
Keywords: shear stress, cement bone, free edge, microvoid, finite element analysis.

1. Introduction

In total hip arthroplasty, the rupture and premature loosening of the cement are directly related to the strength of the cement, which acts as an interface between the bone and the prosthetic component. The choice made by the surgeon agrees with the patient's age and the quality of the bone support [1]. The cement allows the distribution of antibiotics by porosities witch acting as transport path of these medications. But, from the mechanical point of view, it can be prejudicial if the porosity is present locally in the shear stress concentration region priming generally to the free edges of the structure may thus lead at the rupture of the cement due to notch effect [2].

2. Distribution of the stress in the bone cement

A three-dimensional numerical analysis of the distribution and the level of shear stress and that equivalent Tresca induced in the bone cement binder the cup to the bone under the patient's weight the effect was conducted (Fig. 2). The stresses are not homogeneously distributed in the cement. Thus there are areas of this material which are strongly mechanically stressed and located close to the free edge at the interface with the bone are the stress concentration seat. Shear stresses are greatest and solicits the free edge of the cement.



* Corresponding author

E-mail address: zouambileila@yahoo.com

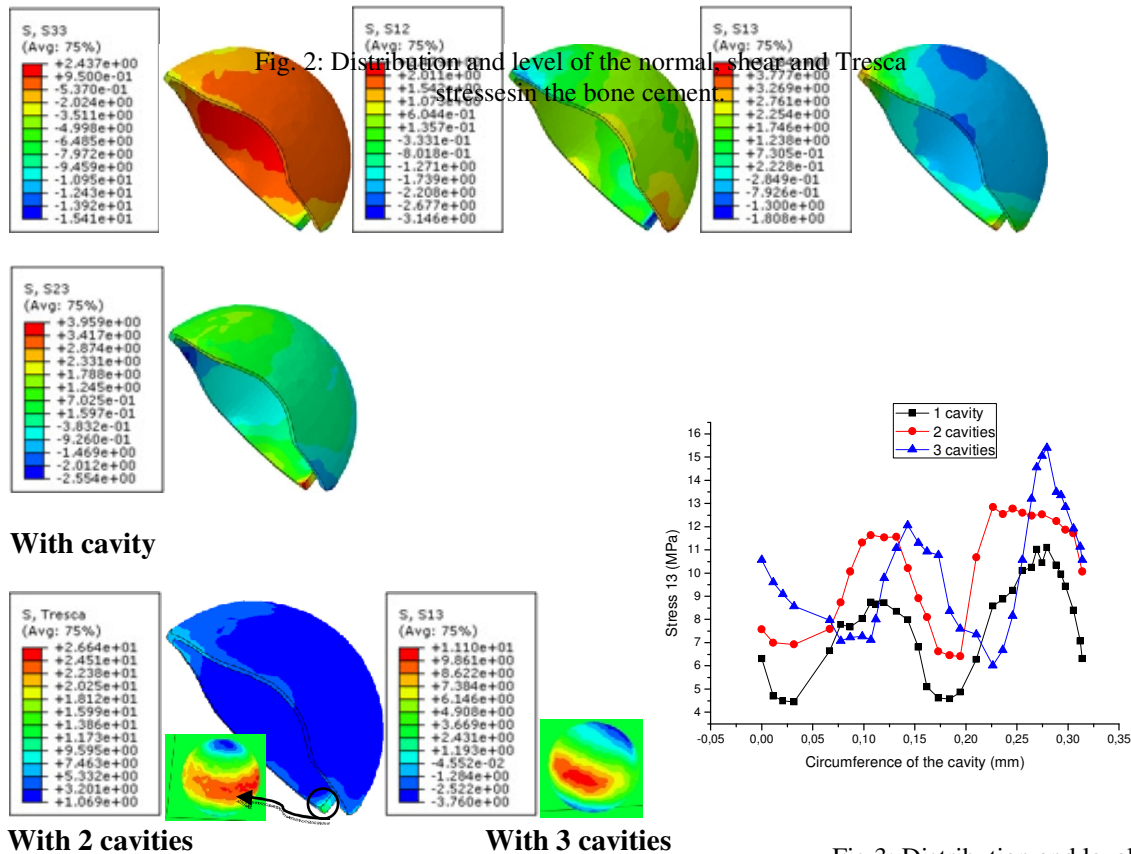


Fig 3: Distribution and level of shear and Tresca stresses around the microvoid located near the free edge of the cement.

These stresses have two maxima thus the level increases strongly when the cavity is close to the free edge and the cement-bone interface. The location of adjacent cavities generates the very high stress intensities in the cement can lead to a risk of damage.

3. Conclusions

The free edge and the cement-bone interface are stress concentration seats in the bone cement; the presence of microvoids in this region strongly concentrated shear stresses that can lead to the risk of loosening of the prosthesis.

References

- [1] D. Foucat, (2003), Effets de la présence d'un grillage métallique au sein du ciment de scellement des cupules des prothèses totales de hanches: Etude mécanique et thermique. Thèse de doctorat, Université de Strasbourg.
- [2] BachirBouiadjra B, Belarbi A, Benbarek S, Achour T, Serier B. (2007), FE analysis of the behaviour of microcracks in the cement mantle of reconstructed acetabulum in the total hip prosthesis; Elsevier; Comput Mater Sci;40:485–91.

THE MONTE CARLO METHOD FOR STRUCTURAL FAILURE PREDICTION OF CIVIL ENGINEERING INFRASTRUCTURES

N. Kazi Tani^{1,2,5}, T. Tamine², D. Nedjar³, M. Hamane³

1 Superior School of Applied Sciences of Tlemcen (ESSA-T), BP 165 RP Bel Horizon, 13000 Tlemcen, Algeria

2 Laboratory LCGE, Faculty of Mechanical Engineering, University of Sciences and Technology of Oran M-B, 1505 El M'NAOUER 31000 Oran, Algeria

3 Laboratory LM2SC, Faculty of Architecture and Civil Engineering, University of Sciences and Technology of Oran M-B, 1505 El M'NAOUER 31000 Oran, Algeria

Abstract: A failure prediction of cracking possibilities of buried foundation sections is studied basing on databases issued from stochastic modeling (Monte Carlo Method) of soil geo-mechanical properties, which represents the support of a part of foundation system. The mechanical behavior of cracked foundation sections resting on soil of random geo-mechanical properties is well described using Line Spring Model (LSM). Numerical model is solved by the method of exact series solutions in structural mechanics for the computation of foundation structural responses at the crack tip and normalized stress intensity factors (SIF) within reasonable accuracy. The effects of the crack position, crack length and probabilistic assessment of soil geo-mechanical properties are discussed in this present a paper, especially on the evolution of normalized stress intensity factors and foundation structural responses. A parametric study based on the obtained numerical results of (SIF) of cracked foundation has been carried out in order to have a suitable prediction of failure occurrences at critical sections. These structural predictions can be very useful to direct engineers and researchers to take optimal solutions to improve the structural reliability of cracked foundations especially the ones of strategic parts of industrial and petrochemical infrastructures.

Keywords: Monte Carlo, Stochastic modeling; cracked foundations; stress intensity factors, Line Spring Model.

1. Introduction

Due to the interaction of foundations with soil that is known as very complex material, foundation mechanical behavior seems very complicated and the detection of critical sections – Section of stress concentration-can allow engineers and structural designers to offer a more optimal design with a suitable mechanical reliability. The apparition of first cracks and notches in concrete foundation parts can help detect critical sections which are governed by a plastic behavior laws and need a very high attention in order to save foundation rigidity and to limit the differential settlements. In the recent decades, a number of studies were conducted in the area of soil-structure interaction modeling the underlying soil in numerous sophisticated ways. The evolution of stress intensity factors are investigated for several crack lengths and crack positions and this, after carrying out a probabilistic study which allows the probably detection of critical foundation sections. The last part of this present paper discusses the efficiency of the proposed numerical model and the impact of obtained numerical results in the optimization of cracked foundation structural design of different parts of urban and industrial infrastructures.

2. Probabilistic assessment of soil geo-mechanical properties

⁵ Corresponding author

E-mail address: kazitani_nabil@yahoo.fr

As a result of the soil natural process of formation and its aggregation, its spatial heterogeneity has been taken into consideration in this research work. This was carried out through probabilistic methods based on Monte Carlo approach in order to quantify the influence of spatial variability of soil stiffness by means of a non-exhaustive parametric study described by the Van Marcke [1] theory of local average. The adopted approach consists to combine the finite element method (FEM) with the possibilities of stochastic modeling. These stochastic methods are essentially of two families, mainly the disturbance methods and Monte Carlo method based on three steps:

- Discretization of random field.
- Finite element method analysis (Deterministic calculation).
- Statistical analysis of structure responses after having carried out a consequent number of simulations for each achievement.

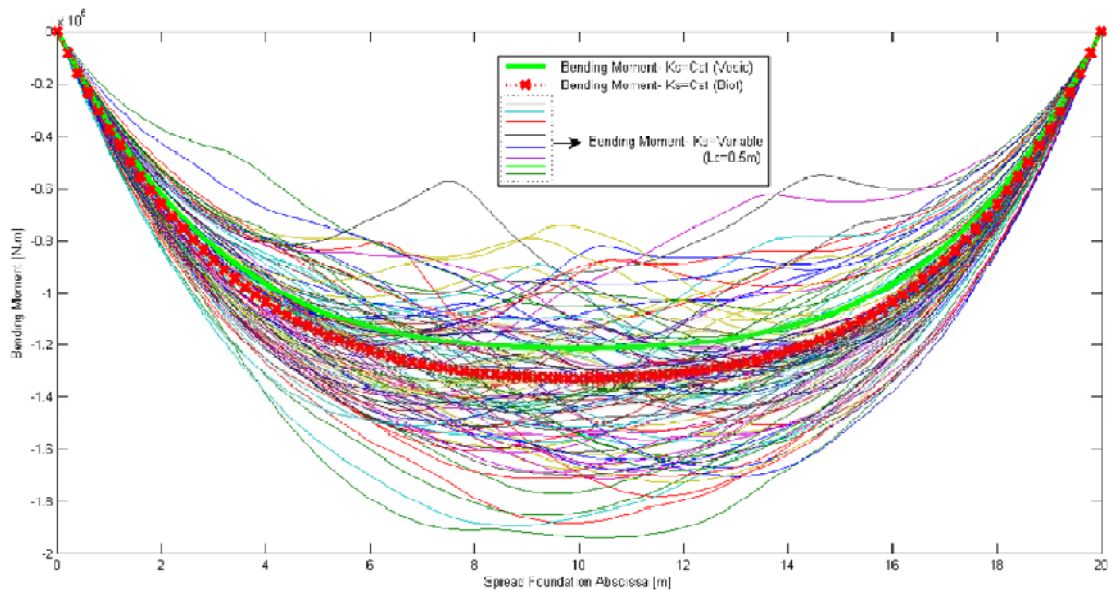


Fig. 1. Bending moment distribution along the foundation for few hazards of soil geomechanical properties ($L_c=0.5m$) and average Bending moment distribution of K_s

3. Conclusions

The aim of this research is to simulate a partially cracked spread foundation supported by spatially random soil. Stochastic modeling technique based on Monte-Carlo method is employed to describe the randomness of soil coefficient of subgrade reaction along the buried foundation. Based on Line Spring Model (LSM), the proposed approach allows computation of stress intensity factors using MATLAB code. The accuracy of this numerical technique depends mainly on Finite Elements meshing density of soil-foundation system and the (LSM) semi-analytical series truncation level. Therefore, the numerical results of structural responses and normalized (SIF) of cracked spread foundation can be very useful to direct the design of such buried cracked structures to more optimal design regarding structural reliability and expected safety level. A parametric study was introduced to investigate the effects of crack length and estimated average values of soil subgrade reaction modulus on the evolution of normalized stress intensity factors KI and KII.

References

- [1] VanMarcke, E. (1983) Random fields: analysis and synthesis, Cambridge, MA, London, England, MIT Press

HEAT TREATMENT OF A PARTICLE INJECTED INTO A PLASMA-PRODUCING MEDIUM

A. Abderahmane, M. Sahnoun, A. Aid

*a Laboratoire de Physique Quantique de la Matière et Modélisation Mathématique (LPQ3M),
University of Mascara, Algeria*

Abstract. Numerical simulation of the interaction between spherical particle (SiO_2) and Ar- H_2 plasma jet is carried out. We are particularly interested on thermal transfer between the plasma gas and metallic particle. In the conditions of molten or semi-molten states of prepared substrate, the medium (plasma jet) affected high velocities of metallic or ceramic particles. To ensuring the fusion of particle materials, the plasma attains the high temperature. The impact velocity of droplets is so important, that it is difficult to describe their behavior on the substrate. The behavior of the impact is directly influenced by thermal and dynamic history of the particle in the plasma jet. Computational analysis by numerical simulation of heat transfer in atmospheric pressure, mid-temperature range (6000K-12000K) of a plasma flow over a metallic sphere has been carried out.

Keywords: constraint, Ranz & Marshall, Computational, plasma Nusselt number.

1. Introduction

Thermal spraying has emerged as an important tool of increasingly sophisticated surface engineering technology. Research and development are increasing rapidly, and many applications are being commercialized. An indication of this rapid development is the fact that over 80% of the advances has been made over the last years [1-2-3-4-5]. Many exciting niches are opening up for metallic and ceramic surface coatings that include such well established markets as aerospace and consumer industries but also more slowly developing coating markets in the automotive, computer and telecommunications industries.

The material covered will discuss the basic nature of the plasma state, plasma-particle interactions, heat and momentum transfer, particle-substrate interactions. The quality of coatings depends strongly on the thermal and dynamical history of particles in flight before impact. For example, obtaining a more or less porous coating strongly depends on the melt and the particle velocity at impact. The advantage of modeling the heat, momentum and mass transfer between plasma-particles is clearly shown by the scientific community working in this domain [6-7].

The heat transfer is calculated from a Nusselt number. This number may be expressed by various semi-empirical formulas. The Ranz & Marshall correlation is frequently used for the spherical particles in gas giving by [8]: $Nu = 2 + 0.6 Re^{0.5} Pr^{0.33}$

The heat transfer correlation examined in this paper is extensions to flow over a sphere and additionally, because of the small diameter involved are for rather low numbers.

2. Modeling

Fig. 1 summarizes the parameters and the phenomena to be considered, to study and model the behavior of a particle of matter in a plasma jet. The modelling of particle treatment in a plasma jet consists the evaluation of its physical characteristics along its trajectory.

3. Results & Discussion

In this paper we will study the heat exchange of a single particle of Silicon dioxide in a field in which the use of this software, COMSOL MULTIPHYSICS, which works with the element finis method. The particle, regarded as immobile, is immersed in a plasma jet Ar/ H_2 at temperature 6000 K and velocity V_∞ is extremely high (100m/s to 500m/s). The SiO_2

particle injected with different diameters (20 μm and 40 μm). It is gradually heated through a boundary layer flow of heat of conduction and convection due to fluid flow.

The model of the transfer of heat plasma-particle and the phase shifts suitable to be carried out in a particle under the conditions of the plasma jet. This therefore makes this particle change many phases, as schematized in Figure 2. Several works shows that in absence of chemical reactions on the surface, the heating by conduction convection in the thermal boundary layer is the principal mechanism of the heating of the particle in the jet plasma [4-17-18-24]. Whereas the particle, under the condition plasma, cooled by radiation towards the ambient conditions. Often the radiative transfer of plasma towards the particle is neglected and plasma is thus regarded as optically thin.

The fin particle achieved our fusion faster than other particle and also rapidly Accelerates. The computed distributions with numerical simulation of plasma temperature for case of inlet gas velocity at x-y-plane of $z = 0$.

4. Conclusion

Following this study, it appears that the interaction of spherical particle (Silicon dioxide SiO₂) and Ar-H₂ plasma jet involves several complex mechanisms. We can conclude that during the injection of a particle in a plasma jet, it can be the seat of various modes of heat transfer and momentum transfer such as conduction, convection, phase change (melting and solidification, evaporation). Although the preponderance of one mode over another is dependent on particle size, nature of the material and the plasma medium but also the dynamic and thermal flow of the jet.

References

- [1] Aissa, A., et al, Ranz and marshall correlations limits on heat flow between a sphere and its surrounding gas at high temperature, Thermal science, Year 2015, Vol. 19, No. 5, pp. 1521-1528
- [2] P Fauchais, G. Montavon, M. Vardelle, J. Cedelle, Developments in direct current plasma spraying, J of Surface & Coatings Technology 201 (2006) 1908–1921.
- [3] Mingheng Li, Panagiotis D. Christofides, Computational study of particle in-flight behavior in the HVOF thermal spray process, Chemical Engineering Science 61 (2006) 6540 – 6552.
- [4] T. Shamim, C.Xia, P. Mohanty, Modeling and analysis of combustion assisted thermal spray processes, J of International Journal of Thermal Sciences 46 (2007) 755–767.
- [4] E. Pfender, Particle behaviour in thermal plasma, Plasma Chem. And Plasma Proc 9-1, (1989), pp 167-194.
- [5] C.H.Beck& al ,Numerical Investigation of the Time Scales of Single Droplet Burning, J of flow Turbulence Combustion (2009) pp 576.
- [6] J.R.Rojas, M.Cruchaga. M .El Ganaoui, B Pateyron , Numerical simulation of the melting of particle injected in a plasma jet, Ingeinaire . Revista chilena de ingenieria, vol. 17 N3 2009 pp 300-302.
- [6] L .Pawlowski 1995 The Science and Engineering of Thermal Spray Coatings (New York: Wiley)
- [7] Fauchais P, Vardelle A and Dussoubs B 2001 J. Thermal Spray Technol. 10 44–66.
- [8] W.E. Ranz and W.R. Marshall, Evaporation from drops. Chem. Eng. Prog. vol. 48 (1952), 141-146.

CHARACTERIZATION AND THERMOMECHANICAL MODELLING OF AN ANISOTROPIC ALUMINUM ALLOY SHEET UNDER BENDING LOADING

N. Benchabne⁶, N. Djaoui, K. Aimen, M. Ould Ouali

Université Mouloud MAMMERRI de Tizi-Ouzou, Laboratoire Elaboration, Caractérisation des Matériaux et Modélisation, BP 17 RP, 15000. Algeria.

Abstract: This paper is devoted to study the mechanical behavior and formability of Aluminum sheet. The aim of this work is to propose and validate a mechanical model that can describe the physical mechanisms governing ductile fracture of sheet during metal forming processes. The mechanical response of the AlMg3Mn has been characterized with uniaxial tensile tests realized within three directions. Flexion tests are carried out in order to determine the material formability. The stress-strain curves obtained during tensile test show the material orthotropic behavior. In this paper, the micromechanically-based Gurson-Tvergaard-Needleman (GTN) model is extended to study fracture of aluminum sheet. The modified model is based on Hill's quadratic anisotropic yield criterion (1948) takes into account anisotropic material behavior with isotropic hardening. The orthotropic behavior formulation is based on the introduction of a coefficient reflecting the plastic anisotropy effect as suggested by Benzerga. Thermal heating due to plastic deformation generally observed during metal forming operation is incorporated into the model. This thermo-mechanical law has been implemented into the finite element package Abaqus/Explicit using the Vectorized User MATerial subroutine (VUMAT) according to an extension of the algorithm proposed by Aravas. Comparison between experimental results and numerical predictions show the capability of the proposed model to reproduce namely the flexion operations with different type of notch (U, V).

Keywords: Ductile fracture, micromechanical modeling, numerical implementation, anisotropy.

1. Introduction

Several steel materials and aluminum alloy are studied and used in shaping (stamping, bending ... etc.). This work describes the experimental tensile test to characterize the hardening and initial anisotropy of the sheet. The bending test complements the tensile test to establish a representative model of hardening at best the actual behavior of the material.

The experimental results obtained are used to study the response of our sheet against bending tests and used for comparison with the predictions of the extended digital GTN model if orthotropic. The experimental results are used to study the response of our sheet against bending tests and used for comparison with numerical predictions. In this paper, we propose an extension of GTN damage model based on hill'48 anisotropic yield criterion. Thermal heating due to plastic deformation generally observed during metal forming operation is incorporated into the model. This thermomechanical law has been implemented into the finite element package Abaqus/Explicit using the Vectorized User MATerial subroutine (VUMAT) according to an extension of the algorithm proposed by Aravas. Comparison between experimental results and numerical predictions show the capacitance of the proposed model to reproduce namely the bending operations with different type of notch (U, V).

2. Experimental part

Tensile tests were performed according to the three direction relative to the rolling direction flat specimen without notch, notched U-shaped (U=3mm) and V-shaped (V=3mm). The results obtained are shown in Figure 1.

⁶ Corresponding author

E-mail address:

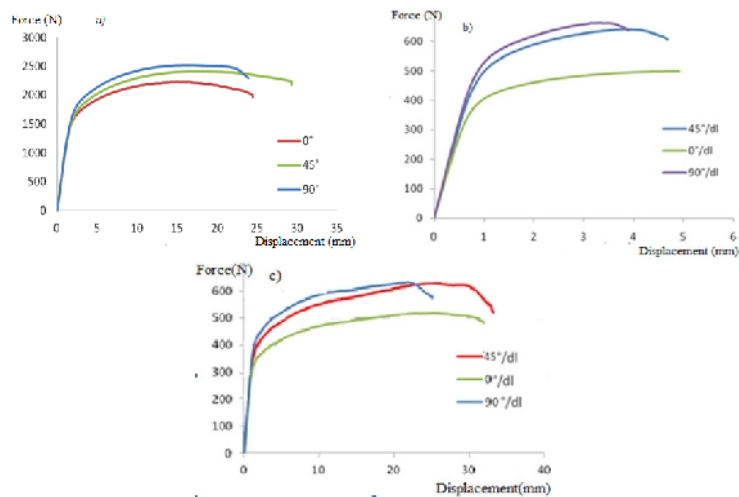


Fig 1. Tensile tests on flat specimen, a) without notch, b) notched U-shaped ($U=3\text{mm}$), c) V-shaped ($V=3\text{mm}$)

3. Results and discussions

Figure 2 shows a comparison between the results obtained experimentally and those predicted numerically on the rolling direction. This comparison between numerical predictions and experimental results showed the relevance of our approach.

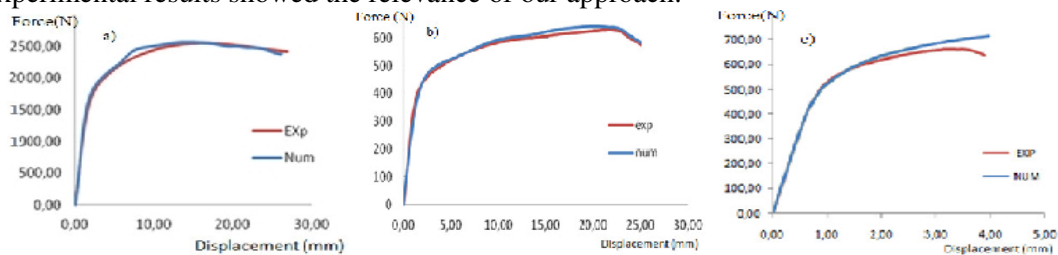


Fig 1. Comparison between numerical and experimental results, a) without notch, b) notched U-shaped ($U=3\text{mm}$), c) V-shaped ($V=3\text{mm}$)

4. Conclusions

GTN micromechanical model, proposed in case of the anisotropic matrix coupled to a ductile damage and temperature, has been successfully used to predict the out of our specimens aluminum alloy: bending specimens notched ($V = 3\text{ mm}$, $U = 3\text{ mm}$) and smooth traction. The results confirm that the extended GTN model for anisotropic matrix coupled with ductile damage and temperature, correctly describes the breaking of these specimens in the case of uniaxial loading essentially.

However, improvements can be made by considering the orthotropic material behavior and an anisotropic damage including the shape effect of the cavities, the cavities shear phenomenon and the kinematic hardening effect. In addition, recent work has shown that the mesh size used also influences the description of ductile fracture.

References

- [1] Hill.A, théorie du rendement et de l'écoulement plastique des solides anisotrope, Pro. Roy. Soc, vol. 193, pp. 281-297, London, 1948.
- [2] M. Almansba, M. Ould Ouali and N.E. Hannachi, micromechanical and phenomenological approaches of the sheet folding proces, Procedia Engineering (Elsevier), vol.10, pp. 3359-3368, 2011.
- [3] . Benzerga, Rupture ductile des tôles anisotropes Simulation de la propagation longitudinale dans un tube pressurisé, Thèse de doctorat. Ecole des Mines de Paris, France, 2000.

Thermomechanical bending analysis of functionally graded sandwich plates

Ahmed Hamidi*, Zidour Mohamed*, Abdelouahed Tounsi** and Adda Bedia El abbes**

*Civil Engineering Department. University of Tiaret Tiaret 14000, Algeria

**Civil Engineering Department. University of Sidi Bel Abbas Sidi Bel Abbas 22000,
Algeriahamidiahmed82@yahoo.fr

Abstract: *In this research, a simple but accurate sinusoidal plate theory for the thermomechanical bending analysis of functionally graded sandwich plates is presented. The main advantage of this approach is that, in addition to incorporating the thickness stretching effect, it deals with only 5 unknowns as the first order shear deformation theory, instead of 6 as in the well-known conventional sinusoidal plate theory. The material properties of the sandwich plate faces are assumed to vary according to a power law distribution in terms of the volume fractions of the constituents. The core layer is made of an isotropic ceramic material. Comparison studies are performed to check the validity of the present results from which it can be concluded that the proposed theory is accurate and efficient in predicting the thermomechanical behavior of functionally graded sandwich plates. The effect of side-to-thickness ratio, aspect ratio, the volume fraction exponent, and the loading conditions on the thermomechanical response of functionally graded sandwich plates is also investigated and discussed.*

Keywords: Sandwich plate; thermomechanical; analytical modelling; functionally graded material; stretching effect.

Theoretical and Numerical Analysis of Stress Intensity Factor in the first mode

(Mode I); Case of a Composite Material.

HAMLI BENZAHAR Hamid¹ and CHABAAT Mohamed²

¹Doctor, University of Djillali Bounaama Khemis Miliana, Algeria.

hzahar2004@yahoo.fr

²Professor, Built Environmental Research Lab., Civil Engineering Faculty U.S.T.H.B, BP32
El Alia, Bab Ezzouar, Algiers 16111, Algeria.

mchabaat@yahoo.com

Abstract: The present study is to evaluate theoretically and numerically the Stress Intensity Factor in first mode (Mode I). The problem is started by consideration of two rectangular shaped materials (flat) which are attached together by an adhesive. Homogenization of the two materials is to say, put same coefficient of Poisson and even shear modulus, leads to a homogeneous material in which one can theoretically determine the strain and calculate stress intensity factor. The numerical analysis of the same material is processed by analysis software (ABAQUS). According to the numerical and theoretical results constraints can limit the stress intensity factor.

COMPREHENSIVE APPROACH TO FRACTURE MECHANICS APPLIED TO POLYMERS (HDPE CASE)

T.Houari¹⁷, M. Benguediab², M. S.Houari³

1 University Mascara, Bab ali city, Mascara, Algeria

2 University Sidi Bel abbes, City 150, Sidi Bel abbes, Algeria

3 University Mascara, Sidi Said city, Mascara, Algeria

Abstract: High density polyethylene (HDPE) is a polymer model of the family of semi-crystalline; it represents a real industrial interest since it is one of the most produced thermoplastic polymers in the world. The study of the deformation and damage behavior and breaking HDPE was proposed from experimental and numerical approaches. Two approaches to energy (J integral and EWF) of fracture mechanics were examined on two types of specimens (CT, DENT) under tension. We conclude that the EWF method for its simplicity is the most suitable parameter for characterizing the intrinsic break our material.

Keywords: High density polyethylene; Triaxiality; Fracture; J integral; EWF method; Damage models; Finite element computations.

1. Introduction

The advanced technology and the evolution of increasingly enhanced in the field of unconventional materials impose a significant competitive technically and economically between metals and polymers for the production of multiform parts for use in areas as varied as the transport sector energy, automotive, aerospace or the medical. High density polyethylene (HDPE), subject of this study, is a polymer family model of semi-crystalline, the specificity of which resides in the combination of an amorphous phase and a crystalline phase. In fracture mechanics, there are two main methods to analyze the sustainability of a structure for a given material: either the global approach which as its name suggests uses measurable quantities such as global energy for the boot, or the local approach which has flourished thanks to the performance of computer codes with which we can access local variables. In this study, we address the fracture mechanics by presenting two global approaches: J integral and essential work of fracture (EWF) can be applied to polymeric materials.

2.EWF Approach

The EWF concept (for "Essential Work of Fracture") is a widely used technique to evaluate the tensile strength of ductile polymers [1]. It is to work on specimens having a size and a variable notch geometry, and measure the material's ability to resist breakage. We present the theoretical foundations and the most commonly used experimental methods.

If L is the uncracked ligament length, t is the thickness and W is the width and is a shape factor, then the total energy absorbed during the breaking process is:

$$w_f = w_e + \beta \cdot w_p \cdot L \quad (1)$$

And so, the essential work of fracture can be determined by plotting a f

⁷ Corresponding author

E-mail address:

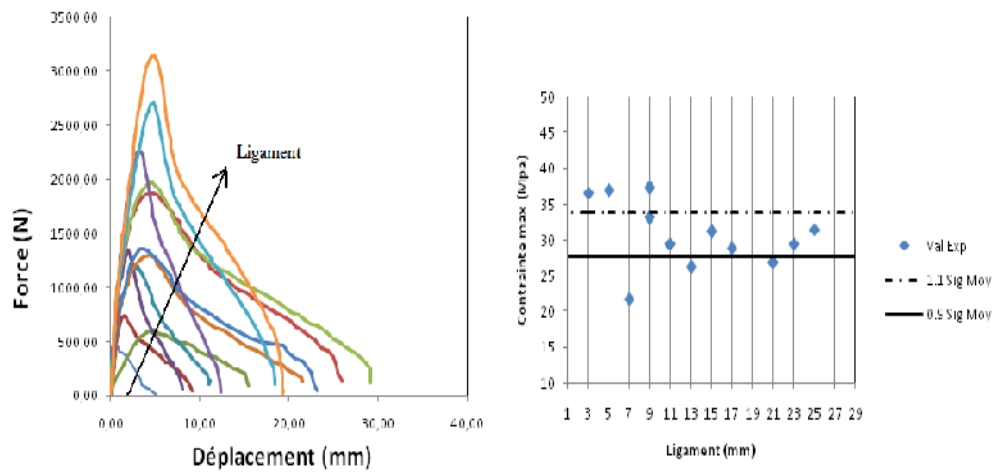


Fig.1. Curve Force - travel for EWF tests; the arrow shows the increase in the length of the ligament. Variation of σ max according to the ligament for DENT samples.

3. Conclusions

The study we have just presented has focused on the characterization and identification of the behavior of HDPE under different loading conditions, such as in quasi-static tensile and breaking with coupling damage. The study of the deformation and behavior to damage and breakage of the HDPE was proposed from experimental and numerical approaches. Two energy approaches (J integral and EWF) of fracture mechanics were examined on two types of specimens (CT, DENT) under tension. The EWF method has allowed us to highlight a very ductile behavior characterized by the existence of a large phase plastic deformation.

References

- [1]. Y-W. Mai, B. Cotterell. On the essential work of ductile fracture in polymers. *Int. J. Fract.*, 32, 105-125, 1986.

VALORIZATION OF NATURAL POLYMERS (LIGNIN) IN THE FORMULATION OF MORTARS AND SELF-COMPACTING CONCRETE

I.Djefour⁽¹⁾, M. Saidi⁽²⁾

(1)PhD student at M'HamedBougara University - Boumerdes Algeria

(2)Research Unit: Materials,

Processes and Environment (UR-MPE); Faculty of Engineering Science;

M'HamedBougara University -Boumerdes Algeria

E-mail: dj_imene90@hotmail.fr

Abstract: The use of lignocellulosic resources known currently undeniable resurgence of interest in the development of building materials. Lignin is a major constituent of lignocellulosic materials. This study focuses on the valorization of mortars and self-compacting concrete incorporating a natural superplasticizer (lignin extracted Aleppo pine woods) and artificial (Tempo 12 Polycarboxylates type SIKA) by reducing the water / cement ratio (W / C). This is to determine the optimal amount of natural superplasticizer will give the mortar and concrete the best physical and mechanical characteristics. Research undertaken in this study were satisfactory on the following points:

- The extraction of lignin by the process Klason and dissolution are perfectly manageable.
- The FTIR analysis confirms the presence of the majority of the functional groups in the extracted lignin structure.
- The performance of these natural adjuvant based mortars and concretes are improved by 20% compared to those of mortars and concretes artificial adjuvant for a W / C ratio = 0.4 identical.
- The amount of solids needed natural adjuvant is 40 times smaller than that of the commercial adjuvant for the preparation of mortars and concretes. So this study of impacts:

1- Scientific: Improved physical-mechanical properties of mortars and concretes by using a biopolymer extracted from the Aleppo pine wood.

2. Economic: valuation of the Algerian wood and use of an amount 40 times smaller than that of the commercial adjuvant.

3- Ecological: recycling of industrial waste from paper manufacturing.

Keywords: Biopolymer (lignin), industrial waste, mechanical resistances, mortars and self compacting concrete.

The influence of the scale coefficients and the mode number on non-local critical bulking load of double-walled carbon nanotubes (DWCNTs)

K. Rakrak¹, M Zidour², A. Chemi³, H Heireche³

¹(Département de physique, Faculté des Sciences, Université Hassiba benbouali, Chlef, Algérie)

²(Laboratoire des Matériaux et Hydrologie, Université de Sidi Bel Abbés, BP 89 Cité Ben M'hidi, 22000 Sidi Bel Abbés, Algérie).

³(Laboratoire de Modélisation et Simulation Multi-échelle, Université de Sidi Bel Abbés, Algérie)

Abstract : The present work indicate the elastic of chiral double-walled carbon nanotubes (DWCNTs) under axial compression. Among the nonlocal elasticity theory, Timoshenko beam model has been implemented. According to the governing, the analytical solution is derived and the solution for non-local critical buckling loads is obtained, and the results shows the influence non-local small-scale coefficient also it indicates the dependence of non-local critical buckling loads on the chirality (SWNT).

Keywords - Double-walled carbon nanotubes, chirality, Buckling, small-scale, Non-local elasticity.

1. Introduction

Iijima [1] and Iijima and Ichihashi [2] discovered the single walled carbon nanotube (SWNT) and multi-walled carbon nanotube (MWNT). This studing indicated that carbon nanotubes (CNTs) have mechanical and thermal properties [3, 4].

The others showed that (CNTs) can be used structures (carbon nanotube-reinforced composite (CNTRC)) [5, 6], can be used for nanoelectronics and nanodevices [7- 9].

Due the limited to systems computation of molecular dynamics (MD) simulations and the difficulties of experimental methods. The continuum mechanics mechanics methods are often used to investigate the behaviour of carbon nanotubes (CNTs) [10, 11]. It has been widely used to study the responses of micro as static and dynamic [12-17], the buckling and thermo-mechanical analysis of (CNTs) [18-23]. More recently, Yakobson et al. (1996) utilize a continuum shell model to predict the buckling of (SWNT) and the results are compared with molecular dynamics simulations.

The Young's moduli used three types of (SWNTs) armchair, zigzag and chiral tubules , are calculated by Bao Wen Xing et al. [22] based on molecular dynamics (MD) simulation. Its represents the dynamics of atoms or molecules of the materials by a discrete solution of Newton's classical equations of motion. The present paper is concerned with the use of the non-local Timoshenko beam model to analyse the non-local critical buckling loads of double-walled carbon nanotubes (DWCNTs).and the solution for critical loads is obtained.

2. Single-walled carbon nanotube (SWCNT):

A single-walled carbon nanotube (SWCNT) is theoretically assumed to be made by rolling a graphene sheet (Fig.1). In terms of the chiral vector (\vec{C}_h), the fundamental structure of carbon nanotubes can be classified into three categories as zigzag, armchair and chiral shown in (Fig.1).

The chiral vector can be expressed in terms of base vectors (\vec{a}_1) and (\vec{a}_2):

$$\vec{C}_h = m \vec{a}_1 + n \vec{a}_2 \quad (1)$$

where the integer pair (n, m) are the indices of translation.

According to different values of integers (n, m), (SWCNTs) can be classified into zigzag ((n or m)=0), armchair (n =m) and chiral (n≠m) (Fig. 1).

The diameter of (SWCNTs) can be expressed in terms of integers (n, m) [25]:

$$d = a \sqrt{3(n^2 + m^2 + nm)} / \pi, \quad (2)$$

where (a) is the length of the carbon-carbon bond which is (1.42 Å).

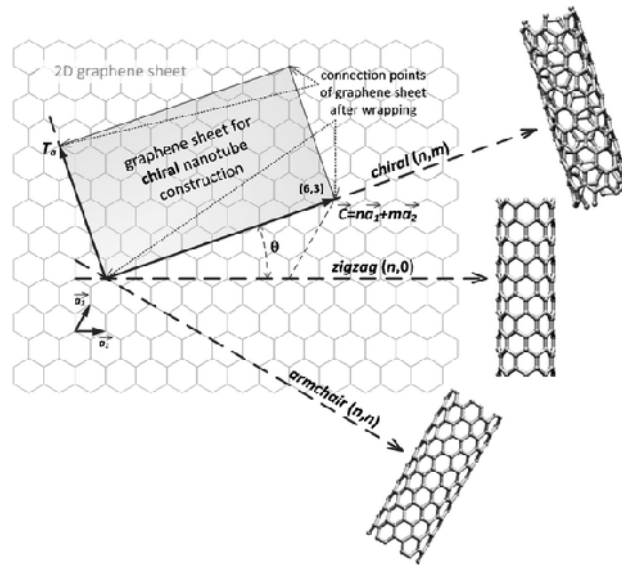


Fig. 1: Schematic the chiral vector of carbon nanotube.

3. Nonlocal Timoshenko beam models of (SWCNTs):

The nonlocal continuum elasticity theory assumed that the stress at a reference point is considered to be a functional of the strain field at every point in the body (Eringen 1983). The nonlocal elasticity theory is applied in various types of nanostructures (nano FGM structures, nanotube.) such as the free vibration [23], wave propagation [11]. For homogeneous and isotropic elastic solids, the constitutive equation of non-local elasticity can be given by Eringen.[24]

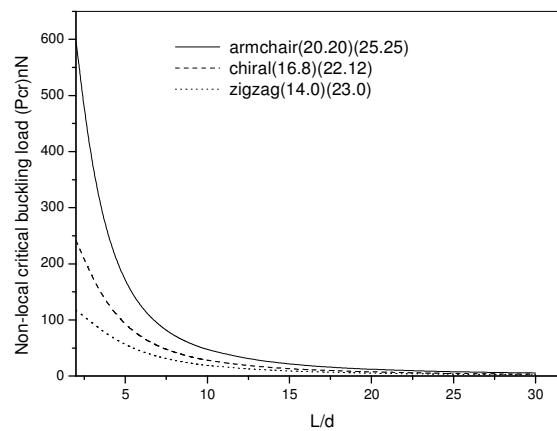


Fig. 2: effect of aspect ratio and chirality of double carbon nanotube on the Non-local critical buckling load in fundamental mode and scale coefficient ($e_0 a = 2 \text{ nm}$).

Conclusions:

This paper studies the Influence of non-local small-scale coefficient, the vibrational mode number, the aspect ratio and the chirality of double-carbon nanotube (DWCNTs) on the nonlocal critical buckling loads using non-local Timoshenko beam theory. The theoretical formulations include the different parameters, the non-local critical buckling loads are obtained.

References

- [1] Iijima, S. (1991), "Helical microtubules of graphitic carbon", Nature, 354, 56–8.
- [2] Iijima, S. and Ichihashi, T. (1993), "Single-shell carbon nanotubes of 1 nm diameter", Nature, 363, 603.
- [3] Dresselhaus, M.S. and Avouris, P. (2001), "Carbon nanotubes: synthesis, structure, properties and application", Top Appl Phys, 80,1-11.

Analyse numérique de la nocivité du phénomène de coup de bélier dans les conduites de transport des hydrocarbures

L. Aminallah^{1,*}, A. Benhamena², A. Merdji¹, S. Habibi¹, A. Daikh¹, B. Medjadji³, A. Aid²
1 Université Mustapha Stambouli de Mascara, Département de Tonc Commun ST, Faculté des Sciences et de la Technologie, BP 763, 29000, Mascara, Algérie
2 Université Mustapha Stambouli de Mascara, Département de Génie Mécanique, Faculté des Sciences et de la Technologie, BP 763, 29000, Mascara, Algérie
3 Université de Sidi Bel Abbès, LMPM, Département de Mécanique, Cité Ben M'hidi, BP 89, 22000, Sidi Bel Abbes, Algérie

Abstract: Dans cette étude la méthode des éléments finis en 3-D est utilisée pour le calcul de l'intégrale J dans les fissures semi-elliptiques dans une conduite en acier A333 Gr 6 soumise à une surpression interne causé par le phénomène de coup de bélier. L'intégrale J a été calculée dans le contour de la fissure (Φ). L'effet de la pression interne et de la configuration de la fissure sur l'intégrale J est analysé. Les résultats obtenus montrent que l'accroissement au niveau de la pression interne entraîne une augmentation remarquable de l'intégrale J . On montre aussi que la direction de propagation de la fissure dépend de sa configuration. L'effet de la profondeur de la fissure sur la valeur de l'intégrale J devient important quand le rapport entre la profondeur de la fissure et l'épaisseur de la conduite (a/t) tend vers 1.

Keywords: coup de bélier, intégrale J , fissure semi-elliptique, rupture, conduite, MEF.

1. Introduction

Les changements du régime d'écoulement d'un fluide contenu à l'intérieur d'une conduite entraînent souvent de brusques variations de pression qui peuvent atteindre des valeurs excessives. Ces fortes variations ont été résulté par un phénomène appelé coups de bélier. Les causes des coups de bélier sont diverses mais elles sont fréquentes lors du démarrage ou de l'arrêt d'une installation hydraulique, par exemple, une prompte fermeture de vanne ou un arrêt rapide de pompe. Ces causes peuvent avoir des conséquences fâcheuses telles que la rupture de canalisations et la détérioration d'appareils traversés par le fluide. Le travail proposé dans cet article a pour objectif l'étude du comportement d'une pipe fissurée soumise à une pression interne causé par le phénomène de coup de bélier. Cette étude est basée sur la détermination de l'intégrale J . Cette dernière est analysée en utilisant le code de calcul WARP 3D utilisant la méthode des éléments finis en trois dimensions.

2. Loi de comportement

La méthode des éléments finis est un moyen d'étude très utilisé actuellement consistant à calculer, après division d'un système en éléments, les variables inconnues pour transformer les équations aux dérivées partielles en équations algébriques. Ces équations peuvent modéliser, moyennant des hypothèses simplificatrices, les problèmes de la mécanique des solides [1], [2] et [3]. Ce travail consiste à l'implémentation de la loi de comportement dans le code de calcul « Warp3D » dans le cadre d'une simulation numérique. Les propriétés mécaniques de l'acier A333 Gr 6 sont : le module de Young ($E = 203$ GPa) ; la limite élastique ($\sigma_e = 302$ MPa) ; et le coefficient de Poisson ($\nu = 0,3$).

3. Effet de coup de bélier sur la variation de l'intégrale J

Dans cette section, nous avons considéré que la pression de service égale à 30 bars. Notons que les changements du régime d'écoulement d'un fluide contenu à l'intérieur d'une conduite entraînent souvent de brusques variations de pression qui peuvent atteindre des valeurs excessives. Ces fortes variations ont été résulté par un phénomène appelé coups de bélier. Cette étude a été réalisée sur une conduite soumise à différentes variations de pressions internes: 20 bars, 40 bars et 60 bars contenant une fissure longitudinale interne avec un rapport a/t égale à 0,3. Cet effet est illustré par les figures 1 et 2. Ces deux figures représentent la variation de l'intégrale J en fonction des positions sur la frontière de la fissure pour une fissure semi elliptique ($a/c = 0,1$) et semi circulaire ($a/c = 0,9$) respectivement. Nous constatons d'après ces deux figures qu'un accroissement au niveau de la pression interne causée par le coup de bélier entraîne une augmentation de l'intégrale J, cette augmentation est plus marquée pour des forte pressions. Cette augmentation au niveau de la pression interne peuvent avoir des conséquences fâcheuses telles que la rupture de canalisations.

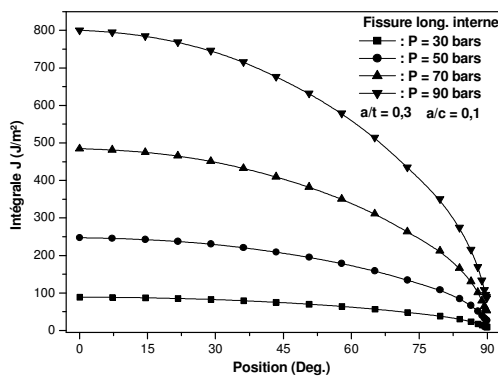


Fig. 1. Variation de l'intégrale J en fonction des positions sur la frontière de la fissure ($a/c = 0,1$) pour plusieurs pressions internes.

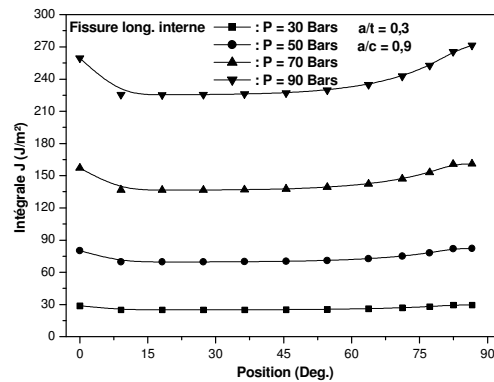


Fig. 2. Variation de l'intégrale J en fonction des positions sur la frontière de la fissure ($a/c = 0,9$) pour plusieurs pressions internes.

4. Conclusions

Dans cette étude, l'intégrale J a été utilisée pour analyser l'effet de coup de bélier sur les critères de propagation d'une fissure dans une conduite en acier A333 Gr 6, les résultats obtenus permettent de déduire les conclusions suivantes :- l'accroissement au niveau de la pression interne causé par le phénomène de coup de bélier entraîne une augmentation de l'intégrale J dans les deux fronts de la fissure ;- la direction de la propagation de la fissure dépend de sa configuration et de sa taille.

Références

- [1] Oden J.T. (1972.), Finite elements of non linear continua, McGraw Hill Company.
- [2] Dhatt G., Touzot G. (1981), Une présentation de la méthode des éléments finis, Ed. Maloine.
- [3] Zienkiewicz O.C., Taylor R.L. (1991), La méthode des éléments finis - formulation de base et problèmes linéaires, Edit. AFNOR

Three-dimensional analysis of the distribution of defects in the bone cement linking the cup to the bone

L. Zouambi^{1,2}, S. Gouasmi¹, F. Bouafia^{1,3}, B. Serier¹

¹LMPM, Mechanical Engineering Department, University of Sidi Bel Abbes, Sidi Bel Abbes 22000, Algeria,

²University Center Of Relizane,

³University of Temouchent.

Corresponding auteur : « zouambileila@yahoo.com »

Abstract

The aim of this work is to analyze three-dimensionally by the finite element method the level and distribution of tangential stresses and the equivalent of Tresca induced in the bone cement linking the cup to the bone under the effect of weight patient. We note that the shear stresses are greater than those of normal by virtue the complex structure of the acetabular cavity. These stresses are localized at the free edge of the cement. The presence of a cavity increases the level of these constraints twofold. These depend on the distribution of these defects in volume and interdistance.

Preheat effects on LiF: Mg, Ti at low dose

M. Halimi ^{1,*}, D. Kadri ¹, A. Mokeddem¹, I. Missoum ².

¹ Department of Materials Technology, Faculty of Physics, University of Sciences and Technology of Oran (USTO-MB), Algeria.

² Energy Physics Laboratory, Department of Physics, Faculty of Exact Sciences, University of Brothers Mentouri Constantine, Ain El bey Road, Constantine 25000, Algeria.

Abstract

Thermoluminescence (TL) is a method used to characterize materials in order to define their potential applications. The pre and post-irradiation annealing is crucial for its response, especially, for long term application in personal monitoring. LiF: Mg, Ti is one of the most important passive dosimeter. Extensive work on pre – irradiation heat treatment has shown that strong modifications to its (LiF: Mg, Ti) glow curve structure are induced.

In this present work we study the Effects of preheat treatment on LiF at low dose. TL measurements were carried out using Riso TL/OSL reader (model TL/OSL-DA-15) equipped with a beta particle source, delivering a nominal dose rate of 0.063G/s.

T-Stress and crack path trajectory in bi-material structures under pure mode I cracking

A. Kablia^{1*}, M. Hadj Meliani^{2,*}, T. Tamine¹

1 Laboratory of LCGE, University USTO Oran, Algeria

2 University of Chlef, LPTPM, Esalem City, 02000, Chlef, Algeria

Abstract: A crack approaching the interface in bi-materials structure has lots of propagation possibilities, it could be rejected by the interface and can achieve it, be either penetrating the interface or deflecting into it, and also the crack can get access to the adjacent material. In this paper, a various numerical analyses using the finite element method have been carried out to investigate the effects of non-singular stress (T-stress) on the crack path direction in bi-material plate under uniform uniaxial tensile stress. The materials on either side of the interface are elastic and isotropic. This problem was studied for a number of cases, the first modeling work examined the effect of the crack length on the path propagation with the presence of the interface, the second one, examines the effect of the oblique angle between crack plane and the interface, also we take on consideration the presence of various materials where the cracks changes its position between the most rigid part and the weak one in the bi-material specimen.

Key words: T-Stress, Bi-material, Interface, crack path

1. Introduction:

The presence of cracks in bi-material structure has a major impact on the reliability of advanced materials. In the few last years this problem has been a topic of considerable research. However, the most of those studies are limited to the solution of the stress singularity and crack tip parameters. For engineering application is very important to estimate the crack path, and the influence of the interface on the crack trajectory. In this paper, a several numerical analyses have been carried out to investigate the effects of the nonsingular stress, known as T-stress on the crack path direction in bi-material plate under uniform uniaxial tensile stress.

2. Crack behavior at interface

If a perpendicular crack reaches an interface, there are at least three possible crack paths. the simplest possible paths in bi-material model: (a) crack penetration across the interface; (b) crack deflection on one side of the interface (singly deflected crack); and (c) crack deflection on both sides (doubly deflected crack).

When crack approaching the interface at an oblique angle, the particularity of the oblique problem for the main crack is the fact that there is a single dominant mode of deformation at the crack tip when the materials across the interface are dissimilar. A consequence of the existence of this single dominate mode, is a tendency for the crack to turn either into or away from the interface, depending on the relative stiffnesses of the materials on either side of the interface.

3. T-Stress

In isotropic linear elastic body containing a three-dimensional crack subject to a symmetric loading, the stresses for each of fields can be written as a series expansion **Williams (1957)[1]**. Near the tip of the crack, where the higher order terms of the series expansion are negligible.

In the mode (I) loading, The first equation of Williams series shows that σ_{xx} comprises of the singular term and T. this implies that T can be determined along any direction where the singular terms of σ_{xx} vanished or can be set to zero by superposing with a fraction of σ_{xx} . This corresponds to mode I position around the crack tip.

$$T = (\sigma_{xx} - \sigma_{yy})_{r=0, \theta=0} \quad (1)$$

* Corresponding author

E-mail address: kablia.usto@yahoo.fr

For different value of θ , the authors [2], [3] and [4] have been calculate the T-Stress for a different orientation

Where

$$T = \sigma_{xx} - g(\theta)\sigma_{yy} \quad (2)$$

The Function of $g(\theta)$ can be determinate for different orientations; for $\theta = \pm\infty$ the function of $g(\theta)$ tend to $+\infty$. Analytically, the T-stress is not calculated in this angle.

Another method proposed by [5] where the T-Stress is

$$T = \sigma_{xx} - \sigma_{yy} + \frac{K_I}{\sqrt{2\pi r}} h(\theta) \quad (3)$$

And $h\theta$ can be also determined for a different orientation.

4. Conclusion

- In this present study, the cracks propagate with a perpendicular an inclined direction toward the interface, and its position are considered for tow cases, the crack located in the material (1) (E=100 GPa, $\nu=0.3$) and in the material (2) (E=210 GPa, $\nu=0.3$).
- The stress intensity factor increase with the normalized crack length L/L_0 . This tendency of K_I has the same evolution as the case when the crack is in a homogenous media, but for the bi-material the evolution was more significant when the crack located in the most rigid part.
- For the perpendicular crack we observed that when the normalized crack length be higher than 0.8 the T-Stress have the attitude to change its value to become positive witch mean that the crack be instable, so it may propagate in the same direction and it can bifurcate, to predict in with way the crack will propagate we proposed a different angle of direction and the result show that, under pure mode I loading the crack will keep his initial direction or he will bifurcate with an angle $-10^\circ < \theta < 10^\circ$
- The T-stress at crack with a perpendicular direction is more important compared with crack with an inclined direction.
- The study of the variation of various ratio of the Young modulus for the same crack length and the same direction toward the interface shows that the evolution of T-stress are strongly depend on this ratio. Weaker is the rigidity of the material where is located the curved crack, more the increase of the T-Stress was remarkable.

5. Reference

- [1] Williams, M. L. (1957). Journal of Applied Mechanics. 24, 109-114.
- [2] Ayatollah, M.R, Pavier, M.J, and Smith, D.J. (1998). Determination of T-stress from finite element analysis for mode I and mixed mode I/II loading. Int. J. of Fracture 91, 283-298.
- [3] M. Hadj Meliani, Z. Azari, G. Pluinage, Y. Matvienko. New Approach for the T-stress estimation for Specimens with a U-notch. CP2009, September 2009, Italy.
- [4] Guy Pluinage, Julien Capelle, Mohamed Hadj Méliani. (2014). A Review Of The Influence Of Constraint On Fracture Toughness Failures of materials and structures by fatigue and fracture, Belgrade, 15–18 September, 2014.
- [5] O. Bouledroua, M. Hadj Meliani and G. Pluinage, A review of T-stress calculation methods in fracture mechanics Computation. Nature & Technology review algeria 2016.

FREE VIBRATION ANALYSIS OF ARMCHAIR DOUBLE-WALLED CARBON NANOTUBES EMBEDDED IN AN ELASTIC MEDIUM USING NONLOCAL THEORY.

M. Zidour^{1,2}, A. Hamidi^{1,2}, T. Bensattalah^{1,2}, B. Adim¹, K. Rakrak³.

1 Université Ibn Khaldoun, BP 78 Zaaroura, 14000 Tiaret, Algeria

2 Laboratoire des Matériaux et Hydrologie, Université de Sidi Bel Abbés, Sidi Bel Abbés, Algeria.

3 Laboratoire de Modélisation et Simulation Multi-échelle, Université de Sidi Bel Abbés, Algerie

Abstract: In the present work, nonlocal Euler-Bernoulli beam theory is used to investigate the free vibration response of armchair double-walled carbon nanotube (DWCNT) embedded in an elastic medium. Winkler-type foundation model is employed to simulate the interaction of the DWCNT with the surrounding elastic medium. It is noticed in the present study that the equivalent Young's modulus for armchair DWCNT is derived using an energy-equivalent model. The results indicate the dependence of nonlocal effects, the mode number and Winkler modulus parameter on the frequency of DWCNT.

Keywords: nanotube, Vibration; armchair, Winkler, nonlocal.

1. Introduction

Since the single-walled carbon nanotube (SWCNT) and multi-walled carbon nanotube (MWCNT) are found by Iijima [1], there have been extensive researches on these nanomaterials. It has been found that carbon nanotubes possess many interesting and exceptional mechanical and electronic properties.

Experiments at the nanoscale are extremely difficult and atomistic modelling remains prohibitively expensive for large-sized atomic system. Consequently continuum models continue to play an essential role in the study of carbon nanotubes. Thereby size-dependent continuum based methods [2-3] are becoming popular in modelling small sized structures as it offers much faster solutions than molecular dynamics simulations for various engineering problems.

The nonlocal elasticity theory initiated by Eringen [4, 5] are captured by assuming that the stress at a point as a function not only of the strain at that point but also a function of the strains at all other points of the domain. Various works related to nonlocal elasticity theory are found in several references [6-7-8].

Recently, considerable attention has been turned to the mechanical behavior of single and multi-walled carbon nanotubes embedded in polymer or metal matrix [9-10]. Vibration and buckling analyses [11-12] of CNTs have shown the employment of Winkler-type elastic foundation for modelling continuous surrounding elastic medium.

In this paper, nonlocal Euler-Bernoulli beam theory has been implemented to investigate the vibration response of armchair double-walled carbon nanotubes (DWCNTs) embedded in an elastic medium. Winkler-type model is employed to simulate the interaction of the DWCNTs with a surrounding elastic medium. The influence of the scale parameter, the van der Waals forces, Winkler modulus parameter and the effect of the chirality of armchair DWCNT is taken into consideration in this study. It is hoped that the present analysis will be useful to researchers and engineers working on carbon nanotubes and CNT based composites.

4. Results and discussions

Based on the formulations obtained above with the nonlocal Euler-Bernoulli beam theory, the effect of both chirality and Winkler modulus parameter on vibration properties of armchair double-walled nanotubes are discussed here. The parameters used in calculations for the armchair DWCNTs are given as follows: the effective thickness of CNTs taken to be 0.258 nm [14], the force constants $K/2= 46900$ kcal/mol/nm² and $C/2= 63$ kcal/mol/rad² [20], the mass density $\rho = 2.3$ g/cm³ [21] and layer distance $h=0.34$ nm [15].

To investigate the effect of scale parameter on vibrations of armchair DWCNTs embedded in an elastic medium, the results including and excluding the nonlocal parameter are compared. In addition, the vibration characteristics of different armchair DWCNTs are compared in order to explore the effect of chirality. It follows that the ratios of the results with the nonlocal parameter to those without nonlocal parameter are respectively given by:

$$\chi = \frac{(\omega)_N}{(\omega)_L} \quad (17)$$

where $(\omega)_L$ and $(\omega)_N$ are the local and the nonlocal higher natural frequency, based on the local and nonlocal Euler-Bernoulli beam model, respectively.

5. Conclusion

This paper studies the vibration of armchair DWCNTs embedded in elastic medium based on Eringen's nonlocal elasticity theory and the Euler-Bernoulli beam theory. Influence of the stiffness of the surrounding elastic medium on the higher frequency of the armchair DCNTs is shown. According to the study, the results showed the dependence of the vibration characteristics on the nonlocal parameter, the mode number, Winkler modulus parameter and aspect ratios of armchair DWCNTs. With the results, the dynamic properties of the DWCNT beam have been discussed in detail; they are shown to be very different from those predicted by classic elasticity when nonlocal effects become considerable. This means that as the length scales are reduced, the influences of long-range interatomic and intermolecular forces on the dynamic properties tend to be significant and cannot be neglected. The investigation presented may be helpful in the application of CNTs, such as ultrahigh-frequency resonators, electron emission devices, high-frequency oscillators and mechanical sensors.

References

- [1] S. Iijima, Nature 354 (1991) 56.
- [2] Zhou S.J., Li Z.Q., J Shandong Univ of Tech 31 (5) (2001) 401.
- [3] Yang, A.C.M. Chong, D.C.C. Lam, P. Tong, Int J Solids Struct 39 (10) (2002) 2731.
- [4] Eringen A C, Int J Eng Sci 10 (1972) 1.
- [5] Eringen A C, J Appl Phys, 54 (1983) 4703.
- [6] Peddieson J, Buchanan G. G, McNitt R. P. Int J Engng Sci 41 (2003), 305.
- [7] Zhang Y Q, Liu G R, Xie X Y, Phys Rev, 71 (2005) 195404-1-195404-7.
- [8] M. Simsek, Steel Compos. Struct. 11 (2011) 59–76.
- [9] C.Q. Ru, J Mech Phys Solids, 49 (2001) 1265.
- [10] Qian, D., Dickey, E.C., Andrews, R., Rantell, T., Appl.Phys.Lett 76 (2000) 2868.
- [11] Ranjbartoreh A.R, Ghorbanpour A and Soltani B, Physica E, 39 (2007) 230.
- [12] Yoon J, Ru C.Q., Mioduchowski A. Int. J. Solids Struct. 43 (2006) 3337
- [13] Y. Tokio, Synth Met 70 (1995) 1511–8.
- [14] Y. Wu, X. Zhang, A.Y.T. Leung, W. Zhong, Thin-Walled Structures 44 (2006) 667 – 676.

FINITE ELEMENT ANALYSIS OF THE INTERFACE CRACKS IN COMPOSITES REINFORCED WITH NATURAL FIBER IN THE PRESENCE OF INTERPHASE.

Mokhtar. KHALDI¹, Nouredine Mahmoudi², Alexandre. VIVET³

IMUSTAPHA STAMBOULI University, Mascara, Algeria.

²*Laboratoire de Génie Industriel et Développement Durable. Centre universitaire de Relizane*

³*University of Normandy, CIMAP-Aleçon UMR 6252 CEA CNRS ENSICAEN, France*

Abstract: In the present work we characterize the interphase between the alfa plant fibers / epoxy resin (Araldite LY 1564 / Aradur 3487) and the longitudinal and transverse rigidities of the alfa fiber by nanoindentation. The experimental characterization results have been introduced in a micromechanical model to estimate, using the finite element method, the evolution of the damage quantified by the stress intensity factor of the interface cracks in the interphase of a unidirectional composite reinforced with vegetable alfa fibers under transverse loading. The results show that the properties and thickness of the interphase have a significant influence on behavior of composites reinforced with vegetal fibers. On the other hand, strong interfaces can also improve crack growth resistance

Keywords: Finite element method, natural fiber, Crack propagation, Interphase.

1. Introduction

Natural fibers (NF) such as alfa, flax, hemp, sisal, coir, jute, ramie, and kenaf have the potential to be used as a replacement for glass or other traditional reinforcement materials in composites, motivated by potential advantages of weight saving, lower raw material price, and ecological advantages of using green resources which are renewable and biodegradable [1-4]. Natural fibers traditionally have been used to fill and reinforce thermosets, natural fiber reinforced thermoplastics, especially polypropylene composites, have attracted greater attention due to their added advantage of recyclability [5]. Since it ensures the interfacial area between fiber and matrix is of a prime importance in the characterization of composite materials and their performance. It is worth noting that many complex phenomena, such as creating links, interdiffusion, and physical interactions may arise and interact in this area. However, the understanding of the damage mechanisms occurring in these composites on different scales is still relatively sparse and lacks of systematic development. One of the most complex micro-scale failure mechanisms of VFRC under transverse loading is associated to the matrix and fiber-matrix interphase failures. The present work focuses on the first step of this failure mechanism: microcrack initiation and growth at the matrix-fiber interphase.

2. Experimental

For identifying the elastic modulus of the matrix, the longitudinal and transverse module of alfa fiber and the interphase we use nanoindentation tests. Table 1 summarizes the results obtained.

Table 1: Properties of the constituents of the composite.

	E_L [GPa]	E_T [GPa]	E_L/E_T	Ref
Alfa fiber	28.8 ± 4.07	4.3 ± 1.4	6.61	[6]
Matrix	3.3 ± 0.2	3.3 ± 0.2		[6]
Interphase	17.157 ± 5.07	17.157 ± 5.07		[6]

3. Numerical analysis

To simulate the evolution of the stress intensity factor of the interface crack finite element method is used. As shown in Figure 1, the model is a representative volume element (RVE) consisting of a single alfa fiber with an idealized circular shape of 10 μm in diameter and an epoxy matrix. The array of the fibers is a square type. The fiber volume content is about 40 %. Under the action of a uniaxial load transverse to the fiber axis, a crack initiated near the interface fiber/ matrix is propagated along the interphase. The results obtained are shown on figure 2 and 3.

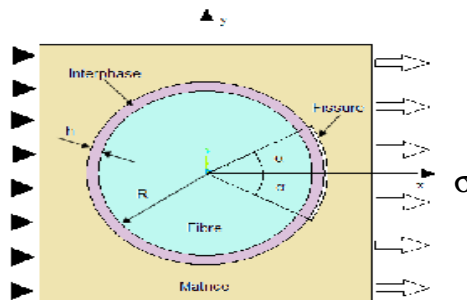


Fig.1: geometry of the model and boundary conditions

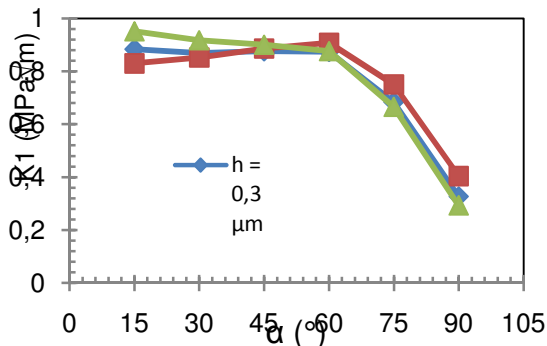


Fig.2: Effect of the thickness of the interphase on the evolution of the stress intensity factor K_I

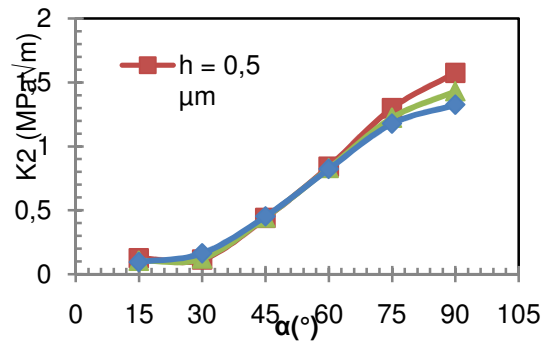


Fig.3: Effect of the thickness of the interphase on the evolution of the stress intensity factor K_{II}

References

- [1] Sherman L.M. Natural fibers: the new fashion in automotive plastics. *Plast Technol*, 1999: 45 (10): 62–68
- [2] Sydenstricker T.H., Mochnaz S., Amico S.C. Pull-out and other evaluations in sisal-reinforced polyester biocomposites, *Polym Test*, 2003, 22 (4): pp. 375–380.

Analysis efforts of shock on the stresses level in the elements of a dental prosthesis

N. DJEBBAR^{*}, B.BACHIR BOUIADJRA, B.SERIER

Department of Mechanical Engineering, University of Hassiba Benbouali,
Hay Salem, N° 19 National road, Chlef 02000, Algeria.
LMPM, Department of Mechanical Engineering, University of Sidi Bel Abbas, BP 89,
Cit  Ben M'hidi, Sidi Bel Abbas 22000, Algeria.

*Corresponding author: e-mail: djebbaredine@gmail.com

From Mr. Madjid Meriem Benziane

Abstract

The aim of this analysis was to determine the intensity and distribution of the stresses in the components of the dental prosthesis (Abutment, Implant and Bone) as a result of the efforts of shock. This numerically study by finite element method was conducted in three zones (proximal, medial, and distal) of these components.

Keywords: Dental implant, bone, efforts of shock, finite element method.

2. Geometrical model

The three-dimensional geometrical model of the dental structure, illustrated in figure 1, to achieve this goal the computer simulations involving the finite element code ABAQUS code version 6.9 was applied. The bone was modelled as full structure (block of bone with size equal to the section of lower jaw: 24.23mm height and 17.43 mm width). It is composed of a spongy center surrounded by 2mm of cortical bone. The implant is presented in form of screw of length 14 mm and diameter 4.1mm. Abutment of conical form is adjusted to the implant. The sizes of the abutment are: length $l=7.2$ mm, lower diameter $d_1=2.6$ mm and great diameter $d_2=3.6$ mm [17].

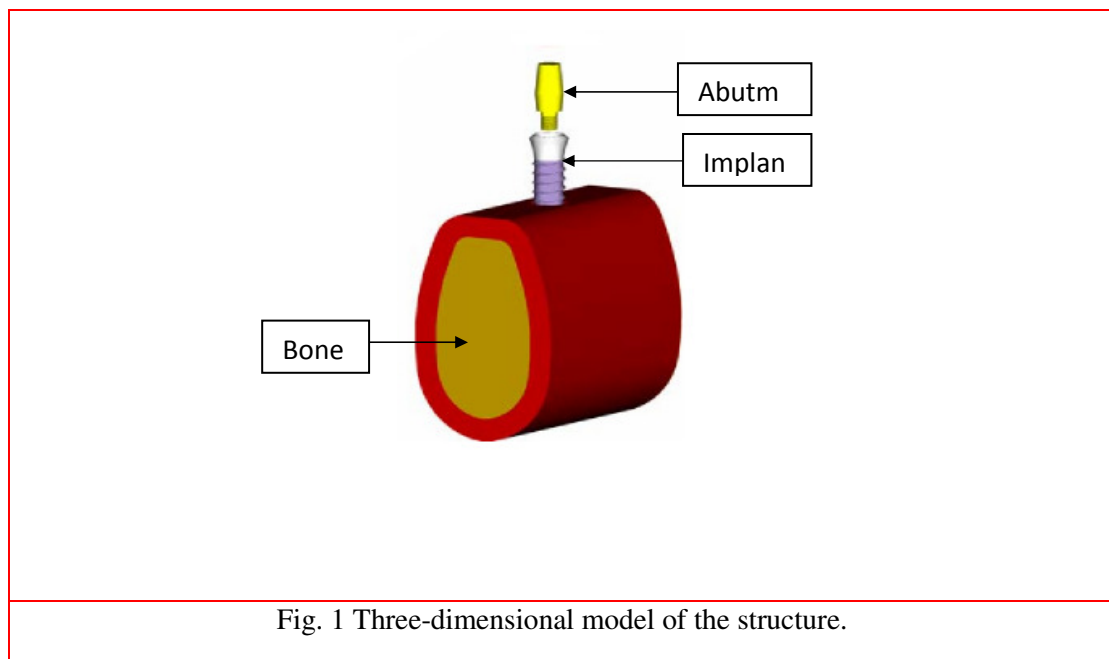


Table 1 gives the elastic properties of the components of the dental prosthesis [17]. The behaviour of the cortical bone is supposed orthotropic.

Matériau	Module de Young E [MPa]	Coefficient de Poisson ν
Implant (Alliage de Titane Ti-6Al-4V)	110000	0.32
Abutement (Alliage de Titane Ti-6Al-4V)	110000	0.32
Os (Cortical Bone)	$E_X=E_Y=11500, E_Z=17000$ $G_{XY}=3600, G_{XZ}=G_{YZ}=3300$	$\nu_{xy}=0.51, \nu_{xz}=\nu_{yz}=0.31$
Os (Cancellous Bone)	2.13	0.3

2.1 Load conditions

A tightening torque abutment - implant and implant-bones of 3500 N.mm and a friction coefficient of 0.28 were retained [17]. Stresses of 6 MPa were applied to the structure according to the directions illustrated in figure 3. This mechanical shock exerted on the bone and abutment following an accident the patient.

Application of depth-sensing microindentation testing to study of interfacial fracture toughness in reinforced Concrete: effect of water to binder ratio and the type of concrete

Said. Grairia¹, Yacine. Chrait¹, Alex. Montagne², Alain. Iost², Mohamed. Bentoumi³,
Didier.Chicot⁴.

¹Laboratory of Civil engineering and Hydraulic LGCH 8 mai 45 Guelma Univesity,Algeria.

²Laboratory of Mechanics, Surfaces and Materials Processing MSMP École
Nationale Supérieure d'Arts et Métiers Lille, France .

³Laboratoire de Mecanique de Précision Univesité Ferhat
Abbas-Setif ,Algeria.

⁴Laboratoire Mécanique de Lille LML UMR 8107 UST Lille IUT
A GMP Villeneuve d'Ascq, France

E-mail : s.grairia@hotmail.fr

Abstract

The resistance to separation of the concrete from its reinforcing steel with which it is in contact is called adhesion .This adhesion constitutes an important property for the use of reinforced concrete. That is why many techniques were developed with the aim of determining this property. Adhesion can be easily found out by standard pull-out test machine. But in this work, the adhesion was measured using Interfacial Indentation test. This technique creates and propagates a crack along the concrete/ steel bar interface and defines the apparent interfacial toughness, which can then be related to the adhesion and mechanical support of the aforementioned interface. Using reinforcing bars, adhesion was measured using Self Compacting Concrete (SCC) and Normal Vibrated Concrete (NVC) specimens. The impact of water-to-binder ratio variations and concrete type on concrete /steel bar adhesion has been the incentive of the present study. Interfacial indentation test on small cylindrical samples have been conducted for 5 SCC and 2 NVC mixtures. Various apparent interfacial toughness have been evaluated. The water-to-binder and concrete type changes seem be better reflected on interfacial toughness, which decrease linearly for higher water content. SCC develops an improved adhesion capacity compared to same strength NVC with similar composition. In this type of studies are rarely those who have tried to characterize the adhesion of matrix/ steel bar reinforcement in Self Compacting Concrete by using the interfacial indentation test as a new methodology. Exclusively, the objective of this research is to fill this gap by characterizing for the first time this concrete/steel bar adhesion by interfacial indentation test and then study the effects of some parameters such as water to binder ratio (w/b) and concrete type on its behavior and on the microstructure of the developed composite material.

In conclusion, the indentation test showed clear advantages over the conventional pullout test and also shows once again its aptitude to study the adhesion of concrete/ steel bar reinforcement couple.

Keywords: Apparent interfacial toughness (Kca), Interfacial indentation test; Water-to-binder ratio (w/b), Nature of concrete; Microstructure, fracture anal

NONLINEAR DYNAMICS OF MECHANICAL SYSTEMS USING TIME INTEGRATION SCHEME "IMPLICIT"

R. Koulli¹, S. Mamouri¹,
University of Tahri M. Bechar, Algeria

Abstract: In this work we focus on improvement of stability and robustness of time-integration energy conserving schemes for nonlinear dynamic analysis of high stiff elastic planar beam. The finite element model chosen is based on the geometrically exact theory beam. A review of the energy conserving scheme for 2D geometrically exact beam is exposed first, and we present the redesign of this schemes, by introducing desirable properties of controllable energy decay in higher modes. The new schemes are based on energy conserving algorithms, presented in the previous work of Gams & al [1]. Multiple of numerical simulations are exposed to illustrate the stability and robustness of decay energy schemes.

Keywords: dynamic, Beam 2D, decay, conserving scheme, Finite elements.

1. Introduction

A large amount of research has been performed to identify effective time integration schemes for the linear and nonlinear analyses of structures.

How to design a stable and robust integration scheme for the stiff equation describing nonlinear elastodynamic of engineering structures, were a matter of intense research (see, Ibrahimbegovic and Mamouri [1,3], Gams & al [2], Bathe [4] and Armero, for state of the art).

In this work we propose an extension of an implicit energy conserving scheme for the dynamic analysis of 2D frame-like structures developed by Gams and al [3]

2. Dynamics of 2D geometrically exact beam

We describe in this section the equations governing nonlinear dynamics of 2D beam undergoing large rotations and displacements, this model is based on the first theory proposed by Reissner, extended to handle an arbitrary space curved beam (see Ibrahimbegovic and Frey).

The virtual strain $\delta\mathcal{E}$ is computed using Lie derivative concept (For details see Ibrahimbegovic and Mamouri [1]), to get

$$\delta\mathcal{E} = \Lambda\delta\Lambda^T(\mathcal{E}) = \delta\phi' - \mathbf{W}\phi'\delta\psi \quad (1)$$

However, due to the planar nature of the problem, $\delta\mathcal{K}$ is obtained directly as:

(2)

$$\delta\mathcal{K} = \delta\psi'$$

Can be rewritten work form :

$$\int_0^L (\delta\phi \cdot \mathbf{A}_\rho \dot{\phi} + \delta\psi J_\rho \ddot{\psi}) ds + \int_0^L (\delta\phi' - \mathbf{W}\phi'\delta\psi) \cdot \mathbf{n} + \delta\psi' m ds = \pi_{ext} \quad (3)$$

3-Mid-point scheme

The time discretization of the weak form of the equations of motion is established, using the mid-point rule approximation. Therefore, the equation (4) must be written at time $t_{n+1/2}$ ($t_{n+1/2} = t_n + \Delta t/2$) is the mid-point of the time step increment $\Delta t = t_{n+1} - t_n$

$$\int_0^L \delta \varphi \cdot A \rho \dot{\varphi}_{n+\frac{1}{2}} ds + \delta \psi J \rho \dot{\psi}_{n+\frac{1}{2}} ds + \int_0^L (\delta \varphi' - \mathbf{W} \varphi'_{n+\frac{1}{2}} \delta \psi) \cdot \mathbf{n}_{n+\frac{1}{2}} ds + \delta \psi' m_{n+\frac{1}{2}} ds = \pi_{ext, n+\frac{1}{2}} \quad (4)$$

4. Numerical simulations

In this section we present the results of several illustrative numerical simulations. All the computations were performed by the computer program FEAP, developed by Prof. R.L. Taylor at UC Berkeley.

4.1 The swinging pendulum

The section of each flexible bar is $A = 0.005 \times 0.01 m^2$, the mass density $\rho = 2700 kg / m^3$, and Young's modulus $E = 73 \times 10^9 N / m^2$

5. Conclusions

A novel design of our time integration scheme has been presented in this work for nonlinear dynamics 2D geometrically exact beam, which are able to enforce the energy conservation or decay. This is needed for long-term simulations and especially for the case when the motion is described by the stiff equations due to large differences in stiffness associates with various deformation modes.

We have demonstrated in several numerical examples that the proposed dissipative scheme is needed, especially for getting improved values of beam stress-resultant internal forces. The proposed scheme leads to better damping of high-frequency content for axial, shear and bending forces compared to a recent approach proposed by Gams et al.

References

- A. Ibrahimbegovic, S. Mamouri: Nonlinear dynamics of flexible beams in planar motion: formulation and time-stepping scheme for stiff problems, *Computers and Structures*, 70 (1999) 1–22.
- A. Ibrahimbegovic, S. Mamouri: Energy conserving/decaying implicit time-stepping scheme for nonlinear dynamics of three-dimensional beams undergoing finite rotations *Comput. Methods Appl. Mech. Engrg.* 191 (2002) 4241–4258.
- M. Gams, I. Planinc, M. Saje: Energy conserving time integration scheme for geometrically exact beam *Comput. Methods Appl. Mech. Engrg.* 196 (2007) 2117–212.
- K.J. Bathe: Conserving energy and momentum in nonlinear dynamics: a simple implicit time integration scheme *Computers and Structures* 85 (2007) 437–445

NUMERICAL INVESTIGATION OF SHAPE EFFECT OF COMPOSITE PATCH ON INCLINED CRACK REPAIRATION.

E.H. Besseghier¹, A. Aid¹, A. Djebli^{8*}, M. Bendouba¹, A. Benhamena¹
1University of Mascara, LPQ3M, Mascara-29000

Abstract: Among the parameters that have an influence on the efficiency of patch are their geometrical and dimensional forms. For this study, a numerical simulation based on 3D by the calculation code abaqus 6.9 of a panel of aluminum that contains a crack $2a=10\text{mm}$ and angled 45° (mixed mode "I and II") repaired with a composite patch as butterfly form with different surface 616, 706, 804 mm^2 and different ratio $C/B=0.4, 0.6, 0.8$ with fixed thickness equal to 1.5mm. In order to measure the efficiency of patch, we have made a comparison with the forms of literature to select the right form of patch that minimizes the maximum of FIC on its mixed mode. For the forms that have a possibility to be in two positions such as rectangular, elliptical, and butterfly the choice of the vertical position is based on the performance is better than the horizontal position and for the octagonal we select the expended octagonal.

Keywords: fatigue, composite patch, mixed mode, analyze by finite element method (MEF), fissure.

1. Introduction

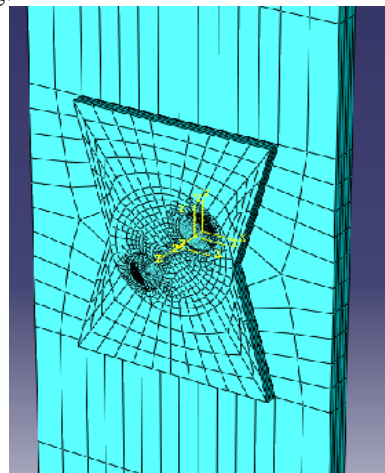
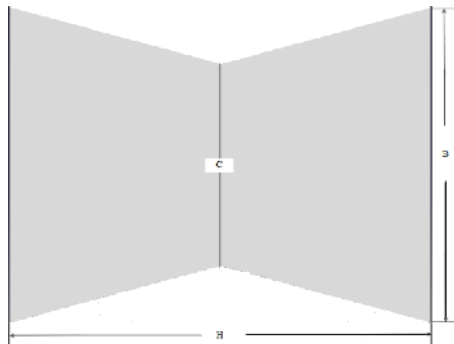
This technique of reparation appears to be adopted as an alternative beneficial one compared to the other conventional techniques. For example, the use of these reparations is a large domain in aeronautics because of its efficiency. The researchers study this method from many sides for example for the patch; the researchers examine the material, the thickness, the form and the dimensions and for the adhesive study the type and its thickness.

2. Resultats and discussion

To evaluate the efficiency, the patch form of a cracked panel in mixed mode during the calculation the parameter R that represents the following equation: [1] :

$$R = \sqrt{\left[\left(\frac{K_I^U - K_I^R}{K_I^U}\right)^2 + \left(\frac{K_{II}^U - K_{II}^R}{K_{II}^U}\right)^2\right]} \quad (1)$$

With K_I^U ET K_{II}^U Represents FIC to the non-repaired panel mode I and II, K_I^R ET K_{II}^R represents FIC to the repaired panel (mode I and II). The combined equation between the FIC mode I and II on the only parameter R that is acquired to compare the performances of the patch form. The patch is efficient to the value of R is big.



* Corresponding author

E-mail address: djebliabdelkader@yahoo.fr

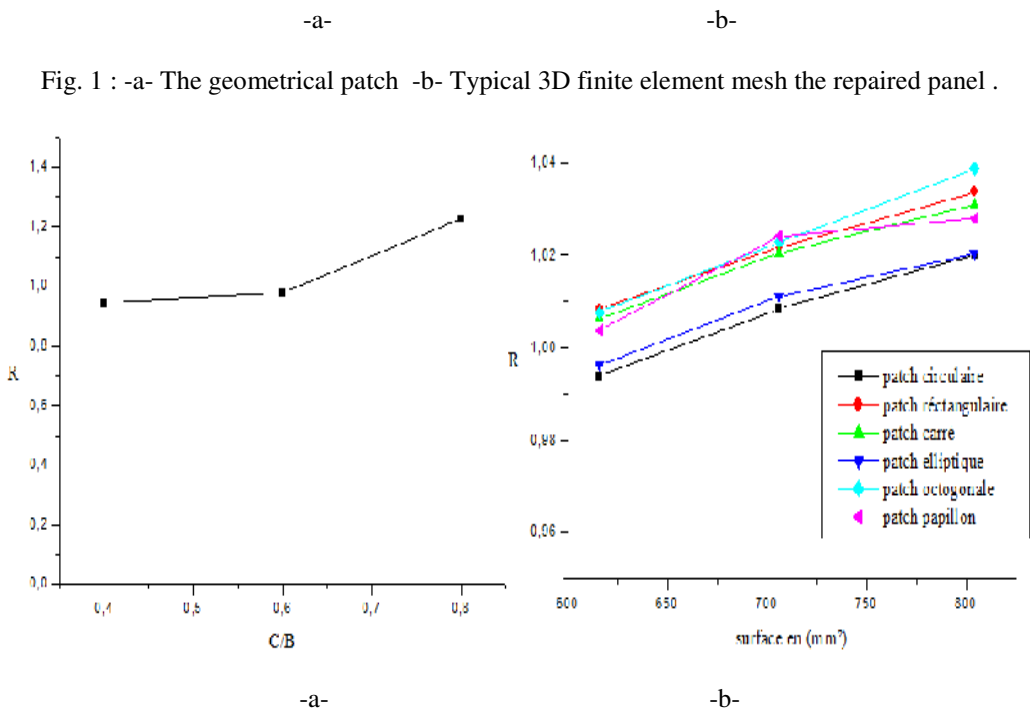


Fig.2: -a- the variation of factor R according to C/B -b- the variation of R according to the surface to different patch form

3. Conclusions

This study examined the comparison of the efficiency of our patch form with the efficiency of patch form of literature [2]. It is a comparison of six patch forms in order to choose the right patch form and for the reparation containing a central crack angled 45°.

The presence of patch reduced significantly the concentration of constraints that can delay the creation of the crack and thereafter the augmentation of the life duration and the structure.

The vertical patch forms are preferable rather than the horizontal forms.

The patch performance increases with the expansion of the patch surface because it reduces the transferred charges or patch.

The butterfly patch performance is better than the octagonal patch on the surface of 706 mm²

References

[1] Murakami Y. Hand book of stress intensity factors. Tokyo: Pergamon Press; 1987.

[2] M. Ramji , R. Srilakshmi, M. Bhanu Prakash . Towards optimization of patch shape on the performance of bonded composite repair using FEM .Composites: Part B 45 (2013) 710–720.

Elastic analyses of the Pipeline API X65 Repaired with Composite Overwrap

D. Belhadri, W. Oudad, H. Fekirini

*Univ Ctr of Ain Temouchent Smart Structures Laboratory (SSL) Po Box 284, 46000, Algeria.
Djamelins@hotmail.fr*

Abstract: In the last 15 years, glass fiber hoop reinforced composite systems emerged as an acceptable, successful method for repairing corroded and mechanically-damaged onshore pipelines where the primary load is internal pressure. The objective of this study was to compare the performance of the repaired rectangular cracks in API X65 pipelines assuming that the material is elastic. The three-dimensional finite element method (FEM) was used to compute the stress intensity factors (SIF) at the crack tip. Repairing cracks under internal pressure using carbon-epoxy composites was investigated where the influence of the depth and the length of the crack, the length of the overwrapping composite and its thickness, and a variation of a mechanical loading were included. In the evaluation of the repair of the pipeline, the failure assessment diagram (FAD) was introduced to obtain the safety factor value. The outcome guided and led to admit that the value of the factor of safety depends on the geometry of the crack and the pressure. In addition, the results showed that the composite gives a best benefit where the length of the overwrapping is between 200-300% of the pipe thickness.

Keywords: API5LX65, composite, J integral, FAD, crack, SINTAP

FATIGUE BEHAVIOR OF COMPOSITE MATERIAL TO USE ORTHOPAEDIC

S. Achouri^{1,2}, B. Redjel²

*1 Research Center in Industrial Technologies CRTI, P.O.Box 64, Cheraga 16014 Algiers, Algeria
souma_sihem@yahoo.fr*

2 Civil Engineering Laboratory, Badji Mokhtar University, 23000, Annaba, Algeria.bredjel@yahoo.fr

Abstract: Cyclic tests of repeated fatigue loads were carried out in three-point bending on a composite laminate material for orthopedic use in glass layers 6 - acrylic perlon- (2P-2V-2P) symmetrical. The tests were conducted to burden with $R = 0$ (ratio of minimum stress to maximum stress), a charging frequency set to a minimum of 75 cycles / min, 1,25Hz and a sinusoidal signal. The test pieces used were cut on medium thickness molded plaques 4 mm, dimensions of 80 mm length and 15 mm width according to the recommendations of the standard EN ISO 14125. These specimens were subjected to various loading levels versus the maximum charge of static failure in three-point bending, either: 90%, 80%, 85%, 70%, 60%, 55%, 45%, 40%. For each load level, a minimum of three test specimens was tested. The curve traced Wohler is distinguished by a wide dispersion in the lifetimes between the specimens subjected to the same level of loading and tested under the same conditions of cycling and was modeled by a straight line. This dispersion is a consequence of the heterogeneity of the studied composites. Indeed, the characteristics of specimens such as reinforcement's rate, distribution, density and shape defects and static strength are not comparable from one specimen to another. This phenomenon of dispersion that the life of forecasts studied composites can be estimated with a high probability by the curve of Wöhler. However, the route of the latter giving the middle part a good and acceptable performance can still be used as a comparison corresponding to variations in compositions, variations reinforcements rate, changes in nature of the resin and fiber, test frequency, cycling parameters etc. The deterioration of the composite takes place in the early fatigue loading cycles and gradually increases on the surface and within the volume to the final fracture. The state of fatigue damage is characterized mainly by a combination of density and orientation of microcracks. This damage is due primarily to a combination of the complexity of the mechanisms microcracking of the matrix, interfacial debonding, of loosening and failure of reinforcements. The stages of evolution of the damage in the case of cyclic loading are the same as those encountered in static loading but chronology and different magnitudes.

Keywords: Perlon, fatigue, damage, reinforcements, Wöhler curve.

1. Introduction

Several studies show that in the case of fatigue of fibre reinforced composite materials, for a given stress level σ_i , a dispersion value of the number of cycles to failure is observed. The problem of dispersal of results is the consequence of the structural heterogeneity of the defects since the elaboration of material [1]. B. Soh Fotsing et al. [2] have been reported that since these defects present in the material are difficult to measure, it is advisable to use as a random variable, for a given stress level, the number of cycles to failure to explain the existence of defects by a probabilistic approach. N. Ngarmaim et al. [3] have formulate a probabilistic model of a new expression of the SN curve in fatigue based on the concept of "weakest link" of Weibull introducing a new parameter N_c , the number characteristic of cycles corresponding to the failure probability equal to 1. His confrontation with the terms of the curve most used SN, particular those Basquin, the Wöhler and the Stromeyer, the fatigue tests and martensite steels P220 100C6 data provided errors of about 5% maximum for models Basquin, Wöhler and that proposed.

2. Results and discussion

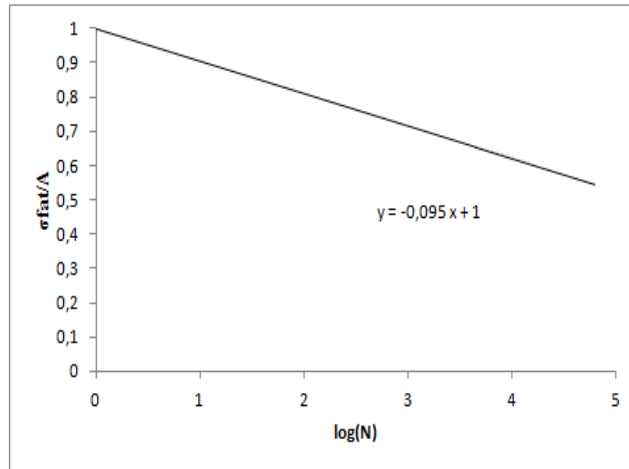


Fig. 2. Normalized curve of Wöhler.

3. Conclusions

- The fatigue lifetime t_r of these composite materials results show a significant scatter.
- Le dommage en fatigue dans ces matériaux est caractérisé par des mécanismes complexes comme, la microfissuration de la matrice, la décohésion fibre/matrice, le délaminage. Ce comportement rend la prévision des durées de vie en fatigue très difficile.
- The general trend of the experimental results on a wide range of number of cycles in the field of the limited endurance shows a convergence of the models of Hwang and Hanf, Wöhler and Basquin around the experimental points
- The straight line of Wöhler remains an interesting approach for its simplicity and offers of the middle part an often acceptable representation in view of the significant dispersif aspect of the material lifetime results.

References

- [1] W. Boukharouba, A. Bezazi, F. Scarpa " Identification and prediction of cyclic fatigue behavior on sandwich panels", Measurement, 53, 2014, pp.161-170.
- [2] Gonzalo M. Dominguez Almaraz. « Prediction of very high cycle fatigue failure for high strength steels, based on the inclusion geometrical properties » Mechanics of Material 40 ,2008, 636-640.
- [3] B. Soh Fotsing, E. maronne, N. Nadjitonon, J.-L. Robert. Intégration d'une démarche fiabiliste dans l'exploitation des critères de fatigue multiaxiaux. 23ème Journée de Printemps de la Commission de Fatigue, du 25 au 26 mai 2004.
- [4] N. Ngarmaïm, B. Tikri, B. Bassa, N. Kimtanger, F. Pennec & J-L. Robert « A New Expression of the Curve S-N in Fatigue based on the Concept of the "Weakest Link" of Weibull » Global Journal of Researches in Engineering: A Mechanical and Mechanics Engineering Volume 14 Issue 3 Version 1.0 2014, pp 21- 26.
- [5] Krawczak P., « Essais des plastiques renforcés », Techniques de l'Ingénieur, traité plastiques et composites, AM5 405, p.8, 26 pages, Doc. 1-10.
- [6] J.F. Mandell, D.D. Huang, F.J. Mc Garry, ASTM STP 772, B.A. Sanders Editor, 1982, pp. 3-32.

REPAIRED CRACK IN AL7075T6 STRUCTURES SUBJECTED TO UNIAXIAL AND EQUIBIAXIAL LOADING

H. Fekirini¹, F. Bouafia^{1,2}, M. Khodja³, L. Zouambi^{1,3,*}

*1*University of SidiBel AbbesLMPM, Department of Mechanical Engineering, 22000, Ben M'hidi City, Algeria

*2*University of Temouchent, 46000, Temouchent, Algeria

*3*University Center of Relizane, 48000, Relizane, Algeria

Abstract: This paper presents a numerical study of the stresses distribution in the bonded repair of Aluminium 7075T6 structure having circular notch damaged by cracking and repaired by bonded composite patch in boron/epoxy with FM73 adhesive. The finite elements model is used to compute the shear stress in the adhesive according to the crack propagation in the plate. However, we compare the effect of the composite patch and plate under uniaxial and equibiaxial loadings on the integral J. The best results are given by the orientation of 0° angle in different ply after evaluation different number of orientation angles. It is ineffective to increase the number of ply in the case of patches where the fiber orientation in the ply is the same. The adhesive layer is more resistant to equibiaxial tension loading as that of uniaxial tension. Which reduces the risk of rupture of this layer thus increasing the life of the damaged structure.

Keywords: FM73 Adhesive, boron/epoxy composite patch, Aluminium 7075T6 plate, uniaxial and equibiaxial loading, crack tip.

1. Introduction

One application that has gained favorable attention in recent years is the use of composites for patches in the repair of cracks in aluminum structures [1] by epoxide adhesive FM73 to increase their service life. However, several studies have been done; W. K. Chiu and R. Jones. [2] discuss the use of a unified constitutive model to predict the behaviour of a thermoset adhesive, FM73. A finite element based study using ABAQUS Software 6.13 focuses on the repair of Al7075-T6 based structures containing a circular notch exhibiting cracking and Boron/epoxy repair patch bonded to the structure with an FM73 epoxy film adhesive layer.

2. Effect of Plies Number of laminated composite patch

We note that the total thickness of the patch is constant regardless of the number of plies. The best results are given by the orientation of 0° angle in different ply after evaluation different number of orientation angles [3-5]. The effect of this number on the performance of the repair is negligible and therefore it is unnecessary to increase the number of plies.

3. Conclusions

The best results of the integral J are given by the orientation of 0° angle in different ply after evaluation different number of orientation angles. It is ineffective to increase the number of ply in the case of patches where the fiber orientation in the ply is the same. The patch and adhesive layer are more resistant to equibiaxial tension loading as that of uniaxial tension. Which reduces the risk of rupture of this layer thus increasing the life of the damaged structure. Comparatively to the plate, the level of these stresses is very significant for the equiaxial loading.

* Corresponding author

E-mail address: zouambileila@yahoo.com

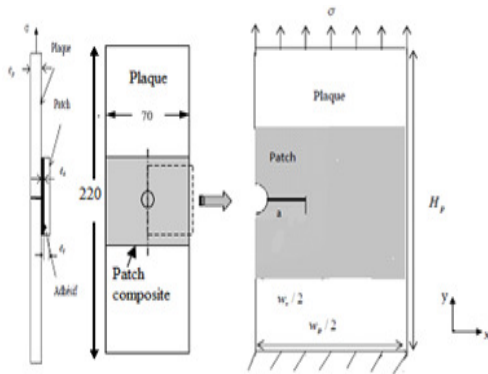


Fig. 1. Geometric model

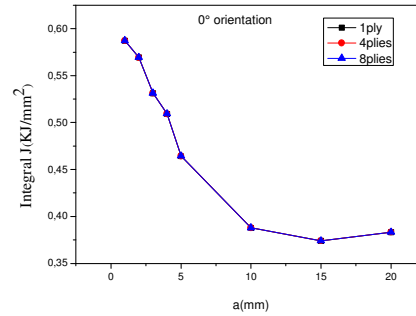


Fig. 2. Variation of the integral J according the crack length (a) 0° orientation

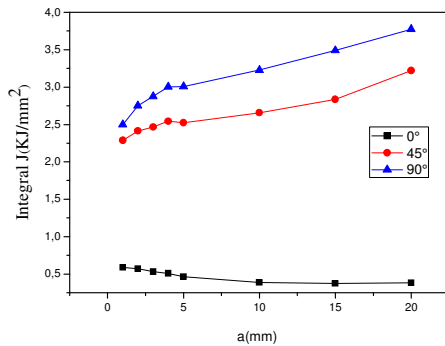


Fig. 3. Variation of the integral J according the crack length for different plies number: (b)

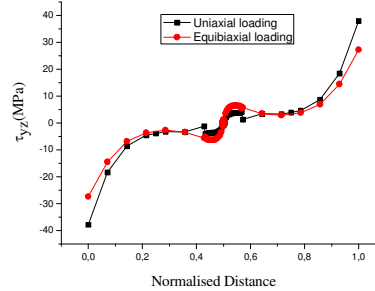


Fig. 4. Variation of the τ_{yz} stress in the adhesive under uniaxial and equibiaxial loading

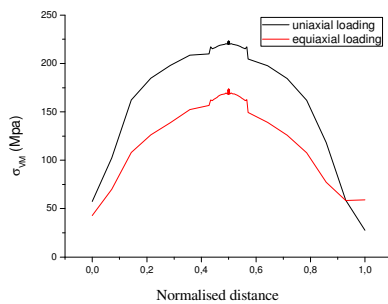


Fig. 5. Variation of the Von Mises stress in the composite patch under uniaxial and equibiaxial loading

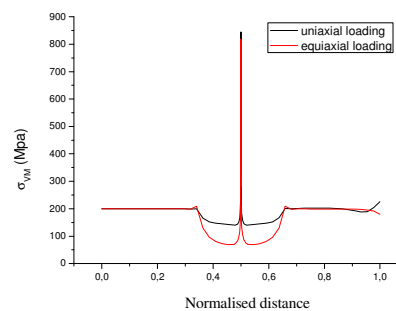


Fig. 6. Variation of the Von Mises stress in the plate under uniaxial and equibiaxial loading for

References

- [1] Kwon, Y.W. and Hall, B.L. (2015), "Analyses of cracks in thick stiffened plates repaired with single sided composite patch", Composite Structures, 119, 727-737.
- [2] Chiu, W. K. and Jones, R. (1995), "Unified constitutive model for thermoset adhesive, FM73", int. j. adhesion and adhesives, 15(3), 131-136.

- [3] SemihBenli and OnurSayman (2011), "The Effects of Temperature and Thermal Stresses on Impact Damage in Laminated Composites", *Mathematical and Computational Applications*, 16(2), 392-403.

EXPERIMENTAL ANALYSIS OF AGING POLY-METHYL-METHACRYLATE PMMA

A. Kaddouri ^{1,9}, S. Ramdoun ¹, N. Serier ¹, k. Kaddouri ¹, B. Serier ¹
1 University Sidi Bel-Abbes, LMPM Mechanical Engineering Department, 22000, Algeria.

Abstract: In general, the behavior of polymers depends on the conditions of their commissioning. Their use leads to long term, usually, to their damage by aging effect. This is an alteration of the mechanical properties, physical and chemical with or without modification of the chemical structure of polymeric materials. The lifespan of these materials is primarily determined by such alteration. Several scientific studies have been devoted to the analysis of aging on the mechanical behavior of polymers. Thus, F. Namouchi and all [1], have studied the effect of heat aging on the electrical properties of Poly Methyl Methacrylate (PMMA). These authors showed that such aging promotes oxidation. O. D. Gonzales and all [2], studied the effect of water content on the optical stress coefficient samples PMMA subjected to forces uniaxial tension. This study shows that this coefficient varies according to the water content. Y. Minhyuk and all [3] analyzed, using silicon micro measures diverter gate, he effect of physical aging on the thermomechanical properties of PS-PMMA polymer. This study showed that the polystyrene PS and PMMA polymers have interacted during the transition from the glass. Our study comes within this context and aims of the experimental analysis of aging on the mechanical properties of PMMA. The effect of temperature, of the environment (sea water, water, UV radiation, solar radiation) have been demonstrated in this work. The mechanical properties have been analyzed in terms of variation of Young's modulus, and break strain, and the strain at break. We show that these physical parameters have been degraded. The degree of degradation is closely related to the nature of the medium. This study is done in order to correlate the diffusion coefficient to damage PMMA.

Keywords: PMMA, UV radiation, aging, mechanical properties.

1. Introduction

By their chemical physico properties, their ease of forming and economic benefits. The polymers are materials of particular interest to the industry. However, the polymers aging is a technological obstacle that opposes their use on an industrial scale in strategic areas. For this, we must initiate and develop research on polymers that become potentially interesting for the industry as ignorance of their durability makes them often limited employment.

2. The mass of water absorbed poly-methyl-methacrylate (PMMA) aged in sea water and fresh water

The water absorption by the polymer was determined in terms of mass change of samples in (fig.1).

Indeed, these were weighed in an ultra-sensitive balance with an accuracy microgram before and after immersion in water; before being tested in tension in (fig2). Mass gain corresponds indirectly to the amount of water absorbed by the material is shown in fig.1.

⁹ Corresponding author

E-mail address: kaddouri.af@gmail.com

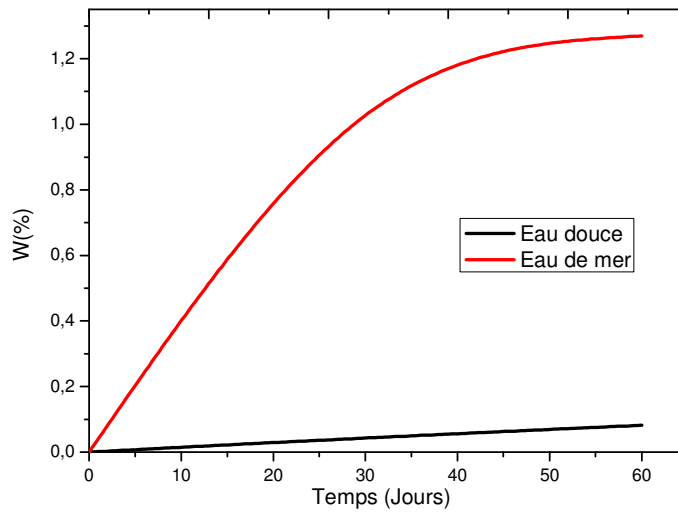


Fig1 comparing the mass of water absorbed PMMA aged to fresh water and sea water



Fig2 Traction test

3.Conclusion

It is concluded that immersion in treated seawater generates greater weight gain than that of fresh water. This shows that the distribution of seawater in the polymethyl methacrylate PMMA is more accelerated than that of fresh water.

References

- [1] F. Namouchi, H. Smaoui, N. Fourati, C. Zerrouki, H. Guerhazi, Bonnet. (2009). J. Alloys and Compounds, Vol. 469, P. 197-202.
- [2] O. D. Gonzales, A. Nicassio, V. Eliasson. (2016). Journal Polymer testing, Vol.50, P. 119-124.
- [3] Minhyuk Y., N. Jung, C. Yim, S. Jeon. J. Polymer,(2011). Vol. (52) P. 4136-4140.

BIOMECHANICAL STUDY OF THE EFFECTS OF THE INLET WAVE FORMS ON THE HEMODYNAMICS INSIDE A PATIENT SPECIFIC CIRCLE OF WILLIS.

D. Sekhane¹, K. Mansour^{1,2}

1 Laboratory of Electronic Materials Study for Medical Applications – Université des frères Mentouri – Constantine 1- Algeria

2 Medical school of Constantine. University Constantine 3 – Chalet des pins – Constantine – Algeria

Abstract: Hemodynamics has important role in the generation of several cerebrovascular diseases. Information about the hemodynamic factors inside a normal cerebral arteries are necessary to understand the providing potential causes of some pathologies inside the cerebral arteries. The aim of this work is to assess the influence of different inlet waveforms flow rates on the hemodynamic factors inside complete healthy circle of Willis (CoW) using patient specific magnetic resonance images (MRI) combined with computational fluid dynamic tool. To study the influence of the inlet waveform we performed a Time Of Flight (TOF) Magnetic Resonance Angiography (MRA) sequence for a young person using GE HDxt system (General Electric Healthcare). The sequence was used to create a 3D surface geometry of the CoW. The geometry obtained was imported to COMSOL Multiphysics software to solve Navies stokes equations in the geometry of interest using finite elements methods. Four inlet flow rate waveforms were used in the simulation. We compared the effect of these waveforms on the arterial pressure, Wall Shear Stress (WSS) and the velocity field stream lines at the systolic time. Results shows that the inlet waveforms have a important influence on the different hemodynamic factors values found, for example the relative difference of the pressure can reach 40%, for the WSS is 26%, and for the velocity 32%. The result found may help to understand the mechanisms of genesis, and the progression of some cerebrovascular diseases.

Keywords: CFD, WSS, Pressure, Hemodynamic, COMSOL Multiphysics.

1. Introduction

Since its introduction, patient specific images combined with Computational fluid dynamic tool (CFD) has been utilized as an alternative tool to predict flow patterns inside various complex geometries [1]. In this work, the effect of different waveforms inlet boundary condition on different hemodynamic factors has been investigated. It was found that the inlet waveform have important effect of the different hemodynamic factors studied which may be a potential cause of the genesis of some cerebrovascular diseases.

2. Material and methods

a- vascular model: Patient specific images of the circle of Willis were obtained from Magnetic Resonance Angiography (MRA), using 3D Time Of Flight (TOF) sequence with the following parameters: TE=3.1ms, TR=25ms and slice thickness=1.4mm. The sequence images was gathered, and the interest zone was truncated, finally a 3D surface geometry of the principal segments of the Circle of Willis (CoW) was obtained for the study fig1.

b- Mathematical and blood model: flowing blood inside the geometry of interest is modelled with Navies-Stokes equation written:

$$\rho \left(\frac{\partial u}{\partial t} + u \cdot \nabla u \right) = -\nabla p + \nabla \left(\mu (\nabla u + (\nabla u)^T) - \frac{3}{2} \mu (\nabla \cdot u) I \right) + F \quad (1)$$

Where ρ is the density, u the velocity and μ the dynamic viscosity. The blood is considered Newtonian and incompressible with a density $\rho=1060\text{kg/m}^3$ and dynamic viscosity $\mu=4\text{mPa.s}$ [2].

Four inlet flow rate waveforms were used in the simulation. We compared the effect of these waveforms on the arterial pressure, Wall Shear Stress (WSS) and the velocity field stream lines at the systolic time.

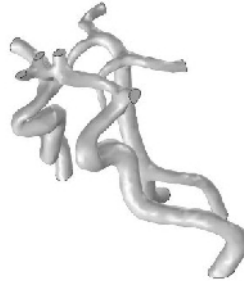


Fig. 1. 3D surface geometry of the circle of willis

3. Results

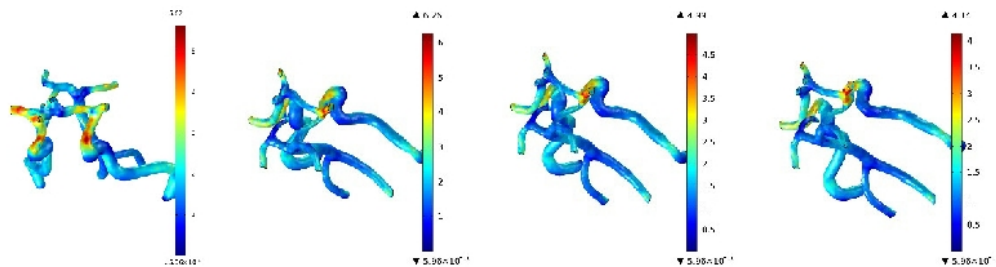


Fig. 2. Simulation results: WSS distribution for the different inlet waveform.

4. Conclusions

In this study we used patient specific images combined with a computational fluid dynamics tool to study the effects of different waveforms on different hemodynamic parameters inside a healthy complete CoW. The results show that the different hemodynamic parameters studied are highly influenced by the inlet waveform.

References

- [1] V. C. Rispoli, J. F. Nielsen, K. S. Nayak et al., "Computational fluid dynamics simulations of blood flow regularized by 3D phase contrast MRI," Biomedical engineering online, vol. 14, no. 1, pp. 110, 2015.
- [2] Y. Hua, J. H. Oh, and Y. B. Kim, "Influence of Parent Artery Segmentation and Boundary Conditions on Hemodynamic Characteristics of Intracranial Aneurysms," Yonsei medical journal, vol. 56, no. 5, pp. 1328-1337, 2015.

PREDICTION OF RESIDUAL FATIGUE LIFE IN REPAIRED CRACKED AL-ALLOY PLATE

F.Z. Seriani¹, N. Benachour¹, M. Benachour¹, M. Benguediab²

1 Laboratoire d'Ingénierie des Systèmes Mécaniques & Matériaux : IS2M

Département de Génie Mécanique, Université de Tlemcen

2 Laboratoire de Matériaux et Systèmes Réactifs, Département de Génie Mécanique

Faculté de Technologie, Université de Sidi Bel Abbès

Abstract: The adhesively bonded composite repair is an efficient and cost-effective method to repair and extend the fatigue life of cracked components in all structures and especially in advanced aerospace structures. In this paper fatigue life of repaired Al-alloy cracked plate was predicted using Nasgro equation when prediction methodology of fatigue life is detailed. Additionally, stress ratio associated with and without patch repair was studied in order to show their influence on fatigue life. Results have shown beneficial effect of patch repair on extension of fatigue life.

Keywords: composite patch repair, graphite/epoxy, fatigue crack, stress ratio, Al-alloy

1. Introduction

Structures, especially the fuselages of aircraft, automotive and car body sheet, are made with aluminum alloys. These structures are subjected to cyclic loading during navigation which consequently leads to damage and creating cracks. The present work covers studying of the fatigue crack growth of a single-sided composite patch repair by Graphite/Epoxy as applied on cracked M(T) specimen in 7075 T73 Al-alloy. Additionally, effect of stress ratio is investigated and a comparison in fatigue life is made between repaired and un-repaired aluminum plate.

2. Methodology in production in fatigue life

In this work we have used AFGROW code [1]. This code allows simulation of fatigue crack growth in opening mode. Tensile plate specimen M (T) is subjected to uniform tensile cyclic load for investigation of effect of repaired structures with composite patch repair. Geometrical parameters of tested specimens are indicated on Fig. 1.

The stress intensity factor " ΔK " for Middle tensile specimen with internal through crack is implemented in AFGROW code. The equation of this factor depends on several parameters and is written below (Eq. 1):

$$\Delta K = \sigma \cdot \sqrt{\pi \cdot a} \cdot f(a/w) \quad (1)$$

where σ is the remote uniform tensile stress, $f(a/w)$ is the crack shape factor correction.

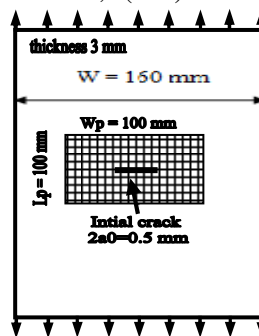


Figure. 1 Patched Al-alloy plate

Patched with six plies (06) and un-patched M(T) specimen with through crack are subjected to a constant cyclic loading ($\sigma_{max} = 100 \text{ MPa}$) for three stress ratio ($R=0.1$; 0.2 and 0.4). The maximal stress intensity "Kmax" criterion was adopted for the limit of crack growth. In prediction of fatigue crack growth for repaired and un-repaired plate NASGRO equation developed by Forman and Mettu is applied for prediction of fatigue life. Results in figure 2 shown that that the fatigue crack growth is also affected by the presence of patch. For example, at $R=0.4$, the fatigue life un-repaired plate is about 93000 cycles for maximum cracked length 28.7 mm but for repaired crack by composite patch, the fatigue life is increased to 123000 cycles for maximum cracked length of 48 mm.

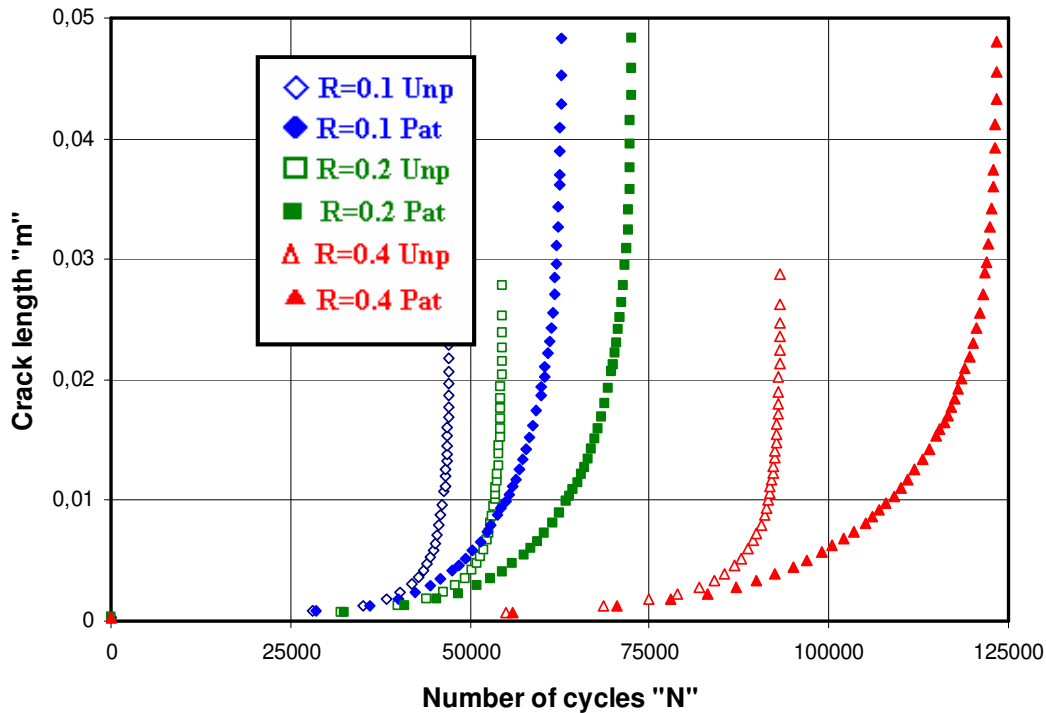


Figure2. Effect of patch repair and stress ratio "R" on fatigue life in M(T) Aluminium alloy plate

3. Conclusion

Fatigue crack growth behavior of cracked plate with bonded composite patch repair was investigated through empirical study with numerical integration. This study involved fatigue behavior of 3 mm thin specimens with center crack M(T) un-repaired and repaired with four directional Graphite/Epoxy patch. This investigation is performed on 2024 T351 Al-alloy used strongly in aerospace structures. Conclusions from this study are cited below:

The fatigue life in repaired cracked plate is increased for all stress ratios.

Ratios in the fatigue life between in repaired and un-repaired plate vary from 1.32 to 1.33. This shown that the fatigue life was increased with 25% and the presence of composite patch repair present beneficial effect on fatigue life.

The fatigue life for the two cases (repaired and un-repaired plate) was affected by stress ratio.

References

- Harter JA. AFGROW users guide and technical manual: AFGROW for Windows 2K/XP. Version 4.0011.14, Air Force Research Laboratory, 2006.
Forman, R.G., Mettu, S.R., In ASTM STP 1131 edited by Ernst, H.A. et al., 1992, 519-546.

FRACTURE BEHAVIOR MODELING OF A 3D CRACK EMANATED FROM BONY INCLUSION IN THE CEMENT PMMA OF TOTAL HIP REPLACEMENT.

M. Cherfi¹, S. Benbarek¹, A. Sahli¹

1University of Sidi Bel Abbes, BP 89, cite Ben M'hidi, Sidi Bel Abbes, 22000, Algeria

Abstract: In orthopedic surgery and in particular in total hip arthroplasty, the implant fixation is carried out using a surgical cement called polymethylmethacrylate (PMMA). This cement has to insure a good adhesion between implant and bone and a good load distribution to the bone. By its fragile nature, the cement can easily break when it is subjected to a high stress gradient by presenting a craze zone in the vicinity of inclusion. The focus of this study is to analyze the effect of inclusion in some zone of cement in which the loading condition can lead to the crack opening leading to their propagation and consequently the aseptic loosening of the THR. In this study, the fracture behavior of the bone cement including a strange body (bone remain) from which the onset of a crack is supposed. The effect of loading condition, the geometry, the presence of both crack and inclusion on the stress distribution and the fracture behavior of the cement. Results show that the highest stresses are located around the sharp tip of bony inclusion. Most critical cracks are located in the middle of the cement mantle when they are subjected to one leg standing state loading during walking.

Keywords: finite element method, total hip replacement, bone cement, biomechanics, bony inclusion, stress intensity factor, submodeling technique.

1. Introduction

The implantation of total hip prosthesis in the human body is a surgical intervention, which requires medical accuracy and more important to that the reliability of total hip prosthesis's components [1,2]. To ensure a good functionality of the cement to reach its expected target (long lifespan); the analysis of the cement is primordial to determine the zones where the crack can appear [3,4]. The arthroplasty is an operation intended to get back the mobility of the articulation, muscle forces, ligaments and other structures constituting the human tissue, which control this articulation by creating a new articular space. It has a target to release the patient from a debilitating pain, bring back a movement and some time corrects a malformation [5]. In the THR, the prosthesis may be sealed with cement or without cement to the bone. In this study, we are interested in the cemented total hip replacement (THR). The acrylic bone cement (PMMA) used in orthopedic surgery (in the mechanical point of view) is the weakest element in the load transfer chain: stem-cement-bone. Therefore, this material is the first responsible of the lifespan of the THR.

2. Geometrical model and Boundary conditions

The obtaining of the 3D solid model of the patient consists in taking images of the interested area using the medical image technique (CT-scan). From these images, one designed this geometrical model using both softwares Solidworks and Amira. The cement has a uniform 2mm thickness around acetabulum.

In this study we took a load in the case of a stumbling patient. This act generates a load of 7 times of a 70 kg human body weight. Contacts between the various components of the THR are considered as stiff and continuous.

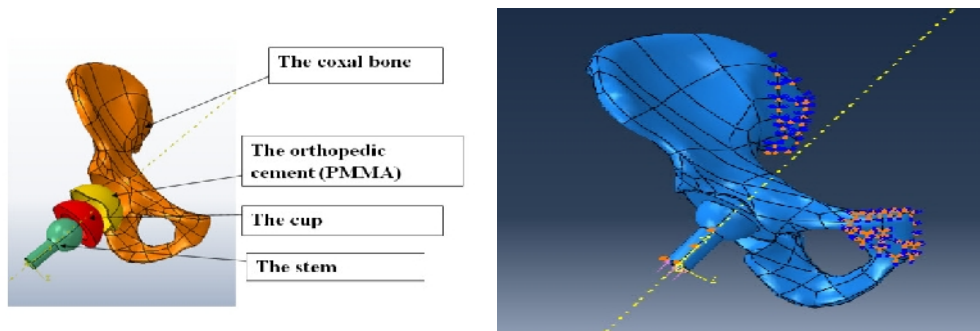
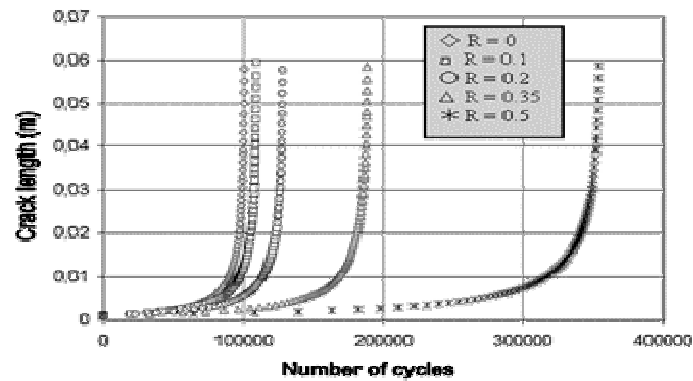


Fig. 1. Geometrical model and boundary conditions.

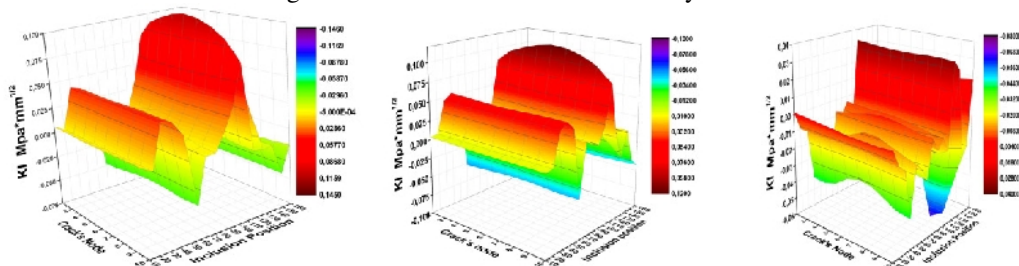


Fig. 2. Distribution of the KI along the crack front according to the inclusion positions (0° , -23° , $+23^\circ$).

3. Conclusions

The loading and the geometry influence directly on the stress state of the orthopedic cement, the stress can be between 16Mpa and 22Mpa. The stem position, (the human body posture), has great effect on the stress state of the orthopedic cement. The first stem position and a radial inclusion position make cement in the highest stress state a head of the bony inclusion that can lead to the crack initiation at this position. When the bony inclusion is oriented toward the radial direction in the radial system, concentrates the stress a head of the inclusion. Stress positions which provoke most risk correspond to 2nd position (23° forward).

References

- [1] C. Naudin and N. Grumbach, Larousse medicale, Larousse,2002.
- [2] F. Pauwels, Atlas zur Biomechanik der gesunden und kranken H'ufte. Springer Verlag, Berlin, 1973.
- [3] D. Merckx, Les ciments orthopediques dans la conception des protheses articulaires. Biomecanique et biomateriaux, Cahiers d'enseignement de la SOFCOT, Expansion scientifique francaise 44 (1993) 67-76.
- [4] J. Tong, K.Y. Wong, Mixed Mode Fracture in Reconstructed Acetabulum, Department of Mechanical and design Engineering, University of Portsmouth, Anglesea road, Portsmouth, PO1 3 DJ, UK.
- [5] R. Huiskes, Failed innovation in total hip replacement, Acta Orthop Scand 64 (1993), 699-716.

Numerical study of low temperature combustion strategies

A. Bendriss^{1,2}, C. Kezrane², Y. Lasbet², M. Makhlouf¹

1 Department of Mechanical Engineering, Sidi-Bel-Abbès University

2 LDMM, University of Djelfa, BP : 3117 Djelfa

Abstract: Low Temperature Combustion (LTC) process is a promising method to decrease NO_x and Soot emissions with low fuel consumption. In this study, a sample CI engine was simulated. After validating the simulated results by comparing with experimental data, the compression ignition was changed into LTC mode. The early injection can create homogeneous air and fuel mixture and advance the changing of fuel to lower hydrocarbons. Also poor and rich fuel was injected in the cylinder and their combustions were compared. It was found that the ignition timing and air-fuel equivalence ratio could control low and high temperature reactions. External EGR can delay the start of combustion effectively, which is very useful for diesel LTC because these fuels can be easily self-ignited and make the start of combustion earlier. Results showed it is possible to gain less pollutions and better performances and optimize the LTC by changing various parameters.

Key words: Low Temperature, Combustion, Emission, Engine

1. Introduction

The main goal in operating ICE homogeneously and leanly is to reduce fuel consumption and to minimize amount of emissions. This latter, can be achieved by using LTC mode which improves emission problems because of its clean burning characteristics (Darrow, 1994) [1]. Regarding to emissions matter, LTC has been the subject of growing interest as an alternative mode to conventional automotive engine.

2. Analysis Methods

In the present work we opt for the Zero-dimensional Thermo-Kinetic Models. Models of this type utilize a single-zone approach to modeling the in-cylinder gases. There are a large number of efforts in this area. The first law of thermodynamics is applied to a homogeneous mixture of in-cylinder gases. The effects of the fluid mechanics are not directly considered except, in some cases, when deriving relevant heat transfer coefficients..

3. Results

The simulated model of CI engine was actuated for several engine speeds and the output information was validated by experimental data. The low and high temperature reaction peak of the heat release rate for SOI between 100° and 30° crank angle can be seen in Fig.1 and Fig.2 .

4. Conclusions

The study was carried out to predict the LTC behavior to improve the efficiency and reduce the pollution of the engine. The results showed that for LTC engine, since ignition occurred in compression ignition mood and the mixture of fuel and air are homogenous, by changing the various parameters and optimizing LTC, it is possible to reach more promising efficiency with less pollution for the engine. The start of combustion outran when fuel was injected earlier and it caused some increases in cylinder pressure and temperature, increases in Soot emissions and decreases in NO_x emissions. Both NO_x and Soot emissions increased due to the rises of equivalence ratio. But it does not result in elevating thermal efficiency.

References

- [1] Darrow, K. G. (1994). Light duty vehicle full fuel cycle emissions analysis: topical report (April 1993-April 1994). Gas Research Institute.

MODELISATION OF THE OPTICAL GAIN IN GAN/GA0.8 AL0.2N/SIC QUANTUM WELL LASERS UNDER STRESS

B. Bouabdallah¹, A.OumSalem², Z.Nabi¹, Y. Bourezig³, S.Kheris¹, B. Benichou³,
O.Benhelal¹, A.Ridah⁴

1 Condensed Matter and Sustainable Development Laboratory, Physics Department, University of Sidi-Bel-Abbès, 22000 Sidi-Bel-Abbès, Algeria

2 Laboratory of Theoretical Physics and material physics, Chlef University, Algeria.

3 Materials Elaboration and Characterization Laboratory, Electronic's Department, University Djillali Liabès, Sidi Bel Abbès, Algeria.

4 LIMAT Laboratory, University Hassan II of Casablanca, Physics Department Casablanca. Morocco

Abstract: The semiconductor's physics, the electronic and optoelectronics components know an immense development. Since the invention of the bipolar transistor, the principal electronic devices are made of Silicon. However, Silicon is not always suitable; in particular in the realization of optical sources because of its indirect band gap. Materials based on Nitride as GaN, InN, AlN, and their alloys are best alternatives. They are used to realise the short wavelength light emitters operating in the region of blue to ultraviolet (U.V), because they have wide direct band gap at room temperature. Quantum well lasers have been developed extensively since they have many advantages, such as very low threshold current density, large modulation band-width, narrow static and dynamic line width, high output power and high lasing temperature. The proposed model is validated on reduced sizes heterostructures (quantum well lasers) based on nitride materials, GaN/Ga_{0.8}Al_{0.2}N/SiC SQW lasers structure under strain (stress) where we detailed the calculation of the optical gain in such a system. Based on these materials (III-N and SiC), the technological development of lasers diode predicts in advance good results considering the good qualities awaited by using the heterostructure GaN/Ga_{1-x}Al_xN and Ga_{1-x}Al_xN/SiC. We have found a low lattice mismatch of GaN and AlN on SiC which is about 3.4% and 0.9% indicating that silicon carbide presents a potential substrate for III-N materials.

Keywords: strain, compressive stress, tensile stress, optical gain.

References

- [1] Ambacher, O., W. Rieger, P. Ansmann, H. Angerer, T.D. Moustakas, M. Stutzman, Sol. State Commun. 97(5) (1996), 365-370.
- [2] W. Fang and S.L. Chuang. Appl. Phys. Lett 67 (6), (1995); 751.
- [3] Yong. Nian. Xu and W.Y. Ching. Phys. Rev B48, (1993), 4335.
- [4] Akasaki, I., H. Amano, ed. Edgar J.H., EMIS Datareviews Series, N11, (1994), an INSPEC publication, 30-34.
- [5] Morkoc, H. Nitride Semiconductors and Devices, Springer Series in Materials Science, Vol. 32, Springer, Berlin, 1999.
- [6] Piotr Perlin, et al. MRS Internet Journal of Nitride Semiconductor Research., 9 (2004).
- [7] M. A. Khan, R. A. Skogman, and J. M. Van Hove, Appl. Phys. Lett., 56 (1990) 1257-1259.
- [8] S. Strite and H. Morkoç., J. Vac. Sci. Technol. B, vol. 10, pp. 1237-1266, 1992.
- [9] P.W.A, McLlroy, A.Kurobe, and Y. Suematsu., IEEE.J.Quantum.Electron., vol 21, (1985), 1958.
- [10] K.J.Vahala and C.E.Zah., Appl.Phys.Phys., vol 52. (1988), 1945
- [11] N.K. Dutta. J.Appl.Phys. 53(11), November 1982. P 7211.
- [12] G. H. B. Thompson: Physics of Semiconductor Laser Devices (Wiley, Chichester, 1980) Chapter 2
- [13] H.C.Casey Jr, and M.B.Panish, Heterostructure lasers, Academic New York, (1978), chap 7.
- [14] W.T.Tsang, Appl.Phys.Lett., Vol. 39, n°2, (1981), 134.
- [15] W.Streifer, R.D.Burnham et D.R.Sciffres. Opt. Lett., Vol. 8, (1983). 283.

ELASTIC ANALYSES OF THE PIPELINE API X65 REPAIRED WITH COMPOSITE OVERWRAP

D. Belhadri, W. Oudad, H. Fekirini

Univ Ctr of Ain Temouchent Smart Structures Laboratory (SSL) Po Box 284, 46000, Algeria.

Djamelins@hotmail.fr

Abstract: In the last 15 years, glass fiber hoop reinforced composite systems emerged as an acceptable, successful method for repairing corroded and mechanically-damaged onshore pipelines where the primary load is internal pressure. The objective of this study was to compare the performance of the repaired rectangular cracks in API X65 pipelines assuming that the material is elastic. The three-dimensional finite element method (FEM) was used to compute the stress intensity factors (SIF) at the crack tip. Repairing cracks under internal pressure using carbon-epoxy composites was investigated where the influence of the depth and the length of the crack, the length of the overwrapping composite and its thickness, and a variation of a mechanical loading were included. In the evaluation of the repair of the pipeline, the failure assessment diagram (FAD) was introduced to obtain the safety factor value. The outcome guided and led to admit that the value of the factor of safety depends on the geometry of the crack and the pressure. In addition, the results showed that the composite gives a best benefit where the length of the overwrapping is between 200-300% of the pipe thickness.

Keywords: API5LX65, composite, J integral, FAD, crack, SINTAP

LIPOLYTIC BACTERIA USE AS BIO-DECONTAMINATING NATURAL IN THE WATER PURIFICATION STATIONS

L. Hachemi¹, M. E. Belgherras², Z. Benattouche³

1, 3University of Mascara, (LBMSS), city Elkararma. Mascara, Algeria.

2University of Sidi bel Abbes, Mechanics and Physics of Materials Laboratory, Djillali Liabes University of Sidi Bel-Abbes, BP89 cité Larbi Ben M'hidi, Sidi Bel-Abbes, Algeria.

laliahachemi@yahoo.fr

Abstract: Different samples were collected from polluted waters by fat materials in the Mascara region for the isolation of bacterial strains capable of degrading fat materials. The objective of this work is the search for new bacterial lipases for biotechnological application that we chose to isolate from polluted water waste fats from slaughterhouses lipolytic bacteria to characterize their microbiological properties and used in the production of extracellular lipase by the fermentation method. A total of two strains were isolated at 37°C from the sample water rich slaughterhouses fat materials. Production of extracellular bacterial lipase was studied as a function of several inductors of lipid nature by the fermentation method. The enzyme activity reached a maximum value, in the presence of olive oil as inducer and glucose as the carbon source and energy at pH = 7.2 at 30 ° C and agitation 125 rpm *Pseudomonas* sp (40 mmol / ml.72h) *Streptococcus* sp (47µmol / ml .72h). The enzyme was purified by precipitation with ammonium sulfate in a yield of 63.73% and 50% in *Streptococcus* sp and *Pseudomonas* sp respectively. The lipase produced by these two bacteria is resistant to 50°C and is strongly inhibited in the presence of 1 mmol Zn + 2 and Mg + 2.

Keywords: bacteria, lipase enzyme, production, fermentation, Purification.

1. Introduction

Industrial waste and fat derived from plants cause irreversible environmental disaster (pollution of water, soil and air). Biological methods use microorganisms to degrade as biodepolluants fat ecological way. [5]

2. Experimental procedure

1. Biological materials: The two bacterial strains used in this study were isolated from sewage water from slaughterhouses.
2. 2. Identification of lipolytic bacteria: We used Sierra method [1]
2. 3. Production of lipase enzyme (fermentation) : Enzyme production is sought in the first place according to several sources carbone. Six media types with various compositions were studied [3]
2. 4. Determination of biomass and lipolytic activity : By applying the law of beer lambert [8]. The determination of biomass g / l is done every 24 (C = DO / ϵ). The lipolytic enzyme activity was measured by the titrimetric method. [2]

3. RESULTS

3. 1. Isolation lipolytic strains:

Among these strains were selected on the basis of its lipase production capacity force.

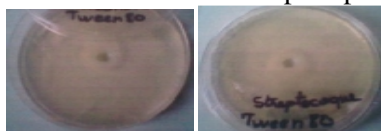


Fig .3. Detection of lipase activity in *Pseudomonas* sp and *Streptococcus* sp.

* Corresponding author

E-mail address: laliahachemi@yahoo.fr

3. 2. Determination of the biomass and lipolytic activity of the inoculum : From the results obtained, the medium of olive oil is favorable to maximize production of the lipase.

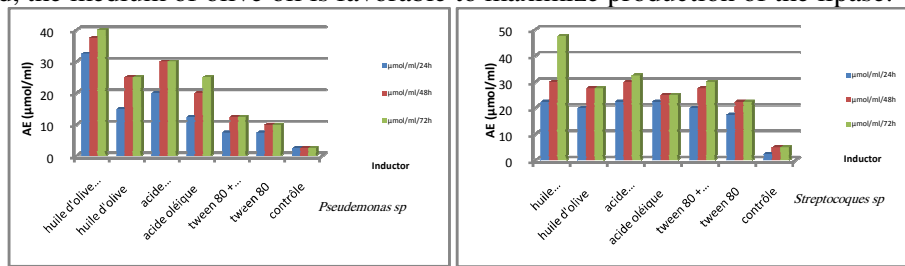


Fig.5. The lipolytic activity during the period of fermentation in ($\mu\text{mol/ml}$).

The results obtained show that the olive oil is effective in inducing the lipase.

3. 4. Purification :

4. 2. The redement and the degree of purity :The purification of the enzyme by precipitation with ammonium sulphate is accomplished by a yield of 63.73 % on Streptocoques sp and 50% for Pseudemona sp.

5. Study of some physicochemical parameters

According to the results, it appears that the purified lipase enzyme is stable at 50°C with a decrease in activity to 13.79 and 51.5 % for Streptococcus sp and Pseudemona sp respectively. Concerning enzyme effectors, the lipase enzyme is strongly inhibited in the presence of $\text{Zn} + 2$ ions and no effect against not detected in the presence of $\text{Ca} + 2$ ions.

4. Conclusion

The two strains studied were selected for their significant lipolytic activity.

Achieving lipase activity ($47 \mu\text{mol} / \text{ml}.72\text{h}$) ; ($40 \mu\text{mol} / \text{ml}.72\text{h}$) for Steptocoques sp and sp Pseudemona sp respectively in the presence of olive oil and glucose at pH 7.2 and 30°C with stirring at 125 rpm .

Both enzymes produced by Streptococcus sp and Pseudemona sp were found resistant (stable) at 50°C pendant 30 minutes with 13.79% of decrease in activity and 51.51 % respectively. So this little enzyme used for the degradation of this waste grease in the warm thermal waters.

So lipase extracted from these little bacteria used as biological decontaminating waters rich in fatty waste or as detergents industries.

References

- [1] A. Delmotte, 1958. L'activite lipolytique microbienne decelee par la methode de Sierra avec reference speciale au *M. pyogenes* var. *aureus*. Journal of Antonie van Leeuwenhoek. Vol 24, Issue 1, pp 309-320
- [2] MA Kashmiri, A Adnan, BW Butt., 2006. Production, purification and partial characterization of lipase from Trichoderma Viride. African Journal of Biotechnology. Vol 5, No 10.
- [3] S.Couri, A.X. Farias., 1995. Genetic manipulation of Aspergillus niger for increased synthesis of pectinolytic enzymes. Rev. Microbiol. 26 (4): 314-317.
- [4] Camacho RM, Mateos JC, Reynoso OG, Prado LA, Codova J., 2009. Production and characterization of esterase and lipase from Haloarcula marismortui. J. Ind. Microbiol. Biotechnol. 36: 901-909.
- [5] Samir CHENNOUF, André MOUREY, Gérard KILBERTUS LERMAB-Microbiologie., 1995. Biodegradation des lipides e t suivi d e l a microflore lipolytique dans des composts

Topic B

CORROSION AND PROTECTION OF CRUDE GAS PRODUCTION AERIAL FACILITIES IN HASSI R'MEL FIELD

K. Gharbi^{1,*}, K. Benyounes^{1,2}, S. Chouicha², O. Bouledroua³

1M'Hamed Bougara University, LGPH, Faculty of hydrocarbons and chemistry, 35000, Boumerdes, Algeria

2Kasdi Merbah University, LENRZA, Faculty of applied sciences, 30000, Ouargla, Algeria

3Hassiba Benbouali University, LPTPM, Faculty of sciences, 02000, Chlef, Algeria

Abstract: Corrosion of crude gas production facilities in HASSI R'Mel manifests inside aerial installations, and this is detected by the corrosion inspection techniques at HR field, in order to reduce the harmful consequences of this problem by the injection of corrosion inhibitor. The study of corrosion inhibitors (chemical A and chemical B) shows that the efficiency of the inhibitor A equals 99,17% with an optimized injection rate at 0,5 litre/million sm³, and the efficiency of the inhibitor B is 85% with an injection rate optimized at 1,02litre/million sm³.

Keywords: Corrosion, production, Hassi R'Mel, inspection, inhibitor.

1. Introduction

Corrosion is the most widespread degradation phenomenon in the hydrocarbons production; it is the origin of the majority pressure equipment failure. Garcia-Arriaga et al [1] reported that the economic costs associated to the corrosion of natural gas processing plants and oil refining plants range between 10% and 30% of the maintenance budget.

In the petroleum and gas fields, the large problem in operating pipe flow lines is the deterioration of pipes because of the internal corrosion. Martinez et al [2] claim that the combination of corrosion and erosion is the main problem in pipe deterioration.

This problem of corrosion manifests inside production aerial facilities of crude gas in Hassi R'Mel field, like piercing and bursting pipes, loss of the fluid circulation, leading to production interruptions and higher costs. Generally the origin of this corrosion in this field is complex; it is triggered by the presence of carbon dioxide (about 0.20 mol% of the crude gas composition) in favorable operating conditions causing the formation of carbonic acid H₂CO₃ and therefore the initiation of corrosion.

2. Application of corrosion inhibitors for production aerial facilities of crude gas in Hassi R'Mel field

The main results obtained after the use of each inhibitor A and B are summarized in the following table:

Table. 1. Results of use of each inhibitor

	Chemical A	Chemical B
Corrosion velocity before inhibitor injection ($\mu\text{m}/\text{an}$)	1200	400
Corrosion velocity after inhibitor injection ($\mu\text{m}/\text{an}$)	10	60
Inhibitor efficiency (%)	99,17	85
Inhibitor injection flow rate (litre / million sm ³)	0,5	1,02
Deposits formation	No	At the treatment plant installations
foaming	No	No

* Corresponding author

E-mail address: gharbikheira17@gmail.com

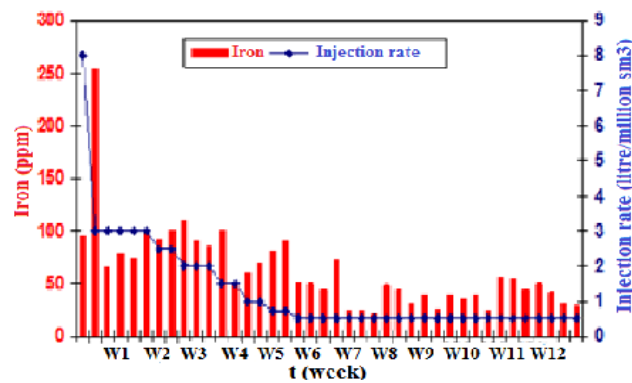


Fig. 1. The evolution of the iron tenor according to the injection of chemical A.

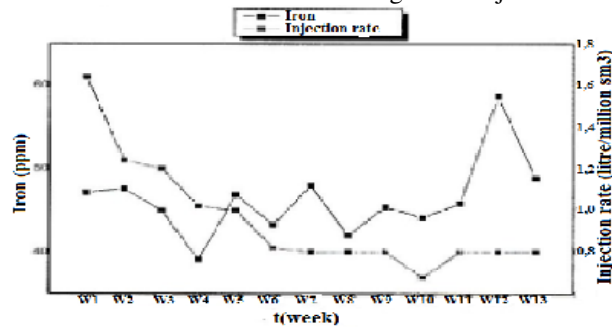


Fig. 2. The evolution of the iron tenor according to the injection of chemical B.

3. Conclusions

The corrosion of the crude gas production facilities in Hassi R'Mel occurs inside aerial facilities by chemical attack of H_2CO_3 , which causes perforations facilities leading to leaks effluent and subsequently to disturbances in the production of the crude gas at Hassi R'Mel field.

Detection of the corrosion problem in the HR field is through the application of specific inspection techniques essentially represented in the chemical laboratory analysis and nondestructive test by piping thicknesses measurement using ultrasound, and therefore it allows us to assess the efficiency of the corrosion inhibitor.

The study of corrosion inhibitors for aerial installations shows that the efficiency of chemical equals to 99,17% with an optimized injection rate to 0,5 liter / sm³ million, and the efficiency of chemical B is 85% with a rate of injection optimized to 1,02 liter / sm³ million. The impact of corrosion inhibitors was analyzed by the chemical examination of pH and iron tenor of the associated water to the effluent, and the piping thicknesses control gave us a good result following the inhibitors used.

References

- [1] Garcia-Arriaga V. (2010). H₂S and O₂ influence on the corrosion of carbon steel immersed in a solution containing 3 M diethanolamine, Corrosion Science.
- [2] Martinez D. (2009). Amine type inhibitor effect on corrosion-erosion wear in oil gas pipes, Wear.

CORROSION AND SCALE GREEN INHIBITORS ON CORROSION EFFECTS ON THE FRACTURE MECHANICS PROPERTIES OF GAS PIPELINES

M. Ould Mbereick¹, M. Hadj Meliani^{1,2}, El-Miloudi Khaled³, C.Fares¹, M.A.Benghalia¹
1LPTPM, FSSI, HassibaBenBouali University of Chlef, Esalem City, 02000, Chlef, Algeria.

2LaBPS-ENIM, île de saulcy 57045, Université Paul Verlaine de Metz, France.

Hassiba Ben Bouali University of Chlef, Algeria

E-mail : mohamedmbeirick@outlook.fr

Abstract: The impact of environment can cause many types of degradations such as pitting corrosion, stress corrosion cracking and sulphide stress cracking of metal structures and one of the serious problems of oil extracting industry is the corrosion process. Recently there were number of assets failures, caused by internal corrosion, recorded in oil and gas industry, the reports confirmed that the failures were due to the effect of traces HCl. Our objectives are to use the plant extracts, such as corrosion inhibitors. Indeed, these natural extracts contain many families of natural organic compounds "Green", readily available and renewable. The mechanics tests carried out on this study of anti-corrosive properties of natural products of plant origin will be to given so far promising results on the fracture mechanics properties. The importance of this area of research is mainly related to the fact that natural products can replace toxic organic molecules present condemned by the world directives for environmentally unacceptable.

Keywords: Corrosion, Green Inhibitors, Failure, Fracture Mechanics, Pipelines HCl acid.

1. Introduction

In this paper we are study influence of the corrosion inhibitors, of the steel grade APL 5L X 65 manufactures for SONETRACH. For this study we are use sour HCl (our aggressive environment). In this paper we are do tow experiment study, in the first experimental we are studied influence of our aggressive environment in the absence of corrosion inhibitors by different concentration of the sour HCl. On the second experimental we are study efficacy of corrosion inhibitors in the same aggressive environment with different concentration for the corrosion inhibitors and our aggressive environment HCl. In this part when we have corrosion inhibitors, we are presented influence of the concentration inhibitors, influence of immersion time of the corrosion rate, variation the energy of rupture of the specimens as a function of immersion time, and finally we are presented evolution of the mechanical properties in three-point bending .

2. Experimental study

2.1 Study in the absence of inhibitors

In this section we studied the influence of the concentration of hydrochloric acid on the corrosion of metal that for the following concentrations 0.25M, 0.5M, 0.75M, 1 M with same time (7 days) immersed in this different concentration. The try are performed after, 6heurs 5days, 10days and 15days of immersion. Table 3 gives the values of the fracture energies in the different concentration acid measured energy to rupture of the specimens when the pendulum tests.

Tab.2: Variation of the fracture energies of the steel relative to the concentration of hydrochloric acid HCl.

Concentration (%)	0.25	0.5	0.75	1
Energy (Joules)	195	180	175	150

Study in the presence inhibitors

In this section we studied the effect of extract of *Ruta Chalpensis* on corrosion of API 5L X65 steel in acidic medium for different concentration. The experimental conditions used are on room temperature of 25 °C with the concentration of 1M HCl acid. The measurements are made after 6 hours, 5days, 10 days, and 15 days of immersion at room temperature. Table 3 gives the values of the energies required to break the test pieces measured at the Charpy test for 5%, 20%, and 30% concentrations of inhibitor in 1M hydrochloric acid medium.

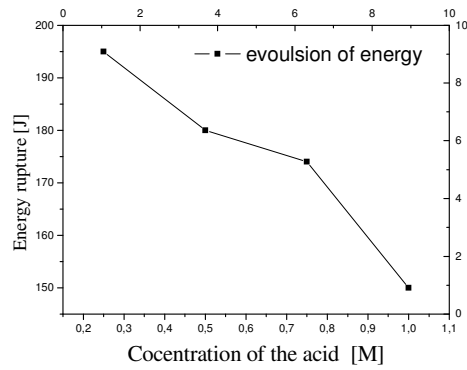


Fig .1.Variation of the energy of ruptur of the specimens according to the time of immersed in HCl acid.

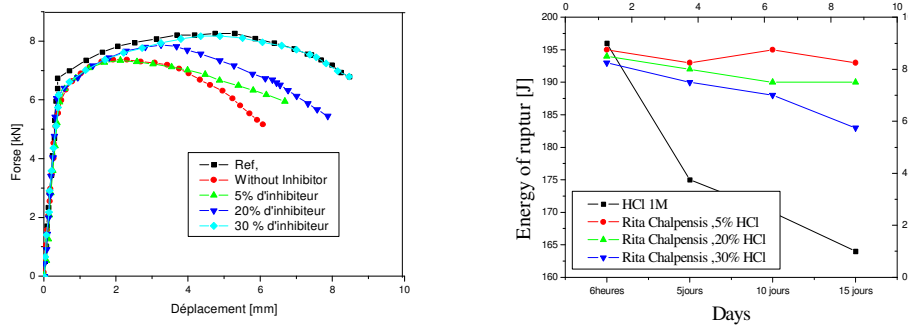


Fig. 2. Evolution of energy fractures of the specimens according to deferent concentrations of Rita Chalpensis. And curve forced displacement for different concentrations of inhibitor

3. Conclusions

This work is devoted to the development of a formulation of corrosion inhibitor used to protect our material. It consists of natural extract of a plant known as the *Rita Chalpensis*. We present the results obtained in the experimental study on the effect of inhibiting the natural extract *Chalpensis Rita* and their interpretations. In the first part, we studied the effect of the concentration of the inhibitor in the aggressive environment (1M HCl acid) on the protective power. In the second part, we are interested in the influence of immersion time on the protective power of the inhibitor. In part of this work we decided to measure the samples breaking energy.

References

- [1] A. M. Abdel-Gaber, B.A. Abd-El-Nabey, E. Khamis, D.E. Abd-El-Khalek. A natural extract as scale and corrosion inhibitor for steel surface in brine solution. *Desalination*. vol. 278, Issue 1-2, pp. 337-342, 2011.
- [2] Salasi, M.; Sharabi, T.; Roayaei, E.; Aliofkhaezrai, M. "The electrochemical behaviour of environment-friendly inhibitors of silicate and phosphonate in corrosion control of carbon steel in soft water media," *Materials Chemistry and physics*, vol. 104, Issue 1, pp. 183-190, 2007.

EXPERIMENTAL STUDY FOR CORROSION INHIBITION OF CARBON STEEL IN ACIDIC MEDIUM

R. Mehdaoui^{1,*}, O. Aaboubi², K. Chouchane¹, A. Khadraoui¹, A. Khelifa¹, O. Aaboubi²

1 Laboratoire de Génie Chimique (LGC), Département de Chimie industrielle, Université de Blida1, B.P. 270, Route de Soumaa 09000, Blida, Algeria.

2 Laboratoire d'Ingénierie et Sciences des Matériaux (LISM), UFR Sciences, BP1039, 51687 Reims Cedex2, France.

E-mail address: mehdaouiraz@yahoo.fr (R. Mehdaoui)

Abstract: The effects of newly synthesized anionic surfactants of two Algerian petroleum fractions: GOS and KES on the corrosion of carbon steel in 1.0 M HCl were investigated using potentiodynamic polarization, electrochemical impedance spectroscopy and scanning electron microscopy (SEM). All measurements showed that the inhibition efficiency increased with increase in the concentration of inhibitor and the effectiveness of these inhibitors was in the order of: GOS > KES. Polarization curves revealed that the studied inhibitors were mixed type inhibitors. Electrochemical impedance spectroscopy technique exhibit one capacitive loop indicating that, the corrosion reaction is controlled by charge transfer process.

Keywords: Corrosion inhibitors, Carbon steel, Electrochemical techniques, SEM.

1. Introduction

Steel corrosion protection in acidic media is of great important for both, industrial facilities and theoretical aspects. Acid solutions are widely used for removal of undesirable scale and rust in many industrial processes. Inhibitors used generally in these processes to control metal dissolution. Among all inhibitors, the most important are the organic ones containing electronegative atoms, unsaturated bonds and plane conjugated systems including all kinds of aromatic cycles; they control corrosion by acting over the anodic or the cathodic surface or both.

In the present investigation two new surfactants: gasoil sulfonate (GOS) and kerosene sulfonate (KES), have been synthesized from Algerian petroleum fractions [1]. The detailed study of surfactants effect on the corrosion of carbon steel in 1.0 M HCl solution was conducted by using potentiodynamic polarization, impedance spectroscopy and scanning electron microscope SEM.

2. Results and discussion

The corrosion behavior of carbon steel in 1.0 M HCl solution at 298 K, in the absence and presence of Algerian petroleum fractions KES GOS, was investigated using the electrochemical impedance spectroscopy (EIS) at 298 K. Nyquist plots of carbon steel in uninhibited and inhibited acidic solutions (1.0 M HCl) containing various concentrations of GOS are given in Fig. 1. The Nyquist plots contain depressed semi-circles with their center located under the real axis, and their size increases with inhibitor concentration, indicating a charge transfer process, mainly controlling the corrosion of carbon steel [2]. In the Bode plots Fig. 2, only one time constant of charge transfer and double layer capacitance were observed.

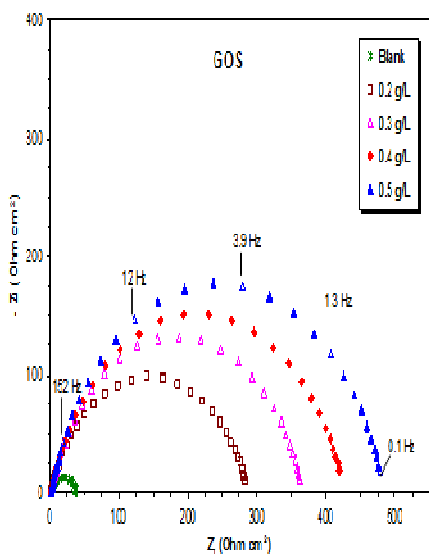


Figure 1. Nyquist plots of the corrosion of carbon steel with different concentrations of GOS at 298 K steel

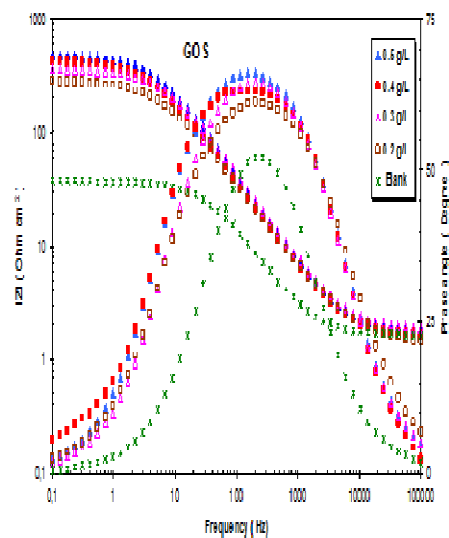


Figure 2. Bode and phase plots of carbon steel in the presence of different concentrations of GOS.

The carbon steel surface in the absence of inhibitor was highly corroded due to aggressive acid. The images taken in the presence of inhibitors show a smooth surface consisting of less pits. This surface property ensures a high degree of protection for the carbon steel surface by inhibitors as shown in Fig. 3 .

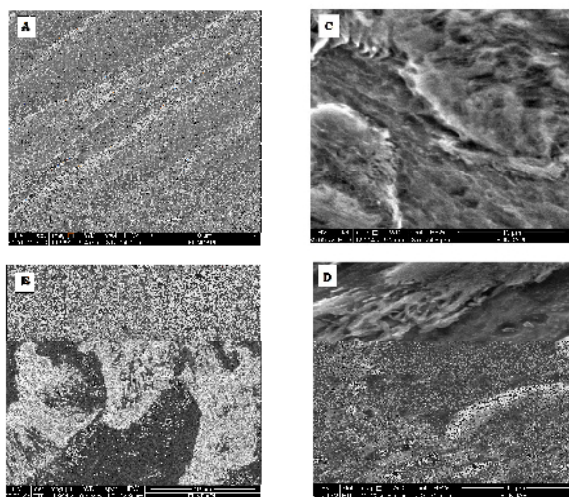


Figure 3. SEM images of carbon steel samples: (A) after polishing, after 24 h of immersion in 1.0 M HCl in the absence of inhibitor (B), in the presence of GOS (C), and in the presence of KES (D).

References

- [1] R. Mehdaoui, A. Khelifa, O. Aaboubi, Res. Chem. Intermed. 41 (2015) 705.
- [2] A. Khadraoui, A. Khelifa, M. Hadjmeliiani , R. Mehdaoui ,Journal of Molecular Liquids, DOI: 10.1016/j.molliq.2015.12.064 (2015).

REDUCTION OF ALKALI SILICA REACTION RISK IN CONCRETE BY GROUND GRANULATED BLAST-FURNACE SLAG

Z. Douaïssia¹, M.F.Habita²

1,2Badji Mokhtar university, Génie Civi laboratory, BP12, Sidi Amar, Annaba, Algeria.

Abstract: The one of significant concerns at designs of durable mortars is alkali silica reaction (ASR). The capillary cracks have formed by ASR increases to permeability of concrete, reduces the strength and lowers the economic lifetime of concrete. The use of mineral and chemical admixtures to prevent expansion due to the alkali-silica reaction (ASR) was first reported 40 to 50 years ago. In this paper, a comprehensive experimental research was carried out to prevent the damages to be able to improve in the reactive aggregated concrete structures by using the ground granulated blast-furnace slag (GGBFS) in the mixtures. Furthermore, the engineering properties of blast-furnace slag, comparison with the other types of mineral additives and the test methodology used in the research were presented and the research findings were also discussed. The alkali silica reaction (ASR) in mortar and the effect of ground granulated blast-furnace slag were studied, The replacement of cement by blast-furnace slag can prevent the alkali-aggregate reaction from causing large expansion in concrete.

Keywords: Alkali-aggregate reaction; Expansion; Aggregate; Cement; Granulated blast-furnace slag.

1. Introduction

Many references concern the use of ground admixtures added to mixtures containing a reactive aggregate coming from a different source, particularly Hobbs [1] and Swamy[2].

The aim of this paper is to verify whether ground granulated blast-furnace slag (GGBS) is an efficient and general solution to counteract ASR expansion. Tests were performed on concrete using two reactive aggregates.

The binder was an ordinary Portland cement, CEM I 52,5R with a moderately high Na₂O_{eq} content (0.8%), Two aggregates were chosen :

- A siliceous limestone (H), mainly composed of calcite
- A crushed waste glass (G), resulting from the crushing of window glasses.

Ground slag (S) is obtained by crushing and sieving at 0,08 mm. In order to study the influence of fineness in counteracting expansion, the slag material is ground to different specific surface (Blaine), which are S1: 100 m² / kg, S2: 400 m² / kg and S3: 600 m² / kg.

2. Mortar tests

The mortar test was an accelerated method using an autoclave apparatus (French Standard P18-594 [3]). This test consisted of measuring the length variations of mortar prisms (4 x 4 x 16 cm) doped with alkalis after a treatment lasting 5 h at 127°C and 0,15 MPa. Mortars had a water/cement ratio of 0,5 and an aggregate/cement ratio of 2,0. The first series of tests were performed on mortars containing only cement, water and reactive aggregates For the second series, cement has been substituted with increasing percentage (by mass) was replaced by the ground slag : 10, 20 and 30% of different finenesses ranging from 200 to 600 m²/kg (Blaine), After 17 weeks of curing, we measured the compressive strength (f_c) of each mortar .

* Corresponding author

E-mail address: douaissiazinebgc@gmail.com

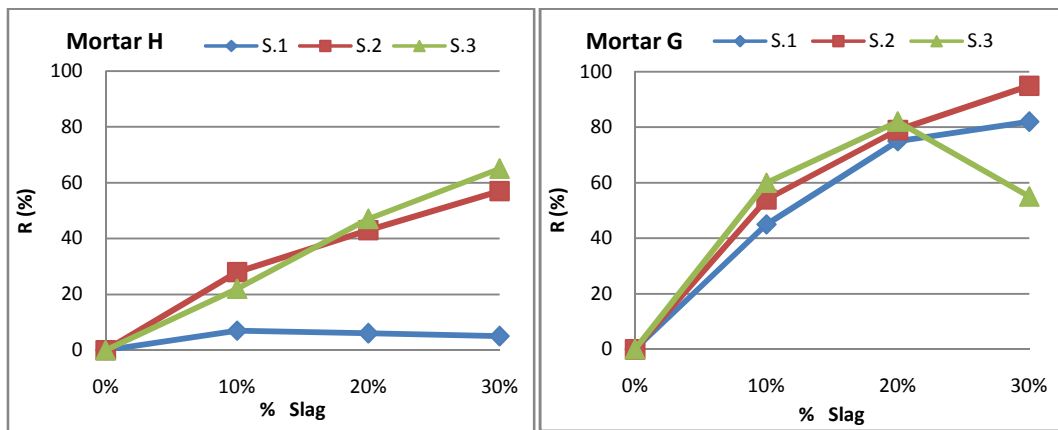


Fig. 1. Reduction of expansion (R%) of mortar versus amount and fineness of slag.

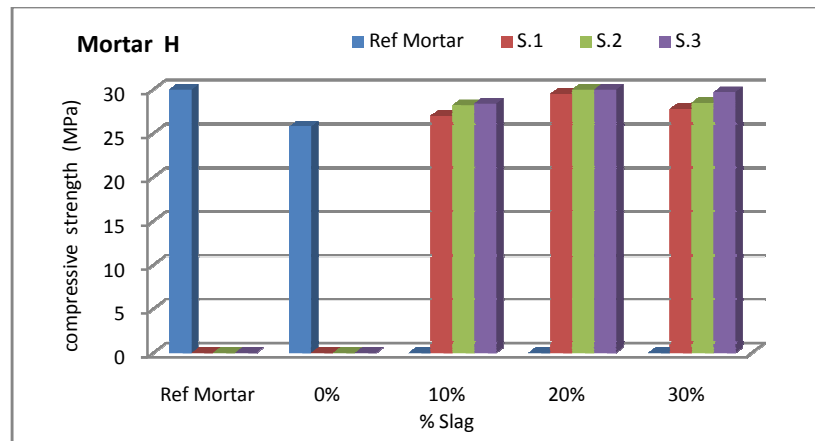


Fig. 2. Slag effect on the compressive strength of mortars

3. Conclusions

The results of the autoclave expansion tests performed on the mortars are given in Figure 1, They confirm that The use of ground slag decreased the expansion of mortars. However, their activity depended on the fineness and quantity used. The main results from compressive tests are reported in Figure 2, we note that :

- The addition of alkali , which causes expansion , occasions a reduction in strength .
- The increasing substitution rate leads to an increase in strength.
- Differences in strength resulting from two antagonistic actions: the alkali-silica reaction that tends to lower the strength, and slag, which probably by a reaction similar to a pozzolanic reaction, increase this strength.
- The slag beneficial effect is measurable by comparing the mortars strength gains with different rate of slag 10%, 20% and 30%, which is 7 MPa, 20 MPa and 16 MPa respectively, mortar strength to 30% of slag is higher than that obtained by the reference mortar did not damaged by alkali-silica reaction.

References

- [1] Hobbs D.W (1989), Effect of mineral and chemical admixtures on alkali aggregate reaction, 8th ICAAR, Kyoto, Japan.
- [2] R.N.Swamy and M.M. Al-Asali (1989), Effectiveness of mineral admixtures in controlling ASR expansion. 8th ICAAR, Kyoto, Japan.
- [3] AFNOR (2004) NF XP P 18-594, Aggregates –Test methods on reactivity to alkalis.

EFFECT OF WELDING CURRENT ON MECHANICAL BEHAVIOR OF RESISTANCE SPOT WELDING OF STAINLESS STEEL 304 L SHEETS

M. Benachour^{1,2,*}, M. Larbi Cherif¹

¹University of Tlemcen, Mechanical Engineering Department, 1300, Tlemcen, Algeria.

²Ingeniery of Mechanical System an Materials Laboratory, University of Tlemcen, 13000, Tlemcen, Algeria

Abstract: In this investigation, 304 L stainless steel sheets were welded by resistance spot welding (RSW) under variation of welding parameters. The sheets were overlay in distance of 30 mm. the welding current varies from 10 KA to 15 KA. The obtained results showed that the parameters, effort and welding time have little effect on mechanical properties compared with respect to the effect of the welding current. The experimental results show also that the welding current is an important parameter for joining structures and its mechanical strength.

Keywords: resistance spot welding, stainless steel, welding current, tensile strength.

1. Introduction

Resistance spot welding process is the joining method used in several industries especially in assembling automobile, furniture and domestic equipment. Stainless steel in special case is used in furniture and domestic equipments. The weld process can be described by a time, current and welding force. The welding current is the most effective and common parameter to influence welding result of a given material configuration. Researchers in welding process by RSW have shown that the formation of nugget in any material depends on optimised combination of spot welding parameters [1, 2]. The effects of welding parameters on the tensile shear strength of the joints were investigated by Qui et al. [3]. The effects of welding current on the mechanical properties of welded joint were investigated by Shawon et al. [4]. An increase in tensile strength of the weld coupon was shown in increasing of welding current. In the investigation conducted by Thakur et al. [5] for assembled 1008 Steel Sheets by RSW, they had shown that welding current is most effective parameter controlling the weld tensile strength.

2. Material and specimen

Stainless steel 304 L sheet with thickness of 2.0 mm was used in this study. Fig. 1 shows the shape of specimens. Mechanical properties are given in Table 1 for receive material. It is difficult to give a precise adjustment of the welding parameters.

Table 1. Mechanical characteristics of 304 L stainless steel

E (GPa)	σ_e (MPa)	UTS (MPa)	A%	HRB
190	336	655	43.2	60

Results and discussion

The welded zone is affected by parameters of welding process (RSW) especially on breaking values of assemblies. Figure 2 shows respectively the variation of the load versus displacement until fracture of the welded assembly by RSW for welding loads 8 and 7 bar at $t=10$ cycles. The increasing in welding current increases the area of the plastic deformation but present a random evolution. The curves load/displacement presents several areas. Points "A" present little distorted points. At points "B", rotation of point to align the sheets in the

* Corresponding author

E-mail address: bmf_12002@yahoo.fr

direction of loading and starts necking. Points "C" give the maximum breaking loads and "D" points present the maximum effort achieved when the fracture propagated in the thickness in the necked region of one of the sheets and propagation of fracture in the base metal MB and tear around the point of the specimen to the final rupture. The effect of welding current on the maximum breaking load (points C) for both welding load is given by figures 3a and 3b. The general appearance shows an increase in the breaking load with increasing welding current. To better understand some interactions of welding parameters and random phenomena, statistical tests are necessary and accompanied by analyzes of fracture surfaces at the interfaces.

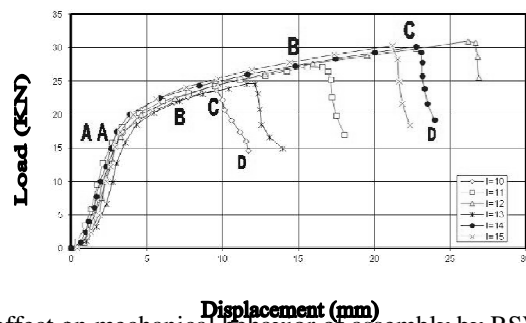


Fig. 1. Welding current effect on mechanical behavior of assembly by RSW at $t=10$ cycles and $F=8$ bar.

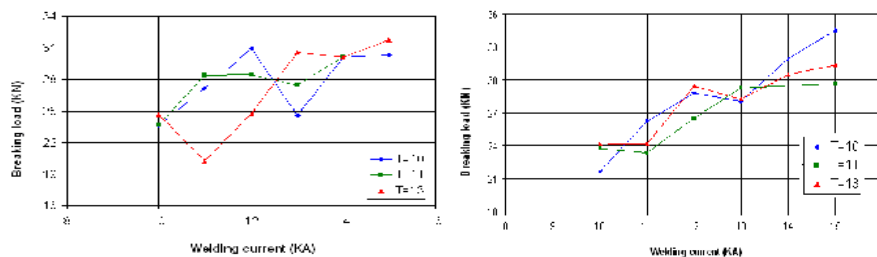


Fig. 2. Effect of welding current on max breaking load at welding force (a) 7 bar (b) 8 bar

3. Conclusions

In this investigation, 304L stainless steels sheets were welded using RSW. The effects of current welding on the tensile shear strength of joint were studied. Tensile/shear tests show that the welding current is dominant parameter over welding time and welding force on the evolution of the load/displacement curves. Also the results show the increases the plastic deformation zone and the breaking load in increasing if welding intensity.

References

- Farizah Adliza G., Yupiter H.P., Manurung, Mohamed Ackiel Mohamed, Siti Khadijah Alias, Shahrum A. (2015), Effect of process parameters on the mechanical properties and failure behavior of spot welded low carbon steel. *J. Mech. Engng. Scie.*, Vol. 8, pp. 1489-1497.
- Charde N., Rajkumar R. (2013), Investigating spot weld growth on 304 austenitic stainless steel sheets". *Journal of Engineering Science and Technology*. Vol. 8, No. 1, pp 69 – 76.
- Qiu R., Zhang Z., Zhang K., Shi H., Ding G. (2011), Influence of welding parameters on the tensile shear strength of aluminum alloy joint welded by RSW. *JMEPEG*, Vol. 20, pp 355–358.
- Shawon M.R.A., Gulshan F., Kurny A.S.W. (2015), Effect of welding current on the structure and properties of resistance spot welded dissimilar (austenitic stainless steel and low carbon steel) metal joints, *J. Inst. Eng. India Ser. D*, Vol. 96 (1), pp 29–36.
- Thakur A.G., Rao T.E., Mukhedkar M.S., Nandedkar V.M. (2010), Application of Taguchi method for RSW of galvanized steel", *J. Engng Appl. Scie.*, vol.5.

MECHANICAL AND NUMERICAL CHARACTERIZATION OF THE MILD STEEL (E235) TUBE UNDER UNIAXIAL COMPRESSION IN QUASI-STATIC REGIME

M.Zerouki^{*1}, M. Haouchine¹, A. Ahmed Ali¹, M.Ould Ouali¹
*1Laboratoire Elaboration et Caractérisation des Matériaux et Modélisation
 Université Mouloud MAMMERRI de Tizi-Ouzou, BP 17 RP, 15000. ALGERIA*

Abstract: In this work, we interested in experimental and numeric study of the mechanical behavior of tubular structures [1] in uniaxial compression (quasi-static regime). Firstly, we characterized the tube of mild steel E235, untreated and not welded, under static conditions (tensile test). Thereafter, the mechanical behavior of the tube under uniaxial compression loading in quasi-static regime is determined experimentally. This behavior is modeled by the law of Johnson-Cook [2] (viscoplastic) implemented in Abaqus/Explicit [3]. A mesh study is made to predict the effect of mesh size on the numeric response. The comparison between the numeric and experimental curves for quantified the numeric response of J-C model.

Keywords: Aabaqus/explicit, crushing tube, Johnson-Cook model, Mild steel.

Introduction

For years, industrial incessantly explore the tubular structures in steels, for their absorptive aspect of energy under compression loading in quasi-static and dynamic regime. This recent work includes the Mechanical characterization and numerical modeling of the crash tubular structures under uniaxial loading in quasi-static regime.

Johnson-cook model

Proposed in 1983 by Johnson and Cook [1]:

$$\sigma = \left(A + B\bar{\epsilon}_{pl}^n \right) \left(1 + C \ln \left(\frac{\dot{\epsilon}_{pl}}{\dot{\epsilon}_0} \right) \right) \left(1 - \left(\frac{T - T_t}{T_{fusion} - T_t} \right)^m \right) \quad (1)$$

Mesh study

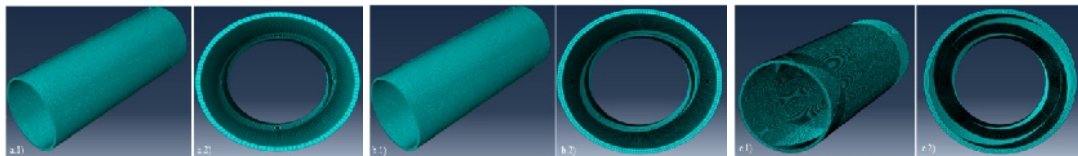


Fig. 1. The mesh size adopted (C3D8R): a) Mesh 1: rude; b) Mesh 2: medium; c) Mesh 3: refined.

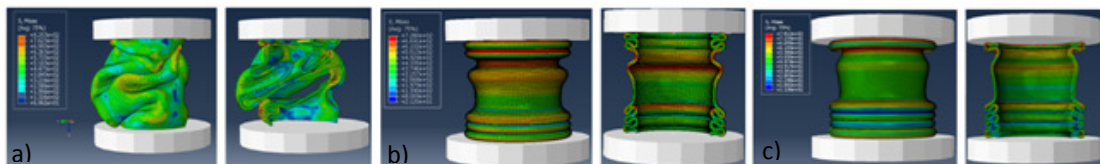


Fig. 2. Tubes after deformation for: a) Mesh 1; b) Mesh 2 and c) Mesh 3.

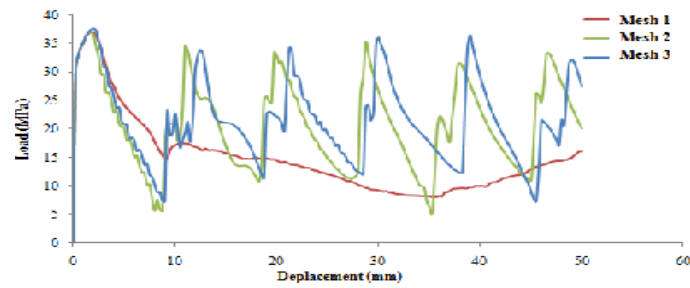


Fig. 3. Comparison of Load/ displacement curves for Mesh 1, Mesh 2 and Mesh 3.

3. Results and discussion

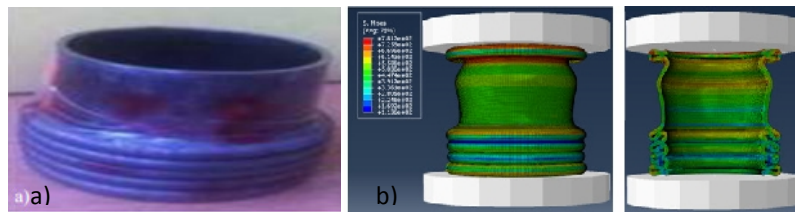


Fig. 4. Comparison between experimental and numerical deformation tube

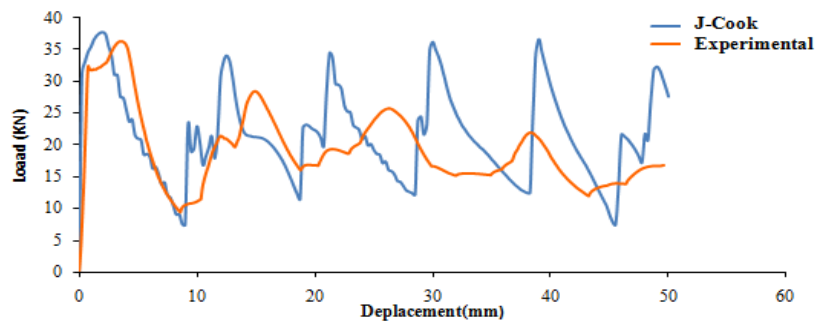


Fig. 5. Comparison between experimental and numerical curve (load-displacement).

Conclusions

According to the results, It was found that:

- The Johnson-Cook numerical model correctly reproduces the mechanical behavior of mild steel E235 under quasi-static compression.
- Mesh size influence on the quality of numerical response: the effect of mesh size is remarkable. The correct numerical reproduction of experimental behavior is observed with a refined specimen. In addition, a coarse mesh can change the overwrite mode (buckling).

References

- [1] WANG Xuguang, Comportement à l'écrasement de structures tubulaires en multi-matériaux, thèse doctorat, Ecole Centrale de Lyon, Novembre 1991.
- [2] G.R. Johnson and W.H. Cook. A constitutive model and data for metals subjected to large strains high strain rates. In Seventh International Symposium on Ballistics, pages 541–547, The Hague, The Netherlands, April 19-21 1983.
- [3] Abaqus standard, version 6.14: Theory manual et Standard user's manual, 2014.

EXPERIMENTAL STUDY OF THE MECHANICAL BEHAVIOR AND KINETICS OF THE MARTENSITIC TRANSFORMATION IN 304L TRIP STEEL: APPLICATION SPOT WELDING

Z. Sidhoum¹⁰, R. Ferhoum^{1,*}, M. Almansba¹¹, R. Bensaada²

¹ Laboratoire Elaboration, Caractérisation des Matériaux et Modélisation (LEC2M), Université Mouloud Mammeri Tizi Ouzou Algeria 15000 algeria

² Laboratoire (LAMOMS), Université Mouloud Mammeri Tizi Ouzou Algeria 15000 algeria

Abstract: In this paper, the effect of different strain on microstructure and mechanical properties of 304L TRIP steel is investigated. So, a tensile test of 304L TRIP steel was carried out at different strain rates. Different tensile tests are performed at 25°C. The microstructure and mechanical properties of 304L TRIP steel are analyzed using Scanning Electron microscopy (SEM), X-ray diffraction and Vickers hardness measurements. The results of Scanning Electron microscopy confirmed that the strain facilitates the formation of martensite even at 25°C, they showed too that the amount of austenite is reduced, and the amount of martensite increases with increasing strain. Secondly, the influence of the annealing treatment on microstructure and mechanical properties of the joint formed by the spot welding are characterized using tensile test, metallographic analysis and Vickers hardness measurements.

Keywords: TRIP steel, mechanical properties, α' -martensite, austenite, Spot welding.

1. Materials.

The material utilized in this work was a cold rolled TRIP sheet steel with the thickness of 3mm. It is characterized by equiaxed γ grains of about 20 μm , containing twins. The microstructure and the X-ray diffraction profiles of this material are given respectively by Fig. 1 and Fig. 2.

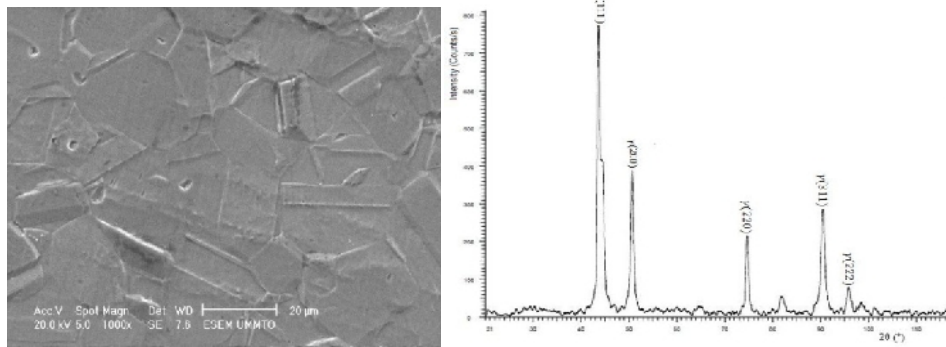


Fig. 1. Microstructure of as received 304L steel Fig. 2. XRD patterns of as received 304L steel

2. Experimental procedure

2.1 tensile tests

Tensile tests were performed on a universal testing machine (Instron 5583). Specimens used for uniaxial tension tests were prepared according to ISO standard 6892 (fig. 3)

* Corresponding author

E-mail address: ferhoum@yahoo.fr

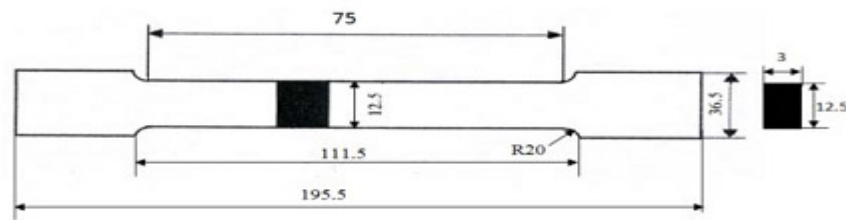


Fig. 3. Geometry of tensile sample (dimension in mm)

2.2. Spot welding

The dimension of sheet are 70 mm length (L), 20 mm width (w) and 3 mm thick (t). Overlap is equal to width of the sheet as per AWS standard. Sheet surfaces were chemically cleaned by acetone before resistance spot welding (effort to 2bar, a welding time of 1.21s and a current of 6.7KA.) to eliminate surface contamination.



Fig. 4. Spot welding specimens

In order to evaluate the effect of the annealing condition on the mechanical and microstructure evolution of the material, the specimens in Fig. 4 were heated at a heating rate of 0.5 Ks⁻¹ to an annealing temperature 850 °C, held there for 120 min, and then cooled down with a cooling rate of 2 Ks⁻¹.

3. Conclusion

In this work, the retention of austenite microstructures of TRIP steel is investigated. The microstructure, particularly retained austenite, is analyzed using electronic microscopy, Vickers hardness measurements, X-ray diffraction. It appears that most of the mechanical properties of 304L are affected. Indeed, significant change in Young's modulus, yield stress, and strain at failure are observed. It is found that after plastic deformation martensitic phase is formed inside the grains in the form of slats packages. The presence of martensite widens to occupy the majority of the grains but with strong heterogeneities and this is with the rise of deformation level. The martensitic transformation is favored in the grains favorably directed compared to the pressure applied.

The spot welding carried out presented defects in the structure such as cavities, pores and impurities which one managed to eliminate by an annealing. The mechanical characteristics obtained after annealing are higher compared to those obtained before annealing. As for hardness it is lower after annealing because annealing is a softening heat treatment.

Numerical analysis of the interaction crack-defect in the cement PMMA

A. Benouis^{1,2*}, A. Boulouar², M. Cherfi³, M. E. Belgherras³, A. Sahli³, B. Serier³
1University of Saida, Bp 138 saida,, Saïda 20000, Algeria.

2Laboratory of Materials and Reactive Systems, Mechanical Engineering Department, University of Sidi-Bel-Abbes, BP. 89, City Larbi Ben Mhidi, Sidi Bel Abbes 22000, Algeria.

3Mechanics and Physics of Materials Laboratory, Mechanical Engineering Department, University of Sidi-Bel-Abbes, BP. 89, City Larbi Ben Mhidi, Sidi Bel Abbes 22000, Algeria.

Abstract: Finite element analysis (FEA) combined with the concepts of Linear Elastic fracture mechanics (LEFM) provides a practical and convenient means to study the fracture and crack growth of materials. In this paper, a numerical modeling of crack propagation in the cement mantle of the reconstructed acetabulum is presented. This work is based on the implementation of the displacement extrapolation method (DEM) and the strain energy density theory in a finite element code. At each crack increment length, the kinking angle is evaluated as a function of stress intensity factors (SIFs). In this paper, we analyzed the mechanical behavior of cracks initiated in the cement mantle by evaluating the SIFs. The effect of the defect on the crack propagation path was highlighted.

Keywords: constraint, Strain energy density; mixed mode; crack propagation; orthopedic cement.

1. Introduction

In the clinical loosening of implants in total hip replacement surgery, fracture of the cement mantle is the main indicated reason [1]. Cracks initiate from micro-voids in cement and propagate due to the cyclic loading of the human body weight during the walking gate cycles [2]. Crack growth analysis is very important to improve the total hip life span. In literature; there has been a little amount of researches carried out in to the crack's growth path in the orthopedic cement, there has been some studies dealing with the fatigue life of orthopedic cement, but not following the crack's growth path [3-6]. Byeongsoo et al. [7] analyzed the fracture parameters (KI, KII and Keff) in a cross section of the femur part of the total hip joint. Benbarek et al [8] used the finite element method to analyze the propagation's path of the crack in the orthopedic cement of the total hip replacement. Results show that the crack propagation's path can be influenced by human body posture.

In linear elastic fracture mechanics, the various fracture criteria for cracks subjected to mixed mode loading have been introduced for the determination of the propagation direction and the critical stress such as maximum tangential stress criterion[6,7,8], maximum principal tangential stress criterion[8], maximum strain criterion[9,10], and strain energy density criterion [11,16]. All these criteria are almost postulated that crack initiation will occur at the crack tip and propagate towards the radial direction.

The strain energy density approach has been found as a powerful tool to assess the static and fatigue behavior of notched and unnotched components in structural engineering [20]. Different SED-based approaches were formulated by many researchers. Labeas et al [21], Zuo et al [22], Nobile et al [23], Balasubramanian and Guha [24], Ayatollahi and Sedighiani [25] and Spyropoulos [26].

The aim of this paper is to present a numerical modeling of crack propagation trajectory in cement of reconstructed acetabulum. Using the Ansys Parametric Design Language (APDL) [27], the direction crack is evaluated as a function of the displacement extrapolation technique and the strain energy density theory. The finite element method is used to carry out

* Corresponding author

E-mail address: alymoh1980@yahoo.fr

this objective. The effect of the inclusions and cavities on the crack propagation in cement orthopedic was highlighted.

2. Results and discussion

2.1 Evolution of Stress intensity factors

For better a study of these parameters, we represented respectively, in Fig. 1a and 1b, the variation of the SIFs KI and KII vs. the inclination angles α , by variation of initial crack size. We note exactly the same behavior of the SIFs KI and KII as in the as in the previous case. In addition, we note that:

The SIF KI increases with the crack length and takes values positive for angles in the range between 90° and -18° , some is the inclination angles α , i.e. it does not depend on the direction of initial crack.

For cracks initiated in the range between -35 and -18° , the factor KI present of the values negative, this can is explained by the existence of the crack in the compression zone.

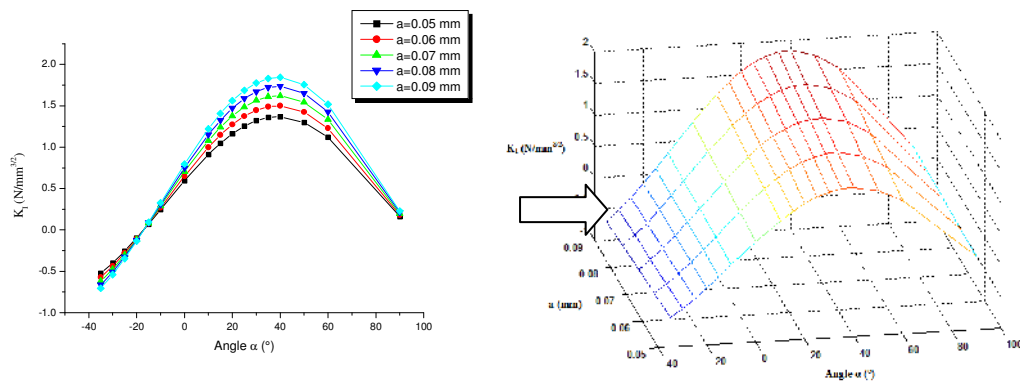


Fig. 1 Variation of SIF KI vs. crack size a and angle α : (a) in 2D and (b) in 3D.

Fig. 2 show that, in the case of the angles α vary between -35° and 90° , the SIF KII takes positive values and its negative values are evaluated in the opposite case, i.e. it depends on the direction of crack orientation. This behavior is seminar with this remark by Boulenouar et al. [52] in the case of cracked plate under mixed mode loading.

The results obtained show that, whatever the crack length, the angle of 40° represents the initial direction of the crack propagation according to the mode-I.

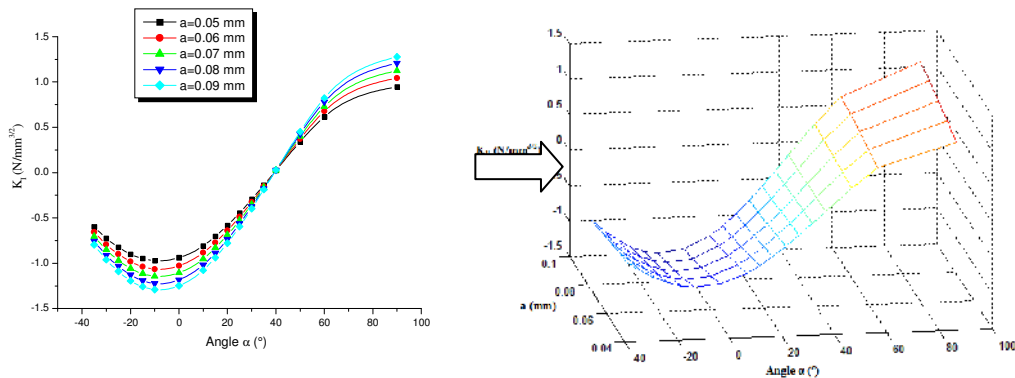


Fig. 2. Variation of SIF KII vs. crack size a and angle α : (a) in 2D and (b) in 3D.

8. Conclusion

In this study, the quarter-point singular elements proposed by Barsoum are used to consider the singularity of stress and deformations fields at crack tip in cement of reconstructed acetabulum.

The displacement extrapolation technique was used to determine the SIFs to predict then the final crack trajectory by evaluation, for each propagation step, the kinked angle using the strain energy density approach.

Numerical calculations made by FEM have shown that the integrated model can correctly describe the stress and deformation field near the crack tip by evaluating the SIFs, and the results are very acceptable on the crack propagation in Biomechanics fracture problems.

The good trajectory of crack under mixed mode conditions is dependent on the crack increment length; over this distance is small, and the closer to the exact solution. The angle of 40° represents the initial direction of the crack propagation according to the opening mode (mode-I) with: $K_I > 0$, $K_{II} = 0$

The implementation of 2D crack propagation process in FE code can account for the influence of inclusions on the path of crack propagation. This feature can be very interesting for propagation in multilayered or in composite parts.

References

- [1] Deb. Sanjukta, Orthopaedic bone cements, Woodhead Publishing in Materials. First publishing, 2008.
- [2] M.A. Pérez, J.M. Garcia-Aznar, M. Doblaré, B. Seral, F. Seral, A comparative FEA of the deboning process in different concepts of cemented hip implants, *Medical Engineering & Physics*, 28 (2006) 525–533.
- [3] Jonathan R.T. Jeffers, Martin Browne, Alexander B. Lennon, Patrick J. Prendergast, Mark Taylor, Cement mantle fatigue failure in total hip replacement: Experimental and computational testing, *Journal of Biomechanics* 40 (2007) 1525–1533.
- [4] P. Colombi, Fatigue analysis of cemented hip prosthesis: damage accumulation scenario and sensitivity analysis, *Int J Fatigue* 24 (7) (2002) 739-746.
- [5] A.B. Lennon, B.A.O. McCormack, P.J. Prendergast, The relationship between cement fatigue damage and implant surface finish in proximal femoral prostheses, *Medical Engineering and Physics* 25 (2003) 833–841.
- [6] B.P. Murphy, P.J. Prendergast, The relationship between stress, porosity and nonlinear damage accumulation in acrylic bone cement, *Journal of Biomedical Materials Research* 59 (2001) 646–654.
- [7] Byeongsoo Kim, Byungyoung Moon, Kenneth A. Mann, Heungseob Kim, Kawng-suck Boo, Simulated crack propagation in cemented total hip replacements, *Materials Science and Engineering A* 483–484 (2008) 306–308.
- [8] Smaïl Benbarek, Bel Abbes Bachir Bouiadjra, Bouziane Mohamed El Mokhtar, Tarik Achour, Boualem Serier, Numerical analysis of the crack growth path in the cement mantle of the reconstructed acetabulum, *Materials Science and Engineering C* 33 (2013) 543-549
- [6] F. Erdogan and G. C. Sih, On the crack extension in plates under plane loading and transverse shear, *J. basic Engng* 85, (1963) 519-527.
- [7] K. J. Chang, Further studies of the maximum stress criterion on the angled crack problem. *Eng. Fract. Mech.* 14, (1981) 125.
- [8] S. K. Maiti and R. A. Smith, Comparison of the criteria for mixed mode brittle fracture based on the preinstability stress-strain field. *Int. J. Fracture* 23 (1983) 281-295.
- [9] H. C. Wu, Dual failure criterion for plane concrete. *J. Eng. Mech. Div. ASCE* 100 (1974) 1167-1181.
- Han-Chin Wu, Dual Failure Criterion for Plain Concrete, *Journal of the Engineering Mechanics Division* Vol. 100 No. 6 November/December (1974) pp. 1167-1181.
- [10] K. J. Chang, On the maximum strain criterion - a new approach to the angled crack problem, *Eng. Fract. Mech.* 14 (1981)107-124.
- [11] G. C. Sih, Strain energy-density factor applied to mixed mode crack problems, *Int. J. Fract.* 10 (1974) 205.
- [12] G. C. Sih, and B. Macdonald, Fracture mechanics applied to engineering problems-Strain energy density fracture criterion, *Eng. Fract. Mech.* 6 (1974) 361-386.

PREDICTING OF VISCOELASTIC DAMAGED BEHAVIOR OF A MULTILAYER COMPOSITE TUBULAR STRUCTURE UNDER A CREEP LOADING

A. Ghouaoula¹, A. Hocine¹, D. Chappelle², M. L. Boubakar²

(1) Controls Laboratory Tests, Measurements and Simulations Mechanics, Benbouali Hassiba

University of Chlef, Hay Salem, National Road N° 19, 02000 Chlef, Algeria

(2) Institut FEMTO-ST, Dept. MécAppli, 24, rue de l'épitahe, 25000 Besançon, France

E-Mail: ghou.amid44@yahoo.fr

Abstract: The aim of this paper is to develop analytical model of viscoelastic behavior for damaged multilayer tubular structures in long fibers. The developed model is used to simulate the viscoelastic response of cylindrical composite structure under a creep loading. The suggested analytical model provides an exact solution for stresses and strains for pipes and on the cylindrical section of vessel submitted to mechanical static loading. Some analytical results are compared with previous works, a good correlation is observed.

Keywords: Tubular structure, Multilayer composite, Viscoelastic, Damage, Pressure loading,

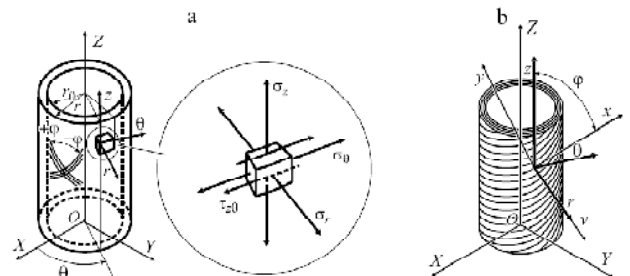
1. Introduction

The use of Fiber reinforced polymeric composites materials has become a current practice in gas transport and storage cylindrical structures due to their lightweight, relative low cost and mainly their high strength over metallic materials. This paper is devoted to extend the analytic modeling tool in order to predict the time remaining before the occurrence of the structure failure. The literature shows that two theoretical approaches are used to predict the composite structures behavior; the classical theory laminates and the so-called theory of elasticity. The first theory assumes that the composite laminates are in a state of planes stress and provides no stress in the direction of thickness. The second shows that the stress developed through radial thickness have a large influence on the choice of stacking sequences[1]. This work aims to propose and validate an analytical model tool dedicated to the designing of a pressure piping and vessel where the viscous nature of the matrix is taken into account in the model, which allows us to model the viscoelastic behavior of a damaged multilayer tubular structure .

2. Determination of the axial strain

The considered material is a thin layer polymer reinforced with long glass fibres .The general stress-strain relationship for each k-th constituent is given by:

$$\begin{Bmatrix} \sigma_z \\ \sigma_\theta \\ \sigma_r \\ \tau_{\theta r} \\ \tau_{zr} \\ \tau_{z\theta} \end{Bmatrix}^{(k)} = \begin{bmatrix} C_{11} & C_{12} & C_{13} & 0 & 0 & C_{16} \\ C_{12} & C_{22} & C_{23} & 0 & 0 & C_{26} \\ C_{13} & C_{23} & C_{33} & 0 & 0 & C_{36} \\ 0 & 0 & 0 & C_{44} & C_{45} & 0 \\ 0 & 0 & 0 & C_{45} & C_{55} & 0 \\ C_{16} & C_{26} & C_{36} & 0 & 0 & C_{66} \end{bmatrix}^{(k)} \begin{Bmatrix} \varepsilon_z \\ \varepsilon_\theta \\ \varepsilon_r \\ \gamma_{\theta r} \\ \gamma_{zr} \\ \gamma_{z\theta} \end{Bmatrix}^{(k)}$$



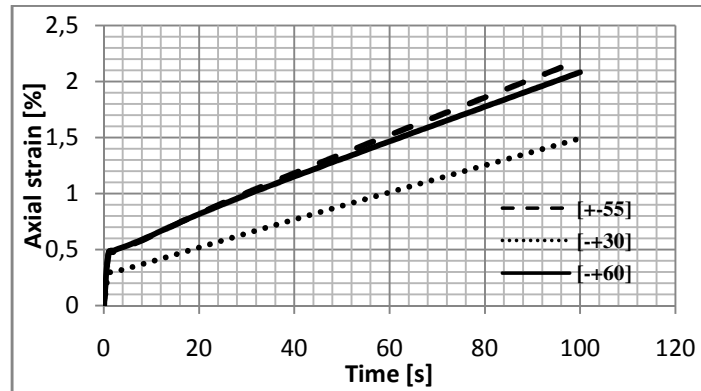


Fig. 1. Evolution of axial deformation versus time.

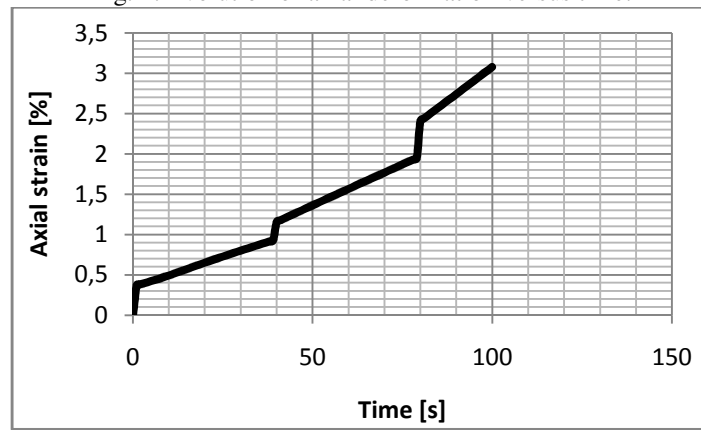


Fig. 2. Evolution of axial deformation versus time for three loading valeure ($P=4\text{MPa}$, $P= 8\text{MPa}$, $P= 10\text{MPa}$).

3. Conclusions

The Williams's type solution has been employed to analyse the stress distribution ahead of the notch tip. It was shown that the T-stress is not constant along ligament ahead of the notch tip for pressurised pipes and Roman tile specimens. It was also found that the non-singular terms are not negligible for a notch as the distance from the notch tip increases. To avoid this difficulty, it has been proposed to use the effective T-stress. The effective T-stress is suggested to be the average T-stress inside the effective distance ahead of the notch tip. Thus, the concept of the T-stress in the case of the crack stress distribution has been extended to the notch stress distributio

References

- [1] Hocine A., Chapelle D., Boubakar L., Benamar A., Bezazi A. Experimental and analytical of the cylindrical part of a metallic vessel reinforced by filament winding submitted to internal pressure. International Journal of Pressure Vessels and Piping, 86, 649-655 (2009).

FAILURE BEHAVIOR AND LOAD TRANSFER IN CONCRETE-STEEL PLATE CONNECTION OF HYBRID CONSTRUCTIONS

L. Madouni¹, M. Ould Ouali², A. Kezmane¹, N.E. Hannachi¹

*1 Laboratoire LAMOMS. University Mouloud MAMMERI of Tizi-Ouzou, BP 17RP. Algeria.
madouni.l@gmail.com, ali.kezmane@hotmail.fr, hannachina@yahoo.fr*

*2 Laboratoire Elaboration et Caractérisation des Matériaux et Modélisation (LEC2M). University
Mouloud MAMMERI of Tizi-Ouzou, BP 17RP. Algeria.
m_ouldouali@ummto.dz*

Abstract: The increasing use of hybrid and mixed building enforce designers to model new systems. Good combination of steel and reinforced concrete structures allow producing efficient structures. In particular, hybrid coupled shear wall are known to be the best systems resisting to horizontal forces due to seismic action. Recent literature has pointed out a need for greater understanding of the interaction of structural steel and reinforced concrete in such systems. In this work, numerical studies were conducted to investigate the behavior of the steel coupling beam–wall connections in terms of the failure mechanism, damage identification evolution and distribution in the concrete, strength, stiffness, and load transfer system. The results obtained from the finite element analysis were verified against experimental results of other researches. A deeper study was conducted to study the effect of the changes of materials properties on the capacity and behavior of the shear connection. It is observed thought cracks and damages in concrete joint different failure mechanism due to the way of load transferring. The first one assumes that the moment transferred by the embedded part of the coupling beam to the concrete shear wall by a couple of vertical forces, while the second one assumes a transfer of the bending moment by a couple of horizontal shear forces. The main objective of the paper is to optimize the performance of the coupled system. So, the interaction between the local stress effects in the concrete wall due to the forces transferred from the beams with the global stresses coming from the overall bending of the walls is analyzed and commented.

Keywords: Shear walls, Failure behavior, coupling beam, Damage identification, Finite Element Analysis

1. Introduction

In high multistory buildings, hybrid coupled shear walls are frequently used, where adjacent reinforced concrete walls are connected together by steel coupling beams. Hybrid coupled shear walls can deliver an effective structural system to resist horizontal forces due to seismic action, where, the overall overturning moments are resisted :partly by the individual flexural action of these walls and partly by an axial compression/tension in the coupled concrete walls. Such a resistance mechanism implies however the transfer of large bending and shear forces in the steel coupling beams. In this paper, numerical studies were conducted to investigate the behavior of the steel coupling beam–wall connections.

2. Load transfer in coupling beam connection

In order to provide a high-efficiency coupling beam, it must be anchored so that its full capacity can be exploited. For safety reasons, all sudden and brittle failure modes should however be avoided. If possible, failure should thus not occur in the concrete since concrete failures are often sudden and low dissipative [1]. The proper way of ensuring that the governing failure mode is not sudden requires an efficient design of the joints.

The specimen test of the experimental studies of Park et al. [2] is chosen as reference for the calibration of the numerical model described in this paper. The geometry of the specimen is shown in Figure 1.

The specimen was modelled by ABAQUS [3] software in three dimensions under monotonic loading only on half of the specimen due to the symmetry. An extended parametric study was conducted.

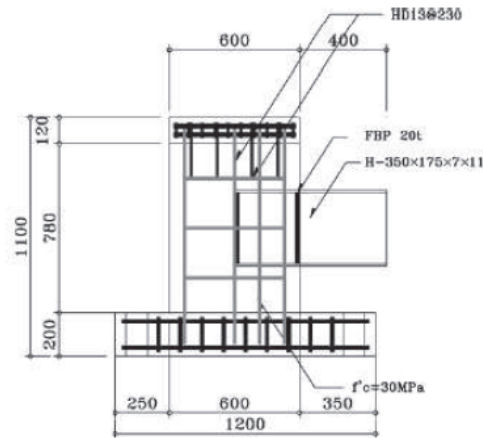


Fig. 1. Geometry details of the specimen.

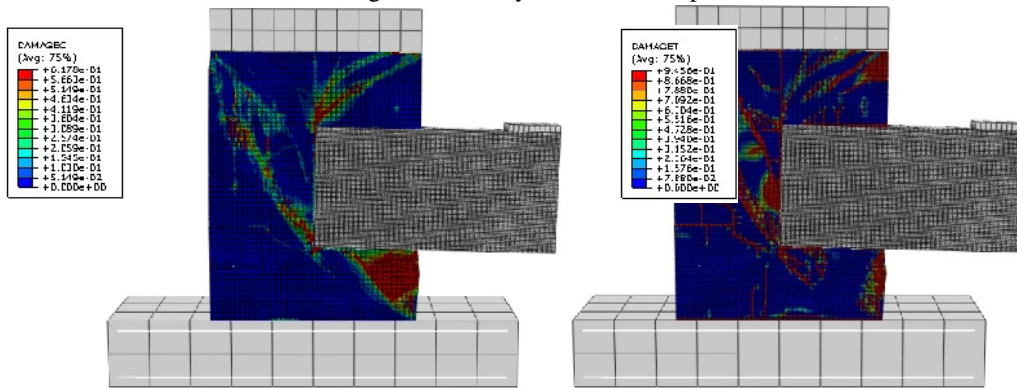


Fig. 2. Compression and tensile damages in shear wall.

3. Conclusions

A finite element model has proved to be effective in terms of predicting the load–displacement response for shear coupled walls, as well as the strain pattern at failure. Useful observations are drawn about the distribution of contact and shear forces between the steel profile and the concrete wall that can make easier the direct control of the embedment conditions in a practical design procedure. As shown in Figure 2, it is observed thought cracks and damages in concrete joint different failure mechanism due to the way of load transferring. The first one assumes that the moment transferred by the embedded part of the coupling beam to the concrete shear wall by a couple of vertical forces, while the second one assumes a transfer of the bending moment by a couple of horizontal shear forces.

References

- [1] Madouni, L., Hannachi, N.E., Degee, H. (2014), Modeling of Steel-Concrete Shear Connection Application to coupled shear walls under seismic action. Eurosteel Proceeding.
- [2] Park, W.S., Yun, H.D., Kim, S.W., Jang, Y. (2012), Structural Performance of Hybrid Coupled Shear Wall System Considering Connection Details, Korean Society of Engineering Structures Vol 16, n ° 3.
- [3] Hibbitt, Karlsson and Sorensen. (2014), ABAQUS standard user's manual.

NUMERICAL ANALYSIS OF CORRODED STRUCTURES WITH ANSYS APDL

H. Berrekia^{1, b*}, A. Chouiter^{2, b}, D. Benzerga^{3, b}

1, 2, 3 University of science and technology Mohamed boudiaf Oran, Oran, Algeria,

b Composite Structures Laboratory and Innovative Materials, Faculty of Mechanical Engineering, PO Box 1505 El M'naouer, USTO, Oran, Algeria

Abstract: Nowadays, pipelines are the most important transportation artery and researches indicate that the pipelines will be a secure tool for energy transmission for over 50 years, which is more significant for petrochemical, oil, and gas industries. The large part of chemical fluids, especially natural gas, transmits with pipelines. These pipelines manufactured with large pipes that they can bear high pressures about several thousand kilogram per cubic centimeter. The gas pressure is obtained by high pressure station in long distances. The function of gas pipelines is very important and vital; therefore, they have to be safe. But unfortunately, utilization of old pipelines in operation increases probability of occurrence. The most important reasons of making these occurrences are the internal and external corrosions that are very effective in damaging gas pipelines, hence safety decreases. So, controlling of corrosion in gas pipelines needs to use cathodic protection with cathodic potential, substance becomes a cathode, and this system decreases the rate of corrosion. Periodic inspections of pipelines are essential, through a method called pigging. A pig is a device inserted into a pipeline which travels freely through it and is driven by the product flow to do specific tasks within the pipeline. In this paper, Algeria and one of the largest hydrocarbon producer and exporter in Africa, it has one of the largest gas pipeline systems in the world. Sonatrach has initiated in 2007 an ambitious integrity of its network management program. An important corollary of this program is the need to have reliable tools for evaluating the performance of each pipeline. However, several accidents have been reported, usually due to the presence of defects, such as corrosion due to metal losses, cracks in welded joints and external aggressions. This work aims to propose a numerical analysis based finite element routine ANSYS, the behavior of a structure, if a pressure tube containing corrosion defects associated with metal losses. The verification of the validity of some rules of thumb about the acceptability of a crevasse is performed simultaneously.

Keywords: Pipeline, Mécanique de la rupture, corrosion, Analyse structurale, Méthode des Eléments Finis par logiciel ANSYS

* Corresponding author

E-mail address: habib.doctorat@hotmail.com

INHIBITORS CORROSION EFFECT ON MECHANICAL PROPERTIES OF API 5L X52 STEEL IN ACID HCL ENVIRONMENT

Y. Rahmani-Kouadri¹, M. Ouled Mbereick¹, M. Hadj Meliani^{1,2}, El-Miloudi Khaled¹,
C. Fares¹, M. A. Benghalia¹, K. Gharbi³

¹University of Chlef Hassiba BenBouali LPTPM, FSSI, Hay-Esalem, 02000, Chlef, Algeria.

²Université Paul Verlaine of Metz, LaBPS-ENIM, île de saulcy 57045, Metz, France.

³M'Hamed Bougara University, LGPH, Faculty of hydrocarbons and chemistry, 35000, Boumerdes, Algeria

Email: mohamedmbeirick911@gmail.com

Abstract: Our objectives are to use the plant extracts, such as corrosion inhibitors. Indeed, these natural extracts contain many families of natural organic compounds "Green", readily available and renewable. The mechanics tests carried out on this study of anti-corrosive properties of natural products of plant origin will be to give so far promising results on the fracture mechanics properties. The importance of this area of research is mainly related to the fact that natural products can replace toxic organic molecules present condemned by the world directives for environmentally unacceptable.

Keywords: Corrosion, Green Inhibitors, Failure, Fracture Mechanics, Pipelines.

1. Introduction

This study is part of the project between UHBC and Sonatrach TRC currency. This project aims to prepare for the use of the existing pipeline network linked to the transportation of natural gas, for the joint transportation of mixing it with hydrogen. Hydrogen is a new sustainable energy carrier which has a scope expanding to date. This has been done within the Theoretical Physics Laboratory of Materials Physics (LPTPM) Chlef. This study is for the purpose of verifying the effect of hydrogenated on the pipeline. Finally it was proposed as a solution to this problem inhibitor protection from the impact test on the X52 steel.

2. Experimental study

In this study we take 28 specimens of standard dimension, and we have by chemical laboratory two solutions were prepared consisting of pure HCl, and 90% HCl with 10% green inhibitor. this specimens has immersed in tow our solution acidity environments by different time.

3. Results and discussion

We are study the influence of the acidity environments on our materials properties, when it immersed in this environments, by the mechanical testing charpy. when we the different parameters explained in the following tables:

Time of immersion	1 day	16 days	7 days	16 days	14 days
HCl	3 specimens	3 specimens	3 specimens	3 specimens	Removal
HCl+10%	3 specimens	3 specimens	3 specimens	3 specimens	Removal

The tables which follow show the results of the energy absorbed by the specimen in the absence of inhibitor and presence of the inhibitor.

Days	Section [mm ²]	K _V [days]	K _{CV} [Joule/mm ²]	K _{IC} [MPa.√m]	Energy report (%)
------	----------------------------	-----------------------	--	--------------------------	-------------------

		without	with	without	with	without	with	without	with
50	75	130	118	1,73	1,57	230,28	219,39	39.81	45.37
39	75	156	151	2,08	2,01	252,26	248,18	27.77	30.09
23	75	175	172	2,33	2,29	267,18	264,88	18.98	20.37
16	75	184	178	2,45	2,37	273,96	269,46	14.81	17.59

The result In this following figure present the Critical intensity Factor K_{IC} by the energy absorbed by specimen, and the energy absorbed by specimen by the time immersed in acidity environment .

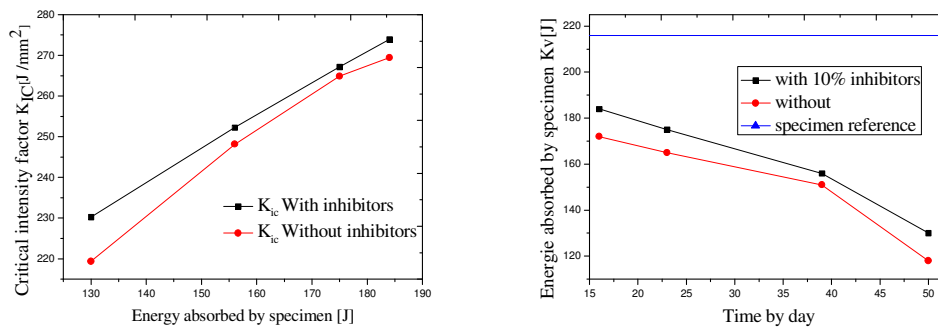


Fig.a.1.evolution the critical intensity factor K_{IC} by energy absorbed and, [a.2]evolution energy absorbed by time .

3.Conclusion

The first medium contains hydrochloric acid (HCl 100%) which is considered aggressive environment, however the 2nd medium contains hydrochloric acid with 90% HCl with 10% green inhibitor. Of the two curves are steadily declining with a significant decrease during the 39th days or the difference between them on referential K_{IC} during the 16th days equals 5.55% for 23 th day equals 4.62%, during the 39th day, the two curves are more and decrease during the 50th day corresponding the final day of the experiment, the difference is the large pus which is 5.56%.

References

- [1] Bazzoni, B. "Criteria for Internal Corrosion Evaluation and Material Selection in Oil & Gas Industry ", Engineering Solutions for Corrosion in Oil and Gas Applications, NACE Conference, Milan, paper No. 12;1989.
- [2] Rahmani raziqa, effet de la temperature sur un inhibiteurs vert a base de ruta chalpensis et l'identification des mecanismes d'adsorption, 24 Juin 2015.

INFLUENCE OF SANDBLASTING ON MECHANICAL PROPERTIES OF PIPELINE API 5L X52 STEEL

A. A. Saadi^{1,*}, O. Bouledroua¹, M. Hadj Meliani^{1,2}, G. Pluvinage²

¹ LPTPM, Faculty of sciences, Hassiba Benbouali University, B.O.Box 151, Hay salem, Chlef 02000, Algeria.

² LaBPS, Ecole Nationale d'Ingénieurs de Metz, 1 route d'Ars Laquenexy, CS 65820 57078 Metz cedex, France.

Abstract: The need to transport petroleum and gas products through pipelines has resulted in the increased erosion of the pipeline materials used in the hydrocarbon industry. Erosion is a mechanical process that causes an eroded volume on the surface of a material. The erosion phenomenon of metallic structures, in petroleum industry, is a problem which affects many industrial sectors. The shocks between the sand particles and the structure surface cause a severe damage. It is manifested by spelling craters of different shapes and depths. The evaluation of dynamic properties and weight loss of a pipeline under the impact of sand has been performed. In this study, was performed using sand blaster erosion machine with different angles and distances to investigate the erosive behavior and mechanism relative to API X52 pipeline steel, caused by sandblasting erosion in Saharan climate conditions. The observation of failure mode shows that the deformation field, after sandblasting, is very important.

Keywords: API 5L X52 steel; Erosion; sandblasting; hardness.

1. Introduction

The sandblasting test is taken account to study the effect on mechanical property for pipeline API 5L X70 steel. This procedure can occur in three cases, the first one in the revetment step, this operation is very important for a good surface (cleaning and increasing the roughness adhesion). The second part is after working in the Sahara, characterized by sand particles impacting on the pipeline walls due to solid-liquid flow, flow restrictions or change in flow direction, the effect of natural sandblasted is small but a long time we have a erosion phenomenal, with a wind speed below 6 m/s [1]. Finally, in the repair pipe with the manual or automatically sandblasted.

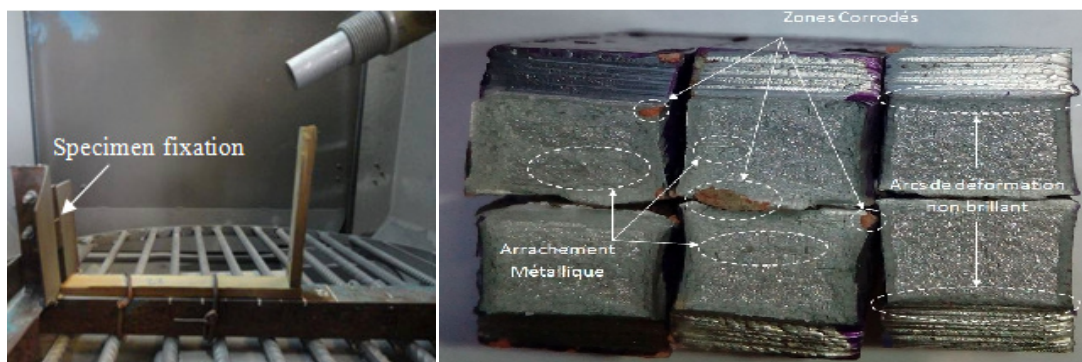


Fig. 1. Procedure of sandblasting with the fixation of the specimen of different angle and distances and description of different zones of Charpy specimen.

* Corresponding author

E-mail address: bouledroua.omar@hotmail.fr (O. Bouledroua)

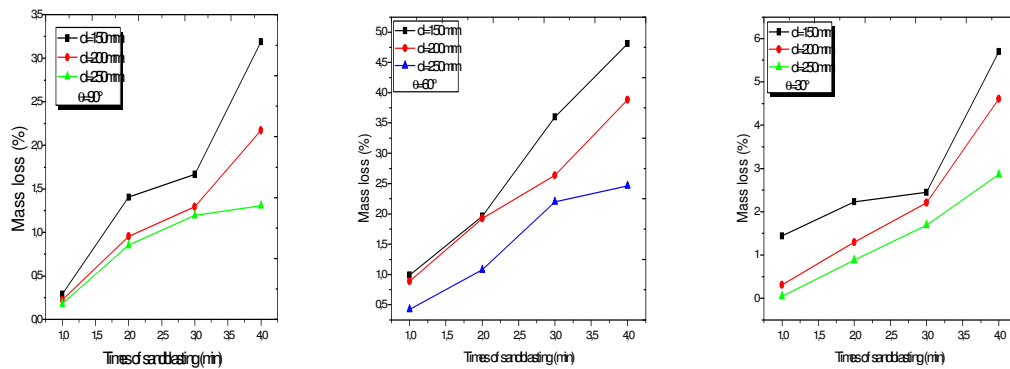


Fig. 2. Evolution the of weight loss on the longitudinal direction (L) as a function of the time of sandblasting for different angle of projection (90°, 60° et 30°)

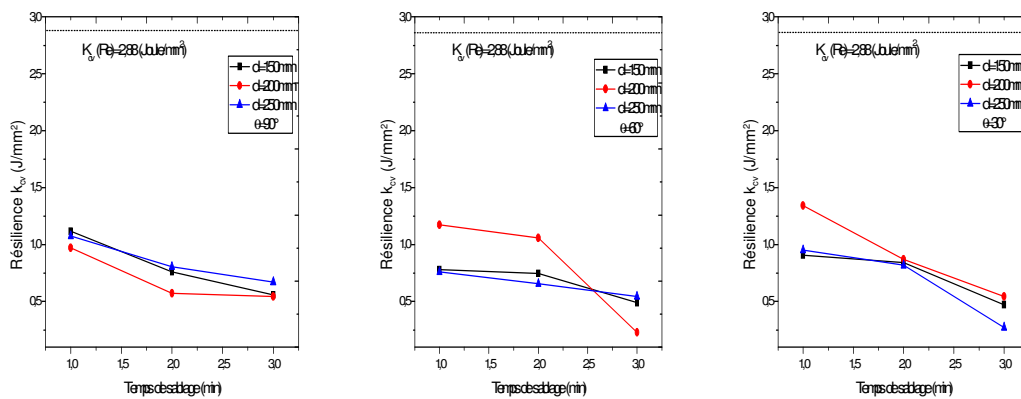


Fig. 3. Evolution the of resilience on the longitudinal direction (L) as a function of the time of sandblasting for different angle of projection (90°, 60° et 30°)

3. Conclusions

The effect of sandblasting on the resilience and weight loss of API 5L X52 gas pipe steels are analysed with different angles and distance. The investigation of the effect of sandblasting duration on the erosion behavior and mechanical property of API X52 steel has led to conclusion that the sandblasting has two principal effects, the first one effect have been achieved at a little decreasing on the resilience and increasing of weight loss and thickness. The observation of failure mode shows that the deformation field, after sandblasting, is very important.

References

- [1] American Petroleum Institute, Specification for Line Pipe, API SPECIFICATION 5L FORTY-SECOND EDITION, JANRY 2000.

CORROSION STUDY OF TERNARY ALLOYS CZT FOR CZTSe SOLAR CELLS

M. Hamla, M. Benaicha, M. Allm

*Energetics and Solid State Electrochemistry Lab, Dept. of Process Engineering, Faculty of Technology,
Setif1 University, SETIF 19000 Algeria*

E-mail: merie200934@hotmail.com

Abstract : The CZT was electrochemically co-deposited in a citrate solution and the CZT+Se were followed by a vacuum post-annealing treatment between 350°-550 °C for 30 mn. Corrosion properties of CZT ternary alloys have been studied in citrate medium at the electroplating platinum substrate (Pt). Cyclic voltammetry is used for the study of electrodeposition processes. the polarization resistance (R_p), the corrosion current density (i_{corr}), the electrolyte resistance (R_L), transfers to the resistance and the capacitance (C) were determined using the techniques Tafel and spectroscopy electrochemical impedance (EIS) respectively. From this study, it was found that the corrosion rate increases with the decrease of potential deposits. Chemical composition and structure of the electrodeposited films were evaluated by energy dispersive X-ray spectroscopy (EDS), scanning electron microscopy (SEM) and X-ray diffraction (XRD)

Keywords: solar cells, ternary alloy CuZnSn, impedance (EIS), corrosion, Electrodeposition

DETERMINATION OF RESIDUAL STRESS IN AL-ALLOYS THIN FILMS

S. Lallouche^{1,2}, M. Y. Debili^{2,*}

1 University of Chlef Esalem City, 02000, Chlef, Algeria.

1, 2 University, Badji-Mokhtar of Annaba, Laboratory of Magnetism and Spectroscopy of Solids LM2S, Department of physics,, Faculty of Science BP12 23200 Annaba, Algeria.

Abstract: Sputter-deposited thin films have wide application in many microelectronic Technologies in which film surface and microstructure have direct implication for device function and reliability, and the progressive reduction of size microelectronic device has generated great interest to apply a metal with low resistivity and superior electromigration in comparison to existing aluminum (Al) or aluminum-alloy interconnections. The physical properties of the film may be strongly influenced by stress in such films. In this work we present a stress-strain evolution of Al-Cu thin films, deposited on glass substrates by RF (13.56 MHz) magnetron sputtering and annealing up to 500°C. Film thickness of both types of coatings was approximately the same 3-4 μm. After characterizing thanks to X-Ray diffraction the structure of these phases, we focused on the study of their microstructural parameters (grain size, microstrain, densit of dislocation). The strain measurement has been performed thanks to Williamson-Hall method classic [1]. The residual stress of the films changes from tensile to compressive with addition of elements (Cu %). The relaxation of stress was observed for all samples after annealing at 500°C.

Keywords: thin films, stress, sputtering, thin films.

1. Introduction

Sputter-deposited thin films have wide application in many microelectronic technologies in which film surface and microstructure have direct implication for device function and reliability, and the progressive reduction of size microelectronic device has generated great interest to apply a metal with low resistivity and superior electromigration in comparison to existing aluminum (Al) or aluminum-alloy interconnections. The physical properties of the film may be strongly influenced by stress in such films.

2. X-ray diffraction

The microstructures of the co-sputtered. Rf sputtered Al(%at.Cu) thin films have been studied by means of X-ray diffraction (XRD). The XRD measurements (Fig. 1). The interplanar spacey measured from X-ray diagrams are identified thanks to JCPDS card [3,4].

3. Size Broadening

Scherrer [5] first observed that small crystallite size could give rise to line broadening. He derived a well known equation for relating the crystallite size to the broadening, which is called the Scherrer Formula.

The microdeformation measurement has been performed thanks to Williamson-hall method [1]. The variation of $B\cos\theta$ according to $\sin\theta$ for annealed deposits, the various line slope obtained determines the micro strain. The negative slopes correspond obviously to micro strain resulting from micro compressive stresses.

* Corresponding author

E-mail address: lallouche_sa@yahoo.fr

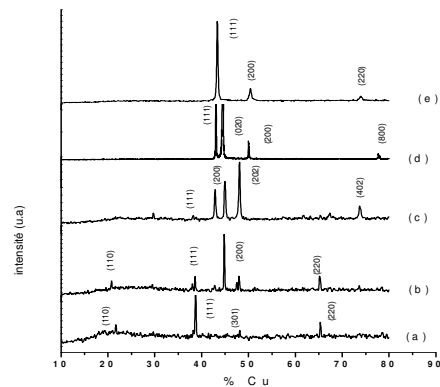


Fig. 1 XRD diagrams for co-sputtered Al-Cu thin films: (a) 1.8 at.%Cu, (b) 7.21 at.%Cu, (c)

The microdeformation measurement has been performed thanks to Williamson-hall method [1]. The variation of $\beta\cos\theta$ according to $\sin\theta$ for annealed, the various line slope obtained determines the micro strain. The negative slopes correspond obviously to micro deformations resulting from micro compressive stresses.

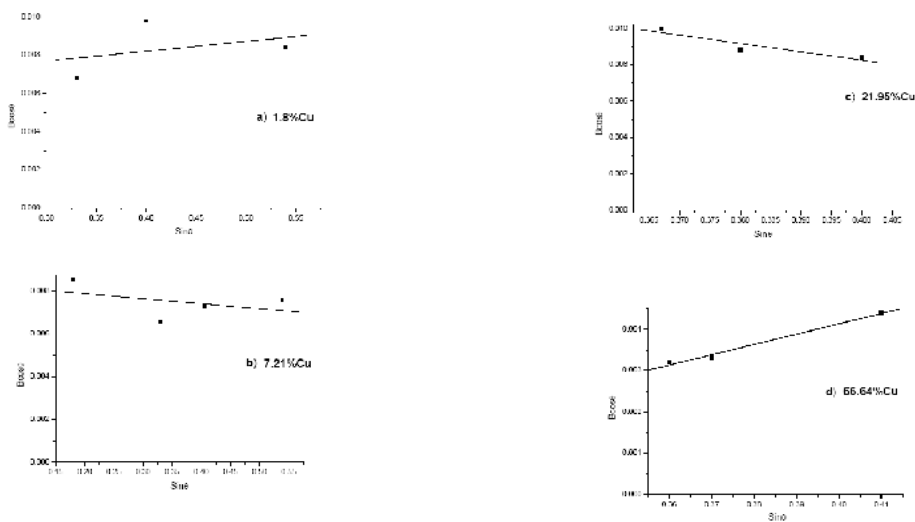


Fig. 2 Variation of $\beta\cos\theta$ according to $\sin\theta$ for various contents of copper of the deposits.

Conclusion

The compressive stress in thin films are the result of the bombardment of the layer by heavy ions or energetic particles during the construction of the deposit and can be interpreted by the mechanism of "atomic shot peening" or "mechanism of hammering".

References

- [1] Hall W.H, "X-ray line broadening in metals", Proc. Phys. Soc.(London) 62 (1949),741-743.
- [3] JCPDS-ICDD CARD 04-0787, (1997).
- [4] JCPDS-ICDD CARD 25-0012, (1997).
- [5] P. Scherrer, Gött Nachr. 2, 98 (1918)

LIPOLYTIC BACTERIA USE AS BIO-DECONTAMINATING NATURAL IN THE WATER PURIFICATION STATIONS

L. Hachemi¹, M. E. Belgherras², Z. Benattouche³

1, 3University of Mascara, (LBMSS), city Elkararma. Mascara, Algeria.

2University of Sidi bel Abbes, Mechanics and Physics of Materials Laboratory, Djillali Liabes

University of Sidi Bel-Abbes, BP89 cité Larbi Ben M'hidi, Sidi Bel-Abbes, Algeria.

Abstract: Different samples were collected from polluted waters by fat materials in the Mascara region for the isolation of bacterial strains capable of degrading fat materials. The objective of this work is the search for new bacterial lipases for biotechnological application that we chose to isolate from polluted water waste fats from slaughterhouses lipolytic bacteria to characterize their microbiological properties and used in the production of extracellular lipase by the fermentation method. A total of two strains were isolated at 37°C from the sample water rich slaughterhouses fat materials. Production of extracellular bacterial lipase was studied as a function of several inductors of lipid nature by the fermentation method. The enzyme activity reached a maximum value, in the presence of olive oil as inducer and glucose as the carbon source and energy at pH = 7.2 at 30 ° C and agitation 125 rpm *Pseudomonas* sp (40 mmol / ml.72h) *Streptococcus* sp (47µmol / ml .72h). The enzyme was purified by precipitation with ammonium sulfate in a yield of 63.73% and 50% in *Streptococcus* sp and *Pseudomonas* sp respectively. The lipase produced by these two bacteria is resistant to 50°C and is strongly inhibited in the presence of 1 mmol Zn + 2 and Mg + 2.

Keywords: bacteria, lipase enzyme, production, fermentation, Purification.

1. Introduction

Industrial waste and fat derived from plants cause irreversible environmental disaster (pollution of water, soil and air). Biological methods use microorganisms to degrade as biodépolluants fat ecological way. [5]

2. Experimental procedure

2. 1. Biological materials: The two bacterial strains used in this study were isolated from sewage water from slaughterhouses.

2. 2. Identification of lipolytic bacteria: We used Sierra method [1]

2. 3. Production of lipase enzyme (fermentation) : Enzyme production is sought in the first place according to several sources carbone. Six media types with various compositions were studied [3]

2. 4. Determination of biomass and lipolytic activity : By applying the law of beer lambert [8]. The determination of biomass g / l is done every 24 (C = DO / ε). The lipolytic enzyme activity was measured by the titrimetric method. [2]

2. 5. Extraction of the lipase:

The crude extract was prepared by centrifugation at 6000tours / min at 4 ° C for 20min.

2. 6. Purification of the lipase: Our method of purification is based on protein precipitation by salts and all product was performed at 4 ° C. [4]

Then determining the protein content, enzyme activity, the purification yield and some physico-chemical parameters of the purified enzyme.

3. Results

3. 1. Isolation lipolytic strains

Among these strains were selected on the basis of its lipase production capacity force.

* Corresponding author

E-mail address: laliahachemi@yahoo.fr



Fig 3. Detection of lipase activity in Pseudomonas sp and Streptococcus sp.

3. 2. Determination of the biomass and lipolytic activity of the inoculum : From the results obtained, the medium of olive oil is favorable to maximize production of the lipase.

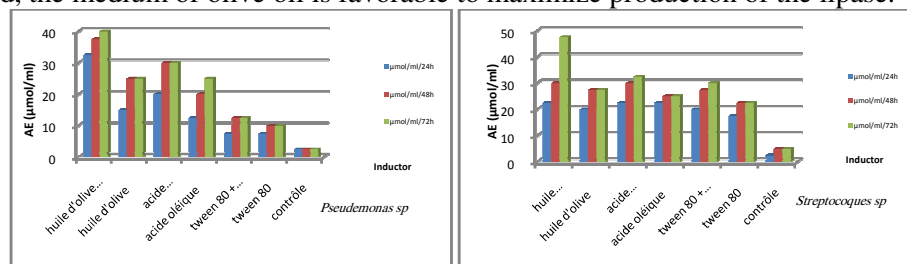


Fig 5. The lipolytic activity during the period of fermentation in (μmol/ml).

The results obtained show that the olive oil is effective in inducing the lipase.

4. Study of some physicochemical parameters

According to the results, it appears that the purified lipase enzyme is stable at 50 ° C with a decrease in activity to 13.79 and 51.5 % for Streptococcus sp and Pseudomonas sp respectively. Concerning enzyme effectors, the lipase enzyme is strongly inhibited in the presence of Zn + 2 ions and no effect against not detected in the presence of Ca + 2 ions.

5. Conclusion

The two strains studied were selected for their significant lipolytic activity.

Achieving lipase activity (47 μmol / ml.72h) ; (40 μmol / ml.72h) for Streptococcus sp and sp Pseudomonas sp respectively in the presence of olive oil and glucose at pH 7.2 and 30 ° C with stirring at 125 rpm .

Both enzymes produced by Streptococcus sp and Pseudomonas sp were found resistant (stable) at 50° C pendant 30 minutes with 13.79% of decrease in activity and 51.51 % respectively. So this little enzyme used for the degradation of this waste grease in the warm thermal waters.

So lipase extracted from these little bacteria used as biological decontaminating waters rich in fatty waste or as detergents industries.

References

- [1] A. Delmotte, 1958. L'activite lipolytique microbienne decelée par la methode de Sierra avec reference speciale au *M. pyogenes* var. *aureus*. Journal of Antonie van Leeuwenhoek. Vol 24, Issue 1, pp 309-320
- [2] MA Kashmiri, A Adnan, BW Butt., 2006. Production, purification and partial characterization of lipase from *Trichoderma Viride*. African Journal of Biotechnology. Vol 5, No 10.
- [3] S.Couri, A.X. Farias., 1995. Genetic manipulation of *Aspergillus niger* for increased synthesis of pectinolytic enzymes. Rev. Microbiol. 26 (4): 314-317.
- [4] Camacho RM, Mateos JC, Reynoso OG, Prado LA, Codova J., 2009. Production and characterization of esterase and lipase from *Haloarcula marismortui*. J. Ind. Microbiol. Biotechnol. 36: 901-909.
- [5] Samir CHENNOUF, André MOUREY, Gérard KILBERTUS LERMAB-Microbiologie., 1995. Biodegradation des lipides et suivi de la microflore lipolytique dans des composts

EFFECT OF SLAG IN THE MECHANICAL BEHAVIOR OF THE ALKALI-SILICA REACTION AFFECTED CONCRETE BEAMS

Z. Douaissia¹, M.F.Habita²

1,2Badji Mokhtar university, Génie Civi laboratory , BP12, Sidi Amar, Annaba, Algeria.

Abstract: Alkali-silica reaction (ASR) can induce the premature distress and loss in serviceability of concrete structures. It is generally agreed that ASR occurs in concretes with reactive aggregates, when there are sufficient alkalis (K₂O, Na₂O), and when relative humidity is higher than 85%. In addition, temperature affects the time of initiation (induction period) and development of the reaction. As ASR takes place, different signs appear inside the concrete, gels and cracks form, gels filling cracks in the aggregates or in the cement paste, gels form reaction rims around aggregate particles, gels fill air-voids in the cement paste and silica gels replacing C-S-H of hydrated cement paste. The aim of this experimental study is to verify if the ground granulated blast-furnace slag (GGBFS) of the region from eastern Algeria, have the ASR- inhibiting effect for affected beams. In this article, the stress-strain behaviour and cracking patterns of the reinforced beams made by concrete affected by alkali-silica reaction with and without the addition of ground granulated blast-furnace slag under an accelerated curing condition of 60 ° C and 100% are investigated in comparison with those of corresponding normal beams by carrying out static load tests. In addition, prisms were used for measurement of the linear expansions and cylinders for tests of compressive strength, elastic modulus and tensile strength were also prepared and cured in the same manner as the beams.

Keywords: Alkali-silica reaction, Granulated blast-furnace slag, Concrete beams, Expansion, Load tests, Stain, Cracking, Strength.

1. Introduction

The specification of concrete containing ground granulated blast-furnace slag (GGBS) is recognised in several countries [1] as an effective measure to reduce the risk of deleterious alkali silica reaction occurring in concrete containing potentially reactive aggregates. However, the effectiveness of GGBS, particularly at levels of cement replacement below 50%, has been questioned by several workers [2-3].

The binder was an ordinary Portland cement, CEM I 52,5R with a moderately high Na₂O_{eq} content (0.8%), Two aggregates were chosen :

- A siliceous limestone (H), mainly composed of calcite
- A crushed waste glass (G), resulting from the crushing of window glasses.

Ground slag (S) is obtained by crushing and sieving at 0,08 mm. In order to study the influence of fineness in counteracting expansion, the slag material is ground to different specific surface (Blaine), which are S1: 100 m² / kg, S2: 400 m² / kg and S3: 600 m² / kg.

2. Concrete Beams tests

The concrete samples were made, stored and tested according to French Standard P18-454 [4]. This test consisted of evaluating the performance of a concrete with respect to ASR by measuring its expansion on 7 x 7 x 28 cm prisms stored at 60°C and 100% relative humidity. The last measurement was taken at 88 weeks. At 34 weeks, map cracking was measured in order to quantify the degree of damage due to ASR. At the same age, compressive strength (f_c) was measured on three cubes (10 x 10 x 10 cm) .

* Corresponding author

E-mail address: douaissiazinebgc@gmail.com

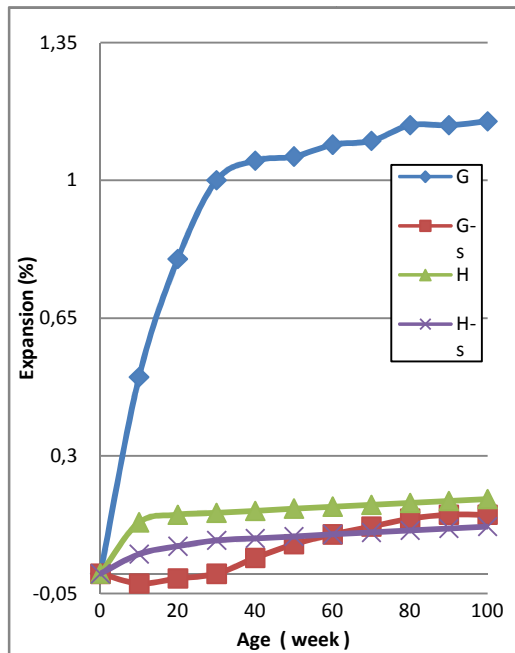


Fig. 1. Expansion of concrete Beams versus time, cured at 60°C and 100% RH.

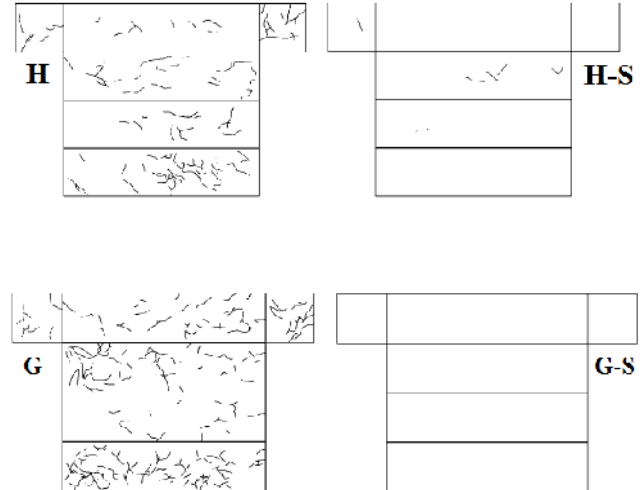


Fig. 2. Influence of ground slag on surface cracking of concrete Beams.

3. Conclusions

The length variations of the concrete beams cured for 88 weeks at 60°C and 100% R.H. are shown in Figure 1. It is noteworthy that the ground slag reduced the expansion of all concretes, different behaviors show concrete with ground slag, concrete G-S shows a slow expansion rate.

After 34 weeks of curing, Crack patterns are shown on Figure 2, The results give information on both the intensity of the damage and the possible isotropic distribution of cracking. We can observe that, the presence of ground slag dramatically decreased the ASR crack development, as was confirmed by the swelling measurements.

At the same age of 34 weeks, the compressive strength (f_c) of each concrete formulation was measured. It can be seen that addition of ground slag enhances the compressive strength of all concretes.

References

- [1] Guidelines for alkali-aggregate reactions in concrete (1986). German Building Standards Committee of the Deutsches Institute für Normung.
- [2] Hobbs D.W (1986), Deleterious expansion of concrete due to alkali-silica reaction: Influence of pfa and slag. Magazine – concrete -recherche.
- [3] Kawamura M. and al (1984), Effet of various pozzolanes additives on alkali-silica expansion in mortars made with two types of opaline reactive aggregates. 38 th annual meeting of Japan Cement Association, Japen, Tokyo, 92-95.
- [4] AFNOR (2004) NF P 18-454, Concrete—Reactivity of a concrete formula with regard to the alkali-aggregate reaction - Performance test.

**THE EFFECT OF THE ELECTRICAL FIELD AND THE POLARIZATION
TEMPRRATURE ON PIEZOELECTRIC PROPRIETES IN THE POLY
(VINYLIDENE FLUORIDE) (PVDF)**

S.DEBILI*, T. CHELOUFI and A.GASMI

*LPS, Department of Physics, Faculty of Science, University Badji Mokhtar, Annaba BP12Annaba
23000, Algeria souha_debili@hotmail.fr*

Abstract: The influence of the electrical field and the poling temperature of the piezoelectric effect in the PVDF films prepared from a solution have been studied by X ray diffraction. The results obtained were discussed on the basis of the dependence of the piezoelectric modulus (d_{33}) as a function of the degree of crystallinity for various modes of vibration. As the polarization temperature increases, the degree of crystallinity decrease, but it increases with the electric field.

Keywords: polymer, PVDF, polarization temperature, piezoelectric effect, crystalline phase

Parametric relation Between Tenacity and Impact Strength in the Zone of Ductile-brittle transition of a Welding Joint

M. TIRENIFI¹, B. BOUCHOUICHA^{2,*}, B. OULD CHIKH³, H.M. MEDDAH³

1 University of Sidi Belabbes, LMSR. BP 89, 22000, Sidi Belabbes, Algeria

2 University of Sidi Belabbes, LMSR. BP 89, 22000, Sidi Belabbes, Algeria

3 University of Mascara, LSTE Laboratory, 29000, Mascara, Algeria.

Abstract: discontinuities in materials require the application of the fracture mechanics. These discontinuities or defects, which are generally responsible for the cracks, have multiple origins internal or external with material, resulting from an unsuitable design, implementation and imperfectly controlled or from an abusive use. More important KIC factor to calculate tenacity. There exist several experimental techniques, which make it possible to determine the critical stress intensity factor. One chose the method of passage of impact strength to tenacity in the zone of ductile-brittle transition from material in this study one aims to apply this method to welding joints, to make a comparison in the three zones (Base metal - Filler and the Heat Affected Zone). Tiredness and impact strength, tensile tests will have to be carried out in order to know the influence of the preparation of the surface of contact on the quality of the welding process. The characterization of welding will enable us to identify the Heat Affected Zone (HAZ) and the Thermo-Mechanically Affected Zone (TMZ)

Keywords: Impact strength, brittle fracture, tenacity, ductile rupture.

1. Introduction

To characterize a material, one needs some of his fundamental properties, like his rigidity, his resistance and his ductility. Rigidity [1] is function of the intensity of the connections which exist between the atoms or molecules constitutive of a material, and is measured by the value of the various modulus of elasticity, in particular by the Young modulus, noted E. resistance [2] characterizes the maximum constraint that a material can support before breaking. This resistance is function of the intensity of its atomic or molecular connections, but also of the influence of certain external parameters, as the shape of the parts or the defects which are present there. The ductility is the property whereby a material can permanently deform before breaking. It thus facilitates working of material in a solid state. For these three properties, it is necessary to add a fourth, fundamental of it, because theoretical resistance is often different from the real resistance of material. This fourth property is the tenacity [Dominique 3], which is characterized by resistance to the brutal propagation of crack. The rupture of a fissured part will be obtained when the stress intensity factor at a peak of crack will be higher than breaking value KIC. One will detail the toughness test and his details of implementation. This one is mainly used when the majority of the structure is in elastic mode, other tests were introduced for the conditions of plastic deformation important or generalized of the structure [1].

2. Relations Between Tenacity and Impact Strength

fracture mechanics tests are long and expensive because the need for a plane strain condition leads to the use of the specimens even thicker than the yield strength of the material is lowered. In contrast, conventional fragility test (Charpy) and the tensile test are inexpensive. The problem of experimental determination of KIC would be greatly simplified if we could link its value to that of other parameters such as KV resilience or yield strength Re. It is just that the following relationships allow us having. The use of correlation between energy

* Corresponding author

E-mail address: ternifi.malika@yahoo.fr

(Charpy) and the toughness K_{IC} has the disadvantage that the stress state (characterized by triaxiality or Q factor) is different for a cut or crack and we know that the stress effective is sensitive to the stress field. [3]. Other empirical correlations between K_{IC} toughness and fracture energy K_V. The relation (1) is used for the fragile zone and by the relation (2) for the ductile zone.

$$K_{IC} = \frac{820\sqrt{K_V - 1420}}{B^{1/4}} + 630 \quad (1)$$

$$K_{IC} = 17K_V + 1740 \quad (2)$$

With

K_{IC} is the stress intensity factor critical in mode I $Mpa\sqrt{mm}$.

K_V is energy of the rupture J/cm^2 .

B is the thickness of the crack.

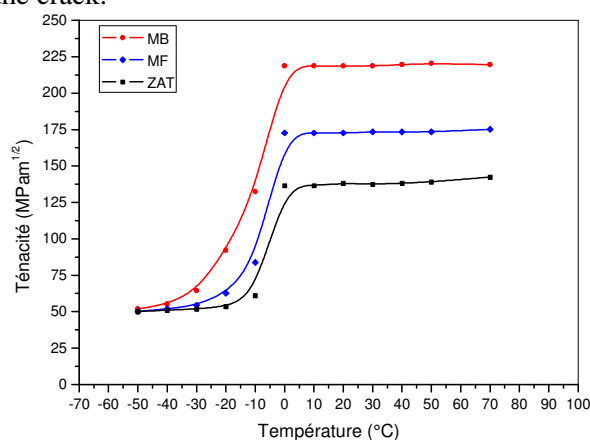


Fig. 1. Curve of tenacity of three zones (BM, FM and HAZ)

3. Conclusions

The results presented by Figure 10 are obtained by the introduction of a factor of uncertainty (distributed according to a law of distribution of Weibull [4], law of the minimum) into the correlation of Wallin [5]. The estimates of tenacity minimal, average for the three zones are relating to the results of impact strengths. One notices for low temperatures a stable average tenacity for the three zones. In the phase of transition, one notices an evolution logical but inversely proportional to the laws of behavior of the three zones, which characterizes steels working under pressure. From 0°C the values of tenacity are stabilized, with higher values in the base metal (MB) that for the molten metal (MF), with less values for the ZAT. Consequently, the parameters used by [5] for the law of distribution of [4] appear reasonable.

References

- [1] Lemaignan Clément "La Rupture Des Matériaux" Dépôt Légal : Septembre 2003 - N° D'imprimeur : 14272..
- [2] Zeghloul A, "Concepts Fondamentaux De La Mécanique De La Rupture", 2004.
- [3] Papanicola Robert "Titanic : Une Autopsie Métallurgique", 2001.
- [4] Weibull S.F.C. Applications de la théorie de la fiabilité à la sécurité d'éléments structuraux d'ouvrage d'art Série ouvrage d'art", OA17, laboratoire des ponts et chaussées 1990.
- [5] Wallin K, New Improved Methodology for Selecting Charpy Toughness Criteria for Thin High Strength Steels", IIW Doc. N° X-1290-94, Commission X, IIW Annual Assembly, Beijing, 1994.

Analyse Numérique du Comportement en Rupture des Conduits sous Pression basé sur une éprouvettes en forme d'arc : Arc-Shaped Specimen : CTPB

A. Benhamena^{1,2,*}, L. Aminallah², A. Aid¹, A. Amrouche³, N. Benseddiqu²

¹ LPQ3M, BP 763, route de Mamounia, Université de Mascara, Algérie

² LML, UMR CNRS 8107, USTL, F-59650 Villeneuve d'Ascq, France

³ LGCgé-E, EA 4515, Université d'Artois, France.

Resumé : L'utilisation croissante des pipelines dans les applications d'ingénierie exige de nouvelles méthodologies afin d'évaluer la capacité de matériau à supporter des charges. La ténacité à la rupture de l'impact de pièces structurales cylindriques telles que les récipients sous pression (Mouzakis et al., 1998) et les conduites sous pression pour gaz combustible et des matériaux de distribution d'eau (Dale et al., 1985, Greig et al., 1992, Han et al., 1999) peut être très important d'un point de vue pratique. Les essais de rupture est parfois ambiguë et n'est pas facile à réaliser, car un échantillon standard ne peuvent pas être facilement fabriqués et préparés pour faire l'essai à partir d'une forme cylindrique. Pour cette raison, les éprouvettes en forme d'arc (arc-shapedspecimen : CTPB, (figure 1) ont été souvent utilisé pour les essais de tuyaux ou récipients sous pression (ASTM E399-09). Afin d'examiner le comportement en rupture de ces structures (pipe sous pression), l'analyse numérique a été faite sur différentes géométries base sur l'application de la mécanique de la rupture élasto-plastique pour déterminer le paramètre de rupture (Intégrale J).

Keywords: pipelines, rupture élasto-plastique, intégrale J, arc-shaped specimen : CTPB.

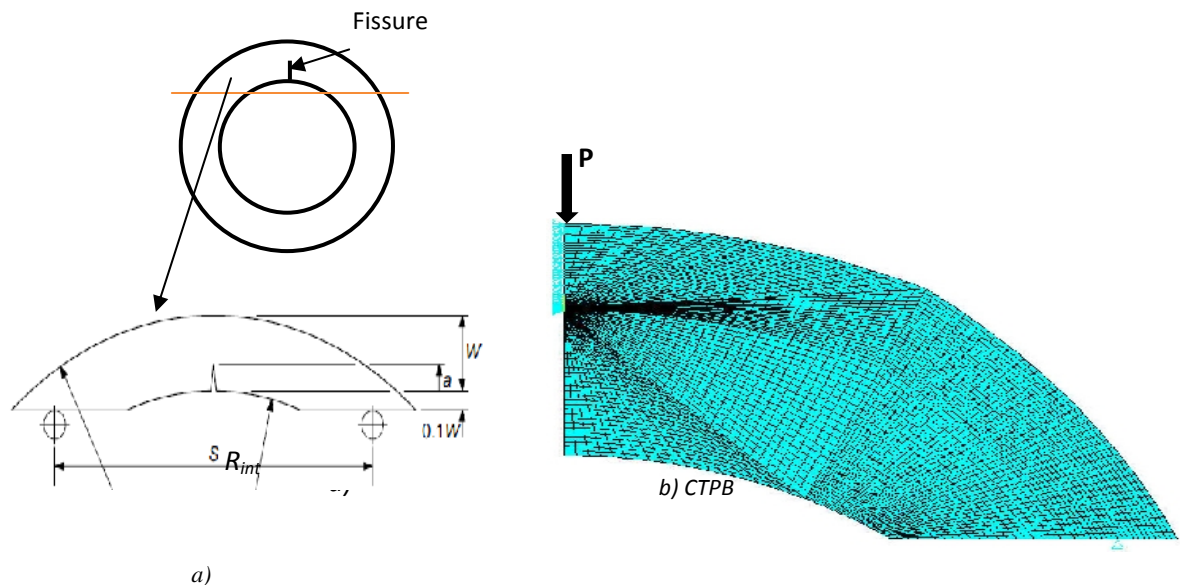


Fig. 1. (a) arc-shaped specimen, (b) maillage avec les conditions aux limites et chargement pour CTPB

* Corresponding author

E-mail address: ali_benhamena@yahoo.fr

NUMERICAL MODELING OF CRACK PROPAGATION UNDER MIXED-MODE LOADING

A. Boulenouar*¹ N. Benamara¹, M. Merzoug¹

1Laboratory of Materials and Reactive Systems, Mechanical Engineering Department, University of Sidi-Bel-Abbes, BP. 89, City Larbi Ben Mhidi, Sidi Bel Abbes 22000, Algeria.

pek_boulenouar@yahoo.fr

Abstract: In this paper, a numerical modeling of crack propagation under mode I and mixed-mode loading is presented. The onset criterion of crack propagation is based on the stress intensity factor, which is the most important parameter that must be accurately estimated and facilitated by the singular element. Using the Ansys Parametric Design Language (APDL), the displacement extrapolation technique (DET) and the maximum circumferential stress (MCS) theory are employed, to obtain the SIFs at crack tip and the crack direction at each step of propagation. The predicted results showed excellent agreement with numerical and analytical results obtained by other researchers.

Keywords: crack propagation, stress intensity factors, mixed-mode loading, displacement extrapolation

1. Introduction

The use of fracture mechanics in the assessment of performance and reliability of structures is on increase and the prediction of crack propagation in structures plays an important part. A software simulation tool, which uses FEA, has been developed to quantitatively predict the propagation of 2D planar cracks through structures. The use of SIFs in crack propagation is one of the most important parameters and successful engineering application in fracture mechanics analysis.

The objective of this study is to present a numerical modeling of crack propagation under linear elastic fracture analysis. Using the APDL code [1], the DET and the MCS theory [2] are implemented, to determine the SIFs and the crack direction, respectively. Therefore, a verification of the predicted SIFs and crack trajectories are validated, with the relevant numerical and analytical results obtained by other researchers.

3. Crack propagation modeling

In order to show the robustness of our numerical developments, three examples are presented:

3.1. Rectangular part with an oblique pre-crack

In the present example, we consider a thin rectangular plate with an oblique pre-crack of length a . A rectangular plate with an oblique crack and final mesh for the first step of the crack propagation are shown in Fig. 1a.

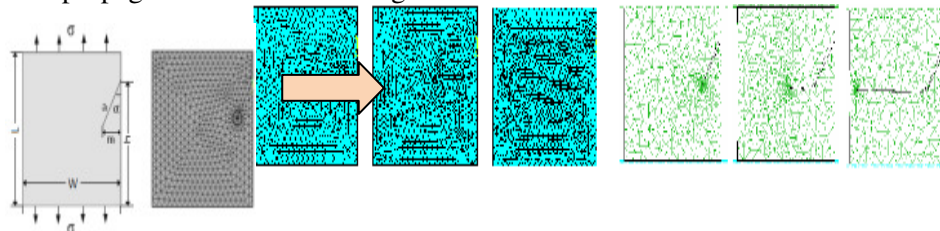


Fig. 1 Crack propagation trajectory of the inclined crack: a) Present study, b) Bouchard et al [3]

3.2 Single edge cracked plate with one hole

In order to determine the effect of a geometrical defect on the crack propagation, we studied the geometry of the single edge cracked plate with one hole. Fig.2a shows the final

configuration corresponding to the last evaluated crack length for the results obtained in Refs [3] and [4], and that obtained in present study.

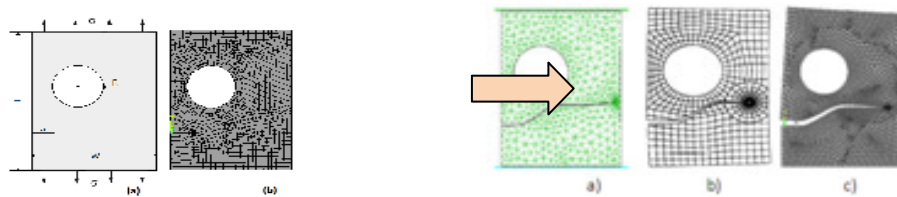


Fig. 2 Crack propagation trajectory: a) Bouchard et al. [3], b) Rashid [4] and c) Present study

3.3 Pre-cracked part with an inclusion

In the last example, the influence of an inclusion on the crack path is studied. A typical FE model of the plate is shown in Fig 3.

The mechanical properties of the material of the plate are: Young's modulus $E1$ and Poisson's ratio $\nu1$ and the inclusion considered is characterized by its Young's modulus $E2$ and Poisson's ratio $\nu2 = \nu1$. The prediction of the final crack propagation trajectory, for three ratios $E2/E1 = 1, 0.1$ and 10 is shown in Fig. 3a.

The same example has been studied by Bouchard et al. [3] using advanced re-meshing technique (Fig 3b). The predicted crack propagation trajectory of the present study is quite similar to that obtained in refs [3] and [5].

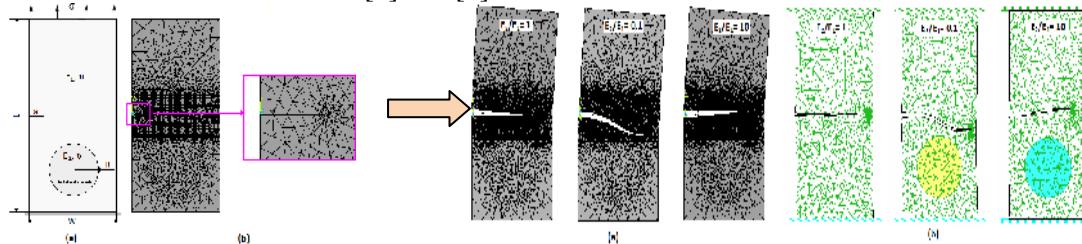


Fig. 3 4 Inclusion effect on the crack propagation path: a) Present study, b) Bouchard et al. [3]

4. Conclusion

In this paper, the FE modeling procedure proposed has been used successfully to simulate the propagation of cracks in plate specimens with holes and inclusions. The crack simulations for mode I and mixed mode cases showed the acceptable crack path predictions. The results of the assessments strongly indicated that the FE simulation for 2D linear elastic fracture mechanics problems has been successfully employed. Based on the results, it was recommended to add further development the APDL code to simulate crack propagation in elasto-plastic materials.

References

- [1] ANSYS, Inc. Programmer's Manual for Mechanical APDL, Release 12.1 November 2009.
- [2] Erdogan F, Sih GC. (1963). On the crack extension in plane loading and transverse shear. J Basic Engng 1963; 85:519-27.
- [3] Bouchard P.O., Bay F., Chastel Y. (2003). Numerical modelling of crack propagation, Comput Methods in Appl Mech and Engrg, 192, 3887-3908
- [4] M.M. Rashid (1998). The arbitrary local mesh replacement method: An alternative to remeshing for crack propagation analysis, Comput. Methods Appl. Mech. Engrg. 154,133-150
- [5] G. Legrain (2006), Extension de l'approche X-FEM aux grandes transformations pour la fissuration des milieux hyperélastiques, Université de Nantes, Thèse de Doctorat.

NUMERICAL ESTIMATION OF STRESS INTENSITY FACTORS AND CRACK PROPAGATION IN CEMENT PMMA

A. Boulenouar^{*1}, B. Benouis², N. Benamara¹

1Laboratory of Materials and Reactive Systems, Mechanical Engineering Department, University of Sidi-Bel-Abbes, BP. 89, City Larbi Ben Mhidi, Sidi Bel Abbes 22000, Algeria.

2University Tahar Moulay of Saida 20000, Algeria.

Abstract: Modelling of a crack propagating through a finite element mesh under mixed mode conditions is of prime importance in fracture mechanics. In this paper, three different crack growth criteria and the respective crack paths prediction in the cement mantle of the reconstructed acetabulum are compared. The maximum tangential stress (MTS) criterion, the minimum strain energy density (MSED) criterion and the new general fracture criterion based on the energy release rate $G(\theta)$ are investigated using advanced finite element technique. The displacement extrapolation technique (DET) is used, to obtain the SIFs at crack tip. Several examples are presented to show the robustness of the numerical techniques. The effect of the inclusions and cavities on the crack propagation in cement orthopedic are highlighted.

Keywords: crack growth path, stress intensity factor, strain energy density, maximum energy release.

1. Introduction

Total Hip Replacement (THR) is one of the most successful surgical procedures ever developed where a ball-socket structure is used to replace a diseased or damaged hip joint. The replacement cup socket is usually attached to the pelvis by acrylic bone cement, which consists of polymethylmethacrylate (PMMA) powder and a liquid component of methylmethacrylate monomer (MMA). When mixing together, polymerization takes place and within a few minutes (10-20 minutes depending on the formulation) of application to the bone cavity, the mixture becomes solid [1, 2]. Fig. 1a show a schematic of a cemented THR where the acetabular cup is fixed by the cement to the pelvic bone. The stability of the fixation critically depends on the integrity of the bone cement under typical physiological loading conditions. At least one million loading cycles per year would be experienced by the hip joint with the maximum hip contact force up to three times of body weight during walking [3].

The presence of defects in the cement during mixing can locally lead to regions of stress concentrations producing a possible fracture of the cement and consequently loosening of the prosthetic cup. There are three major types of defects [4]: porosities, inclusions and cracks.

It is known that cracks are the most dangerous type of defect because of the presence of stress intensity on their front. Most cracks identified in orthopedic cement are [5]:

2. Results and Analysis

In order to simulate the behavior of a crack under mixed mode loading (mode I+II); we considered an example of a crack of length a localized in the cement layer. This crack is inclined to the horizontal x -axis from -35° to 90° .

Figs. 1a and 1b show, respectively, the variations of the SIFs KI and KII according to the crack inclination α , for various crack length. The results obtained show that:

1- The SIF KI is maximum when the angle $\alpha=40^\circ$ (Fig. 8a), then it decreases gradually with the increase of the positive angle and tends to a very low value as one approaches the interface cup/cement.

2- The SIF KI decreases with the angle α , up to a minimal value corresponds to an angle $\alpha=-18^\circ$ from which factor KI takes values negative with the decrease of the angle α . These

negative values of KI indicate that the crack lips are closed due to stress compression around the crack tip.

3- The SIF KII is null when the inclination angle $\alpha=40^\circ$ and increases with this angle (Fig.8b). The factor KII decreases with the angle α up to a minimal value corresponds to an angle $\alpha \approx 18^\circ$ from which the curve takes on a downward look with the decrease of angle α .

Through these results, we can conclude that the initial crack angle of 40° represents the initial direction of the crack propagation according to the opening mode (mode-I) with: $KI=KI_{max}$ and $KII=0$.

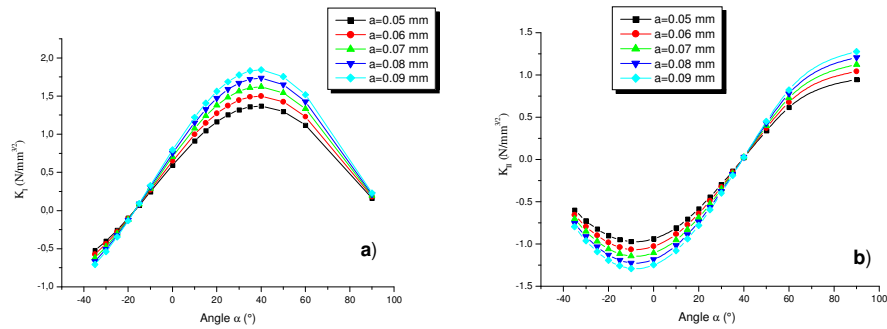


Fig.1. Variation of SIFs vs. crack length a and crack inclination α : a) K_I evolution and b) K_{II} evolution

3. Conclusion

In this paper, three crack kinking criteria and the crack paths prediction for several cases are compared in a PMMA cement layer. The maximum tangential stress criterion, the strain energy density criterion and the general fracture criterion are investigated using advanced finite element techniques. In order to obtain a better approximation of the field near the crack tip in cement of reconstructed acetabulum, special quarter point finite elements proposed by Barsoum are used. The displacement extrapolation technique is investigated to determine the SIFs under mixed-mode loading. Numerical calculations made by the finite element method show that this technique can correctly describe the stress and deformations field near the crack tip.

The initial crack angle of 40° represents the initial direction of the crack propagation according to the opening mode.

The three criteria give good results on the crack propagation path and the results between them are very close, for the cases proposed in this study.

References

- Bouziane MM., Bachir Bouiadjra B., Benbarek S., Tabeti M.S.H., Achour T. (2010), Finite element analysis of the behaviour of microvoids in the cement mantle of cemented hip stem: Static and dynamic analysis. *Materials and Design*. (31): 545-550.
- Achour T., Tabeti MSH., Bouziane MM., Benbarek S., Bachir Bouiadjra B., Mankour A. (2010), Finite element analysis of interfacial crack behavior in cemented total hip arthroplasty. *Computational Materials Science*. (47): 672-677.
- Tong J., Wong KY., (2005), Mixed Mode Fracture in Reconstructed Acetabulum, International Conference on Fracture, ICF11, Italy.
- Benbarek S., Bachir Bouiadjra B., Mankour A., Achour T., Serier B. (2009), Analysis of fracture behaviour of the cement mantle of reconstructed acetabulum. *Computational Materials Science*. 44: 1291-1295..

THE INFLUENCE OF GEOMETRIC DISCONTINUITY ON THE FATIGUE BEHAVIOR OF ALUMINUM ALLOY 7075-T6 AND 6082-T6.

A. Brahami^{1,*}, B. Bouchouicha¹, S. Adim²

1Laboratoire LMSR . Université Djillali Liabès, Sidi Bel Abbes, Algeria.

2Laboratoire LMSS . Université Djillali Liabès, Sidi Bel Abbes, Algeria.

Abstract: This study allowed us to see the influence of geometric discontinuity namely defects or cracks in the aluminum alloys (7075-T6 and 6082-T6), on the fatigue behavior, in other words life using the criteria of fracture mechanics using Ansys finite element code. This discontinuity has multiple internal or external origins resulting from improper design, imperfect implementation or from misuse. This work was performed by simulations on uninterrupted, hole and cracked specimens. Thereafter, the study has allowed to characterize the singularity of the stress field on crack tip by calculating the J-Integral.

Keywords: S-N curve, fatigue life, Aluminum alloy, J-Integral.

1. Introduction

The mechanical design of engineering structures usually involves an analysis of the stress and displacement fields in conjunction with a postulate predicting the event of failure itself. Sophisticated methods for determining stress distributions in loaded structures are available today. Detailed theoretical analyses based on simplifying assumptions regarding material behavior and structural geometry are undertaken to obtain an accurate knowledge of the stress state. For complicated structure or loading situations, experimental or numerical methods are preferable. Having performed the stress analysis, we select a suitable failure criterion for an assessment of the strength and integrity of the structural component.

3. Meshing

In our study the numerical computations happens in 3D and using the finite element method for determining the fatigue behavior, fatigue life, using the computer code ANSYS-WORKBENCH.

The calculations were conducted in plane stress CP.

The mesh size selected in this study for the different specimens is illustrated in the following figures:

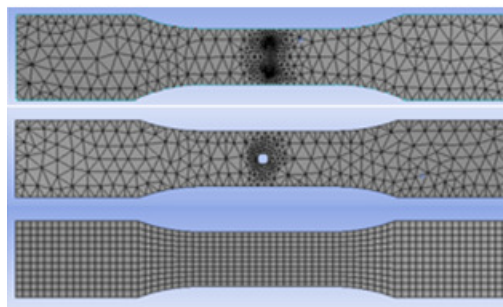


Fig. 1. Mesh used for the various studied specimens.

For the uninterrupted specimen, we chose quadratic elements with 8 nodes. For reasons of computes, I changed the mesh type for the other two specimens, and for that, I have chosen triangular elements.

In all three cases of calculations, I chose a fixed support down and I applied cyclic loading on the top of the specimen.

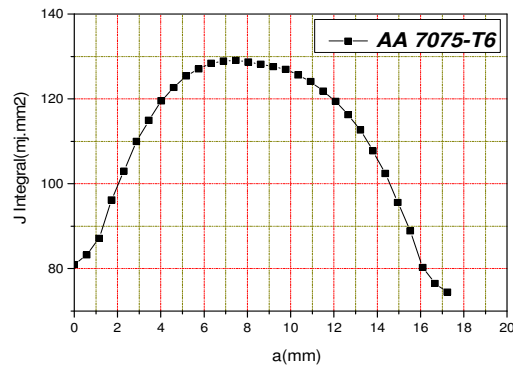


Fig.2. Evolution of I-integral as a function of the crack length.

4. Conclusion

The work of this article is a contribution to the treatment of the prediction life problem in uniaxial fatigue. In order to predict the service life of components subjected to uniaxial fatigue loading. To do this, our integrated study concerns a study of fatigue behavior of uninterrupted specimen then holed specimen finally cracked specimen.

This study has led us to see concretely the influence of the geometric discontinuity. Therefore, a defect that it is a hole or crack, significantly decreases the life of a structure. Also the study allowed us to say that the crack reduces the lifetime more than hole, and that due to the stress intensity factor, which is higher in a crack than a hole.

In order to deepen knowledge on the subject and to verify the validity of the suggested modeling. The work performed in this study could be continued. The main recommendations are:

To see the validity of the proposed geometric modeling and study the impact of the geometry.

To see the influence of other defects in addition to a hole and a crack.

To see the influence of the location of defects

Deepen the study in terms of energy, see the singularity of the stress field in crack tip.

References

- [1] thèse de doctorat, contribution à l'étude de cumul de dommage en fatigue mutiaxiale. SHEN Shen, Lille, France, 2012.
- [2] Laboratoire des matériaux et système réactif (LMSR), Sidi Bel Abbès, Algeria.
- [3] Aluminum: Physical Properties, Characteristics and Alloys, Ron Cobden, Alcan, Banbury, EAA-European Aluminium Association. 1994

CHECKING THE RESISTANCE OF A DRINKING WATER SUPPLY TO CRACKING CONSIDERATION WITH HIS ACTUAL BEHAVIOR

D. Said Lhadji¹

1 National high School of hydraulics, (ENSH), city Soumaa. Blida, Algeria.

Abstract: We study in this work the mechanical behavior polyethylene pipes buried specific property for the distribution of drinking water for the different types of consumers, This work is divided into two phases; in the first we focus on the calculation of the thrust of the embankment on driving by using different methods, bitter presents the results obtained for each calculation method end we choose the most suitable method to be used for the calculation of stresses in second place we analyze the strength of the pipe to stress that tend to crack and those two cases ;the first case or the work we assume that our pipeline operating pressure is the normal state and the other case we have a disturbance of the flow due to a pressure surge can increase the pressure in this case the pipeline be required to work at its limit state. The results obtained demonstrates that the elasticity of the pipe which is a characteristic of the pipe material has a primary role is that of absorption of external and internal stresses.

Keywords: Mechanical ; Pipes; Buried; Stress ;Pressure; Increase ;

1. Introduction

A drinking water supply system (AEP) consists of a set of infrastructure and facilities required to meet all the drinking water needs of urban and industrial area.

The phenomenon of "water hammer" occurs in a closed circuit when the fluid flow is abruptly accelerated or braked by the rapid closure of a valve, a tap or stopping a pump presentation of supply chooses.

To avoid damaging phenomenon can be caused paralysis of the system all the pipe must be dimensioned such that it resists this pressure fluctuation to avoid this problem .the good determination of cracking stress is necessary it is based the type of material and the mechanical characteristics of the pipe.

The pipeline that we will check it t is adduction of Megtaa Lazreg (Blia) [2].

2. Determination of pushed outside and inside the pipeline :

We will determine all the forces exercise on the line (internal and external) without neglecting his real condition which is buried, the determination of the pressure to backfill will be deducted after comparing different methods the general formula is [1]:

$$Q=K.H.Dext.\gamma_{soil} \tag{1}$$

3-determination of stress strain

Constraints will be determined for two cases, case or pipe work with this operating pressure, and the second he or there's a water hammer event that will work are driving a permissible limit state .The constraints will be determined according to the formulas [1].

$$\begin{cases} u(r) = \frac{1-\theta}{E} \frac{r_1^2 P_1 - r_2^2 P_2}{r_2^2 - r_1^2} r + \frac{1+\theta}{E} \frac{1}{r} \frac{r_1^2 r_2^2 (P_1 - P_2)}{r_2^2 - r_1^2} \\ \sigma(r) = \frac{r_1^2 P_1 - r_2^2 P_2}{r_2^2 - r_1^2} - \frac{1}{r^2} \frac{r_1^2 r_2^2 (P_1 - P_2)}{r_2^2 - r_1^2} \\ \sigma(\theta) = \frac{r_1^2 P_1 - r_2^2 P_2}{r_2^2 - r_1^2} + \frac{1}{r^2} \frac{r_1^2 r_2^2 (P_1 - P_2)}{r_2^2 - r_1^2} \end{cases} \tag{2}$$

results of the calculated stresses

* case N°01 :

where $r = r_1 = 0,1637m$.

$$\begin{cases} u_r(r_1) = 4,02 \cdot 10^{-3} \text{ m} \\ \sigma_r(r_1) = -10,05 \text{ bars} \\ \sigma_\theta(r_1) = 33,98 \text{ bars} \end{cases}$$

where $r=r_2 = 0,2 \text{ m}$.

$$\begin{cases} u_r(r_2) = 3,33 \cdot 10^{-3} \text{ m} \\ \sigma_r(r_2) = -2,78 \text{ bars} \\ \sigma_\theta(r_2) = 26,72 \text{ bars} \end{cases}$$

PE 100 we allowable stress equal to 80 bar.

$33,98 < 80 \text{ bars}$

* Case N°02:

where $r = r_1 = 0,1637 \text{ m}$

$$\begin{cases} u_r(r_1) = 7,13 \cdot 10^{-3} \text{ m} \\ \sigma_r(r_1) = -15,88 \text{ bars} \\ \sigma_\theta(r_1) = 64,36 \text{ bars} \end{cases}$$

where $r=r_2 = 0,2 \text{ m}$

$$\begin{cases} u_r(r_2) = 5,84 \cdot 10^{-3} \text{ m} \\ \sigma_r(r_2) = -2,64 \text{ bars} \\ \sigma_\theta(r_2) = 51,12 \text{ bars} \end{cases}$$

PE 100 we allowable stress equal to 80 bars

$64,36 < 80 \text{ bars}$

4. Conclusions

The supply we chose to check behaves well overlooked the point of cracking stress resistance seen even when the latter work for that nominal pressure that is due to the elasticity of the material used. But what we can recommend is that it must not neglect the type of method to be used for the determination of the embankments often pushed into the calculations this overhead is neglected and the pipes are sized as if it was the driving on ground.

References

- [1] A. Mokhtar memory of late study ENSH "Mechanical behavior of buried pipelines, memoires end study" 119p.2000.
- [2] A.Roumane, CTH technical report (ASP building Blida study of steam-hall Melouane Bougara-ouled slama-Larbaa), 2012.

NUMERICAL ANALYSIS OF THE INTERFACE CRACKS IN CONTINUOUS FIBRE REINFORCED METAL MATRIX COMPOSITES

F. Bouafia^{1,2}, H. Fekirini¹, L. Zouambi^{1,3}, B. Serier¹

¹University of SidiBel Abbes, LMPM, 22000, SidiBel Abbes, Algeria

²CenterUniversity of AinTemouchent, 46000, AinTemouchent, Algeria

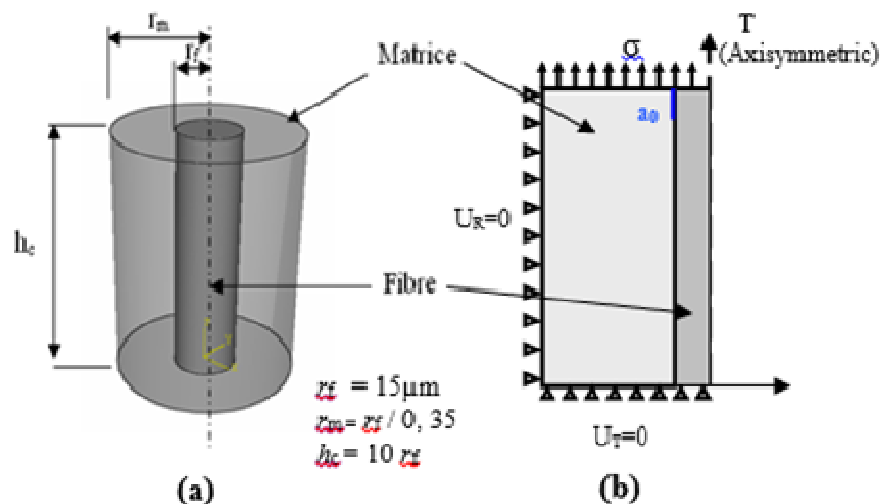
³CenterUniversity of Relizane, 48000, Relizane, Algeria.

Abstract: The main objective of the present paper is numerical analysis of the micro crack propagation along a composite interface. Hence, the finite element technique was used to calculate the opening-mode and sliding-mode stress intensity factors. A two-dimensional linear elastic model was developed to investigate the initiation of a ring-shaped matrix crack from the end of a single sized ceramic continuous-fibre embedded in a metal matrix, subjected to tensile loading. The effect of the applied load, mechanical properties of the composite materials, and fibre volume fraction on crack growth was studied. Moreover, effects of the existence of defects (inclusion, micro-void, and crack) are also discussed. The results show that a sliding mode stress intensity factor is affected more than opening mode stress intensity factor as the loading applied value increases. The existence of the defects in the MMCs generate a resistance to opening mode of the crack. In the other hands they favourite the sliding mode.

Keywords: Crack growth; Metal matrix composite; Finite element method; Stress intensity factor, Void.

1. Introduction

Continuous fibres reinforced metal matrix composites (MMCs) offer superior properties over conventional alloys and have been widely studied because of their many potential applications. Indeed, Liorca [1] revealed during service of highly loaded components fatigue cracks can be initiated. After initiation, these fatigue cracks can grow until final failure occurs. Aslantas and Tas_getiren [2] presented a numerical solution for the problem of interface crack. Variations in the stress intensity factors KI and KII, with load position are obtained for various cases such as different combinations of material of coating layer and substrate, changes in the coefficient of friction on the surface. Aslantas [3], Meguid and Zhao [4] have shown that the finite element technique has been extensively employed to analyze a variety of problems involving two dimensional interface cracks.



2. Geometrical Model

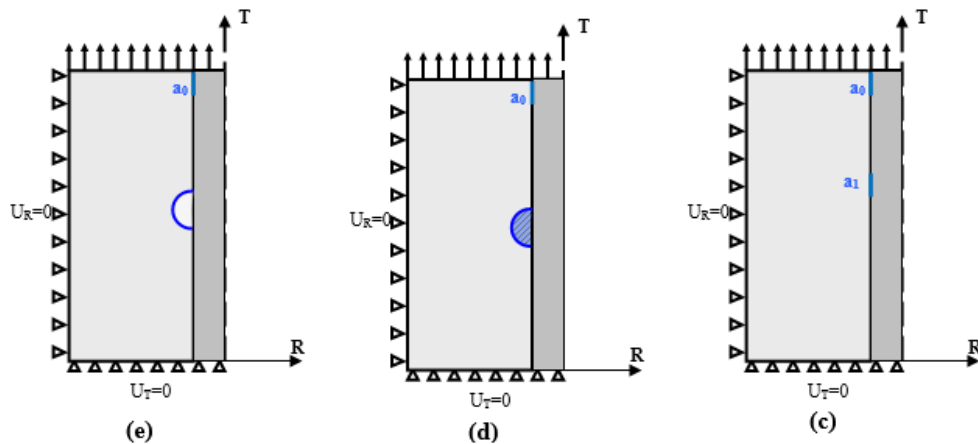


Fig. 1. (a) The composite cylinder model, (b) axisymmetric model of the composite with initial crack, (c) axisymmetric model with crack a_1 , (d) axisymmetric model with inclusion, (e) axisymmetric model with micro-void, (f) Finite element mesh

3. Conclusions

The analysis presented in this paper provides a linear elastic fracture mechanics analysis of interface crack problem in continuous fibre reinforced metal matrix composites. Hence, finite element model has been developed to calculate K_I and K_{II} stress intensity factors at the crack tip. A crack is assumed between fiber and matrix. The effect of the load applied, mechanical properties of the composite materials, fibre volume fraction and the existence of the defects on crack growth has been investigated. The following general results may be drawn as a conclusion of the study.

- The stress intensity factor K_{II} values are much higher than K_I values. Sliding mode K_{II} stress intensity factor is affected more than opening mode K_I stress intensity factor as the loading applied value increases.
- Sliding mode K_{II} stress intensity factor is more affected by the variation of E_f/E_m than opening mode factor K_I . The stress fields in the vicinity of the crack tip are dominated by shear mode. Hence, debonding between fiber and matrix most probably occurs due to shear mode under axial loading.
- The fibre volume fraction is an important parameter. Indeed, it was shown that a weak volume fraction generates strong stress intensity factors K_I and K_{II} . This result reveals the importance of the process of development which must granted a good distribution of fibers in the matrix.
- The existence of another crack on the line of propagation of the first one does not have much effect on K_I and K_{II} stress intensity factor.
- The existence of the defects in the matrix i.e., inclusions and the micro void on the line of propagation of the crack has much effect on K_I and K_{II} stress intensity factor. Indeed it has been shown that the existence of these defects in the MMCs generate a resistance to opening of the crack. In the other hands they favourite the sliding mode.

Finally, all these conclusions highlight the importance of development of a rigorous model, which take into account all welding parameters in predicting spot weld failure.

References

- [1] Liorca, J. "Fatigue of particle and whisker-reinforced metal matrix composites" J. Prog. Mater. Sci. 47 (3), Pages 283–353. (2002).
- [2] Aslantas, K., Tas_getiren, S. "Debonding between coating and substrate due to rolling sliding contact." J. Materials and Design 43, Pages 871–876. (2002).

Comprehensive approach to fracture mechanics applied to polymers (HDPE case):

Houari tarek¹, Benguediab Mohamed², Houari mohamed sidahmed³

¹University Mascara , Bab ali city , Mascara, Algeria

²University Sidi Bel abbes , City 150 , Sidi Bel abbes , Algeria

³University Mascara , Sidi Said city ,Mascara , Algeria

Abstract:

High density polyethylene (HDPE) is a polymer model of the family of semi-crystalline; it represents a real industrial interest since it is one of the most produced thermoplastic polymers in the world. The study of the deformation and damage behavior and breaking HDPE was proposed from experimental and numerical approaches. Two approaches to energy (J integral and EWF) of fracture mechanics were examined on two types of specimens (CT, DENT) under tension. We conclude that the EWF method for its simplicity is the most suitable parameter for characterizing the intrinsic break our material.

Keywords: High density polyethylene; Triaxiality; Fracture; J integral; EWF method; Damage models;; Finite element computations.

1. Introduction

The advanced technology and the evolution of increasingly enhanced in the field of unconventional materials impose a significant competitive technically and economically between metals and polymers for the production of multiform parts for use in areas as varied as the transport sector energy, automotive, aerospace or the medical. High density polyethylene (HDPE), subject of this study, is a polymer family model of semi-crystalline, the specificity of which resides in the combination of an amorphous phase and a crystalline phase. In fracture mechanics, there are two main methods to analyze the sustainability of a structure for a given material: either the global approach which as its name suggests uses measurable quantities such as global energy for the boot, or the local approach which has flourished thanks to the performance of computer codes with which we can access local variables. In this study, we address the fracture mechanics by presenting two global approaches: J integral and essential work of fracture (EWF) can be applied to polymeric materials.

2.EWF Approach

The EWF concept (for "Essential Work of Fracture") is a widely used technique to evaluate the tensile strength of ductile polymers [1]. It is to work on specimens having a size and a variable notch geometry , and measure the material's ability to resist breakage. We present the theoretical foundations and the most commonly used experimental methods .

If L is the uncracked ligament length, t is the thickness and W is the width and is a shape factor, then the total energy absorbed during the breaking process is:

$$w_f = w_e + \beta \cdot w_p \cdot L, \quad (1)$$

And so, the essential work of fracture can be determined by plotting a fig

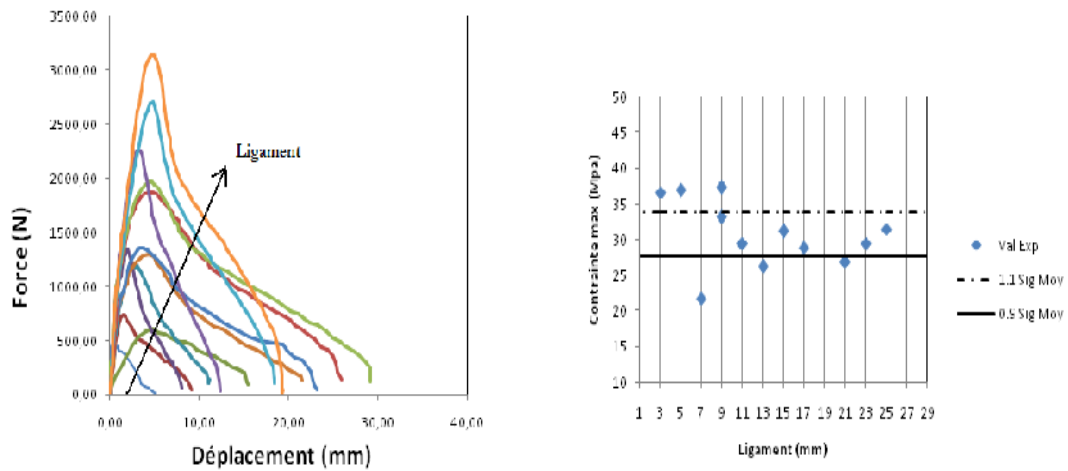


Fig : Curve Force - travel for EWF tests; the arrow shows the increase in the length of the ligament. Variation of σ max according to the ligament for DENT samples.

3. Conclusions

The study we have just presented has focused on the characterization and identification of the behavior of HDPE under different loading conditions, such as in quasi-static tensile and breaking with coupling damage. The study of the deformation and behavior to damage and breakage of the HDPE was proposed from experimental and numerical approaches. Two energy approaches (J integral and EWF) of fracture mechanics were examined on two types of specimens (CT, DENT) under tension. The EWF method has allowed us to highlight a very ductile behavior characterized by the existence of a large phase plastic deformation.

References

[1]. Y-W. Mai, B. Cotterell. On the essential work of ductile fracture in polymers. *Int. J. Fract.*, 32, 105-125, 1986.

STRAIN ENERGY DENSITY PREDICTION OF MIXED-MODE CRACK PROPAGATION IN FUNCTIONALLY GRADED MATERIALS

N. Benamara^{*1}, A. Boulenouar¹, M. Aminallah¹, N. Benseddiq²

1Laboratory of Materials and Reactive Systems, Mechanical Engineering Department, University of Sidi-Bel-Abbes, BP. 89, City Larbi Ben Mhidi, Sidi Bel Abbes 22000, Algeria.

2Mechanics Laboratory of Lille, CNRS UMR 8107, Ecole Polytech'Lille, University of Lille1, 59655 Villeneuve d'Ascq, France

Abstract: The objective of this work is to present a numerical modeling of crack propagation path in functionally graded materials (FGMs) under mixed-mode loadings. The minimum strain energy density criterion (MSED) and the displacement extrapolation technique (DET) are investigated in the context of fracture and crack growth in FGMs. Using the Ansys Parametric Design Language (APDL), the direction angle is evaluated as a function of stress intensity factors (SIFs) at each increment of propagation and the variation continues of the material properties are incorporated by specifying the material parameters at the centroid of each finite element. In this paper, several applications are investigated to check for the robustness of the numerical techniques. The defaults effect (inclusions and cavities) on the crack propagation path in FGMs are highlighted

Keywords: Functionally graded materials; Strain energy density; Mixed-mode; Displacement extrapolation; Stress intensity factor

1. Introduction

There are several techniques used to obtain stress intensity factors (SIFs) in homogeneous and inhomogeneous materials, such as the displacement extrapolation technique (DET) [20,21] the displacement correlation technique (DCT)[22] , the J*k Integral[23,24] and the modified crack-closure integral[25]. In this work, the displacement extrapolation technique is investigated to evaluate the SIFs KI and KII as follows:

$$K_I = \frac{E_{tip}}{3(1+\nu_{tip})(1+k_{tip})} \sqrt{\frac{2\pi}{L_e}} \left[4(v_b - v_d) - \frac{(v_c - v_e)}{2} \right], \quad (1a)$$

$$K_{II} = \frac{E_{tip}}{3(1+\nu_{tip})(1+k_{tip})} \sqrt{\frac{2\pi}{L_e}} \left(4(u_b - u_d) - \frac{(u_c - u_e)}{2} \right), \quad (1b)$$

4.2 Crack propagation simulation in FGM

In present problem, we consider the single edge cracked FGM plate with $L/w=2$ and $a/w=0.5$. The plate is imposed by a plane stress condition under uni-axial loading (Fig. 7a). A typical integration grid of the cracked plate is illustrated in Fig. 7b. For first step of crack propagation, the number of element used in this analysis is 1043 elements with 3196 nodes.

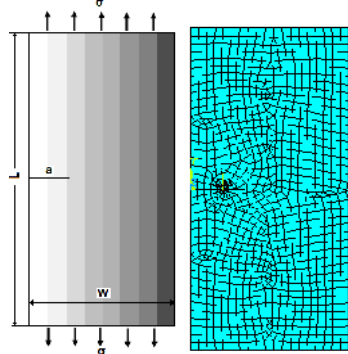


Fig. 1 a) Geometrical model of the cracked FGM plate and b) final mesh for initial configuration

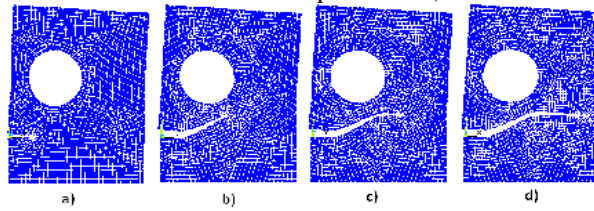


Fig. 2 Four steps of crack propagation trajectory for a single edge cracked FGM plate with one hole

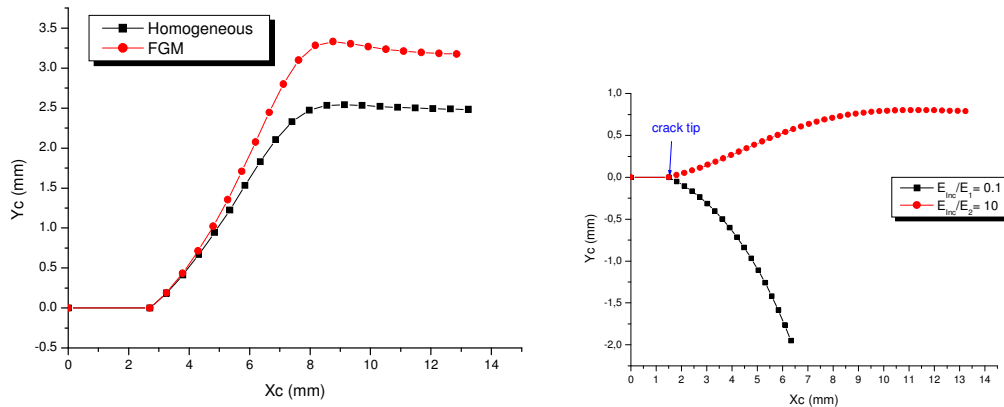


Fig. 3 Positions of the crack-tip obtained for homogeneous and FGM, Positions of the crack-tip obtained for FGM plate with an inclusion.

5. Conclusion

This work investigates mixed-mode crack growth in FGMs plates using the Ansys Parametric Design Language. The SIFs for a single edge cracked plate was evaluated and compared with under mode-I loading. The comparison shows that our numerical techniques is capable of demonstrating the SIF evaluation and the crack path direction satisfactorily. The methodology of crack propagation modeling proposed in this investigation has been used successfully to predict the crack path in FGM plate with holes and inclusions.

The presence of holes and inclusions in the plates disturbed the stress and strain fields providing interesting crack trajectories. The results indicated that FE analysis for fracture mechanics problems has been successfully employed for homogenous and FGM. Based on the results, it was recommended to add further development the APDL code to simulate crack propagation in orthotropic FGMs.

References

- [1] Kim. J.H and Paulino.G.H. Finite element evaluation of mixed mode stress intensity factors in functionally graded materials. International Journal for Numerical Methods in Engineering 2002; 53:1903-1935
- [2] Kim. J.H and Paulino.G.H. Simulation of crack propagation in functionally graded materials under mixed-mode and non-proportional loading. International Journal of Mechanics and Materials in Design 2004; 1: 63-94.
- [3] Rao. B.N and Rahman. S. Mesh-free analysis of cracks in isotropic functionally graded materials. Engineering Fracture Mechanics; 2003, 1-27

NUMERICAL ANALYSIS OF THE DAMAGE OF COMPOSED MATERIALS: METAL-CERAMIC TYPE.

S. Ramdoun^{1,13}, A. Kaddouri¹, H. Fekirini¹, N. Serier¹, B. Serier¹

1 University Sidi Bel-Abbes, LMPM Mechanical Engineering Department, 22000, Algeria.

Abstract: Bimaterials applied in electronics, aerospace, and mechanical etc., are essentially constituted by a ceramic and a metal. These two components present mechanical and physical properties diametrically opposed. To take advantage of these properties, the metal and the ceramic are bonded together at relatively high temperatures. This therefore results in highly localized residual stresses at the interface between these two materials. Added to commissioning constraints, these internal stresses can lead to damage to the Bimaterial. To get, a numerical three-dimensional model by the finite element method has been developed. Abaqus software was used to analyze the behavior of interfacial cracks and ceramic in elastic behavior. The effect of the location of cracks, their sizes, and the load nature has been highlighted. This behavior is studied in terms of variation of the stress intensity factor in modes I, II and III.

Keywords: damage, internal stresses, Bimaterial, cracks, finite element analysis.

1. Introduction

In this work we analyze the mechanical behavior of composite materials. Remember that these materials, ceramic-metal, have been developed either to enjoy the mechanical, thermal and physical properties of materials diametrically opposed, one thus speaks of bimaterial or to improve the initially low stiffness of a material is called composite materials. Composite materials are usually prepared at relatively high temperatures. This temperature is selected depending on the material whose melting point is the lowest. Cooling said temperature than ambient induced internal stresses in close proximity to the interface of the two components of the compound material. Several studies have been devoted to the mechanical behavior of materials subjected to mechanical efforts. Thus, K. Fan et al. [1] showed by the finite element method mechanical damage of a ductile model used to study the effects of conflict on work hardening resistance to fracture behavior of two cracks (interface cracks and near the interface crack) of bimaterial. The results of this study show that for interfacial cracks, the effects of material stress caused by the work hardening mismatch are detrimental to the tensile strength due to the increase in the crack-tip stress triaxiality, and these adverse effects increase with the degree of disparity in work hardening. Using the technique of the hop cycle, A. Moslemian et al. [2] propose an approach based on a finite element analysis to simulate the accelerated propagation of fatigue cracks initiated at the interface of a Bimaterial. This approach appears attractive to the prediction of the growth of interfacial fatigue crack.

2. Finite element modeling

The numerical model developed for this study is a formed three-dimensional structure consisting of two materials (copper and zirconia) assembled together (fig. 1). This assembly (compound material) is subjected to uniaxial tensile stress amplitude (σ) uniformly distributed (fig.1). This width bimatériaux ($l = 8$ mm), height ($h = 12$ mm) and thickness ($e = 2$ mm), contains a size of 0.5 mm, crack initiated at the interface.

¹³ Corresponding author

E-mail address: ramdoun-sara@hotmail.com

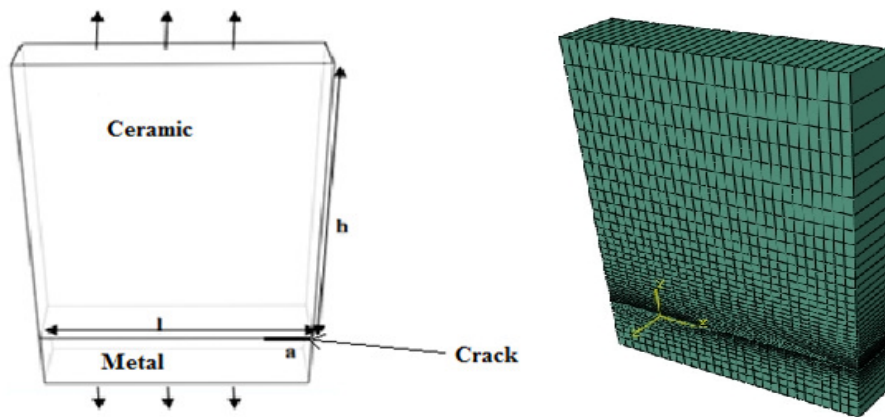


Fig. 1. Cracked model used.

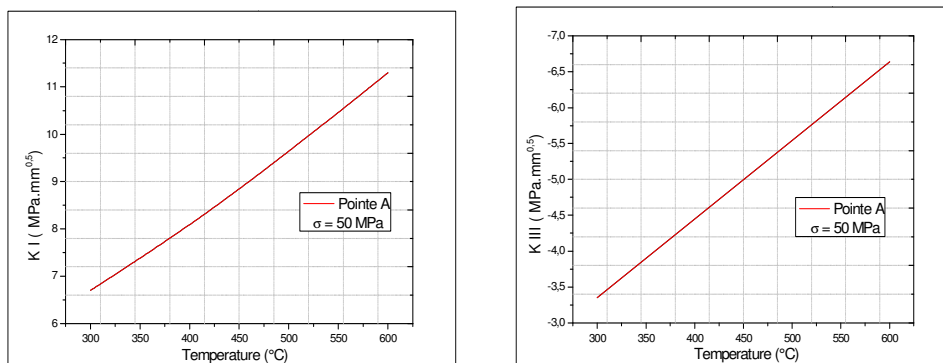


Fig. 2. Effect of thermomechanical loading on the mode stress intensity factor I and III.

3. Conclusions

The results obtained in this work show that:

- Implementation temperature is a physical parameter for the sustainability of materials composed metal-ceramic. It determines the level and distribution of residual thermal stresses;
- Interfacial crack subjected to uniaxial tensile stress perpendicular to his lips, spreads pure opening mode. The propagation kinetics is even stronger than the material compound is more strongly mechanically applied;
- The thermomechanical loading, applied to an interfacial crack, only affects propagation kinetics in open mode. The other two growth patterns appear to be independent of the combination of mechanical and thermal stresses. These two modes are rather sensitive to thermal stresses;

References

- [1] K. Fan, G.Z. Wang, F.Z. Xuan, S.T. Tu. (2015). J. Materials & Design, Vol. 68, P. 186–194,
- [2] R. Moslemian, A.M. Karlsson, C. Berggreen. (2011).J. Fatigue Vol. 33, P. 1526–1532,

CRACK DAMAGE INDICATOR DETECTION USING THE FIRST MODE SHAPE MEASURED.

S. Tiachacht^{1,*}, A. Bouazzouni¹, M. Almansba¹, M. Almansba¹
 IMOULOUD MAMMERI University of Tizi-Ouzou, B.P. N°17 RP, 15000, Algeria.

Abstract: At the design stage and during use, structures must gratify standards of safety and reliability always more demanding. In this sense, we have developed a procedure for detecting damage to a beam structure based first measured and calculated modes (finite element model) of the structure. The procedure was applied to different cases of boundary conditions, and the results are satisfactory in this case structures.

Keywords: beam, damage, mode measure, indicator, finite element.

1. Introduction

During their operation, the machines need to be followed to the anticipation of failures that may be known. Of all the physical parameters, vibration measurements are by far the most reliable and informative data on the machine operating status.

Currently, it is expected that researchers are developing methods of detection, localization and quantification of damage to help every newly recruited engineer to undertake faster and easier maintenance activity.

Pandey et al. [1] first stated that the curvature mode shape at node i on the structure can be obtained by using a numerical formulation called central difference approximation. Radzienski et al [2] applied the Hybrid Damage Detection method to identify structural damage due to fatigue in aluminium cantilever beams.

In what follows, we develop a procedure for locating and quantification of damage in a beam structure and lattice which operates the first measured and calculated eigenvectors (finite element model) of the structure.

2. Damage indicator

Using the first mode of healthy and measured damaged structure, we propose a location indicator of damage as a result:

$$CDI_j = \left| \frac{\vartheta_{i+1}^{FE} - \vartheta_i^{FE}}{\vartheta_{i+1}^m - \vartheta_i^m} \right| ; i = 1 \text{ to } Nn ; j = 1 \text{ to } N \quad (1)$$

where, ϑ_i^{FE} represent the displacement with node i th of the finite elements model; ϑ_i^m represent the displacement measured with node i th; Nn the number of nodes and N the number of elements.

3. Results and discussion

Example 1 - Single damage [3]

The first example, the experiments have been done for a steel cantilever beam fixed free of dimensions: $L \times H \times W = 1 \times 0.02 \times 0.01$ m³. Various damage scenarios have been analysed. As the damage a saw cutting located at $L_1 = 0.3$ m of the beam length L (starting from the fixed end) with cut depth H_c equal to 10% of the beam height has been tested. The width of the crack has been kept constant and equal to $L_c = 0.001$ m. the results of

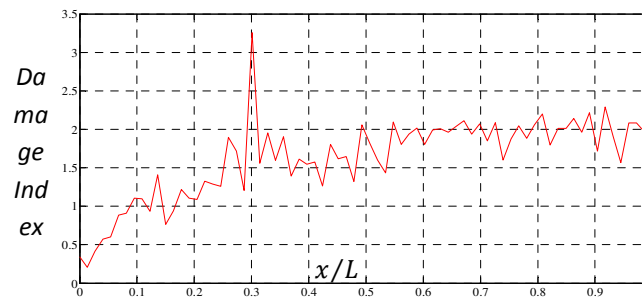


Fig. 2. Damage location results of the beam using the first modal data

The results of the application of the damage indicator on the beam shows in figure 3. It shows the presence of only a damage in the beam which lies at distance 0.3m (9th element).

Example 2 - Multiple damages [4]

An experiment of simple cantilever beams under the loading arrangement shown in Fig. 2 was carried out to illustrate the proposed damage detection method. It was assumed that each beam for the analytical approach was modeled by using the finite element method with 50 beam elements. Assumed, the beams were as steel with an elastic modulus of 1.95×10^5 MPa. The experiment was made on 1m cantilever beams with a gross cross-section of 75mm \times 9mm and the damage section of 25mm \times 9mm. The damage degree of the section was established as the 67% strength loss of the initial second moment of inertia. The damage of the beams was located at 200, 400mm, respectively, from the fixed end, and they had a single damage or multiple damages.

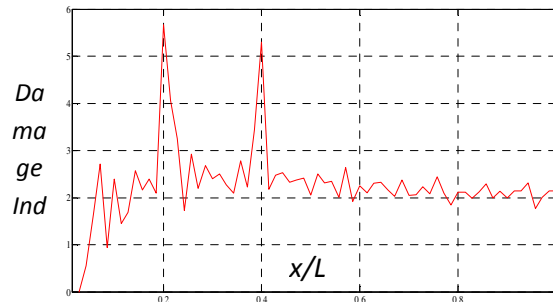


Fig. 4. Multiple Damages location results of the beam using the first modal data

The results of the application of the damage indicator on the beam shows in figure 4. It shows the presence of two damage in the beam, the first at 200mm and the second at 400mm.

5. Conclusions

The procedure developed in this work aims to locate the damage in a beam structure by exploiting modal measures. The advantage of this procedure is that it uses a single mode. several test cases are processed. The place of the damage is localized by exploiting these modal measurements.

References

- [4] E-T Lee, H-C Eun. (2008), Damage detection of damaged beam by constrained displacement curvature, *Journal of Mechanical Science and Technology*.
- [3] M. Radzienski, M. Krawczuk, M Palacz, (2011), Improvement of damage detection methods based on experimental modal parameters. *Mechanical Systems and Signal Processing*.
- [5] N. Hu, X. Wang, H. Fukunaga, Z.H. Yao, H.X.Zhang, Z.S. Wu. (2001), Damage assessment of structures using modal test data., *International Journal of Solids and Structures*.
- [6] H-I Yoon, I-S Son, S-J Ahn. (2007), Free Vibration Analysis of Euler-Bernoulli Beam with Double Cracks, *Journal of Mechanical Science and Technology*.

THE INHIBITION PARAMETERS EFFECT ON CORROSION RESISTANCE OF API X52 STEEL USING DESIGN OF EXPERIMENT

M. A. Benghalia ^{ab}, C. Fares ^a, M. Hadj Meliani ^a,

a Laboratory for theoretical physics and material physics; Department of Process Engineering, Faculty of Technology, Hassiba Ben Bouali University of Chlef, B.P. 151, 02000 Chlef, Algeria.

b Water and Environment Laboratory, Faculty of Technology, Hassiba Ben Bouali University of Chlef, B.P. 151, 02000 Chlef, Algeria

Presenting author: benghalia-amal@hotmail.fr

Abstract: The present study attempted to investigate the best conditions for the use of extract of *Ruta Chalepensis* as corrosion inhibitor of APIX52 steel in 1M HCl. The inhibition of APIX52 corrosion was studied using potentiodynamic polarization of monitoring corrosion rate. A mathematical model is developed by Full Factorial design approach to find the relationship between the various input parameters (factors) and the outputs parameters (response). The proposed Full Factorial design consisted of three factors (bath temperature, inhibitor concentration and stirring speed) at two different levels. The experiments were performed with the selected factors and levels and the results were further processed to find the optimized conditions (inhibitor efficiency). A validation experiment was conducted at the specified conditions at temperature of 323°K, Stirring speed of 6 tr/mn and inhibitor concentration of 18%. It could be concluded that factorial design was adequately applicable in the optimization of process variables and that *Ruta chalpensis* sufficiently inhibited the corrosion of APIX52 at the conditions of the experiment.

Key words: *Ruta Chalepensis* (RC), inhibitor, experimental design, full factorial design (FFD).

EVALUATION OF THE STRESS CORROSION OF 304L STAINLESS STEEL WELDED BY GTAW PROCESS

B. A. Kessal¹, C. Fares¹, L. Milovic², M. Ouchène³

1 Laboratory for theoretical physics and material physics; Department of Process Engineering, Faculty of Sciences, Hassiba Ben Bouali University of Chlef, B.P. 151, 02000 Chlef, Algeria.

2 University of Belgrade, Faculty of technology and metallurgy, Karnegijeva 4, 11120 Belgrade, Serbia

3 IAP, Algerian Oil Institute, 1st November Street, 35000 Boumerdes, Algeria

Author mail: aminelifehouse27000@gmail.com

Abstract: Austenitic stainless steels are widely used in high performance pressure vessels, petrochemical process as ammonia and urea canalization due to their very good corrosion resistance and superior mechanical properties. However, austenitic stainless steels are prone to sensitization when subjected to higher temperatures (673K to 1173K) during the manufacturing process (e.g. welding) and/or certain applications (e.g. Urea transportation). During sensitization, chromium in the matrix precipitates out as carbides and intermetallic compounds decreasing the corrosion resistance and mechanical properties. In the present investigation, 304L austenitic stainless steel was subjected to varying inputs parameters (Number of Pass, Gas Flow Argon, Current) by Gas Tungsten arc welding process using a standard 308L electrode. The purpose of this study was to discuss the effect of three inputs used in GTAW process on microstructure, hardness and corrosion behavior of 304L stainless steel. The radiography was also used in the non-destructive evaluation to recognize various features of the welded specimens. Corrosion behavior of weldments in 30g/l NaCl solution at 25 ± 1 °C was investigated by using potentiodynamic polarization. Result indicated that the microstructure of fusion zones exhibited on the varying of the input parameters effect. Therefore, as the Gas Flow Argon increased, the hardness and corrosion resistance increased.

Keywords: Gas Tungsten Arc Welding (GTAW); Corrosion resistance; Stress corrosion, Microstructure.

Water irrigation in the Chlef region using photovoltaic solar energy

T. Tahri (1,3), H. Zahloul (2), K. E. Meddah(1), H. Lazergue(1)

(1) *Electrical Engineering Department, Hassiba Benbouali University of Chlef*

(2) *Mechanical Engineering Department, Hassiba Benbouali University of Chlef*

(3) *Laboratory of Electrical Engineering and Renewable Energy*

t.tahri@univ-chlef.dz

Abstract

This paper presents a theoretical study that leads to the design of a photovoltaic pumping system to irrigate six hectares of oranges in the valley of Chlef using the software "PVSYST". It was shown that the site of Chlef presents a favorable climate to this type of energy with an irradiation more than 5 kWh/m²/day, and significant resources underground water. Another very important coincidence still promotes the use of this type of energy for pumping water in Chlef is that the demand for water, especially in agriculture, peaked in hot and dry where it is precisely when one has access to the maximum of solar energy.

Keywords: Solar Energy, Irradiation, Water Pumping, Design, Valley of Chlef

1. Introduction

Energy production is a challenge of great importance for the future, indeed the energy needs of industrialized countries continue to increase, and otherwise developing countries will need more energy to carries out their development. Nowadays, a large part of global energy production comes from fossil fuels, the consumption of these sources results in greenhouse gas emissions and thus an increase in pollution. The additional danger is that excessive consumption of natural resources reduces the stock reserves of this type of energy in a hazardous manner for future generations, and also face the numerous economic and oil crises science is interested in the so-called renewable resources which constitute a strategic sector and have a special place in the areas of research and development.

2 Estimation for water needs

The water needs for irrigation depends on the type of culture, the irrigation method and meteorological factors (temperature, humidity, and the season of the year in question). However, practice and local experience are still very essential for proper needs assessment. The water needs of orange for Chlef site are given by the following Table 1.

Table 1: seasonal water needs

Season	Winter	Spring	Summer	Autumn
Debit (m ³ /d)	10	30	70	10

Table 2: Technical data of the controller PS4000 [8].

Power	Max 4000W
Input voltage	Max 375V
Optimal V _{mp}	>238V
Motor current	Max 15A
Yield	Max 98%
Ambient temperature	-30 to 50 °C
Manometric head	Max 80m
Hourly debit	Max 14m ³ /h

Engine ECdrive 4000-C

Table 3: Motor Technical Data ECdrive 4000C. [8]

Rated power	3500W
Yield	Max 92%
Motor speed	900 to 3300 rpm
Immersion	Max 250m

3 Results and discussions

Chlef site design: In the main window of PVSYST software, we choose a new project of a pump design (Fig. 4).

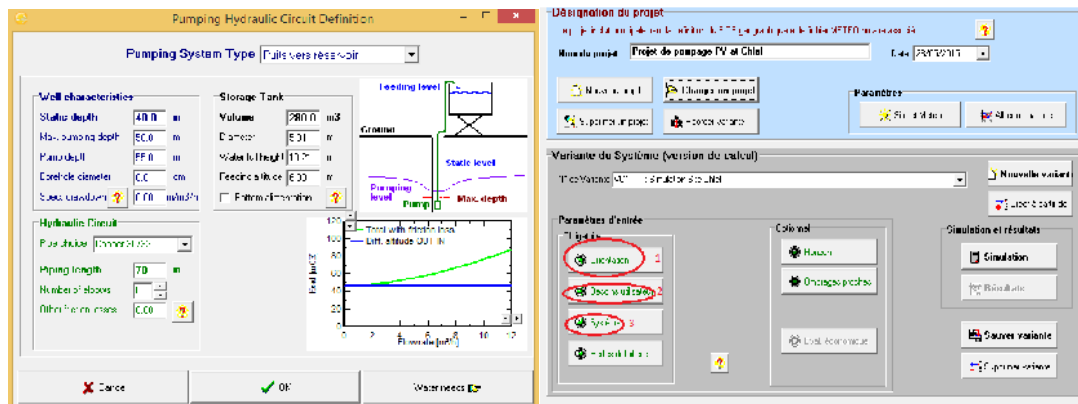


Fig.1,2 : Parameters of hydraulic circuit Choice of input parameters Orientation We choose the inclination of the panel is equal to the latitude of the installation site secured throughout the year.

1- Simulation main results:

Water pumped = 11147 m³
 Needs of water = 11011 m³
 Energy to pump = 9238 kWh
 Unused PV energy (full tank) = 9493 kWh
 System Efficiency = 7.8%
 Pump efficiency = 76.9%
 Unused portion = 8%
 Missing Water = - 1.2%

According to the study, the appropriate PV generator consists of 72 polycrystalline silicon photovoltaic modules with a total output of 18 kWp. Thus, the peak power of the PV generator is 3300 W.

References

- [1] A. Hammidat, A. Hadj Arab et M.T. Boukadoum « Performances et coûts des systèmes de pompage PV en Algérie », Rev. Energ. Ren. Vol. 8 (2005) 157 - 166).
- [2] M. T. Boukadoum, A. Hamidat et N. Ourabia Le Pompage Photovoltaïque Zones Arides (2002)
- [3] Faire de l'électricité avec le soleil IDD « Maison écologique » 2008/2009

NUMERICAL SIMULATION OF DYNAMICS FLOWS OF DIFFUSION FLAMES IN THE COMBUSTION CHAMBER

S. Nechad^{1*}, A. Khelil¹, L. Loukarfi¹, M. Bouketita¹, A. Bennia¹, Y. Bouhamidi¹

¹University Hassiba Benbouali, laboratory C.E.M.S.M. B.P. 151, 2000 Chlef, Algeria

*Corresponding author: s.nechad@univ-chlef.dz

Abstract: This work deals with numerical simulations in three dimensions (3D) non-premixed turbulent diffusion flames in a combustion chamber of a burner with radial swirler coaxial methane injection. The swirl flows remain an important subject of study in the new technologies of the combustion burners because they promote the flame stabilization and are commonly used to efficiently mix the fuel with air. The swirl is an essential element in modern combustion chambers designed to run lean to reduce the formation of pollutants. Thus, swirl movement of the contribution to the mixture makes it possible both to reduce pollutant emissions, increase efficiency and facilitate the stabilization of combustion. It is therefore important to have the air jet of the swirl effect on the burners at different axial and radial configurations on the dynamic and thermal characteristics of the reactant flow and the numerical simulation prediction capabilities. Several factors influencing the combustion process are examined. One of the goals is to study the influence of turbulence models and reaction mechanisms on the prediction of the flow field and temperature. The numerical results are compared with experimental results of N. Merlo, Boushaki T. et al. (2014).

Keywords : non-premixed combustion, swirled flows, turbulent combustion model, burner.

1. Introduction

The control and optimization of non-premixed turbulent combustion is now a priority not only to improve efficiency while avoiding the occurrence of combustion instabilities, but also to reduce polluting emissions. The evolution of the anti-pollution standards and the improvement of the performance of the combustion chambers require the development of new types of burners and combustion techniques. Swirling flow burners are not only used in gas turbines, but also in industrial furnaces because of their significant beneficial influences on flame stability [1], Cozzi and Coghe [2] studied a burner configuration including a swirler for the air flow and examined the influence of air staging on NO_x formation. They compared an axial and a radial fuel injection into the secondary air. They concluded that a radial injection allows a faster centrifugal mixing. Olivani et al. [3] emphasized the influence of radial or axial fuel injection into a swirling air flow on the mixing close to the burner exit. The objective in this work, we study the numerical simulation of three dimensional (3D) diffusion flames of a reactive turbulent flow in a combustion chamber, and to characteristics the effects of the Dynamic Behavior in a burner configuration including a swirler for the axial and radial Air injection. the influence of the turbulence models and the reaction mechanism on the prediction of the flow. The RSM model is used to describe the turbulent flow. The Eddy dissipation used to model the turbulence-chemistry interaction (6 species and 2 reactions). The comparison of the numerical results with the available experimental data shows a good agreement. The numerical results are compared with the experimental data of N. Merlo and al.(2014) [4].

2. Design of swirl burner

A swirl burner uses a set of guiding vanes to give a swirling motion to the combustion air. This creates a recirculation zone, which helps ignite the fuel as well as sustain the flame. The burner of axial swirling vanes configuration consists of two concentric tubes with a swirler placed in an annular part for the oxidant flow (air) as shown in (Fig.1) The central tube delivers the methane through eight holes symmetrically distributed on the periphery of the pipe, just below the burner exit plane. The radial injection of fuel is used to enhance mixing at the near field of the burner exit. In the tangential vane swirl burner (Fig.2) the air enters the

furnace through a set of adjustable tangential guide-vanes. Swirl intensity of the air is adjusted by changing the inclination angle of the guide vanes. The number of vanes varies between 8 and 16.

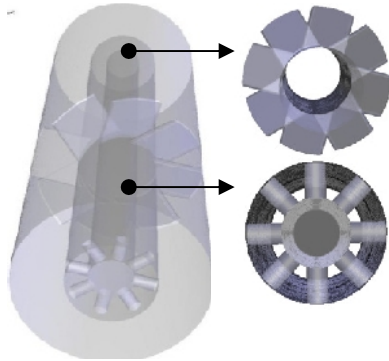


Fig.1 : Axial swirl burner.

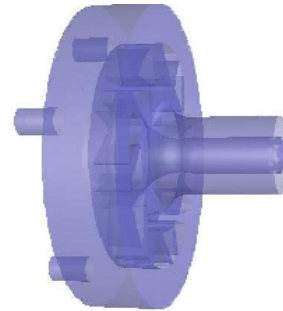


Fig.2 : Tangential vane swirl burner.

3. Results

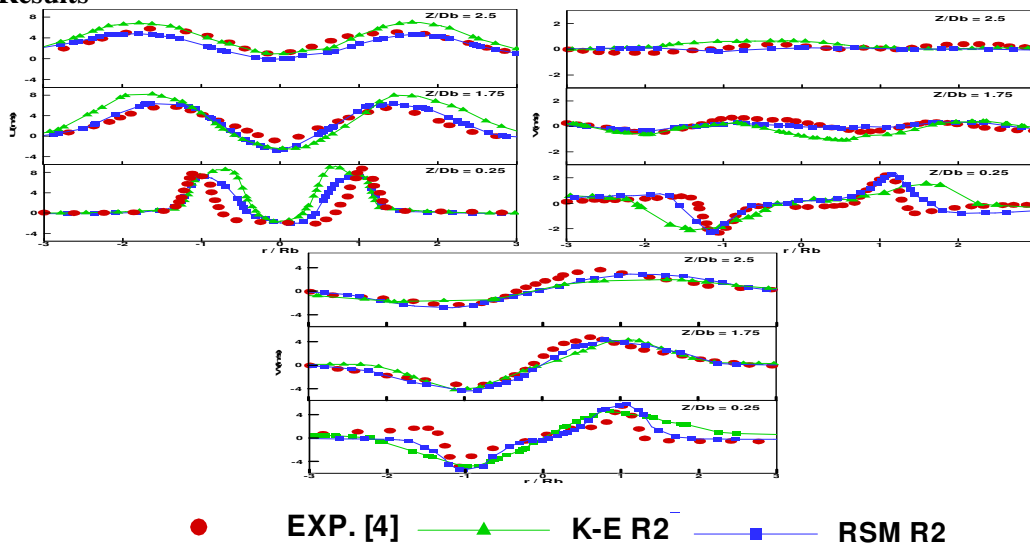


Fig.3: Radial distribution profiles of axial, radial and tangential mean velocities at distances $Z/Db = 0.25, 1.75$ and 2.5 from the exit burner with K-E and RSM models in the axial swirl burner.

4. Conclusions

This study present a three-dimensional numerical simulation has been conducted to the combustion characteristics of methane–air turbulent non-premixed swirling flames with transverse injection of the fuel, and the effects of the Dynamic Behavior in a burner configuration including a swirler for the axial and radial Air injection.

References

- [1] S. Hoffmann, P. Habisreuther, B. Lenze, Development and assessment of correlations for predicting stability limits of swirling flames, Chem. Eng. Process.: Process Intensification 33 (1994) 393–400.
- [2] F. Cozzi, A. Coghe, Effect of air staging on a coaxial swirled natural gas flame, Exp. Thermal Fluid Sci. 43 (2012) 32–39.
- [3] A. Olivani, G. Solero, F. Cozzi, A. Coghe, Near field flow structure of isothermal swirling flows and reacting non-premixed swirling flames, Exp. Thermal Fluid Sci. 31 (2007) 427–436
- [4] N. Merlo et al. Combustion characteristics of methane–oxygen enhanced air turbulent non-premixed swirling flames, Experimental Thermal and Fluid Science 56 (2014) 53–60

Topic C

ON THE FOULING OF ULTRA-FILTRATION MEMBRANE IN THE PRETREATMENT PROCESS OF SEAWATER DESALINATION

A. Adda¹, M. Abbas², S. Hanini¹

1Yahia Fares University, Medea, Algeria

2 Unité de Développement des Equipements Solaires. UDES. /Centre de Développement des Energies Renouvelables .CDER. Bou-Ismaïl.42415.w.Tipaza.Algérie

Email : asmaadda27@gmail.com

abbasdreams@gmail.com

Abstract: The ultra-filtration membranes have been used for the pretreatment rang of seawater desalination based on reverse osmosis process. However, membrane life and permeate flux are primarily affected by the phenomenon of concentration polarization and fouling at its layer. The aim of this paper is to develop a model describing the flux permeate according to various ultra-filtration process parameters. The model is then validated for a given membrane. For this, a program on the MATLAB environment is developed and established and a pre-treatment unit using tangential ultra-filtration has been chosen. The obtained results show the capability of the proposed model and its adequacy to the theoretical results available on the literature.

Keywords: fouling, membrane ultra-filtration, modeling, polarization, desalination, pretreatment.

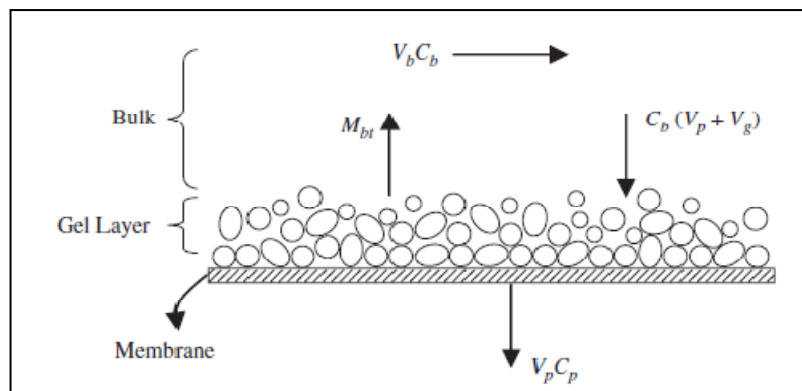
1. Introduction

Faced with growing water demands in the world and particularly in Algeria, producing fresh and drinking water of acceptable quality with minimal cost is the main objective of all researchers [1]. The use of membrane process desalination is increasingly important to solve the water supply problem for human consumption. On the other hand, there are two serious problems in membrane operations: concentration polarization, which has a negative influence on the flux, and membrane fouling, which is an irreversible adsorption of macromolecules [2]. In this way, the ultra-filtration membrane fouling is investigated in this paper. The aim is to develop a model allowing the sizing of seawater desalination pre-treatment system based on cross-flow ultra-filtration process.

2. Methodology

2.1. ultra-filtration modeling

The modeling of permeate flux decline during cross-flow ultra-filtration process aims to predict the flux in order to proceed the sizing of seawater pre-treatment system. During the filtration process, some of the solutes in the bulk are transported into the permeate stream through the boundary layer and gel layer. C_p is the total concentration of solutes in the permeate. C_b is the total concentration of solutes in the bulk. V_g is total volume of gel layer and V_p is the total volume of permeate



J_{C0} : is the rate deposition on the membrane layer and the gel layer thickness is given by:

$$\delta(t) = \frac{1}{C_g} \int_0^t J \cdot C_b \cdot dt$$

The total volume permeate flux can be calculated by Darcy's law as follow:

$$J(t) = \frac{\Delta P - \Delta P_c}{\mu R_m + r_c \delta(t)}$$

In order to validate our model, we make a comparison with experimental results. For this, figure 2 shows permeate flux results (experimental and theoretical) versus filtration time. The simulation results show a good agreement with the experimental data.

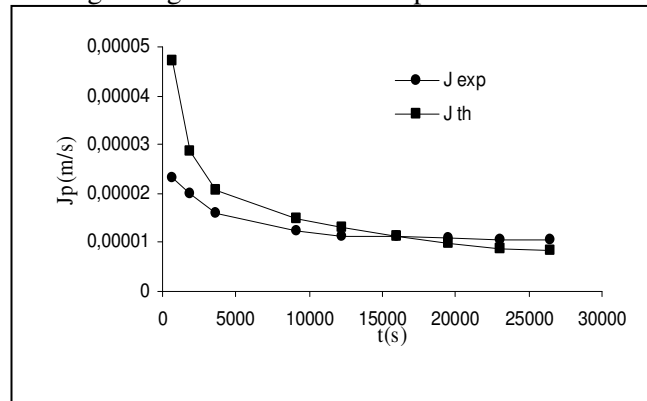


Fig. 2. Comparison between theoretical and experimental permeate flux

3. Conclusions

In this work, a prediction model of permeate flux in pre-treatment process of a desalination plant has been developed. The pre-treatment process considered in this study is based on the tangential ultra-filtration method. The model is then validated for a given ultra-filtration membrane.

The comparison between the proposed model and the experimental data showed a good agreement, the error is less than 4%. It's to mention that the results seem satisfying considering the difficulties to calculate with precision the permeate flux in the ultra-filtration process.

Despite the study is not more detailed but the obtained results are significant enough to get idea about the polarization and fouling phenomenon in ultra-filtration membrane.

References

- [1] Val S. Frenkel. (2011) «Seawater Desalination: Trends and Technologies,Desalination » Trends and Technologies, Michael Schorr (Ed.), ISBN: 978-953-307-311-8.
- [2] S. Lee et al. (1984) Concentration polarization, membrane fouling and cleaning in ultrafiltration of soluble oil, Journal of membrane science, 19, pp 23-38.

COMPUTATIONAL STUDY OF FE-DOPED TiO₂ NANOPARTICLES

B. Bezzina^{1,2,14}, C.E. Ramoul¹, K.E. Slimani¹, O. Ghelloudj¹, M.T. Abed Ghars¹, M. Kahalerras¹, H. Bendjama¹, D.E. Khatmi²

*1*Research Centre in Industrial Technology (CRTI), P.O.BOX 64, Cheraga 16014, Algiers, Algeria

*2*Laboratory of Computational Chemistry and nanostructures LCCN, University May 8, 1945 Guelma - Algeria.

Abstract: The geometries, relative stabilities, and electronic properties of small TiO₂_n (n= 1–4) clusters that are utilized in renewable energy, solar energy (as an active semiconductor metal oxide) were investigated by using density functional theory (DFT) at the B3LYP/LanL2DZ level of theory, as well as the effects of doping of different iron concentrations on the properties of titanium dioxide were given, which some Ti atoms were replaced with Fe atoms. ¶The effects of the size and the concentration of iron all were shown to have a significant influence on the behavior of adsorption of TiO₂ in the field of UV-vis. It was found out that the increase in the size of nanoparticle was accompanied with a reduction in energy of formation and a stability of the clusters. Our results are in good agreement with the experimental and theoretical results available.

Keywords: Solar energy, iron doping, titanium dioxide, clusters.

1. Introduction

Titanium dioxide (TiO₂) is among the important transition-metal oxide material that have a very important role in many areas of chemistry, physics and materials science.

Nanostructure of TiO₂ has attracted considerable attention because of their potential applications: solar cells at low cost, photocatalyst for H₂ production (decomposition of water), the purification of air and water, control of environmental pollution (sorbent CO, NO_x, SO_x, etc.) [1,2], but with certain limitations, for example, TiO₂ works only under ultraviolet light (UV), which represents less than 5% of the entire solar spectrum, but doping techniques change the activity of TiO₂ nano-doped from the UV region to the region of visible light [3,4], in order to improve or correct this defect, we have studied the behavior of growth and stability of small clusters at the molecular level of un-doped TiO₂ and Fe-doped TiO₂ particles as well as their structural, electronic, spectral and thermodynamic properties using the density functional theory (DFT) and time-dependent density functional theory (TD-DFT).

2. Computational method

We simulated the effects of doping Fe by replacement of the Ti atoms with one, two and three iron atoms, respectively; Fe_mTi_n-mO_{2n} [n = 2-3, m = 1 to (n-1)].

The optimization structures, calculation of frequency vibration, electronic and thermodynamic properties of various pure and composite clusters were performed using Gaussian 09W software.

3. Results

In Fig.1, the calculated bond length of the TiO₂ is 1.6 Å with an O-Ti-O angle of 111 degrees, in good agreement with experiment, however the bond length Ti-O vary from 1,6 Å to 2,0 Å with the increase in a size of clusters (number of Ti from 1 to 4).

¹⁴Corresponding author

E-mail address: bezzinabelgacem@yahoo.fr

Whereas Fig.2 illustrates the effect of iron doping on the structural properties of the titanium dioxide clusters, where it shows a net change in the bond length (Ti-O) and the angles (O-Ti-O).

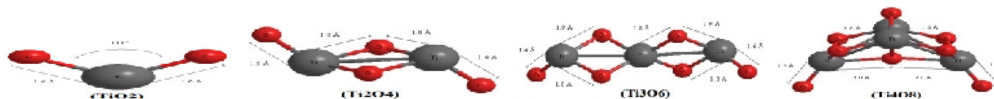


Fig.1. Geometries of un-doped titanium oxide clusters (TiO₂)₁₋₄, the Ti-atoms are indicated by gray spheres and the O-atoms by red spheres.

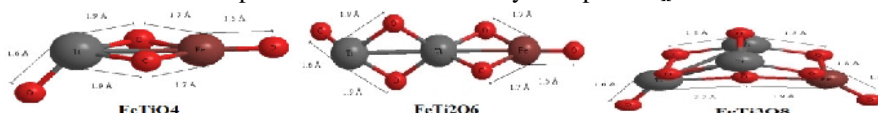


Fig.2. Geometries of 1Fe-doped titanium oxide clusters (TiO₂)₂₋₄, the Fe -atom are indicated by brown sphere.

As shown in Fig.3, generally a regular change in the absorption wavelength (λ) of the clusters with the increase in their sizes, same thing with the substitution effect of iron in the matrix of (TiO₂)₄, which corresponds to a monotonous increase according to the rate of doping.

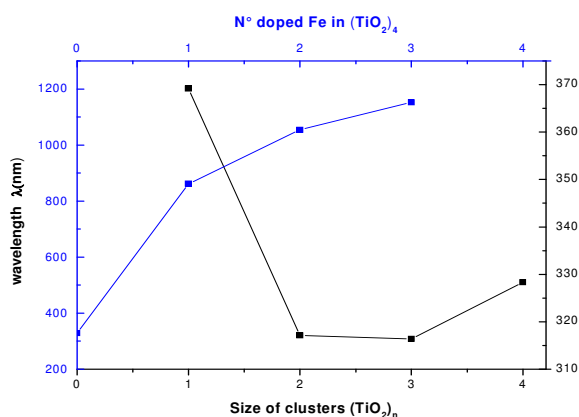


Fig.3: Effect of the size of the clusters of (TiO₂)_n (square black) and numbers of iron atoms doped (blue) in (TiO₂)₄ on their spectral behavior.

4. Conclusion

The electronic structure and stability of un-doped (TiO₂)_n clusters as well as of Fe-doped (TiO₂)_n have been investigated using the density functional B3LYP/LANL2DZ method. For increasing cluster size n, structures become increasingly energetically favored. However the energy gap is reduced continuously with the doping level. The presence of iron in the TiO₂ matrix shifts the band gap of 4.91 eV to 2.6 eV. Whereas a significant shift in the absorption band of light of the titanium oxide to the field of infrared 2500nm < IR > 800nm (bathochromic shift) is obtained as a function of the doping level in Fe.

References

- [1] Lee.C, Aikens.C.M .(2013), Effects of Mn doping on (TiO₂)_n (n= 2–5) complexes, Computational and Theoretical Chemistry, 1013,32–45.
- [2] Tan.Y. N, Wong.Ch. L, Mohamed .A. R. (2011), An Overview on the Photocatalytic Activity of Nano-Doped-TiO₂ in the Degradation of Organic Pollutants,” ISRN Materials Science , Article ID 261219, 18 pages. doi:10.5402/2011/261219.
- [3] Libera .J. A., Elam.J.W., Sather.N.F.,T. Rajh, Dimitrijevic. N.M. (2010), Iron(III)-oxo Centers on TiO₂ for Visible-Light Photocatalysis, Chem. Mater 22, 409–413.
- [4] Carneiro.J.O., Teixeira.V, Portinha.A, Magalhaes.A, Coutinho.P., Tavares.C.J., Newton.R.(2007), Iron-doped photocatalytic TiO₂ sputtered coatings on plastics for self-cleaning applications, Materials Science and Engineering B 138, 144–150.

EFFECTS OF OXYGEN FLOW RATE ON THE PROPERTIES OF ZNO THIN FILMS PREPARED BY DC REACTIVE MAGNETRON SPUTTERING

F. Bouaraba^{1*}, S. Lamri², N. Ziani¹, O. Boussoum¹, M.S. Belkaid¹.

¹ Université Mouloud Mammeri, Laboratoire Des Technologies Avancées Du Génie Electrique, Tizi-Ouzou, Algérie.

² Université de Technologie de Troyes, UMR 6281, CNRS, Antenne de Nogent Pole Technologique de Haute-Champagne, France.

Abstract: ZnO transparent conductive thin films are widely applied in optoelectronic devices such as flat panel displays and photovoltaic cells, because of their excellent optoelectronic properties, non-toxicity, low material cost and stability in hydrogen plasma processes. In present work ZnO thin films were deposited on Corning 7059 glass substrates with direct current reactive magnetron sputtering process from a Zn target, at temperature of 300 °C. The effects of oxygen flow rate on the structural, optical and electrical properties of ZnO thin films were studied using X-ray diffraction (XRD), scanning electron microscopy (SEM), ultraviolet visible (UV-Vis) spectrophotometer, four-point probe. The experimental results reveal that All films demonstrated strong (002) preferential orientation. The minimum resistivity of $1,6 \cdot 10^{-2} \Omega \cdot \text{cm}$ and an average transmittance of 90 % are obtained. This work suggests that oxygen vacancies play an important role in modifying properties of ZnO

Keywords: magnetron sputtering, thin films, ZnO, oxygen flow rate.

1. Introduction

The interest of Transparent Conductive Oxides (TCO) has been growing. The existence of their two properties, electrical conductivity and transparency in the visible, making them ideal candidates for applications in photovoltaic and optoelectronics [1-2].

Among these TCOs, ZnO is one of the most favorable material for its direct and wide band gap (3.37 eV) [3] its abundant, relatively low cost, good stability in hydrogen plasma process, large exciton binding energy of 60 meV, and non-toxicity. ZnO has been recently investigated for surface acoustic wave (SAW) devices, transparent conducting coatings for thin-film solar cell applications, gas sensors, ultraviolet photo-detectors and potential applications in the realization of nanoscale devices.

2. Results

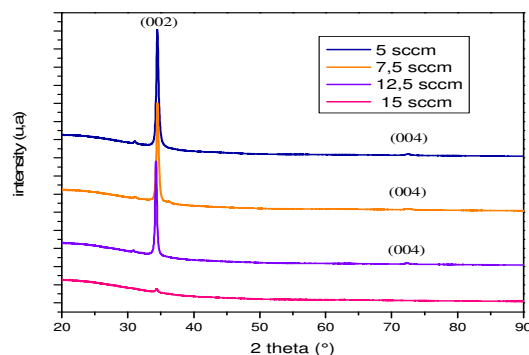


Fig. 1. The XRD patterns of ZnO films deposited with different oxygen flow rate

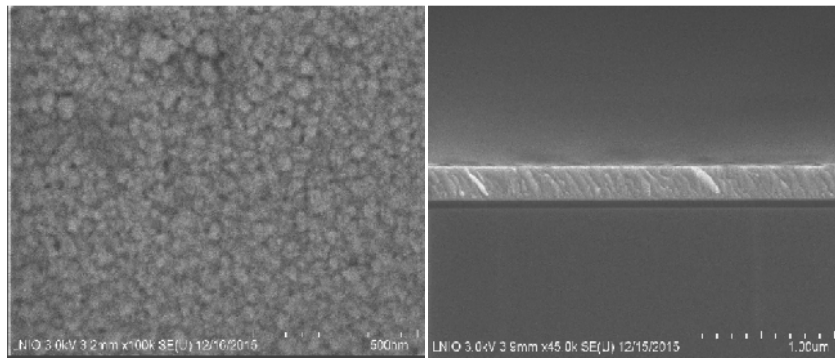


Fig. 2. The Surface and Fracture Cross-Section Morphologies of ZnO Thin Film.

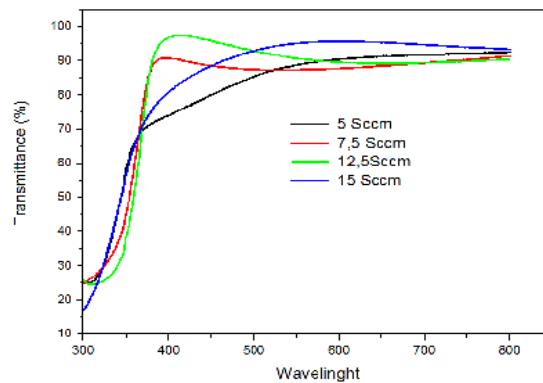


Fig.3.The transmittance spectra of ZnO thin films.

3. Conclusions

In this paper undoped ZnO thin films with different oxygen flow rate were prepared on glass substrates by DC reactive magnetron sputtering. Microstructure, surface morphology, electrical and optical properties were investigated. The XRD patterns reveal that all films have a polycrystalline structure and a preferred orientation with the c-axis perpendicular to the substrate and that the films prepared at 5 sccm of oxygen flow rate present the most intense peaks. The growth rate of the film decreases dramatically with increasing O₂ flow rate,

The SEM studies show that the films are uniform and homogeneous. We observe also that the resistivity of the ZnO films decreases with increasing of oxygen flow rate.

The average transmittance in the visible range (400–800nm) for all the films was over 90 %.

In conclusion The results show that oxygen flow rate significantly affects the crystallinity, resistivity, and optical properties of ZnO thin films.

References

- [1] E. Fortunato, L. Raniero, L. Silva, A.G. Alves, A. Pimentel, P. Barquinha, H.A. Guas, L. Pereira, G.G. Alves, I. Ferreira, E. Elangovan and R. Martins, Highly stable transparent and conducting gallium-doped zinc oxide thin films for photovoltaic applications, *Materials Letters*, 96, 237–239, 2013.
- [2] M. Berginski, J. Hüpkes, M. Schulte, G. Schöpe, H. Stiebig and B. Rech, The effect of front ZnO:Al surface texture and optical transparency on efficient light trapping in silicon thin-film solar cells, *Journal of Applied Physics*, 101, 074903, 2007.
- [3] L. Zhengwei, W. Gao, ZnO thin films with DC and RF reactive sputtering, *Materials Letters*, 58, 1363-1370, 2004.

Study on the parameters influencing length interface in multiproduct pipelines

D. Bennacer^{15,*}, R. Saim¹, F. Benkhenafou², B. Benameur¹

1University of Tlemcen, Energetic and Applied Thermal Laboratory (ETAP), P.O.Box 119, 13000, Tlemcen, Algeria

2University of Tlemcen, Department of Physics, PO Box 119, 13000, Tlemcen, Algeria

Abstract: Knowledge of the parameters influencing interface length (mixing volume) occurred between two fluids in contact and in sequential flow, in a multiproduct pipeline is of paramount and of economic importance (costs). Having tested some empirical correlations of the diffusion coefficient in a previous work and developed mathematical formula governing the mixing phenomenon [1], which occurs between two fuels during their sequential flow in a multiproduct pipeline which extends over a length of 168km. This last links the refinery in western of Algeria to storage and fuel distribution centers.

1. Introduction

The mode of transport by pipeline contributes significantly to the reduction of costs, delivery times, the road traffic and also ensures massive transport of hydrocarbons. It is often necessary to pump successively into the same pipeline two or more different products in a well-defined sequence, instead of reserving for each product immense lengths of pipes which make the pipeline system too bulky, generating more expenditure and maintenance.

Owing to the importance of pipelines in the petroleum industry, it is necessary to better understand the relationship between theory and field results for the mixture that occurs when products are transported in batches in the same pipeline [2]. The mixing interface estimating problem is common in multiproduct pipelines, where batching involves the continuous shipment of different products through a single pipeline without any physical separation between these products [2].

3. Experimental Device

3.1 Notion of batching

Batching refers to the process of successive transport of batches of petroleum products through a single pipeline. Large quantities of different types and categories of refined petroleum products are transported from the refinery to the storage and distribution centers. These pipelines are commonly called "multi-product pipeline". The speed of transport and operating economics make the batching and multiproduct pipelines are extremely popular in the oil transport industry [3], and almost all transport pipelines operate today in this way.

* Corresponding author

E-mail address: bennacer.djamel@yahoo.fr

3.2 Presentation of the experimental device (multiproduct Pipeline)

The multiproduct pipeline serving as an experimental device is one of the multiproduct pipelines in Algeria. It is more than 168 km long (figure 01), and it's composed of three sections of different lengths and diameters (12", 10" and 8"). It transports fuels and mostly diesel and gasolines. It feeds the western and southwestern region of Algeria. The flow rates along the pipeline are defined as a fixed value during pipeline operation and are controlled automatically by control valves (figure 02) [1].

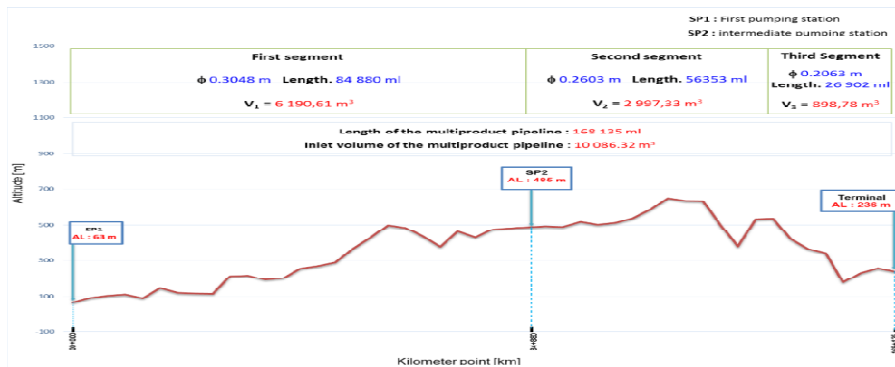


Fig. 1 Lengthwise profile of multiproduct pipeline

Other system components include (figure 2):

- A refined-products tank farm at the refinery.
- Two pumping stations.
- A receiving center including fuel storage.

Fuels moved in batches from the refinery tank farm through the SP1 pumping station. A vertical contact was established between batches as each was introduced, with the subsequent

Results and discussion

We present hereafter the influence of the different parameters on the evolution of the volume of the mixture (length of the interface).

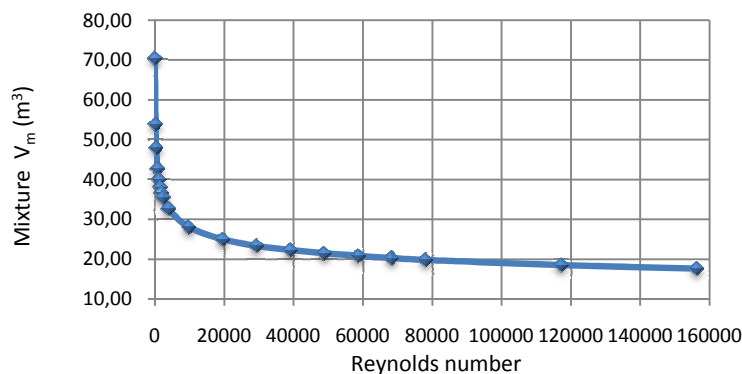


Fig. 1 Influence of the flow regime on the volume of the mixture

Figure 1. covers the two flow regimes (laminar and turbulent) showing clearly that the volumes recorded are very large at low flow rates (Low Reynolds numbers) and more particularly for the laminar regime, in contrast to the turbulent regime, which greatly improves the area of the mixture (Reduces the interface length).

References

- [1] Bennacer D. et al. (2014), Evaluation analytique et expérimentale de l'interface générée entre deux fluides en contact et en écoulement séquentiel dans un pipeline multiproduit, Le 3^{ème} Séminaire sur les Technologies Mécaniques Avancées (STEMA). 08 et 09 Novembre, Tlemcen, Algérie.
- [2] Etim S Udoetok, Anh N Nguyen, (2009). A disc pig model for estimating the mixing volumes between product batches in multiproduct pipelines. *Journal of Pipeline Engineering*, 8, 3, pp 195-204.

NUMERICAL AND EXPERIMENTAL INVESTIGATION OF DYNAMIC BEHAVIOR OF LAMINATE COMPOSITE UNDER FLEXURAL VIBRATION

A. Rahmane¹, T. Benmansour¹

1Department of Mechanical engineering, Constantine 1 University, Road of ,Ain El Bey, Constantine,Algeria

Abstract: Nowadays, the use of composite materials has taken a large place in civilian industries as well as in military and aerospace industries. Therefore, significant investigations about their mechanical and physical properties are needed. The present study addresses the effect of the measurements technique on dynamic properties of laminate composite FRP. An experimental investigation is implemented using an impulse technique. The various specimens are excited in free vibration by the use of bi-channel Analyser. The experimental results are compared by model of finite element analysis using ANSYS. The results studies (natural frequencies, magnitude vibration,) show that the effects of significant parameters such as lay-up and stacking sequence, boundary conditions and place of accelerometer mass under measurements. The findings of this study indicate that the dynamic characteristics of the laminate composite are sensitive to the mass of accelerometer as function of his positions.

Keywords: Natural frequencies, Stacking sequence, ANSYS, Carbon-epoxy.

1.Introduction

The Composite materials are fabricated to have better engineering properties than the conventional materials as metals. Some of the properties that can be improved by forming composite materials are: stiffness-to-weight ratio, strength, corrosion resistance, thermal properties, fatigue life and wear resistance. As regard to the vibration behavior of the composite structures, many studies were carried out to control and determine the dynamic characteristics of those materials.

2. Experimental Set-up

Experimental tests have been carried out with the aim of understanding the correct physical behavior of carbon/Epoxy laminate composite and validating the numerical models constructed using ANSYS software. The dimensions of the specimens are: 290 mm x300 mm x1mm (fig.1). They are consisted from 8 layers of unidirectional fiber carbon/ epoxy. The mechanical properties of the laminates are given in [1].

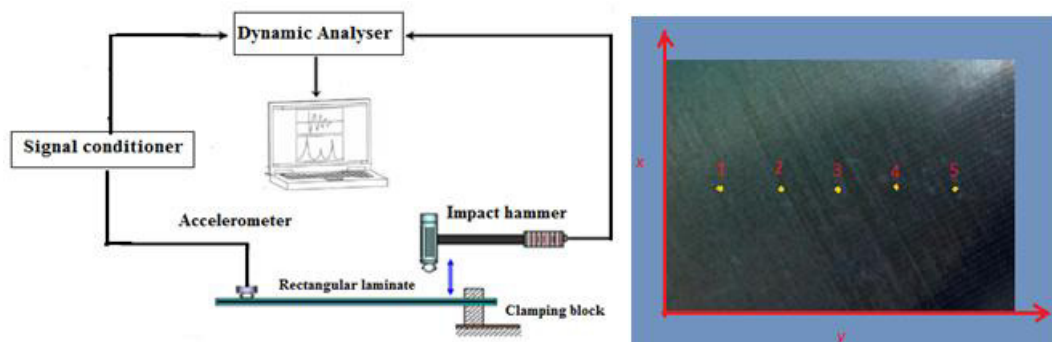


Fig .1 Laminates composite is used to identify the effect of excitation place of accelerometer Six laminated composites with the symmetrical stacking sequences of $[\pm 20]_2s$, $[\pm 25]_2s$, $[\pm 30]_2s$, $[\pm 60]_2s$, $[\pm 65]_2s$, and $[\pm 70]_2s$ are excited in free vibration. The specimens are tested for two boundary conditions, namely clamped-free-free-free and clamped-free-clamped-free

The experiments are carried out to identify the effect of accelerometer mass on natural frequencies. The experimental tests are carried out by using a vibration analyzer type B&K 2035. It is connected to an impact hammer. A low mass accelerometer (2g) is used to detect vibration response. The experimental set-up is shown in Fig. 2.

3. Results

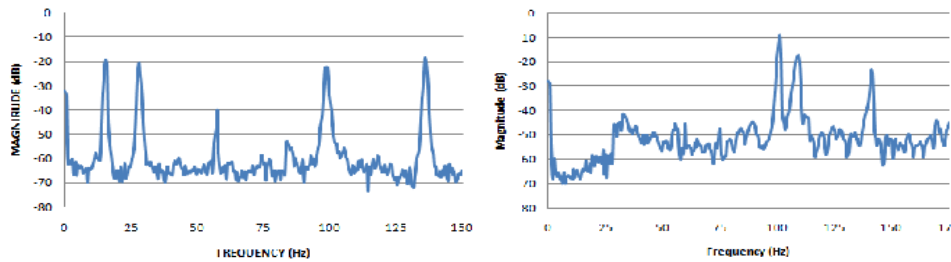


Fig. 3 Frequency spectra for one measuring point for specimens with the stacking sequences of $[\pm 20]_2s$: a) CFFF, b) CFCF

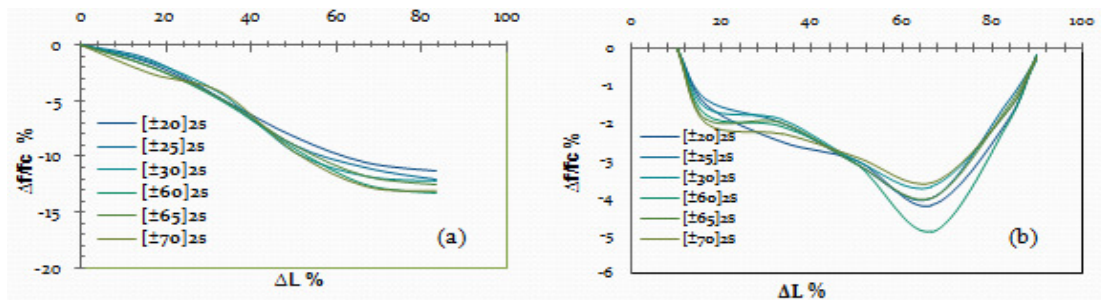


Fig. 4 Effect of accelerometer position on the natural frequency for first mode for: (a) CFFF and (b) CFCF

Table 1 Experimental and numerical natural frequencies of the CFFF specimens.

Stacking sequence	Experiment Frequency (Hz)			FEM Frequency (Hz)		
	1 st mode	2 nd mode	3 rd mode	1 st mode	2 nd mode	3 rd mode
$[\pm 20]_2s$	15.55	28.15	57.51	15.723	28.944	58.495
$[\pm 25]_2s$	14.15	29.50	62.05	14.503	30.928	63.239
$[\pm 30]_2s$	13.10	31.45	64.10	13.142	32.470	65.969
$[\pm 60]_2s$	06.00	27.85	33.96	05.767	28.124	34.630
$[\pm 65]_2s$	05.55	24.85	30.81	05.160	25.333	31.467
$[\pm 70]_2s$	05.10	21.85	28.90	04.773	22.216	29.482

4. Conclusion

A low mass accelerometer is used to measure the vibration response of the composite specimens, though, it is proved that the accelerometer mass affects the measurements. To reduce this influence it is essential to consider the average of all grid points' measurements. The natural frequencies of symmetrical laminate composite specimens increase with the reduction of the stacking sequence, due to the increase of the laminate stiffness. That is to say, this work has been able to set up a method of non-destructive characterization, which could minimize the errors of the experimental protocols able to disrupt the final results.

References

[1] Liljedahl CDM, Crocombe AD, Wahad M.A, Ashcroft I.A (2006). Damage modeling of adhesively bonded joints. Springer Science Business Media, 141: 147-161

OPTICAL SIMULATIONS OF P3HT/PCBM BULK- HETEROJUNCTION ORGANIC PHOTOVOLTAIC FOR IMPROVING ABSORPTION

F. Brioua^{1,*}, C. Daoudi¹, H. Bourouina², M. Remram¹

¹Laboratoire LEMEAMED, Département d'électronique, Université des Frères Mentouri Constantine,
Algerie

²Laboratory FUNDAPL, Faculty of science, University of Blida, Blida BP. 270 09000, Algeria

Abstract: In this study, we have investigated on two-dimensional model of the optical modeling for a multilayer system in an organic solar cell based on (the top of the a transparent anode layer made of indium tin oxide (ITO)-electrode (110 nm thick) since it has high transmittance in visible region. The following layer is a thin layer (40 nm thick) of poly(3,4-ethylenedioxythiophene): poly (styrenesulfonate) (PEDOT:PSS) and the bulk heterojunction blend varied between 40 and 220 nm of poly(3-hexylthiophene) (P3HT) and 6,6-phenyl C61-butyric acid methyl ester (PCBM) as photo-active material, and the layer of the calcium (Ca) (5 nm) as electron transporting layer , finally by and the aluminum cathode (80 nm thick). From the distribution of the electromagnetic field inside the solar cells of each layer, we can computed the exciton generation rate (G) in the active layer (P3HT:PCBM).

Keywords: P3HT:PCBM; Organic solar cells; Finite-Element method (FEM), Optical modeling, electromagnetic field.

1. Introduction

The research of organic solar cells (OSCs) has attracted much attention recently due to the advantageous properties such as their mechanical flexibility and the potential benefits of low cost production methods [1]. However, these organic photovoltaic advantages do not allow obtaining conversion efficiency as the silicon ones. The poly(3-hexylthiophene) (P3HT) and phenyl-C61-butyric acid methyl ester (PCBM) a typical active layer has been used. Optical modeling has been performed to find the optimal device structure under normal incidence sunlight, in order to enhancement performance responses optical of device.

2. Determination of the absorption in optimum thick active layer

At base the complex refractive indices of $\tilde{n} = n + ik$ of different layers in device structure, that are given from refs [2], where n and k are the refractive index and extinction coefficient, respectively. And taking into consideration the Floquet periodic boundary conditions are used on the one-period cell boundaries. Add to the device structure is divided into tiny meshes and spatial distribution of the electric field intensity enhancement, as shown in figure 1. (b and c). Under AM 1.5 100 mW/cm² illumination, where the solar light waves strike in normal incidence. A optical model is proposed, based on Maxwells equations solved by finite element method (FEM) using means of the commercial software Comsol Multiphysics [3]. The optical absorption and electric field amplitude are enhanced by optimizing the thickness of the active layer. This exciton generation is computed by to the following expression [4] :

$$\varphi(x, \lambda) = \frac{1}{2} c \varepsilon_0 \alpha n |E(x)|^2 \quad (1)$$

$$G_{\text{optical}}(x) = \frac{\lambda}{hc} \sum_{300}^{900} \varphi(x, \lambda) \quad (2)$$

α is the absorption coefficient:

$$\alpha = 4\pi k / \lambda \quad (3)$$

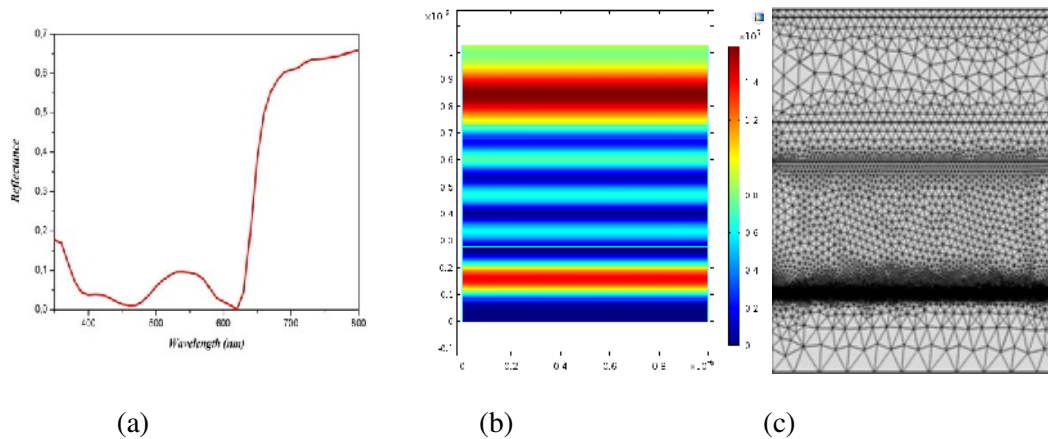


Fig. 1. Calculated reflectance for a 220 nm thick active layer (a), and spatial distribution of the electric field intensity enhancement, namely the normalized incident intensity, along a cross section of the (OSC) (b), typical 2D finite element mesh used in the model (c).

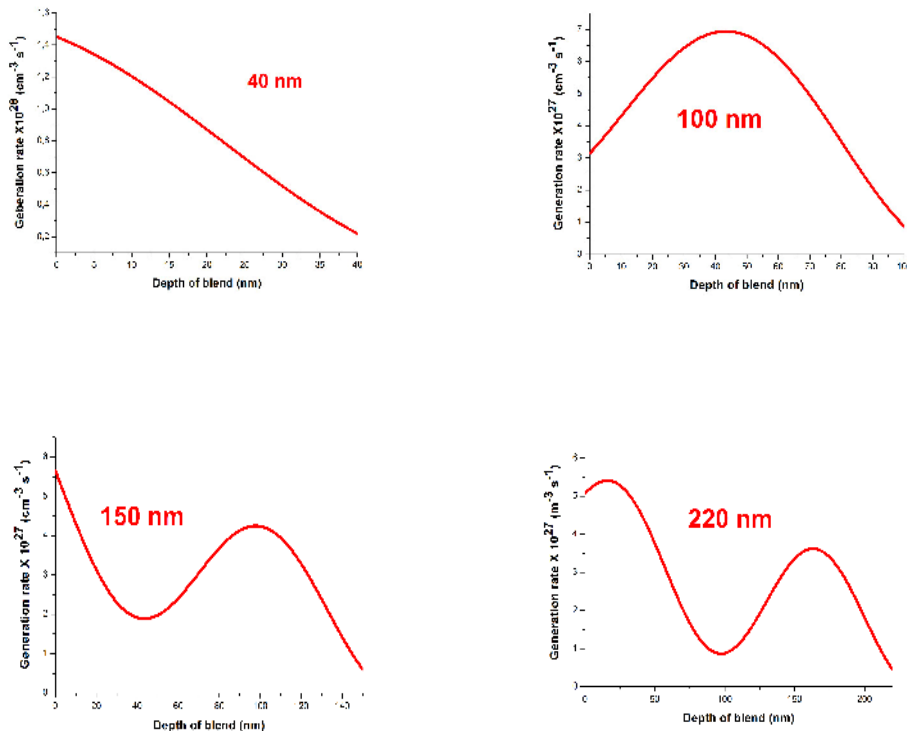


Fig 2 . Profiles of exciton generation rate for various blend thicknesses (40, 100, 150, and 220 nm), a good agreement compared with literature results [4]

3. Conclusion

In summary, From the optical modeling of organic solar cells (OSCs) using fine element method with the COMSOL software. The response optical such as the generation rate and electric field amplitude are enhanced by optimizing the thickness of the active layer, taking into account optical interference effect have a very important influence on enhancement of absorption. A good agreement compared with literature results have been found, particularly in the case of 40 nm is the optimum value of active layer thickness, a value obtained around 1.43×10^{28} ($1/\text{cm}^3 \cdot \text{s}$).

STUDY OF DYNAMICS OF CARRIERS IN INSB/GAAS QUANTUM DOT SOLAR CELL

F.Benyettou^{1,*}, A.Aissat¹

1University of Blida, LASICOM, Route de Soumaa, 09000, Blida, Algeria.

Abstract: One of the most widely used in the field to improve the photovoltaic conversion efficiency of a solar cell technology is the use of nanostructures including Quantum Dot Solar Cell QDSC. The electric field, recombination, photogeneration and the photoabsorption rates of carriers in Quantum Dots Solar Cell QDSCs have a big impact on the collection and extraction efficiency of these carriers from the confinement zones. In this latter, the behavior of these magnitudes and the mains characteristics: current-voltage J(V) and External Quantum Efficiency EQE of InSb/GaAs QDSCs are studied. Our results have shown that the insertion of 30 InSb/GaAs QD layers inside the intrinsic region of GaAs based pin solar cell provide a relative enhancement of about 22.33 % and 29.31 % of short-circuit current and efficiency respectively. Moreover, the absorption range edge of photons with low energy extended from 900 to 1400 nm. This reveals that introduction of QDs in the intrinsic region of GaAs pin structures enhances significantly the device characteristics beyond what has been thus far reported for conventional semiconductor-based solar cells.

Keywords: QDSC, efficiency, EQE, photogeneration, photoabsorption, recombination.

1. Introduction

Currently, quantum dot solar cells are one of the most active researches field in the third generation solar cell. Comparing with quantum well, quantum dot has more quantum confinement effects, which is in 3-dimension. Typically, the research in the quantum dots solar cell has been performed and focused on InAs/GaAs QDs. Contrary; InSb/GaAs have a few reports due to growth difficulties associated with Antimony Sb compounds [1, 2]. In this paper, we are interested to study the dynamics of carriers in InSb/GaAs QDSC, such as the recombination, photo-generation, and electric field. Simulation results show that the incorporation of InSb/GaAs QD layers inside intrinsic region of GaAs based pin solar cell can improve the conversion efficiency and enhance the dynamics of carriers in this later.

2. Theoretical models

Several models have been used in literature to determine the main characteristics of a solar cell and dynamics of carriers. The Drift-Diffusion model and current continuity equations for the quantum well systems are used to calculate the current density of electrons and holes in the bulk and well regions and it is given in equations (1) and (2) respectively. Photo generation rate is given by equation (3).

$$\frac{dn_b}{dt} = G_b - U_b - \frac{n_b}{\tau_{cn}} - \frac{n_{qw}}{\tau_{en}} + \frac{1}{q} \frac{dJ_n}{dx} = 0 \quad (1)$$

$$\frac{dn_{qw}}{dt} = G_{qw} - U_{qw} - \frac{n_b}{\tau_{cn}} - \frac{n_{qw}}{\tau_{en}} = 0 \quad (2)$$

$$G(x) = G_0 \cdot \exp(-\alpha(\lambda) \cdot x) \quad (3)$$

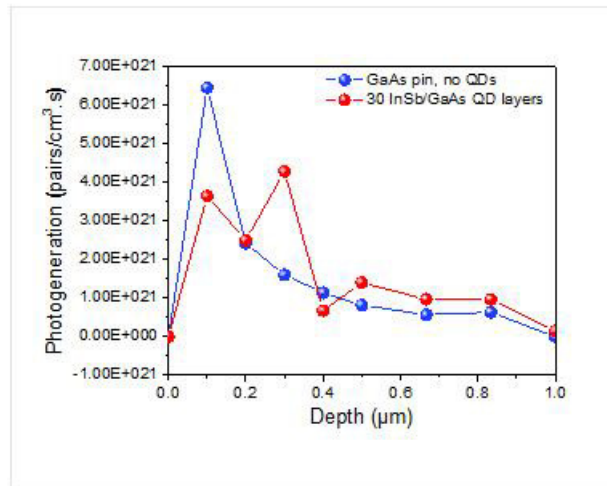


Fig. 1. Photogeneration rate of pin and 30 InSb/GaAs QD layers solar cell.

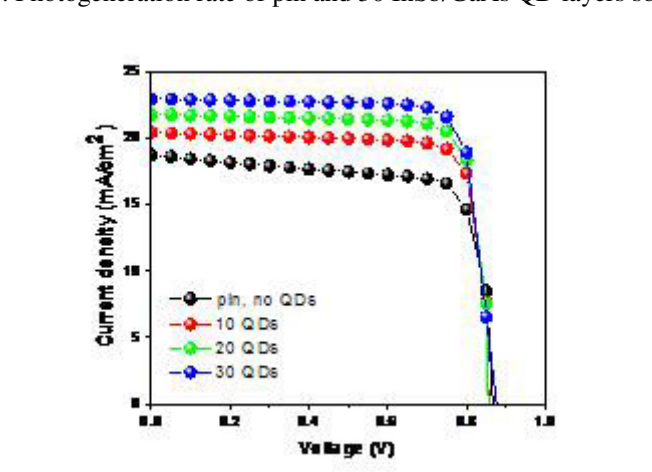


Fig. 2. J(V) of InSb/GaAs Quantum Dot Solar Cell for variable QD layers inserted.

3. Conclusions

In the present work, we have shown the influence of InSb/GaAs QDs layers introduction on the main characteristics of GaAs pin solar cell and on the dynamics of carriers. Based on our simulation results, 30 InSb/GaAs QD layers gives a maximum conversion efficiency of about 33.34 %, this means an relative improvement of 29.31% and enhance significantly the dynamics of carriers. Otherwise, the absorption range limit has extended from 900 nm to 1400 nm.

References

- [1] Tsatsul'nikov, A. F.; Ledentsov, N. N.; Maksimov, M. V.; Mel'tser, B. Y.; Volovik, B. V.; Krestnikov, I. L.; Sakharov, A.; Bert, N. A.; Kop'ev, P. S.; Alferov, Zh. I.; Bimberg, D. Semiconductor 1997, 31, 55.
- [2] Ueta, A.; Gozu, S.; Akahane, K.; Yamamoto, N.; Ohtani, N. Jpn. J. Appl. Phys. 2005, 44, No. L696.

HEAT TRANSFER ENHANCEMENT INSIDE A SOLAR CHIMNEY

M.T.Bouzaher¹, M. Lebbi¹, L. Boutina¹, H. Boualit¹

1 Unité de Recherche Appliqué en Energies Renouvelables, URAER, Centre de Développement des Energies Renouvelables, CDER, 47133, Ghardaïa, Algeria.

Abstract: A computational investigation is carried out to enhance heat transfer inside a solar chimney collector. The study examines the effect of the collector entrance height ratio and the tilt location of the collector roof. It is aimed to achieve the optimal geometric parameters of the collector that ensure a maximum mass flow rate. The momentum and energy equations are solved using a computational fluid dynamics (CFD) software Ansys-Fluent. Both, the collector entrance height ratio ($H=H_e/H_c$) and the tilt location ratio ($Ar=r/R_c$), are encompassed between 0.125 and 1. Firstly, to validate the current solver, the obtained numerical results are compared with experimental data. The main results show that the collector entrance height ratio and the tilt location influence intensely the flow control inside the solar chimney. In addition, they indicate that the collector entrance height ratio must be as small as possible compared to the collector height value.

Keywords: Solar Chimney, Finites volume method, collector entrance height ratio, Flow control, tilt location effect.

1. Introduction

The improvement of the collector performance provides a very promising strategy to harvest solar energy. From an economic point of view, this performance enhancement makes the cost of a solar chimney power plant competitive as compared to other renewable energy resources. From the analysis of the previous literature, it is clear that a number of researchers were focused on optimizing the geometries of a solar chimney due to high performance that can be achieved. However, it is observed that, insufficient information about the effect of the collector entrance height and its location are available. This reason was the motivation to investigate numerically the effect of the collector entrance height ratio and where is the best tilt location in the collector?

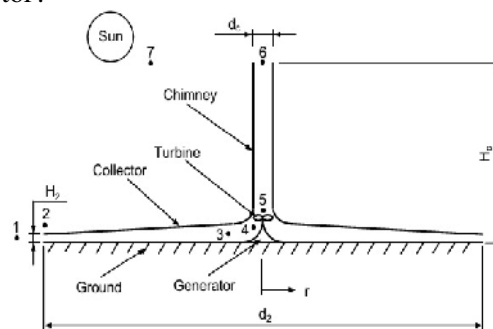


Fig.1. Schematic view of solar chimney power plant (SCPP) (Maia, C. B et al 2009)

2. The effect of the tilt location and the collector height entrance ratio on the magnitude velocity field

Figure 6 (a-d) presents the magnitude velocity contours development inside the solar chimney cavity for different position configurations with collector entrance height ratio ($H=0.375$). From this figure we observed that the maximum velocity (red color) is concentrated at the tower regions. Besides, it is noted that the maximum velocity is registered for the tilt location ratio $AR=0.875$ and for collector entrance height ratio $H=0.375$. Thus, a greater volume of air will be heated in the collector for the same period, so, decreasing the maximum velocity values in the tower. In addition, when we advanced to the collector center the velocity is

decreasing, but at collector outlet the velocity is growing according to the flow area reduction.

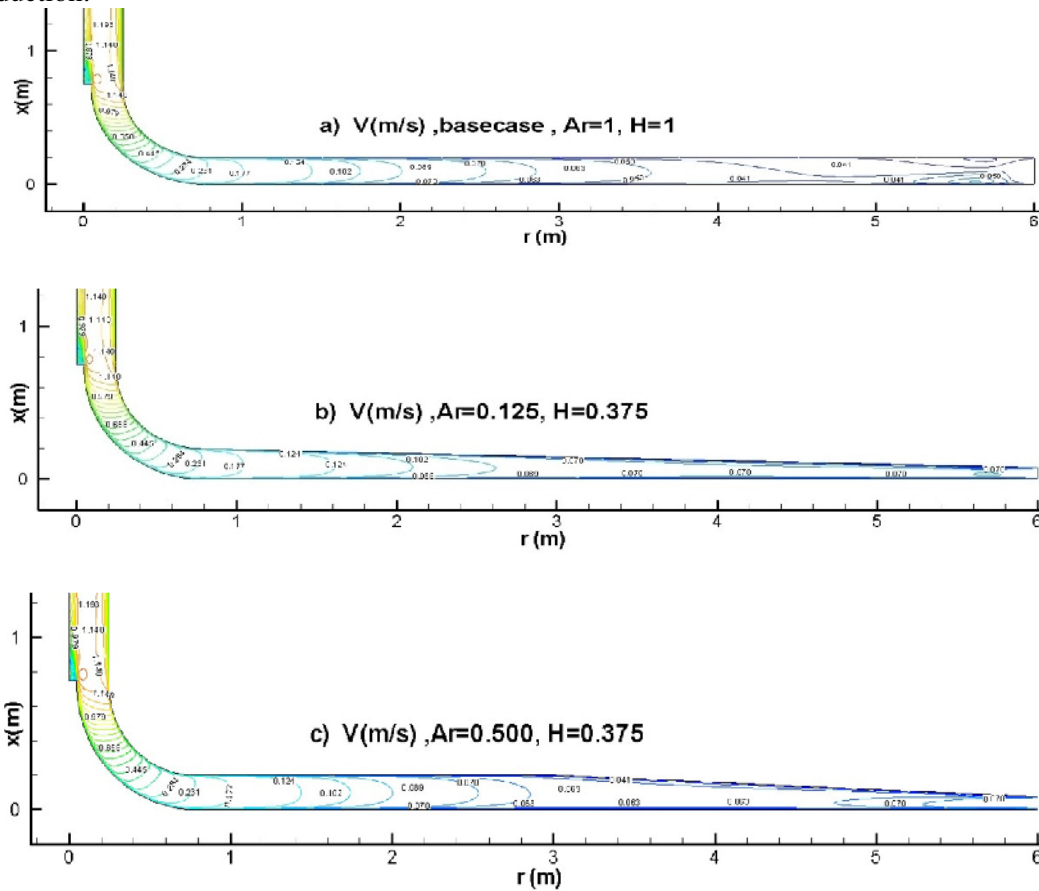


Fig.6. Magnitude velocity contours for different location of tilted collector roof for $Ra= 1.51E+07$

3. Conclusions

Two-dimensional asymmetric numerical simulation is performed to investigate the collector entrance height ratio effects on the flow behavior in a small-scale solar chimney. The following main conclusions can be extracted:

1. The collector entrance height ratio ($H=H_e/H_c$) is an important parameter that in the SSCP system for increasing the production mass flow rate.
2. The best tilted location ratio of the collector roof $Ar=0.875$ that produces a maximum of mass flow rate in the system.
3. The best collector entrance height ratio is for the value of $h=0.375$ that produces a maximum of mass flow rate in this configuration.
4. The variation of the tilt location and the reduction of the collector entrance height have significant effects on the thermal characteristic of the collector, but they have limitations values that should not be exceeded. Moreover, the importance of the collector entrance tilt is to keep the heated air that can be lost in the exterior media.

References

- [1] Stambouli, A. B. (2011). Promotion of renewable energies in Algeria: Strategies and perspectives. *Renewable and sustainable energy reviews*, 15(2), 1169-1181.

COMPUTATIONAL ANALYSIS OF FLOW AND HEAT TRANSFER CHARACTERISTICS IN A FLOATING SOLAR CHIMNEY POWER PLANT FSCPP

A. M.T.Bouzaher^{1*}, M. Lebbi¹, L. Boutina¹

¹ *Unité de Recherche Appliqué en Energies Renouvelables, URAER, Centre de Développement des
Energies Renouvelables, CDER, 47133, Ghardaïa, Algeria.*

Abstract: Typically, the conventional solar chimney power plant is built by rigid and reinforced material. Even if it has a long life span, the tower of this chimney is required to be high as possible to improve the efficiency; this tower can be destroyed easily by the external wind. A concept of floating solar chimney (FSC) is developed to be used instead of the conventional rigid solar chimney power plant. The aim of the present investigation is to analyze the thermo-hydrodynamic behavior of a floating solar chimney having a flexible tower. The effect of incoming wind velocity on the natural convection process is considered.

Keywords: solar chimney, natural convection process, flexible tower.

1. Introduction

Many potential negative effects were recorded because of the utilization of fossil fuels, which is until now the dominating source of energy. So it is necessary to replace the fossil fuels sources by renewable and clean energy sources to solve the above problems. Solar chimney power technology is an effective solution for large-scale production of energy. The first idea was displayed in a publication by Gunter in 1931 (Zou 2008) and the real prototype was constructed later in 1980 (the 50 kW Manzanares prototype). The solar chimney consisted of a solar collector, a tower situated in the center of the collector, and wind turbine generators. The floating FSC tower can theoretically extend several thousands of meters, which improves considerably the energy conversion efficiency [Papageorgiou CD(2003), Bernal-Agustin JL(2006), Zhou XP et al(2008)]. The purpose of the present study is to analyze the Thermo-hydrodynamic behavior of a floating solar chimney having a flexible tower. In literature, no study investigated computationally this type of solar chimney.

2. Problem description

The proposed device consists of a solar chimney power plant with flexible tower (Fig.1,2,3). The chimney tower is divided into two parts, flexible one and rigid one. The incoming wind flow is considered as a pulsatile flow with sinusoidal form. Therefore, the flexible part is animated by a simple flexure motion in which the governed equation is given as :

$$h(x) = \frac{a_{\max}}{h} \cdot h(y)^2 \cdot \sin(\omega t + \varphi) \quad (1)$$

where $h(x)$ is the instantaneous tower position along the x axis, $h(y)$ is the instantaneous tower position along the y axis, a_{\max} is the deflection amplitude, $\omega = 2\pi f_{\text{flexion}}$ is the frequency, φ present the phase, and t is the time.

3. Dynamic mesh strategy

The adopted calculation strategy of the flow contemplates dividing the calculation domain in three zones as illustrate in Fig. 2.b. The Zone 1 presents the rigid part of the moving tower, and is animated by a rotation motion. The Zone 1 slides in Zone 2 in which this sliding is performed through the layering technique which consists of adding or removing layers of cells adjacent to the moving boundary, based on its height. The dynamic mesh model in ANSYS FLUENT 15.0 allows us to specify an ideal layer height on each moving boundary. The layer of cells adjacent to the moving boundary (layer j in Fig 3-a) is split or merged with the layer of cells next to it (layer i in Fig. 3-a) based on the height (h) of the cells in layer j .

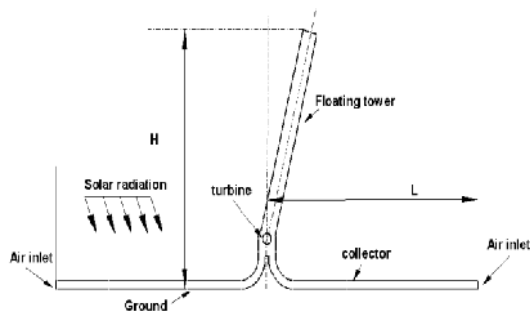


Fig. 1. Overall view of FSC plant

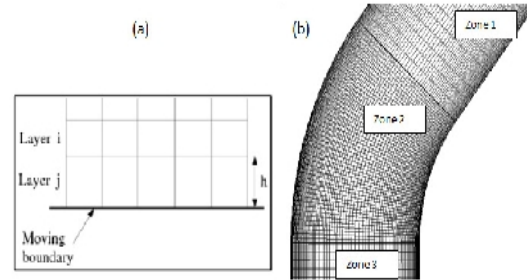


Fig. 2. (a) Dynamic layering Method (b) Tower

Zones.

4. Influence of tower deflection in the temperature contours

Fig. 3 illustrates the isothermal contours inside of the chimney with various tower inclinations. It is noted that the maximum temperature in the chimney is registered at the tower base and this is related to the fact that a recirculation zone appears in the tower base and prevent heat transfer (Fig.3). Then the temperature decreases toward the outlet with the increase of the tower inclination, a decrease about 5% in the temperature is recorded along the tower due to the change in the velocity magnitude. It should recall that the ground temperature is fixed to 320 K and the collector cover temperature to 300 K.

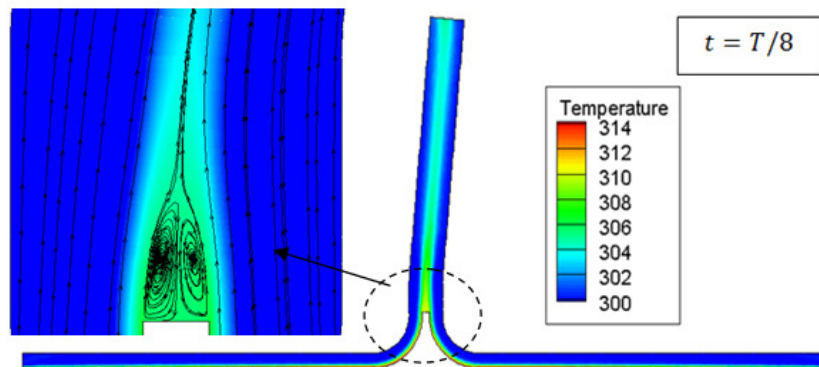


Fig.3. Temperature contours in the FSC plant

3. Conclusions

This study present the heat transfer process and the fluid dynamics in a floating solar chimney (FSC) chimney. The effects of the tower deflection is considered. The analysis has shown that a requirement for a more parametric study of such type of chimney is necessary for a full definition of the design. Results show that the velocity at the tower base remain the same during the tower deflection, which mean that the turbine can rotate with the same tip speed ratio during the tower deflection.

References

- [1] Zhou XP, Yang JK, Xiao B, Hou GX.(2007) Experimental study of the temperature field in a solar chimney power setup. Appl Therm Eng 2007;27:2044–50.
- [2] Haaf W, Friedrich K., Mayer G., and Schlaich J. (1983) Solar Chimneys, Part I: Principle an Construction of the Pilot Plant in Manzanares. Int J Sol Energy 1983; 2:3–20.

THE EFFECT OF AL₂O₃-WATER NANOFLUID ON THE PERFORMANCE OF A HEAT EXCHANGER

N. Benamara*1, M. Aminallah1, A. Boulenouar1 and M. Serier

1Laboratory of Materials and Reactive Systems, Mechanical Engineering Department, University of Sidi-Bel-Abbes, BP. 89, City Larbi Ben Mhidi, Sidi Bel Abbes 22000, Algeria.

Abstract: A nanofluid is the mixture of nanoparticles into base liquids such as water, ethylene glycol (EG), oils, etc. The nanoparticles used in nanofluids are typically made of metals, oxides, carbides, or carbon nanotubes. In this paper AL₂O₃-water nanofluid is considered. Nanometer-sized particles added to one or both fluids flowing in a heat exchanger; improve the yield of the latter due to their high thermal conductivity. To this effect, we plan to numerically study the heat exchange between a hot fluid another cold in a heat exchanger consists of two coaxial tubes in which are discussed the effects of the hot fluid flow, its capacity nanoparticles and the direction of the flows on changes in temperatures of these fluids, the Nusselt number and the efficiency of the exchanger. In order to validate the model used, we investigué in experiments the changes of the temperatures of these two fluids without nanoparticules in an exchanger same length and diameters. In this paper, The numerical simulation is performed using the two-equation k-ε SST turbulence model (Fluent) with a Reynolds number range 3054.44-7636.1 in the hot fluid and fixed to 3000 in the cold fluid. The results obtained show: a good match between the numerical and experimental, positive effects of increasing the fluid flow rate and the percentage of nanoparticles on the efficiency of the double tubes heat exchanger and the Nusselt number especially in the case where the flows are counter.

Keywords: Nanofluid; turbulence; heat exchanger; parallel flows; Al₂O₃ nano-dispersion.

1. Introduction

The heat exchangers are different in their design and their behavior. The choice of a particular exchange is dictated by various parameters such as coefficient of total exchange, obstruction minimal that possible, nature of the fluids used, exchanged flow and maintains easier. Once selected exchanger, the need to improve performance is required, which is faced with dynamic and thermal behavior problems. However, the application of nanotechnology in the field of heat transfer contributes to such improvement in adequate kinetic and thermal conditions and thermics and constitutes a challenge for future years.

2. Results and discussions

The studied axisymmetric geometry is discretized in 500.000 quadrilateral elements. Considering the simplicity of the examined model, we chose a structured mesh very refined near to the interface between the two mediums and less refined further.

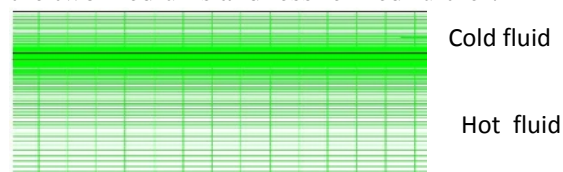


Fig. 3 Typical mesh model

4. Results and Discussion

$$Nu=0.023Re^{0.8} Pr^{0.3}$$

(5)

$$Nu_D = \frac{(f/8)(Re_D - 1000)Pr}{1 + 12.7(f/8)^{1/2}(Pr^{2/3} - 1)} \quad (6)$$

with

$$f = (0.790 \ln Re_D - 1.64)^{-2} \quad (7)$$

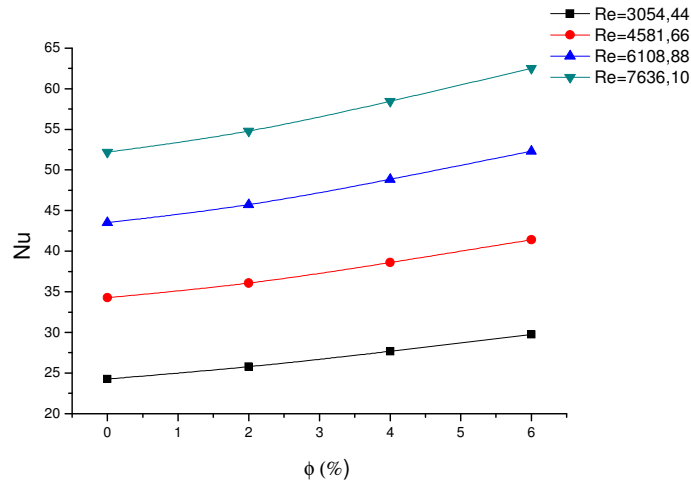


Fig. 10 Effect of volume fraction for different Reynolds number.

Conclusions

In this study, we examined the properties kinetics and thermics of the turbulent flows of two fluids (heat and cold) in a heat exchanger constituted of two concentric tubes. The cases of flows parallel and anti parallel are considered. The effects of the hot fluid flow and the quantity of nano-particles on the variation of temperatures of the two fluids, Nusselt number along the exchanger and the exchange area are investigated. The obtained results allow us to deduce the following conclusions:

The effectiveness of the exchanger increases with the flow and the volume fraction of nano-particles in the hot fluid.

The exchange surface decreases as the volume fraction of the nano-particles increases.

The heat exchanger for the flows anti parallel is more effective than the parallel flows.

References

- [1] Choi, S., Enhancing thermal conductivity of fluids with nanoparticles, In Developments Applications of Non - Newtonians Flows, D.A. Siginer and H. P. Wang. New- York : American society of Mechanical Engineers, Vol. 66, pp. 99-105, 1995.
- [2] Li Y., Zhou J., Tung S., Schneider E., Xi S., A review on development of nanofluid preparation and characterization, Powder Technology, 196(2009), 89-101.
- [3] Humnic G., Humnic A., Application of nanofluids in heat exchangers: A review, Renewable and Sustainable Energy Reviews, 16/8 (2012), 5625-5638.

THE LOCAL NUSSOLT NUMBER A LONG SQUARE CYLINDER IMMERSSED IN POWER-LAW FLUIDS UNDER AIDING THERMAL BUOYANCY

H. Laidoudi^{1,*}, M. Bouzit¹, O. Bouledroua²

¹Laboratoire des Sciences et Ingénierie Maritimee (LSIM), Faculty of Mechanical engineering, USTO-MB, BP 1505, El-Menaouer, Oran.

²Laboratoire de Physique Théorique et Physique de Matériaux, LPTPM, Faculté des Sciences Exactes et Informatique, Université Hassiba benbouali de Chlef

Abstract: This paper examines the effect of thermal buoyancy on momentum, and heat transfer characteristics of confined square cylinder submerged in incompressible power-law fluid. The detailed flow is visualized in term of streamlines contours. The numerical results have been presented and discussed for the range of conditions: power law index $n = 0.4$ to 1.2 , $Ri = 0$ to 0.5 , $Re = 40$, $Pr = 50$, at a fixed value of blockage ratio $\beta = 0.2$. The governing equations are solved by using the package ANSYS-CFX 14.0. The obtained results showed that the augmentation of power law causes separation to grow, the thermal buoyancy delays the flow separation in different power-law indexes gradually and at some critical value of the buoyancy parameter it completely disappears resulting a creeping flow around a cylinder. Moreover, the local Nusselt number is computed to predict correctly the heat transfer rate of power-law fluids under superimposed thermal buoyancy.

Keywords: power-law fluid, local Nusselt number, mixed convection, heat transfer, steady state.

1. Introduction

The flow separation is undesirable flow phenomenon which can be found in many engineering applications, it basically causes increase of drag force. Accordingly, a lot of attention is devoted to control the flow separation. Several methods have so far been developed.

In this paper, our objective is to analyze through numerical simulation the effect of superimposed thermal buoyancy of the flow field and heat transfer rate for non-Newtonian power-law fluids. To do so, the governing equations (continuity, momentum, and energy) are carried out by finite volume based commercial CFD package ANSYS - CFX 14.0. However, this work addresses the combined characteristics of power-law fluids and thermal buoyancy. The mixed convection is controlled by the number $Ri = Gr/Re^2$ [1]. If $Ri > 1$, natural convection dominates over the forced convection, if $Ri < 1$, the forced convection dominates. The Oswald relationship is type of generalized Newtonian fluid for which the apparent viscosity characteristic depends with shear rate. If $n < 1$ shear-thinning fluid, $n = 1$ Newtonian fluid, $n > 1$ shear-thickening fluid [2].

2. Numerical methodology

The problem under consideration is shown schematically in Fig.1. The fluid flow enters the channel with fully developed velocity profile, and constant temperature (T_{in}), and passes the cylinder, whose surface is maintained at constant temperature (T_w). The blockage ratio ($\beta = d/H$), (L_u) is 10 times of the cylinder height; (L_d) is 20 times of the cylinder height. The unstructured trilateral cells of non-uniform grid spacing were generated using the package GAMBIT (version 2.4.6). The grids points are distributed in a non uniform manner with higher concentration near the cylinder as shown in Fig. 2.

The dimensionless governing equations for this 2-D, laminar, incompressible flow with constant thermo-physical properties along with Boussinesq approximation and negligible viscous dissipation can be expressed in the following conservative forms:

$$\text{Momentum} \quad u^* \frac{\partial v^*}{\partial x^*} + v^* \frac{\partial u^*}{\partial y^*} = -\frac{\partial p^*}{\partial y^*} + \frac{1}{Re} \left(\frac{\partial \tau_{xy}^*}{\partial x^*} + \frac{\partial \tau_{yy}^*}{\partial y^*} \right) + Ri T^* \quad (1)$$

The fluid viscosity is defined by Oswald law which can be expressed:

$$\eta = m \left(\frac{I_2}{2} \right)^{\left(\frac{n-1}{2} \right)} \quad (2)$$

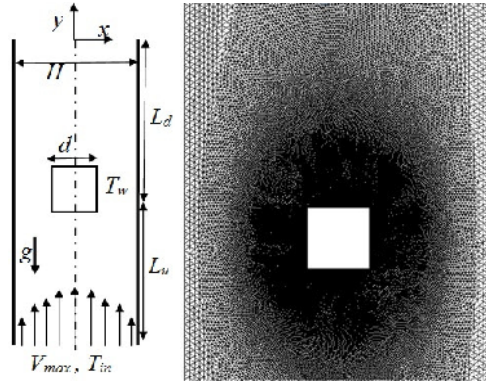


Fig. 1. Schematic diagram.

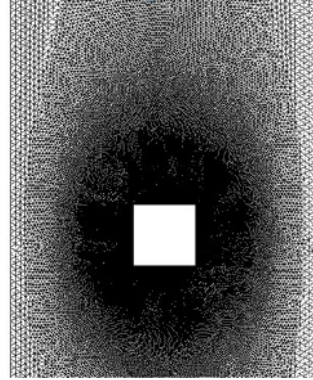


Fig. 2. Typical grid.

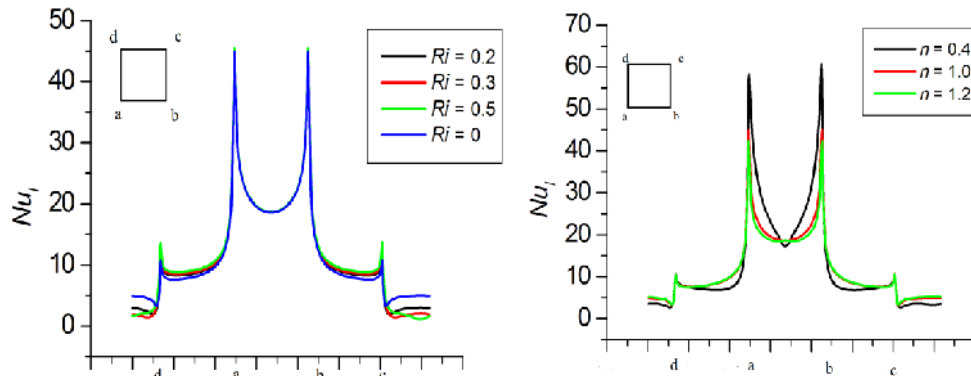


Fig. 3 Variation of Nu_l at fixed $Re = 40$, for different Richardson number and power law index.

3. Conclusions

The mixed convection heat transfer of Non-Newtonian power-law fluids from a heated confined square cylinder is examined numerically in this paper, for these range of conditions: $Ri = 0$ to 0.5 , $n = 0.4$ to 1.2 at fixed $Re = 40$, $Pr = 50$, and $\beta = 0.2$. The governing equations (continuity, momentum, and energy) are solved using the commercial package ANSYS-CFX (14.0), the obtained results showed that, increase the thermal buoyancy strength causes the separation to delay, and eventually there is no flow separation at all behind the cylinder, resulting a creeping flow around the object. The computation of local Nusselt number presents that, the heat transfer rate increases with increasing Richardson number at the right and left sides of cylinder, whereas it decreases at the rear surface of cylinder, increase in the Richardson number keeps the same heat transfer rate at the front surface of cylinder. Furthermore, decrease in the value of power law index promotes the heat transfer rate at the right and left sides of the cylinder whereas it decreases on rear edge due to the rheological behavior of the apparent dynamic viscosity around the square cylinder.

References

- [1] Dipankar Chatterjee, Bittagopal Mondal (2014). Control of flow separation around bluff obstacles by superimposed. International Journal of Heat and Mass Transfer 72 :128–138. thermal buoyancy, Publisher.
- [2] R.P. Chhabra, J.F. Richardson, Non-Newtonian Flow and Applied Rheology, 2nd ed., Butterworth-Heinemann, Oxford, 2008.

EFFECT OF THE SUBSTITUTION OF THE CALCINED BENTONITE ON THE CHEMICAL DURABILITY AND RHEOLOGICAL PROPERTIES OF CEMENT MORTARS

N. Mesboua ^{1*}, K. Benyounes ², A. Benmounah ¹

**1 Research Unit Materials, Processes and Environment (UR-MPE), University M'Hamed Bougara Bumerdes, Avenue of Independence, Bumerdes, 35000, Algeria.*

2 Laboratory of Physical Engineering Hydrocarbons, Faculty of Hydrocarbons and Chemistry (FHC), University M'Hamed Bougara Bumerdes, Avenue of Independence, Bumerdes, 35000, Algeria.

Email: mesbouhnour@hotmail.fr

Abstract: In cementing industry, the search for a less expensive binder by using industrial waste and natural resources has become a major concern for the deficit level in the manufacture of Portland cement. However despite the technical, economic and ecological benefits reported by the use of blended cements, these are associated with disadvantages. It is therefore necessary to know whether cements several components have synergistic effects so that their ingredients manage to compensate for each other's weaknesses. The aim of our work is the study of the influence of the substitution of CEM I cement in the local Algerian calcined clay such as: the calcined bentonite on the rheological properties, physical-mechanical and chemical durability of mortars prepared according clay-based contents, in the presence of fine (silica fume). This will select the optimal dosages for binary cements, the best in the rheological side, both from the standpoint of mechanical strength of the sustainability perspective. Results from this research confirms that 12% of calcined bentonite improves resistance binary high performance mortars at early age and long term, and for clay mortar is significantly notable for the attack of these mortars solutions hydrochloric, sulfuric and nitric.

Keywords: Cement replacement; Bentonite calcined; Silica fume; acid.

1. Introduction

Given this situation, partial substitution of perspective of the cement by the clay is a promising solution. This calcined product (Sarah C. Taylor-Lange and al 2015; S. Andrejkovic̃ova and al 2015), has missing plastic properties to the cement while participating in curing reactions necessary for obtaining the required strength. Furthermore, Clay production produces no CO₂, making products s interesting from an environmental point of view. The calcined clay is an eco-material that improved rheological properties and structure of cementitious products. Given the general trend on the use of high environmental quality products, Clay and contributes to sustainable development of building materials respecting the best natural resources and the environment. (Nurhayat Degirmenci and al 2009)

2. Rheological of the Saturation Point

The saturation point of high-range water-reducer (HRWR) is determined by the viscometer NF EN 934-2. Is varied dosage of high-range water-reducer (HRWR) until the grout has a nearly Newtonian behavior that is to say at a constant plastic viscosity versus shear rate. Determining the saturation point of our cement (CEM I) - high-range water-reducer (Medaflo 145) is performed using the viscometer VT550.

The results of changing the viscosity according to the shear rate are shown in the following curve. The results of development of the shear stress versus the shear rate are shown in Figure 1.

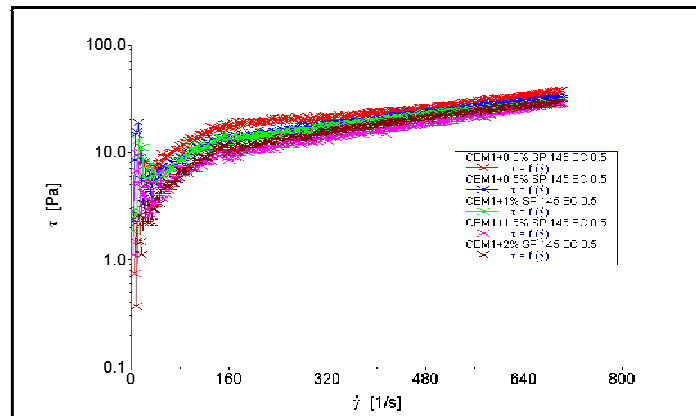


Fig. 1. Evolution of the shear stress versus shear rate.

3. Durability

3.1. Attack of the specimens with chlorhydric acid (HCl)

We used a solution of 05% hydrochloric acid with a pH = 1.34. The percentage mass loss of the different mortars for a period of 28 days is given by the following figure.

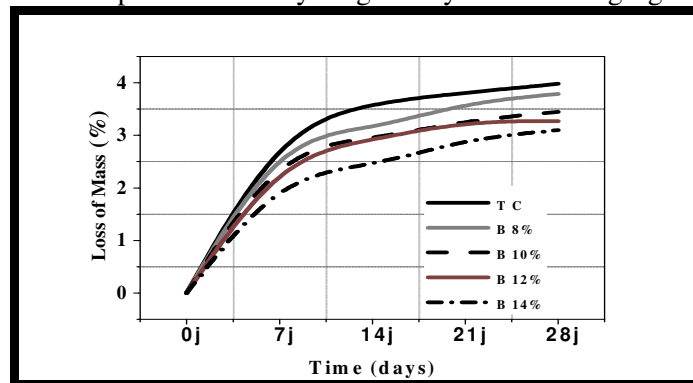


Fig. 2. Mass loss as a function of Time.

3. Conclusions

Our practical study allowed us to understand the formulation, characterization of high-performance mortar by chemical durability, the effect of calcined clays on the properties of mortars and in particular the role of the calcined Bentonite.

From the results obtained; It can be concluded:

In the chemical durability plane, clay (calcined bentonite), thereby generating a coherent skeleton, a relatively impermeable mortar skin and therefore a more resistant mortar etching when the increase in clay content.

Attack of inorganic acids (hydrochloric acid) is more aggressive), the degradation is related not only to the concentration of the acids but also their solubilities.

References

- [1] J. Mirza , M. Riaz , A. Naseer , F. Rehman , A.N. Khan , Q. Ali. Pakistani bentonite in mortars and concrete as low cost construction material, Applied Clay Science 45 (2009) 220–226.
- [2] Shazim Ali Memon, Rao Arsalan , Sardar Khan , Tommy Yiu Lo, Utilization of Pakistani bentonite as partial replacement of cement in concrete, Construction and Building Materials 30 (2012) 237–242.
- [3] S. AHMAD, S. A. BARBHUIYA, A. ELAHI AND J. IQBAL, Effect of Pakistani bentonite on properties of mortar and concrete, Clay Minerals, (2011) 46, 85–92

EFFECTS OF WELDING PARAMETERS ON FSSW: EXPERIMENTAL AND NUMERICAL STUDY

M. Merzoug^{*1}, A. Boulenouar¹, N. Benamara¹, B. Bouchouicha¹, M. Mazari¹

1Laboratory of Materials and Reactive Systems, Mechanical Engineering Department, University of Sidi-Bel-Abbes, BP. 89, City Larbi Ben Mhidi, Sidi Bel Abbes 22000, Algeria.

Abstract: In this paper, the Aluminum A6060-T5 plates of thickness 2mm was friction stir spot welded (FSSW), and the effects of welding parameters (rotation speed, plunge speed and distance from the center of pin) on the temperature variation of the joints were investigated. The experimental design method is used to investigate the effects of welding parameters in order to achieve an optimization of the FSSW process. This optimization allows the development of experimental results and may help to better understand the complexity of the phenomena resulting from contact parts/tool during the stirring process.

Keywords: FSSW, penetration, rotation of the tool, temperature, design of experiments.

1. Introduction

As a relatively new manufacturing process, there is limited published research work on FSSW process as compared to friction stir welding (FSW). Several works, however, have been discussed in symposia and conferences. Lin and al. [1] investigated microstructures and failure mechanisms of FSSW in aluminum 6111-T4 based on experimental observations. Mechanical properties are critical for an FSSW joint which are mainly affected by tool geometry and process parameters. Recently, some researchers studied the thermal and heat generation aspects of FSSW process. Gerlich and al [2] measured peak temperature in aluminum and magnesium alloys friction stir spot welds. Two thermocouples were embedded in a welding tool assembly in the experiment. Kulekci and al [3] studied the tensile-shear-strength and hardness variations in the weld regions. Cavaliere and al [4] analysed the effect of welding parameters on the mechanical and microstructural properties of dissimilar AA6082-AA2024 joints produced by friction stir welding. Analysis of variance (ANOVA) test was performed to identify the process parameters that are statistically significant. The purpose of the ANOVA test is to investigate the significance of the process parameters, which affect the temperature of FSSW joints. In addition, the rotational speeds used have a significant effect on temperature.

2. Results and discussions

Fig.1 presents data points, represented by the open square symbols, for relative temperature vs ω . It can be seen that the temperature increases with increasing rotational speed at a constant welding speeds tool. It can be inferred that the temperature is inversely proportional to the rotational speed [5]. For the tensile/ shear samples welded at the rotational speed of 1000 rpm, the crack initiates in the tip of the hook and then propagates along the hook. Fig. 2 shows that the deformation has not occurred in the weld interface, total shear started on the side of the melting zone in the heat affected zone. The application of response surface methodology to a welding procedure can be dealt elsewhere. The temperature of friction stir spot-welded is a function of the welding parameters such as tool rotational speed (N), plunge speed (Pw), welding time (Time), and distance from the center of pin (d) and it can be expressed as, Temperature = f (N, Pw, Time, d), $y = f(X1, X2, X3, X4)$

After omitting insignificant factors, the mathematical model is obtained as shown in Eq (1).

The effect of welding parameters on the transient temperature distribution is shown graphically in Fig.3. (Figure 3.a) shows the effect of the rotational speed is important in decreasing the speed of rotation, the temperature increases toward the maximum value. At a rotation of 1000 rpm, the temperature reaches 320 °C and 312 °C to devoid the rotational

speed for the same 1400 tr/min welding speed 20 mm / min. Fig(3.b) shows the difference of temperature, 310 °C to 321 °C and 16mm/min at 20 mm / min which confirms that the slope of the line is positive. The curve in (Fig. 3.c) is upward, in other words over time tends to increase and its maximum value, the more the temperature increases, but with a small slope. That is to say the temperature increases from 313 °C for a time of 48 s at 317 °C for 53 s. It can be concluded that this affects the variation of the temperature. The (Fig. 3.d) shows the influence of the distance. 12 mm A temperature = 314 °C whereas for a distance 15 mm the temperature reaches 317 °C.

$$Y = 315,06 - 4,56X_1 + 4,93X_2 + 2,18X_3 + 2,56X_4 + 4,81X_1X_2 + 9,06X_1X_3 - 5,81X_1X_4 - 3,18X_2X_3 + 2,18X_3X_4$$

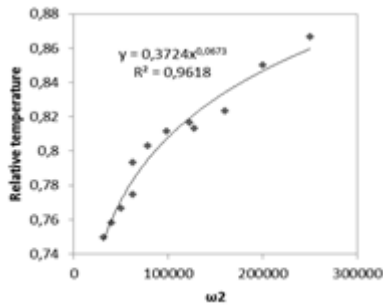


Fig. 1. Relativetemperature vs. w2 experimentalresults and modeling

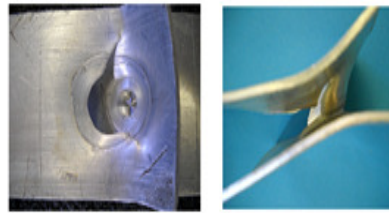


Fig.2. Tensile/shear mixed fracture observed with the parameter: 1000 rpm and 16mm/min

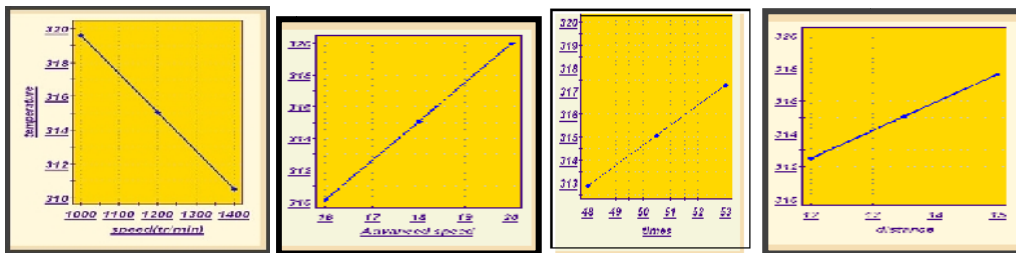


Fig.3.Effect of weldingparameters on temperature variationduring FSSW

3. Conclusions

The FSSW process does not use any external heat source. In general, the temperatures reached do not exceed 80% of the melting temperature of the base metal of 6060-T5 aluminium. This study focuses on the influence of four factors (N, Pw, Time, d). To predict these effects, the method of experimental design is a tool that, combined with experimental measurements, allows us to understand and control the consequences that can result from the friction stir welding process.

References

- [1] P. Lin, S. Lin, J. Pan, T. Pan, L. Nicholson and M. Garman, "Microstructures and Failure Mechanisms of Spot Friction Welds in Lap-Shear Specimens of Aluminum 6111-T4 Sheets", Proc. of the SAE. W.Cong. Michigan. (2004).
- [2] A. Gerlich, P. Su, and T. North, "Peak Temperatures and Microstructures in Aluminum and Magnesium Alloy Friction Stir Spot Welds", Sc and Tech of Wel and Joi, vol. 10, p.647-652. (2005).
- [3] M. Kemal Kulekci, O.E. Ugur Esme, "Experimental comparison of resistance spot welding and friction-stir spot welding processes for the en aw 5005 aluminum alloy", MTAEC9, 45(5)395(2011).

MECHANICAL PROPERTIES AND ADHESION BEHAVIOUR OF THERMAL BARRIER COATING

Y. Fizi, Y. Mebdoua, H. Lahmar

Centre de Développement des Technologies Avancées, Cité 20 août 1956, BP.17 Baba Hassen, Alger, Algérie

**Corresponding author: yfizi@cdta.dz*

Abstract: Thermal barrier coatings are commonly used in high temperature parts of gas turbines, to protect the underlying metal substrate from deterioration during high temperature exposure. The yttria-stabilized zirconia (YSZ) thermal barrier coatings (TBCs) prepared by atmospheric plasma spraying were studied. In the experiments, a combination of optical microscopy and scanning electron microscopy (SEM), energy dispersive X-ray spectroscopy (EDS) and X-ray diffraction (XRD) analysis was used to evaluate the microstructural characteristics. Instrumented indentation measurements were also performed on the coating cross-sections in order to obtain experimental load–displacement curves of the composite coating. Tensile bond strength tests were carried out, in this study, following requirements stated in the standard ASTM C633-79. In the computational analyses, the methodology based on the combination of oriented finite element and a non-linear finite element was conducted to determine elastic-plastic properties of TBCs. Due to the complexity of the coatings and difficulty of conducting tensile test, The elastic–plastic behavior law optimized from instrumented indentation tests allowed calculating the coating adhesion. A comparison between the experimental results was also investigated. On the other hand, a three-dimensional of diametrical compression model with the incorporation of fracture by extended finite element simulation (XFEM) was developed to analyze the crack propagation.

Key words: Mechanical properties, Thermal barrier, Finite elements, XFEM.

STUDY THE EFFECT OF ADHESIVE AND PATCH IN THE PLUG SAFETY BY THE FINITE ELEMENT METHOD

I. Gadi, B. MadjidMeriem, B.B. Bouiadjrab

aLRM, Mechanical engineering department, University of chlef, chlef Algeria

b LMPM, department of Mechanical engineering, University of sidiBel Abbes, sidiBel Abbes, Algeria.

Abstract: The aim of this study is to analyze for a circumferential crack on the plug of cylinder. The stress intensity factors along the crack front are computed by the 3D finite element method for the mode I. taking into account many parameters, including the repair process such as the composite layer thickness of adhesive and patch, and composite material properties. The obtained results show that the repaired by the composite materials allows reducing significantly the stress intensity factors, which can increase the life of the cylinder [1]

Keywords: Crack, cylinder, finite elements, adhesive, patch, stress intensity factor.

Introduction

Nowadays, many factories are faced rehabilitating pipelines due to damage and defects caused by different factors such as the environmental and the quality of crude oil. The main reason of pipeline failure in the many fields is corrosion. The most defects in the original material are results of installation process such as cracks during loading and welding [2].

In fact, the composites materials in the pipeline repairing are one of the most important elements for using in the piping system. Ozdenet. al. [3] work to develop guidelines to assist regulators, operators, and manufacturers in using composite technology to repair the pipelines.

The main aim of this work is to evaluate the role of cylinder composite material (plug) for piping system under the internal pressure in order to calculate the stress intensity factors for the mode I. We used the finite element model in order to analyze the crack repaired by the composite material of circumferential under the internal pressure at the plug of pipeline.

2. Geometry and finite elements method

In this study, the circumferential crack at different positions in the wall of cylinder was investigated. The crack sizes are characterized by dimensions of a single patch, and an adhesive. The geometrical characteristics are described in Fig. 1.a, where R_i ($R_i = 605$ mm) is the inner radius, and t ($t = 20$ mm) is the wall thickness [1].

In this study, we were used three-dimensional finite element method. The finite element model is based on three parts to model the cracked cylinder, the adhesive, and the composite patch (fig (1.b)).

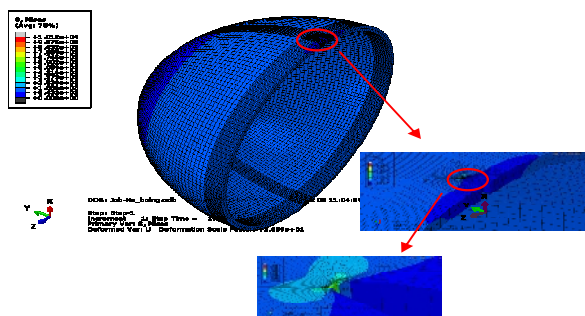


Fig. 1a. Geometrical and mesh models.

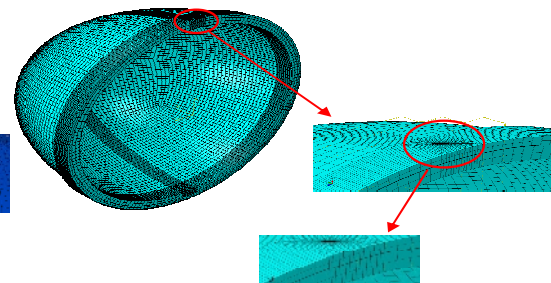


Fig. 1b. Geometrical and mesh models.

3. Results and discussions

The objective in this study is to show the importance of patch composite materials repair for cylinder crack under internal pressure through investigation by the stress intensity factor for the mode I. The numerical results show results for cylinder cracks and their repair by patch. The crack cylinder results using the finite element simulation (Abaqus)[4].

The results of SIF for cracked cylinder under internal pressure were investigated along of the crack front for two cases: firstly study the cracks in cylinder without patch and secondly repaired by patch in order to analyze the role of the materials composite for increasing the lifetime of the piping systems.

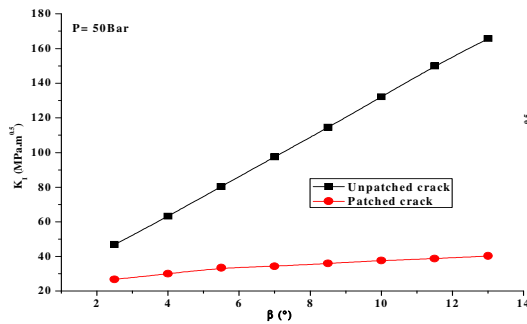


Fig. 2 Stress intensity factor (SIF) vs. crack angle for external position crack patched and unpatched.

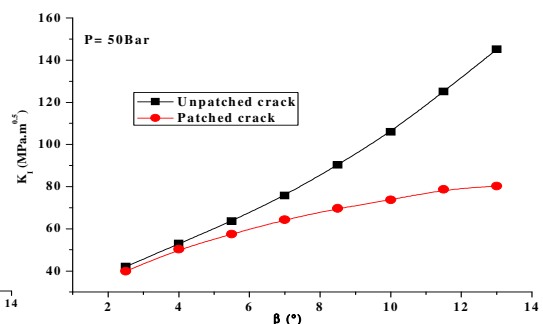


Fig. 3 Stress intensity factor (SIF) vs. crack angle for internal position crack patched and unpatched.

The numerical results of KI (Figure 2) allow presenting the behavior of crack along of the elbow crack front at external position for different crack angles where the repairing system by composite material is important to decrease the SIF values where they decreased to 20 MPa.m^{0.5}.

The effect of patch is shown through the difference between reparation with patch and without repair. At the external crack tip the SIF is decreased from 46.80 MPa.m^{0.5} to 26.77 MPa.m^{0.5}.

At 13° angle of crack, The SIF for the patch is decreased until 75.7% compared with the without patch.

Figure 3 is showed the results of the SIF versus crack angles along the internal crack elbow for repaired by patch and unrepaired.

The results is presented the important of the SIF at the internal crack tip between two angles 2.5° and 4°, where the role of the composite patch in this interval isn't efficiency, but the angles between 5.5° and 13° are important.

The results are shown that the patch at the internal crack is significantly important where The SIF at 13° angle of crack for the reparation with patch is decreased almost 44.7% compared with the without patch.

4. Conclusion

This study demonstrates that the reduction in the stress intensity by the composite patch repair of cracked cylinder subjected to under pressure is significant, which can improve the lifetime of repaired cylinders. Using the mechanical properties of the adhesive and the composite patch can develop the repair operation and improve of efficiency significantly.

This technical operation allows to reduce the stress intensity and to increase the lifetime where it can be the best solution for decreasing the risk of adhesive layer failure.

References

- MadjidMeriem-Benziane, Gadi Ibrahim, ZahloulHamou and, BelAbbesBachir-Bouiadjra, Stress intensity factor investigation of critical surface crack in a cylinder, AdvAnces in MAterIAls And Processing technologies, 2015,vol. 1, nos. 1-2, 36-42 .
- H. Toutanji, M. Han and ,J. Gilbert. Stress Modeling of defected pipelines Strengthened with FRP composite; ICERP 2008 February 7-9, 2008, Mumbai, India © FRP Institute
- O. O. Ochoa, C. Alexander, Composite Repair Methods for Steel Pipes, Stress Engineering Services, Inc., USA, Final Project Report, MMS Project Number 558, June, 2007

INVESTIGATION ON THE CONSTRAINT EFFECT FOR THE STAINLESS AISI 304L THIN SHEETS USING AN HYBRID METHOD

R. Bensaada¹, M. Almansba^{2,*}, R. Ferhoum³, Z. Sidhoum⁴, N.E. Hannachi⁵
1,2,5 University of Tizi-Ouzou, LAMOMS Lab. Hasnaoua II, 15000, Tizi-Ouzou Algeria.
3,4 University of Tizi-Ouzou, LEC2M Lab. Hasnaoua II, 15000, Tizi-Ouzou Algeria.

Abstract: It has been recognized by several researchers that the global fracture mechanics criteria 'K and J' are strongly dependent on the geometrical and shape parameters of specimens and defects. Among the consequences of this dependence, we find the variation of the constraint effect in the vicinity of the crack front, this dependence plays a key role in the variation of fracture toughness and crack propagation. The purpose of this work is to study the geometrical parameters effect on the fracture toughness of stainless AISI 304L thin sheets using a combined experimental-numerical approach. Compact Tension (CT) specimens are machined in conformity with the ASTM E 1820 standard. Experimental tests were performed in accordance with the standard including three thicknesses (0.8, 1.5 and 3 mm), three crack lengths are considered for the 0.8 and 3 mm sheets and four for the 1.5 ones. Numerical simulations were performed using the FE package ABAQUS including a damage model for the crack propagation assessment. A general tendency is found when we assess the evolution of the critical energy to fracture dependently of the crack length/ligament ratio.

Keywords: J-R Curve, crack propagation, damage, constraint, geometric parameters.

1. Introduction

In the last decades, the global approach of fracture mechanics is widely used for the study of the behavior of engineering materials and structures. Unfortunately, criteria related to this field suffer strongly from transferability problems. Many works are performed [1, 2] considering geometric parameters effect. Many authors proposed the association of a second parameter as T-Stress or Q-Parameter [3-5] but this method is limited by inaccuracies for non linear problems. In this work, we use a combined approach consisting to perform both experimental tests and F.E. Analysis to study the constraint effect on the critical fracture toughness for stainless AISI 304L thin sheets with different thicknesses and crack lengths.

2. Assessment of the geometric parameters effect on the fracture toughness J_{IC}

Experimental tests are performed on CT specimens and the load-displacement curve results are calibrated by 3D finite element analysis using the ABAQUS package [6] as illustrated in Fig.1 for $a/w = 0.2$ and $b = 1.5$ mm (a is the crack length, w and b are the width and the thickness of the specimen), the GTN model (eq.1) is used for the determination of crack propagation, where σ_e is the von Mises stress, q_i are the Tvergaard calibration parameters, f is the porosity, σ_h is the hydrostatic stress and $\bar{\sigma}$ is the actual flow stress.

$$\phi = \frac{\sigma_e^2}{\bar{\sigma}^2} + 2q_1 f^* \cosh\left(q_2 \frac{3\sigma_h}{2\bar{\sigma}}\right) - (1 + q_1^2 f^{*2}) = 0 \quad (1)$$

Since the load-displacement curves from experimental tests and crack propagation data from numerical simulation are available, the ASTM E 1820-13 procedure [7] is used for the J-R curves determination, the result of the critical fracture toughness versus the ratio a/w is illustrated in Fig. 2 and the cracked specimen is given by the Fig.3. We conclude that the shape of this evolution is the same as the works reviewed by Neimitz [8].

* Corresponding author

E-mail address: almansbm@gmail.com

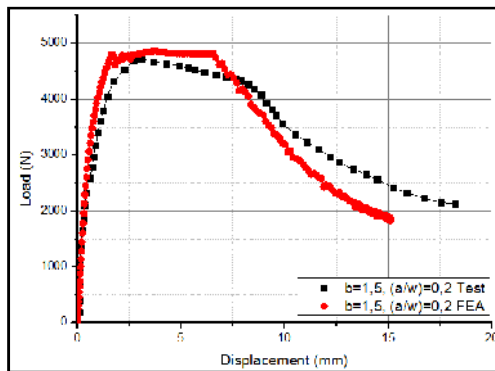


Fig.1. Capacity curves of CT Test $(a/w)=0.2$, $b=1.5$, experiments with F. E simulation

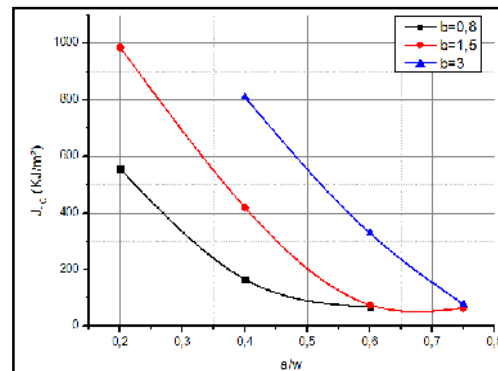


Fig.2. J_{1C} evolution with geometric parameters

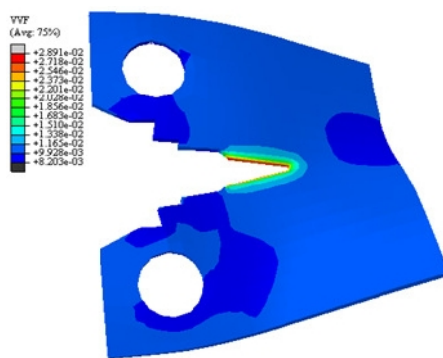


Fig.3. Determination of the crack propagation from FE Analysis

3. Conclusions

The aim of this work is to assess the geometric effect on the fracture toughness of stainless AISI 304L thin sheet, we can conclude that the GTN model predict successfully the ductile fracture of the material and the shape of evolution of fracture toughness with the evolution of geometric parameters is in conformity with the works available in the literature.

References

- [1] A. R. Shahani, M. Rastegar, M. B. Dehkordi, and H. M. Kashani, "Experimental and numerical investigation of thickness effect on ductile fracture toughness of steel alloy sheet," *Engineering Fracture Mechanics*, vol. 77, pp. 646-659, 2010.
- [2] X. Qian, Y. Zhang, and Y. S. Choo, "A load–deformation formulation with fracture representation based on the J–R curve for tubular joints," *Engineering Failure Analysis*, vol. 33, pp. 347-366, 2013.
- [3] Y. Y. Wang and D. M. Parks, "Limit of J – T characterization of elastic-plastic crack-tip fields. Constraint effects in fracture theory and application," *ASTM STP1244: American Society for Testing Materials*, Philadelphia, PA, vol. 2, pp. 43–67, 1995.
- [4] Y. J. Chao and X. K. Zhu, "J-A2 characterization of crack-tip fields : Extent of J-A2 dominance and size requirements," *International Journal of Fracture*, vol. 89, pp. 285-307, 1998.
- [5] J. H. Kim and G. H. Paulino, "T-stress, mixed-mode stress intensity factors, and crack initiation angles in functionally graded materials: a unified approach using the interaction integral method," *Comput Methods Appl Mech Engrg*, vol. 192, pp. 1463–1494, 2003.
- [6] HKS, "ABAQUS 6.12 User Manual," Providence R.I 2012.
- [7] ASTM, "E1820-13 : Standard Test Method for Measurement of Fracture Toughness " 2014.
- [8] A. Neimitz, "Fracture toughness of structural elements : the influence of the in- and out-of-plane constraints of fracture toughness," *Materials Science*, vol. 42, pp. 61-77, 2006.

THEORETICAL STUDY OF INASXSb1-X /GAAS QUANTUM WELL SOLAR CELL

S.Taleb^{1,*}, I.Lagraa¹

1Applied Materials Laboratory (AML), University of Sidi Bel Abbes, Sidi Bel Abbes, Algeria

Abstract: This article presents a theoretical study of a new InAsSb/GaAs Quantum Well Solar Cell QWSC that has a few reports [1]. The influence of the insertion of InAs_xSb_{1-x} QW layers inside the intrinsic region of a GaAs pin solar cell on the main characteristic parameters of a solar cell and on the External Quantum Efficiency EQE have investigated. The results have shown that the insertion of 20 InAs_{0.8}Sb_{0.2}/GaAs QW layers provide a relative improvement of about 17.06 % and 2.14 % of short-circuit current and efficiency respectively. Otherwise, the absorption range edge of photons with low energy extended from 870 to 950 nm.

Keywords: QWSC, efficiency, EQE, Short-circuit.

1. Introduction

The Quantum Wells QWs are among the first approaches proposed to achieve the challenge to overcome Shockley-Quisser limits in a solar cell [2]. Such a configuration permits the charge carriers confinement in the quantum wells while generating an optimal photocurrent, respecting some parameters, such as the width, the number and geometry of the quantum wells. It's reported that III-V alloys have difficulties to control their growth in the laboratory. Recently, InAsSb ternary semiconductor has gained an importance on optoelectronic field thanks to their excellent electronic properties and its lower bandgap [3]. In this paper, an InAsSb/GaAs QWSC structure is studied originally in theory.

2. Theoretical models

Several models have been used in literature to determine the main characteristics of a solar. The Drift-Diffusion model and current continuity equations for the quantum well systems are used to calculate the current density of electrons and holes in the bulk and well regions and it is given in equations (1) and (2) respectively. The EQE is given by equation (3)

$$\frac{dn_b}{dt} = G_b - U_b - \frac{n_b}{\tau_{cn}} - \frac{n_{qw}}{\tau_{en}} + \frac{1}{q} \frac{dJ_n}{dx} = 0 \quad (1)$$

$$\frac{dn_{qw}}{dt} = G_{qw} - U_{qw} - \frac{n_b}{\tau_{cn}} - \frac{n_{qw}}{\tau_{en}} = 0 \quad (2)$$

$$J_{ph} = q \int_{\lambda_1}^{\lambda_2} F(\lambda) \cdot EQE(\lambda) d\lambda \quad (3)$$

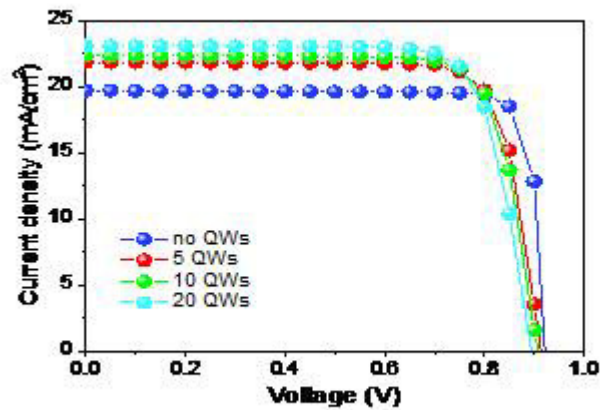


Fig. 1. J(V) of InAs_{0.8}Sb_{0.2}/GaAs Quantum Well Solar Cell for variable QW layers inserted.

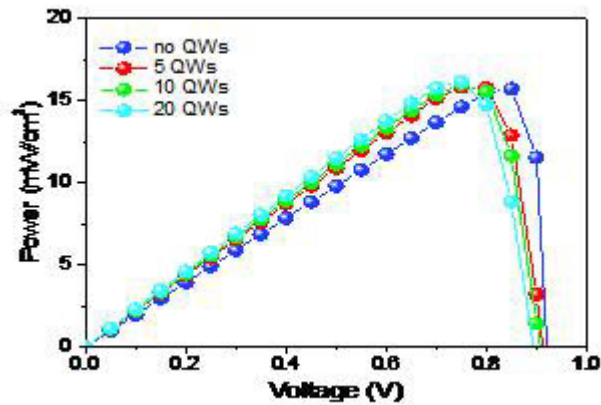


Fig. 2. P(V) of InAs_{0.8}Sb_{0.2}/GaAs Quantum Well Solar Cell for variable QW layers inserted.

3. Conclusions

In the present work, we have shown the effect of InAsSb/GaAs QW layers introduction on the main characteristics of GaAs pin solar cell. Based on our simulation results, 20 InAs_{0.8}Sb_{0.2}/GaAs QW layers gives an optimal conversion efficiency of about 16.03 %, an increase of 0.34 % comparing to its GaAs baseline efficiency. Otherwise, the absorption range limit has extended from 870 nm to 950 nm.

References

- [1] K. Suzuki and Y. Arakawa, Phys. Status Solidi B 224, 139 ~2001.
- [2] Shockley W and Queisser H J 1961 J. Appl. Phys. 32 510.
- [3] S. Tsukamoto, P. Battacharya, Y. C. Chen, and J. H. Kim, J. Appl. phys. 67,6819 (1990).

Ab initio study of structural , electronic ,optical and thermal propertieess of AgInTe2

H.Bendjeddou¹, A.Gassmi¹, H.Meradji², S.Ghemid²

1Laboratoire LPS, Département de Physique, Faculté des Sciences, Université Badji Mokhtar, Annaba BP12Annaba 23000, Algeria

2Laboratoire LPR, Département de Physique, Faculté des Sciences, Université Badji Mokhtar, Annaba BP12Annaba 23000, Algeria

Abstract: Structural, electronic and optical properties of AgInTe₂ have been investigated using Full Potential Linear Augmented PlaneWave (FP-LAPW) method within density functional theory (DFT) as implemented wien2k code. The exchange-correlation potential was calculated using the Wu-Cohen Generalized gradient approximation (WC-GGA). Moreover, the modified Becke Johnson approximation (mBJ) was also used for band structure calculations. The ground state properties such as lattice constants and bulk modulus are in good agreement with available experimental and theoretical data. The band gaps obtained by mBJ approximation are better than those obtained by WC-GGA and engel-Vosko GGA and are closely to experimental results. A direct band gap (Γ - Γ) is observed for the compound. The optical properties were analyzed, the imaginary and real part of dielectric function, the reflection coefficient (R), refractive index(n) and extinction coefficient (k) are computed.

Key words: FP-LAPW, DFT, WC-GGA , structural properties, electronic properties, optical properties

MECHANICAL CHARACTERIZATION OF THE BEAD WELDING OF HIGH-DENSITY POLYETHYLENE (HDPE)

A. Belaziz ^{1*}, M. Mazari ¹

1University Djillali Liabes (LMSR), BP 89, 22000, Sidi Bel Abbes, Algeria.

Abstract: High-density polyethylene (HDPE) is widely used for many years for pipes of industrial facilities. The range of applications was extended to construction industry: transmission of gas, water, sewage disposal. Among the consolidation process of pipes made from high-density polyethylene (HDPE), fusion welding or butt weld fusion is considered to be a widely used technique in the thermoplastics industry whereby the mechanical behavior of the weld may approach that of the initial materials. This study was devoted to the experimental study of the mechanical behavior of a HDPE structure welded by butt fusion welding technique solicited in traction. We are based on experimental tests that were performed to characterize the material studied, introduce the ductility of the welded section and see the effectiveness of the displacement speed and the welding parameters, namely the melting temperature relative to the dimension of the internal diameter of the pipe.

Keywords: high-density polyethylene (HDPE), tensile testing, behavior, characterization, deformation.

STUDY OF A NEW GEOMETRY OF BEAM WELDED RECONSTITUTED (COMPOSITE BRIDGES)

A. Houda¹, H. Zedira^{2,*}, B. Redjel³

1University, Abbas Laghrour, khenchela, Algeria

2University of Abbas Laghrour, 40000, khenchela, Algeria.

3University, Badji Mokhtar, Annaba, Algeria

Abstract: This study pertains to the numerical analysis or AUTODESK ROBOT structural analysis software professional 2009 was used for modeling and calculation of two different geometry beam welded reconstituted (beam welded reconstituted solid core and another pleated soul). After completing the various calculations it was found that the beam welded reconstituted pleated soul is the most economical and architecturally the most successful

Keywords: beam welded reconstituted, reinforced concrete, pleated soul, composite section, digital simulation

1. Introduction

The history of steel bridges lived all ages of cast iron, puddle and finally the age of steel through these different periods, metal bridges have gradually evolved to their present form. They are the result of the combination of a cover and a metal frame in which each one has different shapes and designs.

Of all the forms of apron, twin boom is the most economical. It works economically in a range of slenderness of the order of 20 to 30, to ensure the bracing, the twin-boom can be braced by either bridge piece with or without brackets or by simple braces with or without transverse prestressing [1].

Concern the beams must be sized according to the requirements of the euro code 3, point of view they are making functioned from three props welded together by four welds these are respectively the top flange, and the soul the lower sole [2]

Before beginning the study of a composite section; it is obvious to focus the mind on the main benefits resulting from it are:

The reduction of 20 to 30% of the own weight of the metal structure to equal loading. This advantage leads to a significant reduction of the height of the BWR.

The increase in flexural rigidity resulting in a considerable decrease in service .This advantage allows the metal structure to have greater ranges for equal loading [2]

2. Study of comparison between BWR in I solid core and soul BWR pleated

We found that virtually all the beams are I-shaped, made from cut sheet metal, welded reconstituted.

Pictures of a girder bridge caught our attention because the geometry of the beams out of the ordinary. Indeed, the soul of the beams has a different special form which usually does (vertical solid core); it is a pleated core. We decided to do a comparative study between a BWR reach 30m a vertical line and a soul BWR littermates has folded to me.

* Corresponding author

E-mail address: houdaaminagc@gmail.com

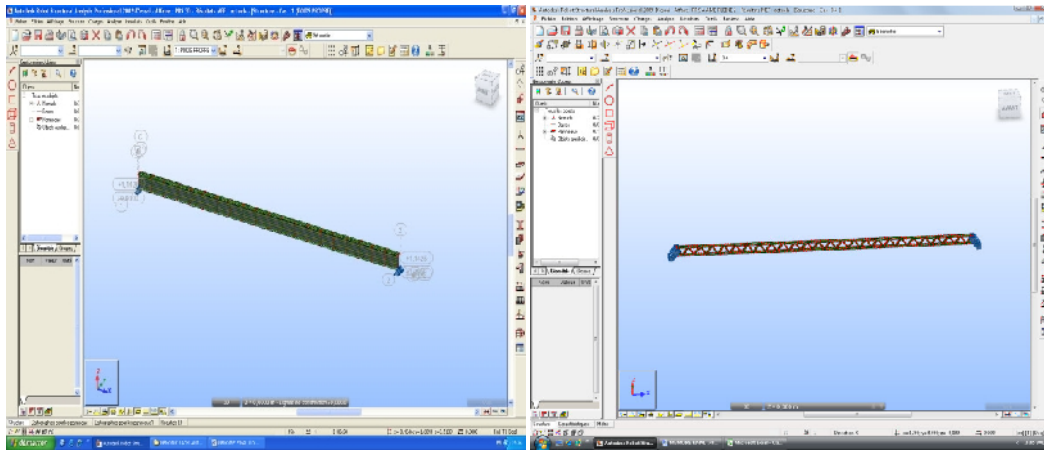


Fig. 1. BWR in I solid core modeled in 3D.

Fig. 2. BWR pleated soul modeled in 3D

Tab. 2. Resulted obtained

	σ_c MPA	σ_t MPA	U_z cm	weight " T"
I fully 3D soul	411.86	206.79	-17.7	22.67
3D pleated soul	467.30	241.37	-10.9	17

3. Conclusions

The results show that the beam welded reconstituted pleated soul brings significant economic benefits; hence it requires a height of 80cm to cross a 30m range at the same time as ordinary BWR requires 1.2m to cross the same scope for equal loading. ; it was found that the beam welded reconstituted pleated soul brings considerable economic reliefs.

References

- [1] Bennett D. (2000) the history and technical bridges, Vol. 1, edition Eyrolles.
- [2] Bourrier P and Brozzti, J, (1996) Steel and Composite steel-concrete constructions Vol 2 ,n°2, Vol. 6, editions Eyrolles et Delta

INTERFACIAL STRESS ANALYSIS IN MULTIMATERIAL METAL / CERAMIC / METAL BY THE METHOD OF FINITE ELEMENT

W. Bensmain¹, B. Serier^{2,*}, H. Fekirini³
123 Laboratoire de Mécanique Physique des Matériaux

Université Djilali Liabes de Sidi Bel Abbès BP89, Cité Ben M'hidi, Sidi Bel Abbès, 22000, Algérie

Abstract: This work presents three-dimensional analysis of the interfacial stress in a Multimaterial. This study shows the effect of physical and mechanical properties on the intensity of the residual stresses. In order to determine the level and distribution of internal stresses numerically by the finite element method in the assembly silver-copper-zirconia. This multi-material is assembled with different physical and mechanical properties. Results are achieved under mechanical loading, thermal and thermomechanical. This approach was successfully used to quantify the constraints of notch-tip fields for various geometries and loading conditions. The variation of normal and shear stresses is obtained in close proximity to the interface.

Keywords: Interfacial stresses, multi-matérial Metal/Ceramic/Metal, finite element.

1. Introduction

Open multi-materials have a wide field of research and application in many industrial sectors. The assembly analyzed in this study is designed such that simultaneously one can use the characteristic properties of ductile and ceramics, while having a structure. The use of a ceramic finds its justification by its electrical insulation properties even at high temperature [1], high wear resistance and chemical inertness. Meanwhile, the ductile parts allow to bind the ceramic part to the rest of the component, and they can act as an electrical conductor. Finally, the assembly is performed such that sealing is total. This work can analyze the internal stresses of thermal and mechanical assembly in the Ag / ZrO₂ / Cu. this multi material was chosen for three reasons. First is their broad application in the electronics industry, electrical and thermo-mechanical and aerospace. The second is that it is three different materials with Young's modulus ($E_{ZrO_2} \approx 2E_{Cu}$, $E_{ZrO_2} \approx 3E_{Ag}$) and coefficients of different thermal expansion ($\alpha_{ZrO_2} = 3\alpha_{Cu}$, $\alpha_{ZrO_2} = 2\alpha_{Ag}$). Finally, the difference between the mechanical and physical properties of the multi-material led to the birth of interfacial stresses which can cause damage to the multi-material Ag / ZrO₂ / Cu [2]. A considerable fall of KIC stress intensity factor in close proximity to ceramics, which leads to embrittlement of the metal-ceramic joint. Therefore, it is interesting to analyze the stress state, level and distribution.

2. Determination of the T-stress in the case of a notch

The structure consists of a type of Multi-material assembly (Ag / ZrO₂ / Cu) which has the same thickness ratio ($t_m / t_c = 6$) t_m is the thickness of metal and is t_c that of the ceramic. The numerical analysis was developed as part of the calculation of finite element code Abaqus 6.11. The mesh was refined at the interfaces so that the results is accurate and converge with optimum time (fig.1). Figure 2 shows the variation of normal internal stresses σ_{xx} multi-material Ag / ZrO₂ / Cu according to the distance from the interface under a mechanical load.

* Corresponding author

E-mail address: bensmainwafaa@yahoo.com

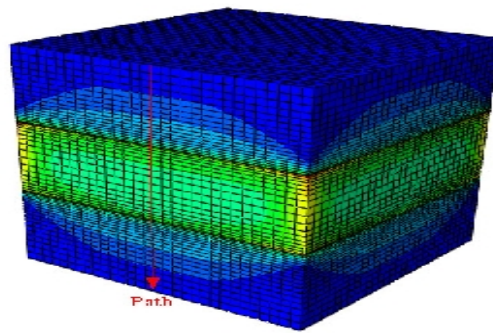


Fig. 1. Typical 3D finite element mesh used in assembling of the multimaterial

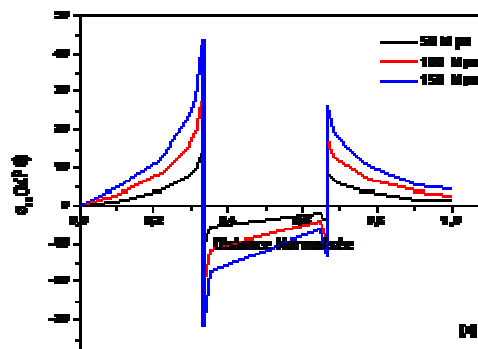


Fig. 2. Variation of the normal stress σ_{xx} depending on the distance input to the interface Ag / ZrO₂ / Cu, a) Mechanical Loading.

3. Conclusions

The results obtained in this study from an analysis by the finite element method show that:

The presence of interface metal / ceramic / metal is the stress concentration seat;

The normal residual stresses σ_{xx} , σ_{yy} and σ_{zz} in close proximity to the interface are more intense at the center than at the edge of the multi-material studied. They decrease away from the interface and bring the silver and copper in tension and compression in zirconia;

The σ_{yy} normal residual stresses are much greater than the normal stresses and σ_{xx} σ_{zz} . Their level is more pronounced near the first interface (Ag / ZrO₂).

Internal σ_{yz} tangential stresses are highly distributed near the interfaces between the constituent assembly materials. Compared with the normal stresses σ_{xx} , σ_{yy} and σ_{zz} , these constraints are of a lower level.

Under a thermomechanical loading multi-material Ag / ZrO₂ / Cu generates normal residual stresses and tangential little marked compared to stresses induced by purely thermal or mechanical stresses.

The difference between the thermal expansion coefficients and Young modulus induced more intense internal stresses in the assembly.

References

- [1] G. Aliprandi, Matériaux réfractaire et céramiques techniques, Edition septima Paris, 1979.
- [2] J.L. Chermant, " Les céramiques thermomécaniques", Press du CNRS, 1989

Study of phase stability of AlN under high pressure.

¹N. BOUTELDJA, ²S. DAHMANE, M. TRAICHE, ⁴A. CHENOUNE, ⁵A. ALIBENAMARA

1,2,3,5 University of Chlef, LTPM, Esalem City, 02000, Chlef, Algeria.

4 University of Oran LCGE USTO BP-1505 El-M'naouar, Algeria

Abstract:

This research work us to know the calculated structural properties of different phases of semiconductor AlN crystal (Wurtzite, Zinc Blende and Rocksalt), using an ab-initio method of Linearized Augmented Plane Wave with Full Potential (FP-LAPW) based on the Density Functional Theory (DFT), the results include; the lattice parameters, the volume of the lattice, the total energy and the equilibrium compression modulus and its derivative with for the pressure. Most of the structural properties calculated are higher than the experimental values and a 1% error for the GGA approximation and lower a 1% error for the LDA approximation.

Introduction:

The Aluminum Nitride semiconductor (AlN) is of great interest given their applications in electronics and optoelectronics, this is due to their very interesting properties and first, their gap energy (EG=6.12eV)[1] of the wavelength $\lambda= 0.2\mu\text{m}$ which corresponds with the electromagnetic coverage spectrum in the Ultra-Violet

Method of calculations:

In our calculations, we used the Wien2K code with full potential linearized augmented plane waves based on density functional theory in the generalized gradient approximation and local density approximation, the calculations are based on the structural properties of AlN semiconductor in three phases Würtzite (WZ), Zinc Blende (ZB) and Rocksalt (RS), to determine the more stable phase, the crystal structure of the Würtzite phase is defined by three parameters a , c and an internal parameter u , the Zinc Blende phase and the Rocksalt phase can be defined by the lattice parameter a .

The atomic sites for the Würtzite phase of the Al atom are (0,0,0) (2/3,1/3,1/2) and the atom N (0,0,u) (2/3,1/3,u+1/2), for the Zinc Blende phase, the atomic sites of the atom Al (0,0,0) and the atom N (1/4,1/4,1/4), and for the Rocksalt phase, the atomic sites of the atom Al (0,0,0) and the atom N (1/2,1/2,1/2). The values of Muffin Tin rays (R_{MT} is the mean radius of the Muffin Tin spheres MT), for Al and N at the three phases the R_{MT} is represented as a good choice to avoid overlapping spheres Muffin Tin, for AlN Würtzite ($R_{MT}=1.75$), AlN Zinc blende ($R_{MT}=1.80$), AlN Rocksalt ($R_{MT}=2.00$) and for N ($R_{MT}=1.75$).

The determination of the structural properties of AlN by the Wien2K code for the GGA and LDA approximations is carried out by calculating the variation of the energy as a function of volume, and minimizing this energy to find the optimal parameters.

These parameters are adjusted with the Murnaghan state equation [1] which is given by the following expression:

$$E(V) = E_0(V) + \left[\frac{BV}{B'(B'-1)} \right] \times \left[B' \left(1 - \frac{V_0}{V} \right) + \left(\frac{V_0}{V} \right)^{B'} - 1 \right]$$

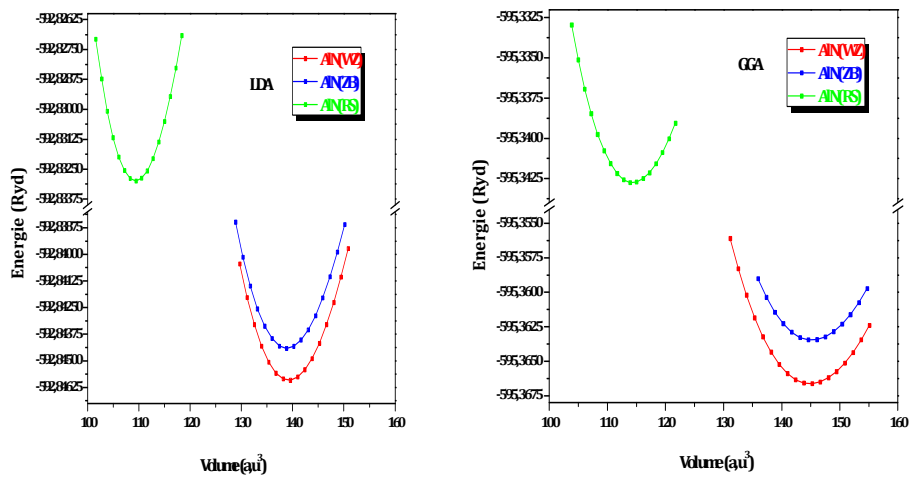


Fig 1,2: The variation of the total energy as a function of the volume of AlN in the GGA approximation. Fig 2: The variation of the total energy as a function of the volume of AlN in the LDA approximation

Conclusions:

We have presented detailed calculations of the structural properties of AlN semiconductor in the zinc-blende, rocksalt and wurtzite phases using the ab-initio method of Linearized Augmented Plane Waves with Full Potential (FP-LAPW) based on the Density Functional Theory (DFT) in the Local Density Approximation (LDA) and Generalized Gradient Approximation (GGA). The structural properties of AlN obtained by the use of GGA are in good agreement with the experimental results compared to LDA, the LDA/GGA error are very similar. We conclude that AlN crystallizes in the Würtzite phase, which is the most thermodynamically stable state, but can crystallize in the Zinc Blende phase, which is a metastable state.

Référence:

- [1] I. Vurgaftman, J. R. Meyer and L. R. Ram-Mohan, «Band parameters for III–V compound semiconductors and their alloys» *J. Appl. Phys.*, Vol. 89, No. 11, (2001).
- [2] Qimin Yan, Patrick Rinke, Matthias Scheffler, and Chris G. Van de Wall, «Strain effects in group-III nitrides: deformation potentials for AlN, GaN, and InN» July 14, (2009).
- [3] B. Daoudi, M. Sehil, A. Boukraa, H. Abid, «FP-LAPW calculations of ground state properties for AlN, GaN and InN compounds» *J. Nanoelectronics and Materials* (2008).
- [4] M. Abu-Jafara, A.I. Al-Sharif, A. Qteish, «FP-LAPW and pseudopotential calculations of the structural phase transformations of GaN under high-pressure» *Solid Stat. Comm.* 116, 389 (2000).
- [5] M. Van Schilfgaarde, A. Sher and A. B. Chen, *J. Cryst. Growth.* 178, 8 (1997).

ANALYZE OF INTERFACIAL CRACKS IN A COMPOSITE MATERIAL SUBJECTED TO DIFFERENT LOADS

Y. Chahraoui¹, L. Zouambi^{1,2,*}, F. Bouafia^{1,3}, B. Serier¹

*1*ILMPM, Mechanical Engineering Department, University of SidiBel Abbes, 22000, SidiBel Abbes, Algeria,

*2*University Center of Relizane, 48000, Relizane, Algeria

*3*University of Temouchent, 46000, Temouchent, Algeria.

Abstract: In this investigation, a numerical model was developed to study the effect of both thermo-mechanical load in SIC fiber-reinforced Al2024 matrix. The finite element technique was used to analyze the level of the stress intensity factors (SIF) KI, KII for crack growth in the matrix composites at the interface matrix/fiber. Influences of the applied load on the stress intensity factors for crack in matrix have been investigated. The behaviour of inclined cracks has been analyzed. We show the variation of the SIF KI, KII depending on the intensity of the applied load and the angle of orientation θ of cracks relative to the interface. KI grows very strongly with the crack propagation. This factor is insensitive to increased cracking defect. These cracks are even more unstable than the intensity applied tension forces grows. The shear mode is governed by the direction of crack propagation. The values of the stress intensity in KII are negligible compared to those resulting mode I. This intensity leads to a strong interaction between the highly localized stress fields in close proximity to these defects and resulting intensification of mechanical energy to the crack tip, and therefore an increase in the speed of propagation of fatigue cracks.

Keywords: composite SIC/Al2024, crack, stress intensity factor, thermo-mechanical stress, finite element analysis.

1. Introduction

The problems related to durability of composites require a better understanding of damage process. They occur when these materials are subjected to thermo-mechanical stresses and / or environmental. Under these conditions, their mechanical properties can change over time. The estimate of the residual life of the composite structure requires the development of experimental methods, sensitive to changes in service of mechanical properties, and the development of models taking into account the progressive damage of these materials to predict these developments mechanical properties.

2. Mechanical, thermal and Thermo-mechanical loading

The composite material (Fig. 1) is subjected to thermo-mechanical loads (tensile loading in the direction xx and temperature). The angle θ of the orientation of the crack compared to the interface tends towards 45° , the shear stress becomes maximum τ and the SIF KII approaches its maximum value. 45° to 90° , the SIF KI approaches its maximum value, while the value of the SIF KII tends to 0, it shows that the movement of the crack lips being in mixed mode (I and II), the mode I in this case is paramount, it is the mode of opening of the most dangerous crack. The thermal effect is visibly clear. The level of the curve of the SIF increases considerably with increased thermal load (Fig. 2 (a, b & c)).

* Corresponding author

E-mail address: zouambileila@yahoo.com

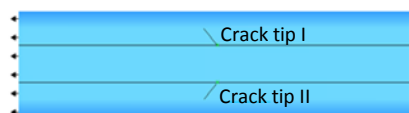


Fig. 1: Geometric model

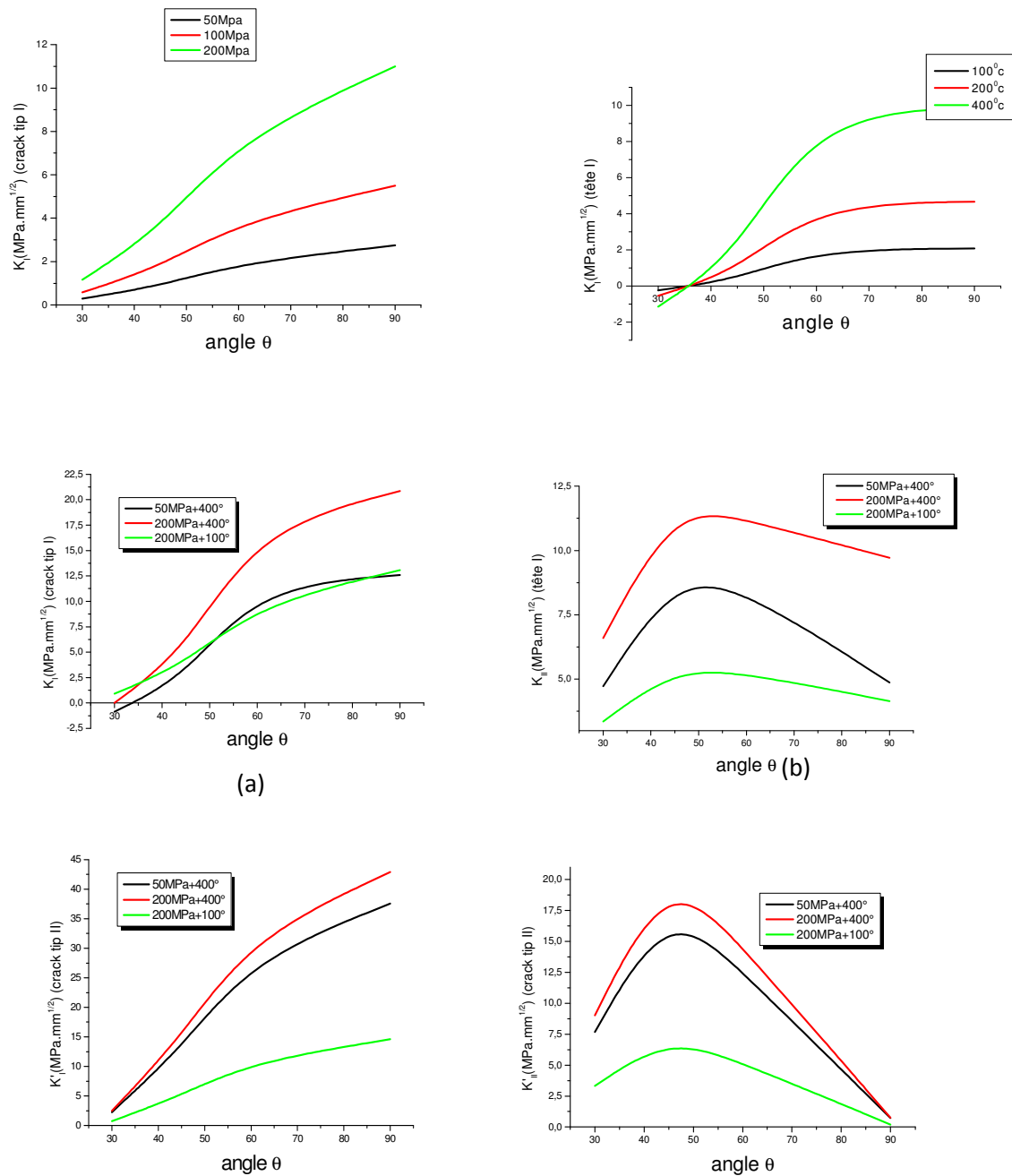


Fig. 2: Variation of the SIF according to the crack orientation θ (a) Mechanical, (b) Thermal and (c) Thermo-mechanical loading

3. Conclusions

The stress intensity factor (SIF) in mode I and mode II depends on the location of the crack initiated from the matrix to the fiber-matrix interface. The angle of orientation of crack propagation determines the predominant mode. The level of the SIF increases with the increase of the thermo-mechanical loading.

References

- [01] KHIAT Sidi Mohamed Amine. (2012), Etude de la probabilité d'endommagement des composites unidirectionnels aux interfaces Fibre/Résine. Thèse. Université des Sciences et de la Technologie d'Oran
Mohamed Boudief.

L.

Comportement dynamique des poutres sandwiches fonctionnellement graduées (FGM)**Free Vibration Analysis of Functionally Graded Sandwich Beams**L. Hadji^{1,16}, N. Zouatnia², Y. Tlidji¹, A. Kassoul²¹*Département de Génie Civil, Faculté des Sciences Appliquées, Université Ibn Khaldoun, BP 78 Zaaroura, Tiaret, Algérie.*²*Laboratoire de Structures, Géotechnique et Risques, Université Hassiba Benbouali de Chlef, Algérie.*

Abstract: In this paper, a hyperbolic shear deformation beam theory is developed for free vibration analysis of functionally graded (FG) sandwich beams. The theory account for higher-order variation of transverse shear strain through the depth of the beam and satisfies the zero traction boundary conditions on the surfaces of the beam without using shear correction factors. The material properties of the functionally graded sandwich beam are assumed to vary according to power law distribution of the volume fraction of the constituents. The core layer is still homogeneous and made of an isotropic material. Based on the present refined beam theory, the equations of motion are derived from Hamilton's principle. Navier type solution method was used to obtain frequencies. Illustrative examples are given to show the effects of varying gradients and thickness to length ratios on free vibration of functionally graded sandwich beams.

Keywords: Vibration, Sandwich Beam, Shear Deformation, Hamilton's principle

1. Introduction

In recent years, the application of functionally graded (FG) sandwich structures in aerospace, marine, civil construction is growing rapidly due to their high strength-to-weight ratio. There exist two common types: sandwich structures with FG core and sandwich structures with FG skins. With the wide application of FG sandwich structures, understanding vibration of FG sandwich structures becomes an important task.

Analytical solution

The equations of motion admit the Navier solutions for simply supported beams. The variables u_0 , w_b , w_s can be written by assuming the following variations

$$\begin{Bmatrix} u_0 \\ w_b \\ w_s \end{Bmatrix} = \sum_{m=1}^{\infty} \begin{Bmatrix} U_m \cos(\lambda x) e^{i\omega t} \\ W_{bm} \sin(\lambda x) e^{i\omega t} \\ W_{sm} \sin(\lambda x) e^{i\omega t} \end{Bmatrix}$$

¹⁶Corresponding author

E-mail address: had_laz@yahoo.fr

where U_m , W_{bm} , and W_{sm} are arbitrary parameters to be determined, ω is the eigenfrequency associated with m th eigenmode, and $\lambda = m\pi/L$.

Substituting the expansions of u_0 , w_b , w_s from Eqs. (10) into the equations of motion Eq. (8), the analytical solutions can be obtained from the following equations

$$\begin{pmatrix} a_{11} & a_{12} & a_{13} \\ a_{12} & a_{22} & a_{23} \\ a_{13} & a_{23} & a_{33} \end{pmatrix} - \omega^2 \begin{pmatrix} m_{11} & m_{12} & m_{13} \\ m_{12} & m_{22} & m_{23} \\ m_{13} & m_{23} & m_{33} \end{pmatrix} \begin{pmatrix} U_m \\ W_{bm} \\ W_{sm} \end{pmatrix} = \begin{pmatrix} 0 \\ 0 \\ 0 \end{pmatrix}$$

Results and discussion

In this section, various numerical examples are presented and discussed to verify the accuracy of present theories in predicting the free vibration responses of simply supported FG beams. The FG beam is taken to be made of aluminum and alumina with the following material properties:

Ceramic (P_C : Alumina, Al_2O_3): $E_c = 380$ GPa; $\nu = 0.3$; $\rho_c = 3960$ kg/m³.

Metal (P_M : Aluminium, Al): $E_m = 70$ GPa; $\nu = 0.3$; $\rho_m = 2702$ kg/m³.

And their properties change through the thickness of the beam according to power-law. For convenience, the following dimensionless form is used:

$$\bar{\omega} = \frac{\omega L^2}{h} \sqrt{\frac{\rho_m}{E_m}}$$

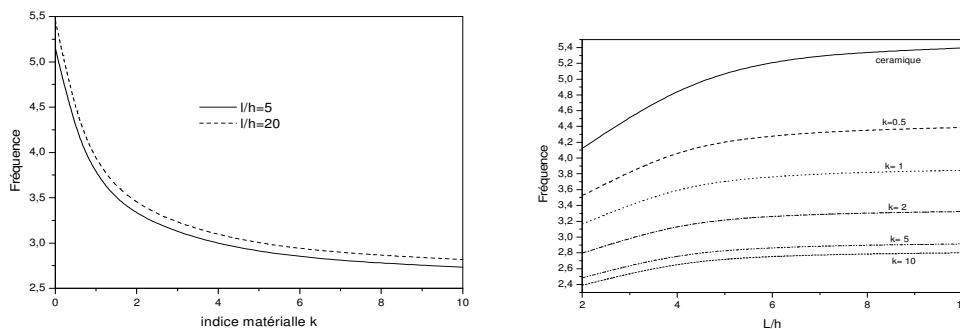


Fig. 2 Variation of fundamental frequencies $\bar{\omega}$ versus the material parameter k for (2-1-2) simply supported FG sandwich beams with homogeneous hardcore. Fig. 3 Fundamental frequency $\bar{\omega}$ as a function of span-to-height ratio L/h of symmetric FGM sandwich beam (2-1-2) with homogeneous hardcore for various values of k .

Conclusions

A new hyperbolic shear deformation theory for the free vibration analysis of FG sandwich beams is developed. The theory accounts for parabolic distribution of the transverse shear strains and satisfies the zero traction boundary conditions on the surfaces of the beam without using shear correction factors. It is based on the assumption that the transverse displacements consist of bending and shear components.

References

- [1] Aydogdu M, and Taskin V. (2007), Free vibration analysis of functionally graded beams with simply supported edges, Mater. Design, 28(5), 1651-1656.
- [2] Sallai B.O., Tounsi A., Mechab I., Bachir B.M., Meradjah M., Adda Bedia E.A. (2009), A theoretical analysis of flexional bending of Al/Al₂O₃ S-FGM thick beams, Comput. Mater. Sci., 44(4), 1344-1350.

A SIMPLE QUASI-3D THEORY WITH FIVE UNKNOWNNS FOR THE STATIC ANALYSIS OF FGM SANDWICH PLATES

A. Hamidi¹, M. Zidour², A. Tounsi³, E. A. Adda Bedia³

1University of Bechar, Department of Civil Engineering, P.O.Box 417 Road of Kenadsa 08000, Bechar, Algeria

2University of Tiaret, Department of Civil Engineering, P.O.Box 78 zaâroura 14000, Tiaret, Algeria.

3University of Sidi Belabbes, Department of Civil Engineering, P.O.Box 89 22000, Sidi-Bel-Abbès, Algeria.

Abstract: In this research, a simple but accurate sinusoidal plate theory for the thermomechanical bending analysis of functionally graded sandwich plates is presented. The main advantage of this approach is that, in addition to incorporating the thickness stretching effect, it deals with only 5 unknowns as the first order shear deformation theory, instead of 6 as in the well-known conventional sinusoidal plate theory. The material properties of the sandwich plate faces are assumed to vary according to a power law distribution in terms of the volume fractions of the constituents. The core layer is made of an isotropic ceramic material. Comparison studies are performed to check the validity of the present results from which it can be concluded that the proposed theory is accurate and efficient in predicting the thermomechanical behavior of functionally graded sandwich plates. The effect of side-to-thickness ratio, aspect ratio, the volume fraction exponent, and the loading conditions on the thermomechanical response of functionally graded sandwich plates is also investigated and discussed.

Keywords: Sandwich plate; thermomechanical; analytical modelling; functionally graded material; stretching effect.

1. Introduction

In recent years, astonishing advances in science and technology have motivated researchers to work on new structural materials. Functionally graded materials (FGMs) are classified as novel composite materials which are widely used in aerospace, nuclear, civil, automotive, optical, biomechanical, electronic, chemical, mechanical, and shipbuilding industries. Due to smoothly and continuously varying material properties from one surface to the other, FGMs are usually superior to the conventional composite materials in mechanical behavior. FGMs may possess a number of advantages such as high resistance to temperature gradients, significant reduction in residual and thermal stresses, and high wear resistance. Since the main applications of FGMs have been in high temperature environments, most of the research on FGMs has been restricted to thermal stress analysis, thermal buckling, fracture mechanics and optimization.

In this article, for the first time, the new four variable refined plate theory is developed for thermomechanical bending of FG sandwich plates. Navier solution is used to obtain the closed-form solutions for simply supported FG plates. The effects of the variation of the volume fractions of the constituent materials and thickness-to-side ratio on the through-the-thickness deflections, in-plane displacements, and axial stress distributions are studied in detail. Numerical results for deflections and stresses are investigated. Numerical examples are presented to illustrate the accuracy and efficiency of the present theory by comparing the obtained results with those computed using various other theories.

* Corresponding author

E-mail address: hamidiahmed82@yahoo.fr

Problem formulation

Consider the case of a uniform thickness, rectangular FG sandwich plate composed of three microscopically heterogeneous layers referring to a rectangular coordinates (x, y, z) . The top and bottom faces of the plate are at $z = \pm h/2$, and the edges of the plate are parallel to axes x and y .

The sandwich plate is composed of three elastic layers, namely, "Layer 1", "Layer 2", and "Layer 3" from bottom to top of the plate (Fig. 1).

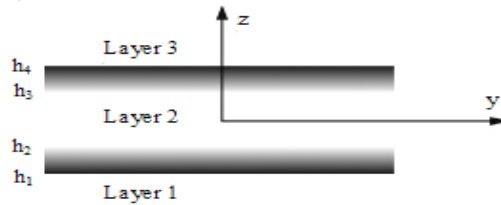


Fig. 1. The material variation along the thickness of the FG sandwich plate.

Numerical Results

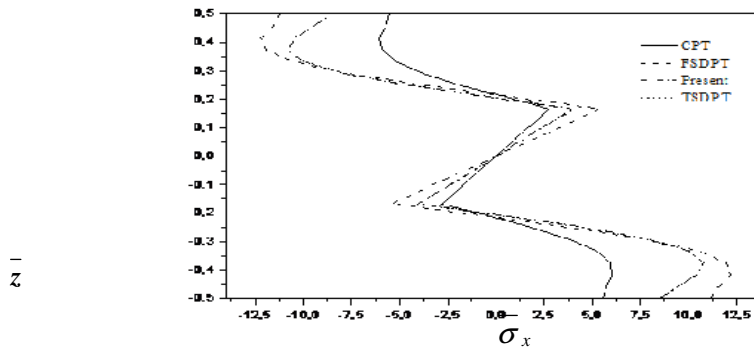


Fig. 2. Comparison of the variation of nondimensional axial stress $\bar{\sigma}_x$ across the thickness of symmetric and nonsymmetric FG sandwich plates ($k=1.5$) by applying different shear deformation theories.

3. Conclusions

In this paper, a new four variable refined plate theory (RPT) has been developed to investigate for the first time the thermomechanical behavior of simply supported FG sandwich plates. Unlike any other theory, the theory presented gives rise to only four governing equations resulting in considerably lower computational effort when compared with the other higher-order theories reported in the literature having more number of governing equations. The results of the shear deformation theories are compared together. Hence, it can be said that the proposed theory RPT is accurate and simple in solving the thermomechanical bending behavior of FG plates.

References

- [1] Reddy J. N. (2000), Analysis of functionally graded plates, *Int. J. Num. Methods Eng.*, 47: 663-684.
- [2] Cheng Z.Q. and Batra R.C. (2000), Deflection Relationships Between the Homogeneous Kirchhoff Plate Theory and Different Functionally Graded Plate Theories, *Archives of Mechanics*, 52(1): 143-158.
- [3] Vel S.S. and Batra R.C. (2002), Exact Solution for Thermoelastic Deformations of Functionally Graded Thick Rectangular Plates, *AIAA Journal*, 40(7): 1421-1433.

DESIGN AND ANALYSIS OF TWO GANTRIES IN STEEL STRUCTURES

O. Belaidi^{1*}, F. Taouche-kheloui¹, Kh. Iftene, M. Almansba¹, N.E Hannachi¹
1University of Tizi Ouzou, LAMOMS Lab. Hasnaoua II, 15000, Tizi-Ouzou Algeria.

Abstract: This work is a comparative study between two gantries made with a steel-concrete mixed specific assembly system. The first assembly of conventional structure, for the second, composite steel-concrete. The gantries are made of tubular steel columns. The first assembly is carried out with metallic reinforcing plates providing the connection between the columns and beams; the second consists of assemblies of conventional plates. For this, we used a local approach by modeling the loading gantries requested by the form of horizontal displacement. Calculations are performed using the numerical model "concrete damage plasticity" for concrete. The model is defined by a nonlinear behavior law. The numerical model used for steels is the elastic-plastic model linear hardening. Both models are implanted into the calculation software finite element "ABAQUS". The models used to visualize the damage and determine the mode of failure.

Keywords: Simulation, gantry, finite element, damage, stresses, assembly.

1. Introduction

Two models are studied. The first model is a gantry made with tubular steel columns filled with concrete (concrete steel model (CSM)). The second model, reference model, only made with tubular steel columns (steel model (SM)) [1, 2, 3,4, 5].

2. Numerical simulation

Both models are acted upon by a horizontal force imposed at the top of each gantry and a static explicit boundary condition at the base. Steel is modeled using an elas-toplastic behavior with isotropic hardening based on the three-dimensional criterion of Von Mises stresses. An elastic-plastic behavior is used to model the behavior of concrete. The models are implemented in the finite element code ABAQUS [6]. The force displacement curve for the two models is given in Figure 1. Figure 2 shows the stress-strain curve at the base of both models.

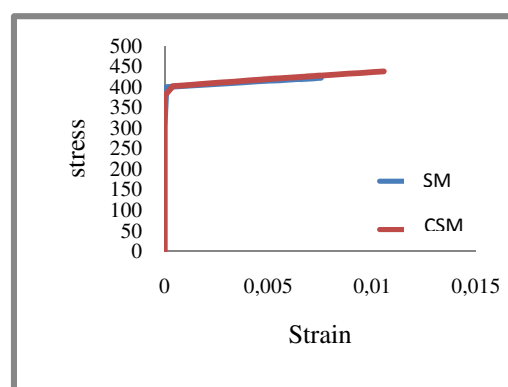


Fig. 1. Curve strains stresses at the base of the two models (CSM, SM)

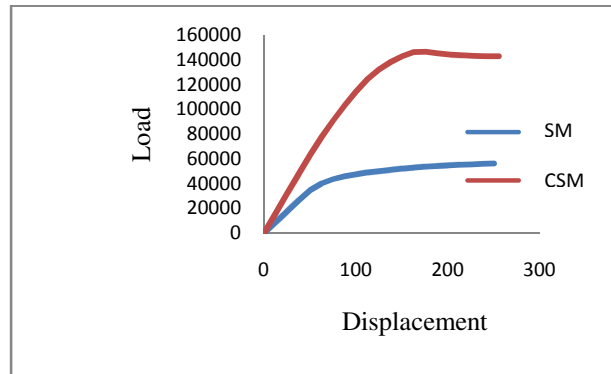


Fig. 2. Load-displacement curve of the two models (CSM, SM)

3. Conclusions

The model without concrete (SM) has a ductile behavior in relation to the concrete model (CSM). It is found that the concrete improves the behavior of the frame in terms of stiffness, load bearing capacity and ductility.

References

- [1] M., Landowski, B., Lemoine, 2005. Concevoir et construire en acier.
- [2] A.K., Kim, G.D., Loughheed, 1997. *Rapport CNRC- Institut de recherche en construction du Conseil national de recherches*. CNRC- Conseil national de recherches du Canada ISSN 1206-1239.
- [3] N., Haouam, 2010. System for building in steel-reinforced concrete; "WO/2010/048966.
- [4] R., Mbelounis 2008. Mémoire de magister en génie civil. Etude de la performance des poteaux mixtes Acier-Béton Sous différentes sollicitations.
- [5] R., Maquoi Dubruykere, J.F., Demonceau, et Lincy, 2005. Guide de construction métallique (construction mixte)
- [6] M., Abbas, 2005. Présentation du logiciel ABAQUS Principes et fonctionnement, Université de Technologie de Compiègne Laboratoires Roberval /UMR UTC- CNRS.

POLY-SILICON FOR HETEROJUNCTION SOLAR CELLS BASED ON NUMERICAL SIMULATIONS

N. Ziani¹, M.S Belkaid¹, R. Zedek¹, O.Boussoum¹, F.Bouaraba¹

1Universite Mouloud MAMMERI of TiziOuzou, Campus Hasnaoua BPN17, TiziOuzou, Algeria

Abstract: In order to give a real understanding and realization of all the phenomena occurring inside the photovoltaic cell devices, the development of a reliable simulated model first is also essential. In this paper simulation study with the design evaluation of ZnO/p-cSi and ZnO/p-polySi heterojunction solar cells using two dimensional numerical computer aided design tool (TCAD). A program in ATLAS simulator from SILVACO international has been developed. The device performance is evaluated by implementing special models (i.e., surface recombinations, interface traps, thermionic field emission tunneling model for carrier transport at the heterojunction etc) at the semiconductor-semiconductor interfaces. A current density of 27.19 mA/cm², open circuit voltage of 0.47 V and fill factor of 66.10 % was achieved for ZnO/p-polySi heterojunction. Contrary to ZnO/p-cSi structure, ZnO/p-polySi heterojunction shows height photovoltaic response and low Isc. Simulation results gives dark current of the order of 10⁻⁸ A for both heterojunction solar cells.

Keywords: simulation, solar cell, ZnO-polySi, heterojunction, atlas silvaco.

1. Introduction

Poly-crystalline silicon solar cell modules currently represent between 80% and 90% of the PV world market resulting from the stability, robustness and reliability of this kind of solar cells compared to those of emerging technologies. Polycrystalline silicon solar cells are considered to be one of the most promising alternatives to bulk crystalline silicon solar cells, decrease the cost of crystalline silicon wafers significantly. With the purposes of reducing the cost further and promoting the performance of heterojunction solar cells, the heterojunction based ZnO/p-polySi solar cell is proposed and simulated. Proposed solar cell has a wide band gap Zinc oxide (ZnO) deposited on polysilicon to form a heterojunction. With a wide bandgap, high transparency and low resistivity material, ZnO can be used as a window layer and simultaneously heterojunction partner for heterojunction based solar cells [1 -2]. Note that the ZnO/Si based heterojunction solar cells can efficiently collect the solar light through the double band structure: high energy photons in the ultraviolet region can be absorbed by ZnO while low energy photons in the visible range collected at the depletion region of Si after they transmit through ZnO layer. The main purpose of this work is to thoroughly investigate the design investigation of ZnO/p-polySi based heterojunction solar cells compared with ZnO/p-cSi solar cell using two dimensional numerical simulation and the true potential of ZnO/p-polySi heterojunction solar cells.

2. Device simulation and results

A simulation program for proposed ZnO/Polysilicon heterojunction solar cell structure has been developed in ATLAS simulator from SILVACO international. Fig.1 shows the structure of the ZnO/Polysilicon hetero-structure. Light is assumed to be falling from the top of the heterojunction. After defining the physical structure of device, material properties of ZnO and poly-Si has been defined. The simulation results of ZnO/p-polySi heterostructure solar cells has been presented and the results of the solar cells are compared with ZnO/c-silicon solar cell. ZnO/p-cSi solar cell shows superior results as compared to ZnO/p-polySi solar cell because the polysilicon have less conduction due to dislocation of atoms and crystalline silicon has high conductivity as compared to polysilicon.

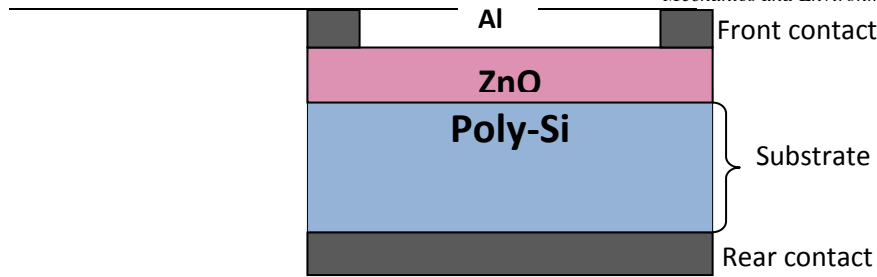


Fig. 1. Schematic representation of the sample structure.

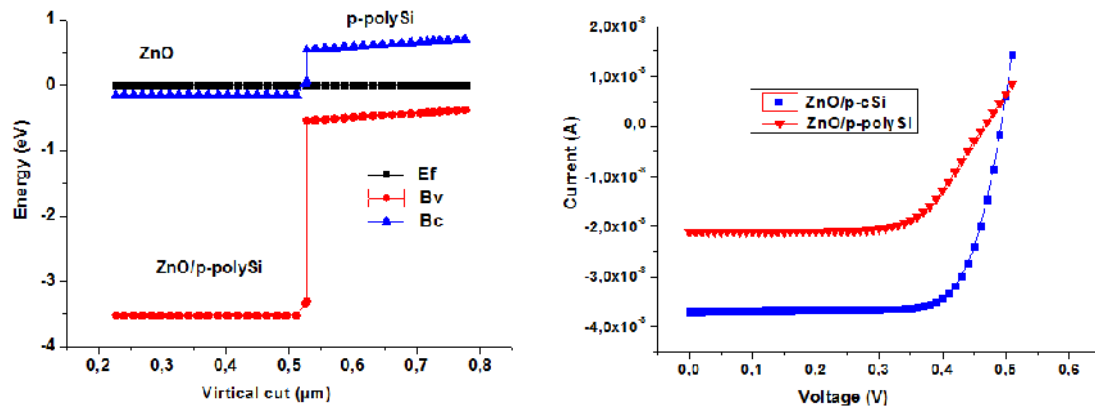


Fig. 4. Photocurrent spectra of the heterojunction solar cells.

3. Conclusions

A theoretical design assessment using two dimensional numerical simulations for ZnO/Si heterojunction structures is presented. The ZnO/p-polySi device exhibits the open-circuit voltage, short-circuit current density and fill factor of this device are 0.47 V, 27.19 mA/cm², 66.10 % and 8.48 %, respectively. ZnO/p-polySi heterojunction shows height photovoltaic response and low I_{sc} because the height absorption at the atoms dislocation for the polysilicon. Therefore, our study on the device formed by the ZnO/p-polysilicon is very significant in exploring the high efficiency poly-silicon solar cell.

The proposed ZnO/p-polySi based heterojunction solar cell shows great potential alternative from the viewpoint of performance efficiency, simple and low temperature processing steps and hence low cost candidate.

References

- H. H. Afify et al., (2005), Egypt. J. Solids, Vol. 28.
 Tingfang Yen et al., (2006), 4th photovoltaic energy conversion conference.

THE INFLUENCE OF THE METHODS OF PREPARATION ON THE TEXTURAL AND STRUCTURAL PROPERTIES OF THE TITANIUM DIOXIDE

A.Mennad^{1*}, A.Mahiout²

*1*Unité de Développement des Equipements Solaires, UDES / Centre de Développement des Energies Renouvelables, CDER, Bou-Ismaïl, 42415 Tipaza, Algeria.

*1**E-mail: .mennad.abdelkader@udes.dz

2 Helsinki Metropolia University of Applied Sciences, P.O. Box 4071, FI-00079 Metropolia, Finland.

Abstract: Titanium dioxide has a wide range of applications depending on its textural and structural characteristics. Two types of titanium dioxide powder are prepared, xerogel and aerogel, using respectively the incipient wetness impregnation and the extraction of the organic solvent in the autoclave at the hypercritical conditions. The physical characteristics and the crystalline structure of the titanium dioxide powder are related to the technique used for the preparation. The aerogel powder presents some physical characteristics more interesting in application as catalyst.

Keywords: Titanium dioxide, anatase, rutile, photocatalysis, textural and structural properties, aerogel, xerogel.

1. Introduction

The semiconductor character of the crystalline nanoparticles of the titanium dioxide is of great interest of research for various principal technological applications such as the photocatalysis [1, 2], electronics [3], pharmacy [4], optics [5], paper industry, environmental depollution [6]. In addition to its extremely interesting photocatalytic properties, it is also used as a catalytic support to improve the textural properties of catalyst in chemical reactions [7-9]. There exist several modes of preparation of titanium dioxide particles corresponding to the classical techniques of aerosol and aerogel [8], or with the advanced techniques such as PVD [10], CVD [10, 11], electrochemistry [10]. The technique used depends on the scope of application of the titanium dioxide particles. The present study is to highlight the influence of the modes of preparation of aerosol and aerogel on the textural and structural properties of the titanium dioxide for applications in catalysis or photocatalysis. The characterizations are carried out after the preparation of the aerogel and the commercial aerosol Degussa P 25.

2. Preparation and characterization of the titanium dioxide

The titanium dioxide aerogel is prepared using an autoclave SAE (Société Autoclave Engineers). It is a cylindrical form device of a volume of one liter, which can function until a temperature of 350°C and a pressure of 340 bar. The heating is ensured by an electric oven. Programming of the temperature ensures a linear rise of this one. A pyrex container of a volume of 340 cc containing the gel dispersed in an organic solvent is put in the autoclave which contains a complementary volume (q.s.p. 500 cc) of same solvent necessary to reach the hypercritical conditions of this solvent. The device is closed, then purged with nitrogen. The oven is then put in heating until reaching the hypercritical parameters of the solvent (temperature, pressure) which are maintained approximately 30 minutes. The solvent is then evacuated very slowly in order to avoid the training of the solid. When the evacuation is finished, the device is purged with dry nitrogen so that cooling is done under anhydrous and inert atmosphere. Chemicals: Orthotitanate of butyl – FLUKA product, density = 1; Methanol R.P. NORMAPUR- PROLABO product, purity 99,8%, (H₂O < 1 %), Pb, Cu, Ni, Zn, Fe = 0.1 ppm; Nitrogen R – L' AIR LIQUIDE, purity 99,995%; Deionised water.

Heat treatments under O₂ 500 °C 2 h, and H₂ 500 °C 15 h, are carried out separately on the aerogel TiO₂(A) and the aerosol Degussa P25 in order to analyse the evolution of their structure with the X-rays diffraction and to relate the results to the modes of preparation of the aerosol (xerogel type) and aerogel.

Table 1: Crystalline phases and mean size of the titanium dioxide particles of the aerosol Degussa P25 (xerogel) and the aerogel TiO₂(A)

Solid B.E.T surface area	Crystalline phase	Mean size of particles, (Å)		
		After preparation	O ₂ 500 °C 2 h	H ₂ 500 °C 15 h
Aerosol Degussa P25 50 m ² /g	Anatase	203	244	253
	Rutile	291	331	319
Aerogel TiO ₂ (A) 121 m ² /g	Anatase	94	90	152

3. Conclusions

The preparation of aerogels by extraction under the hypercritical condition of the organic solvent contained in the gel solution has the characteristic to obtain solids with a large specific surface area that any other technique can reach easily. Moreover, the single crystalline phase of anatase obtained with the aerogel makes it possible to proceed research studies for other applications implying intermediate phase to the nonreversible rutile phase. The preparation of aerogel makes it possible to obtain a powder with a large specific surface area which is one of the m properties of a catalyst or a catalytic support used in a chemical reaction.

References

- [1] S. Craig, Turchi and David F. Ollis, *J. Catal.* 122 (1990), 178-192.
- [2] A. Fujishima, Donald A. Tryk, *Energy Carriers and Conversion Systems- Vol. I Photochemical and Photoelectrochemical Water Splitting.*
- [3] Kai-Liang Zhang, Chang-Qiang Wu, Fang Wang, Yin-Ping Miao, Kai Liu, Jin-Shi Zhao. *Optoelectronics Letters*, vol.9, 4 (2013), 263-265.
- [4] Cuong Phan Huu, Influence des propriétés morphologiques et structurales de TiO₂ pour la destruction de cellules cancéreuses, (2012-2013). Laboratoire des Matériaux Surfaces et Procédés pour la Catalyse UMR 7515 CNRS/ECPM/Uds, Strasbourg.
- [5] Claire Duchesne, Université Sciences et Technologie-Bordeaux I, Thèse (26-11-1993).
- [6]- Patrice Blondeau, Abadie Marc, Communication, Observatoire de la Qualité de l'Air Intérieur (OQAI- juin 2012).
- [7] Jimmie G. Edwards, Julian A. Davies, David L. Boucher, Abdelkader Mennad. *Angew. Chem. Ed. Engl.* 31 (1992), No. 4, 480-482.
- [8] Abdelkader Mennad, Thèse no. 520 (1986), Laboratoire de Thermodynamique et Cinétique Chimiques, Univ. Claude Bernard, Lyon I.
- [9] David L. Boucher, Julian A. Davies, Jimmie G. Edwards, Abdelkader Mennad. *J. Photochem. and Photobiol., A: Chem.* 88 (1995) 53-64.
- [10] Xiaobo Chen and Samuel S. Mao, *Chem. Rev.* 2007, 107, 2891-2959.
- [11] Christos Sarantopoulos. Thèse no. 2523 (19 octobre 2007), Institut National Polytechnique de Toulouse, Ecole doctorale : Matériaux-Structure-Mécanique.

NATURAL CONVECTION IN A CAVITY SIMULATING A THERMOSYPHON

A. BENNIA^{*1}, S. RAHAL², A. KHELIL¹, G. MEBARKI² and L. LOUKARFI¹

¹ *Laboratoire de Contrôle, Essai, Mesure et Simulation Mécaniques, Université Hassiba Benbouali de Chlef, Hay Salem, route nationale N° 19, 02000, Algérie.*

² *Laboratoire L.E.S.E.I, Département de Mécanique, Faculté de Technologie, Université Hadj Lakhdar de Batna, rue Boukhlouf Med el Hadi, 05000 Batna, Algérie.*

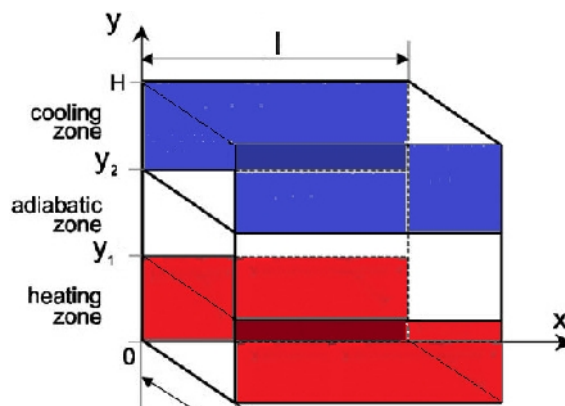
Abstract: In this work, we present a numerical study of natural convection in a vertical rectangular enclosure simulating a thermosyphon. The governing equations have been solved by a numerical approach based on the finite volume method using the fluent code. An initial validation was conducted by comparing our results with those of other authors. Thereafter, has been varied as well as the material of the solid walls as well. We considered the influence of the parameters mentioned above on the temperature fields, the heat flux density and the average Nusselt number. The optimal conditions that allow obtaining maximum heat transfer rates have been determined.

1. Problem description

The schematic configuration Studied is shown in Figure (1). It is a rectangular cavity of height (H), length (l) and thickness (e) filled with Silicone oil. The dimensions of the cavity are: 100 mm x 100 mm x 5 mm.

Walls localized in [1]:

$[z = 0 \text{ and } e, 0 \leq x \leq 1, 0 \leq y \leq y_1 \text{ and } y_2 \leq y \leq H]$ are subjected to conditions of Dirichlet temperature while the other walls are kept adiabatic (Neumann conditions $Q = 0$) [2].



The boundary conditions associated with the problem are:

- Dirichlet conditions

$T = T_h$ if $z=0$ and $e, 0 \leq x \leq 1, 0 \leq y \leq y_1$ corresponding to the heating zone.

$T = T_c$ if $z=0$ and $e, 0 \leq x \leq 1, y_2 \leq y \leq H$ corresponding to the cooling zone.

- Neumann conditions

All of the other parts of the surfaces are adiabatic.

2. Results

In the present work, the results of section I. Ishihara et al. [2] were used. For this, we considered the same conditions (the silicon oil used as a working fluid, rectangular cavity dimensions (100mm x 100mm x 5mm), laminar, the temperature difference, ΔT , between the

heating and cooling surfaces is $1K$, $Pr = 212$ and $Ra = 1,95,10^5$) than I. Ishihara et al. [2] who obtained numerical results (Figure 2-a) and experimental (Figure 2-c).

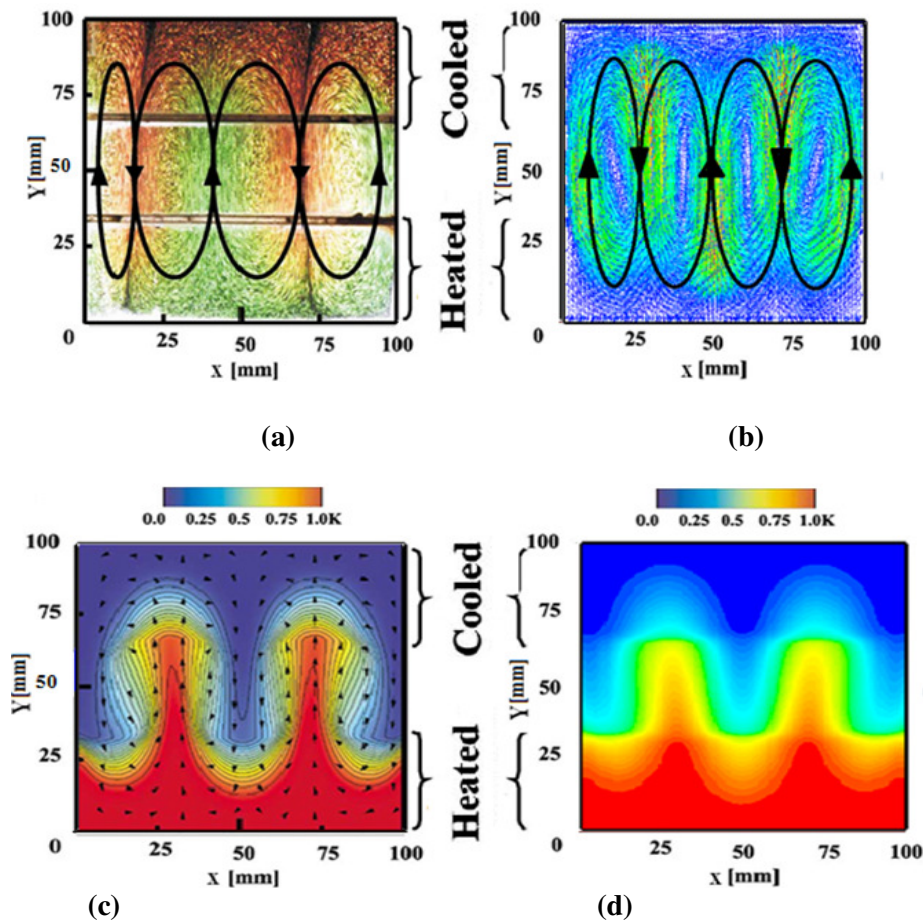


Fig. 2. Comparison of results for $Pr = 212$ and $Ra = 1,95.10^5$. (b), (d) study. (a), (c): results of I. Ishihara et al [2].

Based on these figures, we note that our results are in good qualitative agreement with those presented in [2]. So our numerical simulation procedure was validated by comparison with experimental and numerical results of the work contained in the reference [2].

3. Conclusions

In this study, we conducted a parametric numerical study of natural convection in a square cavity with baffle was also conducted. a detailed study with mercury as convective fluid was conducted. Mercury has been chosen because it allows for the greater density of thermal flux in both cases (with or without fins). To show the influence of the nature of the solid on the walls of the cavity, we compared the plexi-glass and the steel for the same dimensions of the cavity and the same temperature gradient. There after a study to show the influence of a vertical temperature gradient in the heat flux was also conducted.

References

- [1] M. Chaour, Interaction des structures tourbillonnaires avec la couche limite dans une cavité différentiellement chauffée, mémoire de magister, *Université Mentouri-Constantine* 2010.
- [2] I. Ishihara, T. Fukui and R. Matsumoto, Natural convection in a vertical rectangular enclosure with symmetrically localized heating and cooling zones, *Int. J. of Heat and Fluid Flow*, 23, 366-372,

EXPERIMENTAL THERMAL STUDY OF TURBULENT JET SWIRLING: APPLICATION IN THE HVAC SYSTEMS

A. BENNIA^{1*}, L. LOUKARFI¹, A. KHELIL¹, H. FELLOUAH², M. BRAIKIA¹ and Y. BOUHAMIDI¹

¹*Laboratoire de Contrôle, Essai, Mesure et Simulation Mécaniques, Université Hassiba Benbouali de Chlef, Hay Salem, route nationale N° 19, 02000, Algérie.*

²*Department of mechanical engineering, Université de Sherbrooke, 2500 boul. Université, Sherbrooke, Québec, Canada*

Abstract: Research into the physics of mixing and the mechanisms for enhancing mixing is necessary for many engineering applications. During the past decades, it has become clear that an enormously powerful mechanism for enhancing flow mixing is the generation of streamwise vortices in a mixing flow by using some vortex generators such as swirling nozzles. In order to improve the air diffusion efficacy at least cost taking account of the esthetic aspect in the design of the air diffusion terminal units, we found a «passive» mean which consists of blowing the jet through the swirl nozzle. In this work, we present an experimental study of a turbulent jet issued from a swirling diffuser applied to new air diffusers for heating, ventilating, air conditioning (Heating, Ventilation and Air Conditioning “HVAC”) systems. We noted that the swirling jet with angle of inclination 60° ensures better expansion radial of temperatures relative to the lobed jet. The swirling jet saw his advantage the expansion point of view would be more appropriate in the case of large volumes.

1. Introduction

In order to improve the air diffusion efficacy at least cost taking account of the esthetic aspect in the design of the air diffusion terminal units, we found a «passive» mean which consists of blowing the jet through the swirl diffuser. Concerning the applications, they are numerous: heating, ventilation and air conditioning used in habitation [1, 2]. They are also used in the combustion domain and in the design of injectors offering good combustion stability [3, 4, 5, 6]. The mixing improvement by Passive control is of wide practical interest. This type of control enables the improvement of the air diffusion in the building [7]. To ensure the occupant’s comfort, the blowing velocities and temperatures should be homogeneous, which is not ensured by the classical terminal units. The principal objective of this study is to establish, the distribution of the temperatures, experimentally, for a configuration of a jet from a swirling diffuser. This type of flow has been studied in sight of its application to the ventilation of the residential premises.

2. Test experimental assembly and working conditions

The experimental assembly is essentially designed to generate an air jet from a lobed diffuser. The experiments have been carried out in a room of a length of 3.0 m, a width of 2.5 m and a height of 2.5 m. These dimensions enable to carry out tests at a vertical free and hot jet conditions with unfavorable pressure forces. The room has been isolated from the exterior environment during experiments. Because of the absence of the room walls thermal control the temperature was not maintained constant. The temperature difference between the jet and the environment is then controlled by readjustment of the blowing air jet temperature. Consequently, the Archimedes number of the jet is conserved during the experiments. The installation is composed of a chassis on which the blowing device is fixed (Figure 1). This latter contains a hot air blowing diffuser oriented towards the bottom. The flow temperatures and velocities are measured with a multifunctional thermo-anemometer. The probe is supported by a stem guides vertically and horizontally in order to sweep the maximum space. The thermal sensor precision is ± 0.5 °C. A digital thermometer is placed outside the flow in the test room in order to enable the instantaneous measurement of the ambient temperature

(T_a). The experimental devices for measurement in the free mode are represented on figure 1. The ambient temperature T_a , the jet temperature T_i and velocity U_i at different points are taken simultaneously.

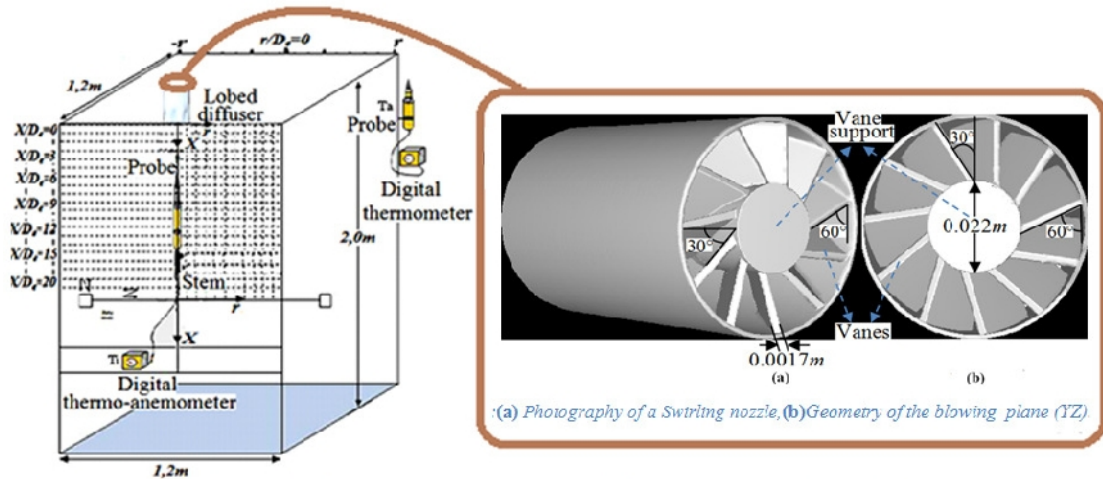


Figure 1 : Schematic description of the experimental installation.

Figure 1 shows a swirl nozzle composed of eleven aluminum vanes arranged on an aluminum holder of a diameter d equal to 0.022 m . In order to achieve a vortexing effect, the vanes are oriented at inclination angles α_a of 30° and α_b of 60° with respect to the jet axis and the plane of blow, respectively. The vanes are arranged such that they are connected to a fixed support (support fins), behind which develops a recirculation zone whose length depends on the blowing device having a diameter D_e (D_e refers to the diameter of the origin of the blow).

3. Conclusion

To ensure the occupant's comfort, the residences temperatures and blowing velocities should be homogeneous, which is not guaranteed by simple air diffuser of the classical terminal units. We noted that the swirling jet with angle of inclination 60° ensures better expansion radial of temperatures. The swirling jet saw his advantage the expansion point of view would be more appropriate in the case of large volumes.

- [1] Dia A., « Simulation de jets d'air lobés pour l'optimisation des Unités Terminales de Diffusion d'Air », *Université de La Rochelle, Doctorat en sciences*, 2012.
- [2] Dimotakis P.E., « The mixing transition in turbulents flows », *Journal of Fluid Mechanics*, 2000. **409**: p.68-69.
- [3] Meslem A., Nastase I., Allard F., « Passive mixing control for innovative air diffusion terminal devices for buildings », *Building and Environment*, 2010. **45**: p. 2679-2688.
- [4] Meslem A., Elhassan M., Nastase I., « Analysis of jet entrainment mechanism in the transitional regime by time-resolved PIV », *Journal of Visualization*, 2011. **14**: p. 41-52.
- [5] Elhassan M., Meslem A., Abed-Meraïm K., « Experimental investigation of the flow in the near-field of a cross-shaped orifice jet », *Phys of Fluids*, 2011. **23**: p.16.
- [6] Nastase I., Meslem A., Iordach V., Colda I., « Lobed grilles for high mixing ventilation - An experimental analysis in a full scale model room », *Building and Environment*, 2011. **46**: p. 547-555.
- [7] Meslem A., Bode F., Nastase I., Martin O., « Optimization of lobed perforated panel diffuser: numerical study of orifice geometry », *Modern Applied Science*, 2012. **6**(12): p59.

NUMERICAL INVESTIGATION OF HEAT TRANSFER ENHANCEMENT INSIDE A PARABOLIC TROUGH SOLAR COLLECTOR USING GEOMETRICAL MODIFICATION AND HYBRID NANOFLUID.

A. Benabderrahmane*, A. Benazza, M. Aminallah, S. Laouedj.
Faculty of Technology, Djilali Lyabes University, Sidi Belabbes. Algeria.

Abstract: Three dimensional numerical investigation of heat transfer enhancement in a non-uniformly heated parabolic trough solar collector using several passive techniques under turbulent flow was incorporated in the current paper. The governing equations were solved using the finite volume methods (CFD) with certain assumptions and appropriate boundary conditions. The Monte Carlo ray trace technique was applied to obtain the heat flux distribution around the absorber tube. The numerical results were validating with the empirical correlations existing in the literature and good agreement was obtained. The present results demonstrate that the inclusion of inserts provide a good performance in heat transfer, also the receiver temperature gradient are shown to reduce with the use of geometrical modification, the inserts have a remarkable effect on the HTF velocity distribution. Heat transfer enhancement increases with combining different kinds of nanoparticles with several volume fractions; however it was accompanied by increasing skin friction coefficient.

Keywords: numerical investigation; parabolic trough solar collector; heat transfer enhancement; Monte Carlo ray trace technique; passive techniques; hybrid nanofluids.

1. Introduction

Heat transfer enhancement is an active and important field of engineering research. Many studies are carried out to improve the heat transfer following both numerical and experimental methods. Heat transfer achievement techniques are typically classified into three categories: active techniques, passive techniques and compound techniques in which two or more passive or/and active techniques are employed together.

The aim of this numerical investigation is to estimate the convective heat transfer enhancement in the fully developed turbulent flow under a non-uniform heat flux using two different methods; the first is the use of geometrical modifications by several inserts type; the second is the utilization of nanofluids using the mixture two-phase model and the study of the combination of two or more different nanoparticles, the results of these studies are presented in the form of Nusselt numbers and Darcy friction factor.

2. Model description

In this work; we have considered a simplified model of the parabolic trough receiver in which the effect of the central rod and other supports is considered negligible. A detailed schematic diagram of the receiver is presented in Fig. 1. The principal objective of this paper is to improve heat transfer inside PTC receiver using simple geometrical mechanisms by incorporating longitudinal inserts in the absorber tube which are easily realizable in the industry

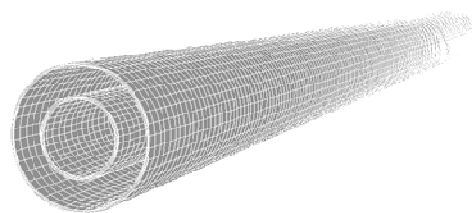
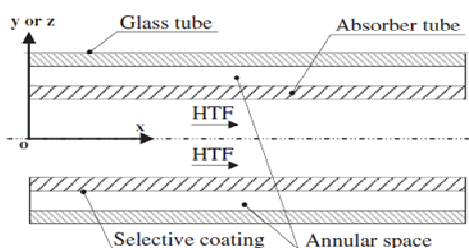


Fig.1. Schematic of longitudinal section of the receiver

3. Effect of using inserts inside the absorber

The numerical results illustrate that the enhancement of the average Nusselt number with Reynolds number due to the presence of inserts, for all models Nu increases with increasing Re. As can be noticed, the solution of the absorber with insert fins retrieves a higher Nusselt number compared to the smooth tube model. On the other hand, the friction factor augments likewise; the higher values are the results of the swirling flow induced by the longitudinal inserts. The results show also that the inserts have a remarkable effect on HTF temperature distribution, absorber temperature and HTF velocity distribution.

4. Effect of using nanofluid as HTF

For the present study, we used two-phase mixture model which solves the mixture momentum equation as well volume fraction transport equation for each secondary phase. The results demonstrate that the use of nanoparticles produces an interesting heat transfer improvement, furthermore transfer enhancement was increasing with the combination of two or three different type of nanoparticles however it was accompanied by increasing wall shear stress values.

5. Conclusion

Three-dimensional numerical simulation on enhancing heat transfer in a non-uniformly heated parabolic trough solar collector under turbulent flow by using multiple passive techniques is performed in this paper. The following conclusion can be drawn:

The Nusselt number for absorber fitted with inserts increases by around 104 to 190%.

The skin friction coefficient of tube with inserts augments 1.14 to 1.45 times compared to the smooth tube.

The heat transfer enhancement is strongly dependent to the geometric parameters of inserts.

The PEC ranges from 1.1 to 1.5 shows that the augmentation of heat transfer can cover the penalty of increased flow resistance and this is a sign of good performance in heat transfer enhancement.

Combining two or more inserts provide better heat transfer.

The inserts have remarkable effects on HTF temperature, on the inner wall absorber temperature distribution and on HTF velocity.

The inclusion of nanoparticles produced an interesting increase of the heat transfer with respect to that of the base liquid.

The Nusselt number is responsive to material type of nanoparticles used.

Heat transfer enhancement was increasing with the combination of two or three different type of nanoparticles however it was accompanied by increasing wall shear stress values.

The mixture conductivity increases with increasing the metallic nanoparticles volume fraction.

SIMULATION STUDY OF THE SURFACE AERATOR POWER FOR THE CHLEF SEWAGE STATION

D. Aoumeur, B. MadjidMeriem

aL.R.M, Mechanical Engineering Department, University of Chlef PO. Box 151, Chlef 02000 Algeria
bal-pha@hotmail.fr

Abstract: The present work is to investigate the sewage flow in the Chlef station through the three-dimensional. Studying the flows in single phase for the surface aerator case allows to calculate the power consumed during the treatment operation. The CFD (Computational Fluid Dynamics) is one of important method to study this phenomenon where it can show the mesh in the critical zone of the wall with high accuracy. The choice of boundary conditions is very interesting to develop many parameters such as the station geometry, velocity of sewage, regime of flow and the rheological behavior.

Keywords: Basin, surface aerator, single phase, Modeling, Chlef station.

GLASS FORMING ABILITY AND CRYSTALLIZATION BEHAVIOR OF NICKEL-BASED AMORPHOUS ALLOY MEMBRANES FOR HYDROGEN SEPARATION BY ELECTRONIC AND CALORIMETRIC MEASUREMENTS

B. Smili¹, M. Mayoufi¹, I. Kaban^{2,3}, J. G. Gasser⁴

*1*Laboratory of Inorganic Materials Chemistry, Chemistry Department, University Badji Mokhtar of Annaba, BP: 12, Algeria

2 IFW Dresden, Institute for Complex Materials, P.O. Box 270116, 01171 Dresden, Germany

3 TU Dresden, Institute of Materials Science, 01062 Dresden, Germany

4 Université de Lorraine, Institut de Chimie, Physique et Matériaux, Laboratoire de Chimie et Physique Approches Multiéchelles des Milieux Complexes LCP-A2MC, 1 boulevard Arago, 57078 cedex 3 Metz, France

*Corresponding author: smili.billel@yahoo.fr

Abstract : The future energy will slowly shift from fossil fuels to green sustainable energy solutions, such as hydrogen energy. Hydrogen fuel is a revolution in the energy future of the world due to their high ability to convert into electricity, heat or motive power based on their end use. The separation of hydrogen through the amorphous membranes from contaminant gases such as carbon dioxide (CO₂) and methane (CH₄) becomes very important for the production of energy. In recent years, amorphous alloy membranes Ni-Zr and Ni-Nb-Zr based alloys have been proposed to overcome the low cost of Pd-based alloys for hydrogen separation, and having excellent hydrogen permeation properties. Thermal and structural behavior studies of amorphous alloy membranes for the separation of hydrogen are focused on adapting and optimizing their functional properties for industrial applications. The thermal stability of the amorphous state is a very important factor for the use of amorphous membranes at high-temperature. The operating temperature of amorphous alloy membrane is influenced by the glass transition temperature T_g and the crystallization temperature T_x, that must be studied to have clear and precise information on the behavior and the scope of these membranes, in order to prevent this crystallization phenomenon. In this paper, the thermal stability, structural changes and electronic properties of Ni₆₀Nb₂₀Zr₂₀ hydrogen-selective alloy membrane will be characterized by electrical resistivity, absolute thermoelectric power, Differential scanning calorimetry (DSC), X-ray diffraction (XRD), and by scanning electron microscopy (SEM). A very good agreement between the phase transition temperatures determined using different techniques has been determined. Thermal stability and crystallization kinetics of Ni₆₀Nb₂₀Zr₂₀ amorphous alloy were evaluated under isothermal and non-isothermal conditions by using electrical resistivity measurements. From TER data it was found that the Ni₆₀Nb₂₀Zr₂₀ metallic glass has a wide supercooled liquid region of 63 K and high activation energy of crystallization E_x evaluated from four measurements of resistivity as a function of temperature with different heating rate (0.5, 2.5, 5 and 10) °C/min, is determined to be 510,2 kJ/mol and 498,6 kJ/mol using the Kissinger and Ozawa equations respectively. This demonstrates the very high thermal stability of this glassy alloy. The isothermal crystallization process of the melt-spun Ni₆₀Nb₂₀Zr₂₀ amorphous alloy described by the Johnson-Mehl-Avrami equation, and the Avrami exponents obtained are in the range of 2.17 to 2.41 with an average value of n = 2.26. This indicates that the crystallization process is basically characterized by the three-dimensional diffusion-controlled crystal growth with an increasing nucleation rate. In the isothermal process the activation energy, calculated by the Arrhenius equation decreases as the volume fraction converted between 10 % and 90 %, and giving an average value of E_x = 427.2 kJ/mol. The crystal structure and the morphology in the raw state and after thermal treatment have been investigated by X-ray diffraction (XRD) and scanning electron microscope (SEM).

Key words: Metallic glass, Thermal stability, Electronic transport properties.

Three dimensional numerical simulations of fluid flows generated by anchor stirrers

Y.KAMLA¹, H.AMEUR^{2,*}, A.HADJEB³, D.SAHEL³

¹Department of Science and Technology, Faculty of Technology, Hassiba Ben Bouali's University, Chlef, Algeria

²Department of Technology, Institute of Science and Technology, Ahmed Salhi's University Center, Ctr Univ Naâma, 45000, Algeria²

³Faculty of Mechanical Engineering, University of Science and Technology USTO-MB, Oran, Algeria

Abstract: The present paper provides results of the 3D numerical investigation of flows generated by anchor impellers in a cylindrical vessel. For a Newtonian viscous fluid, effects of the impeller design on the hydrodynamics and power consumption are explored. We focus on the design of the lower part of impeller by realizing three different geometrical configurations. The influence of impeller rotational speed is also examined. All calculations are achieved with the CFD computer code CFX (version 16.0). Some predicted results are compared with experimental data available in the literature and a satisfactory agreement has been observed.

Keywords: Anchor impeller; Impeller design; Mixing vessel; 3D hydrodynamics; Power consumption.

1. Introduction

The mixing operation is widely encountered in many industrial processes. Indeed, the processes of homogenization and physical or chemical transformations of mass or energy transfer are the basis of many industrial sectors, such as: food, petrochemical, pharmaceutical, paint, etc. The close-clearance impellers are highly recommended for the mixing of highly viscous fluids [1-3]. Several experimental and numerical studies were carried out to improve the efficiency of the anchor impellers in mixing systems. Among others, we cite the following works. Baccar and Abid [4] studied by numerical simulation the efficiency of several kinds of anchor impellers in terms of mixing and heat transfer for Reynolds numbers ranging between 10^3 and 10^4 .

2. Description of the problem

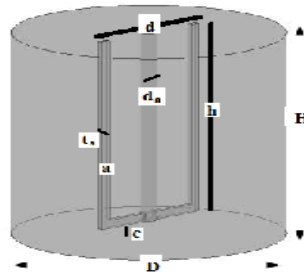


Fig. 1. Geometry of the problem studied

* Corresponding author

E-mail address: y.kamla@univhb.dz

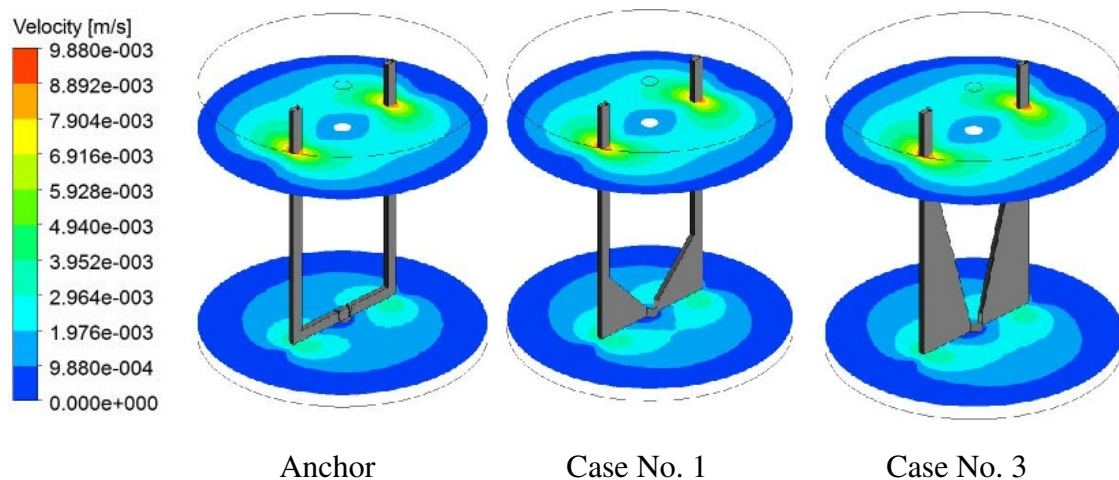


Fig. 2. Velocity contours for $Re = 10$, $Z^* = 0.05$ and $Z^*=0.83$

The agitation of viscous fluids requires always special impellers. As other impellers, the anchor has some issues which should be remedied. As shown on Figure 2, a well-mixed region is observed in the lower part of vessel. On the basis of these results, a new design is suggested.

The geometry of the classical anchor and three others with modifications in the lower part, namely: Case 1, 2 and 3. The new suggested design concerns a triangular plate inserted at the vertical arm of blade.

In a comparison between the new geometries, the increase of the triangular plate surface has found efficient for further intensification of fluid motion in the whole vessel volume.

Conclusion

Series of numerical simulations of mixing systems equipped with anchor impellers have been achieved for a Newtonian fluid. Effects of the impeller design have been explored. Poor mixed regions were observed near the vessel base when mixing with the classical anchor. Therefore, a new design was suggested which concern a triangular plate inserted to the vertical arms of the classical anchor. Effects of the triangular plate surfaces have also been investigated by realizing three geometries, namely: case 1, 2 and 3. The obtained results revealed that the classical anchor requires less power consumption but the lower part of vessel is poorly stirred. Case 3 have been found more efficient than both other cases, since it provides wider well-mixed region size and requires just an additional increase in power consumption (compared to case 1 and 2).

References

- [1]Kazemzadeh A., Ein-Mozaffari F., Lohi A., Pakzad L. (2016). Intensification of mixing of shear-thinning fluids possessing yield stress with the coaxial mixers composed of two different central impellers and an anchor. *Chemical Engineering and Processing: Process Intensification*. In press, doi: 10.1016/j.cep.2016.10.019.
- [2]Ameur H., Kamla Y., Hadjeb A., Arab I. M., Sahel D. (2016). Data on mixing of viscous fluids by helical screw impellers in cylindrical vessels. *Data in Brief*, 8: 220-224.
- [3]Prajapati P., Ein-Mozaffari F. (2009). CFD Investigation of the mixing of yield- pseudoplastic fluids with anchor impellers. *Chemical Engineering and Technology*, 32: 1211-1218.

SOLAR DRIVEN AIR CONDITIONNING SYSTEM BASED ON DESSICCANT MATERIALS

L. Merabti¹, M. Merzouk², N. Kasbadji Merzouk³, W. Taane⁴, M. Abbas⁵.

1,3,4,5 Unité de Développement des Equipements Solaires, UDES/ Centre de Développement des Energies Renouvelables, CDER, 42415, W. Tipaza, Algérie

2Faculté des Sciences de l'Ingénieur, Département de Génie Mécanique, Université Blida 1, Algérie

Abstract: Reducing the energy demand for air conditioning applications is an important goal to achieve for energy saving. It is so that necessary to develop alternative techniques to existing refrigeration equipment. The use of new technologies using clean and non harmful materials for the environment appears unavoidable. Furthermore, the use of the heat generated by solar panels is an interesting option for new air conditioning processes since the cold in demand coincides with the most warm and sunny period. The 'desiccant cooling' is an innovative technology allowing refreshing atmosphere by the changes of state of water, the solar energy exploitation and the use of desiccants materials which have the distinction of dehumidifying the air. The air drying by these porous materials is a needful operation especially in hot and humid climates like coastal areas of our country. The proposed air conditioning system is a solid desiccant system powered by solar energy; a simulation study is done to optimize the energy consumption of the system depending on the properties of the desiccant material used.

Key words: porous materials, solid desiccant, air conditionning, solar driven system, energy saving.

1. Introduction

The "desiccant cooling" system is proposed as an alternative to traditional air conditioners. Cooling systems potentiated by evaporative drying produce directly fresh air, unlike the mechanical compression refrigeration units, absorption or adsorption units, which cool an intermediate fluid. One feature of this system is the desiccant wheel containing a porous, silica gel or other, called desiccant, able to dehumidify the air by adsorbing the water it contains before starting cooling it. This system has the particularity of consuming a little amount of electric power comparing to traditional air conditioning systems and do not use refrigerants harmful to the environment, giving however its most important potential during the days of strong sunlight when demand is greatest.

2. Modeling and simulation of solid desiccant cooling system

The most important part of drying systems is the desiccant wheel, it is modeled from the equations of heat and mass balance in a small part of volume element of the wheel [1-2]. Solar cooling technology by dehumidification with a desiccant material allows obtaining significant energy savings. The main results as the collector surface, the diameter of the wheel and its efficiency and the thermal coefficient of performance are obtained from the inputs that are the efficiencies of the various components (humidifiers, rotary heat exchanger and regeneration heater), basic external conditions, the desired conditions in the room to be conditioned and the characteristics of the solar collectors were used. For the desiccant material used we took the hydraulic diameter and the thickness of the desiccant. [3]

The results show the evolution of the solar collector's field depending on the thickness of the desiccant and the variation of the rotation speed of the wheel based on the hydraulic diameter for different thicknesses of the silica gel.

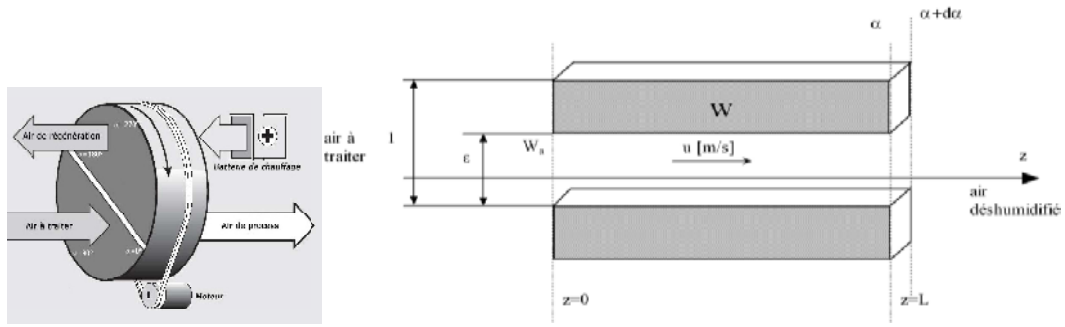


Fig. 1 : Elementary channel representation in a desiccant wheel

$$M_d \frac{\partial W}{\partial t} + \frac{1}{v_a} \varepsilon \left[\frac{\partial w_a}{\partial t} + u \frac{\partial w_a}{\partial z} \right] = 0 \quad (1)$$

$$M_d \frac{\partial W}{\partial t} = h_m \cdot S (w_a - w_{eq}) \quad (2)$$

$$M_d \frac{\partial H}{\partial t} + \frac{1}{v_a} \varepsilon \left[\left(\frac{\partial h_a}{\partial t} \right) + u \left(\frac{\partial h_a}{\partial z} \right) \right] = 0 \quad (3)$$

$$M_d \frac{\partial H}{\partial t} = h_m \cdot S (w_a - w_{eq}) (h_{fg} + C_{pv} T_a) + h_c \cdot S (T_a - T_m) \quad (4)$$

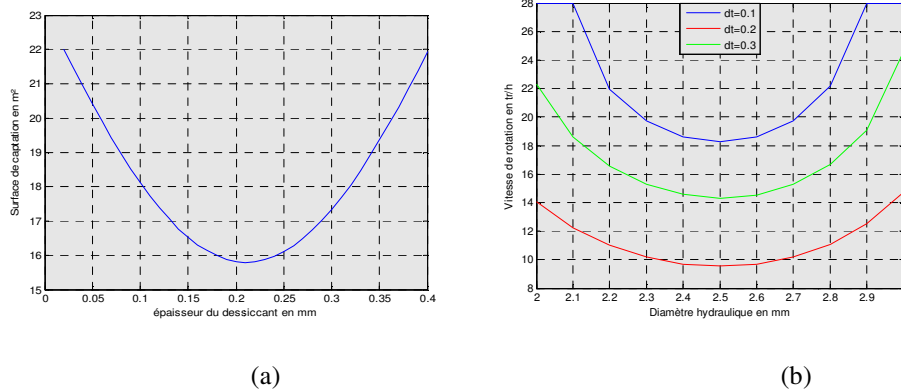


Fig. 2. (a) Collector's surface variation as a function of the thickness of desiccant (b) Rotary speed variation as a function of hydraulic diameter for different thicknesses of desiccant

3. Conclusion

The various parameters of desiccant material were considered for the study and optimization of the collector area needed to operate the solar desiccant cooling system. The optimization of this surface allows for substantial energy savings. The thickness of the porous material used affects the collector surface, if the thickness of the desiccant is lower or higher than its optimum value, the exchange between the regeneration air and the silica gel will be less, and the collector's surface must increase to compensate.

References

- [1] Maalouf C., Wurtz E., Mora L., "Impact of night cooling techniques on the operation of desiccant evaporative system" soumise à International Journal of Ventilation fin Avril 2006, acceptée en Juillet 2006.
- [2] M. Behne, "Alternatives to compressive cooling in non residential buildings to reduce primary energy consumption", Final Report LBL, mai 1997.
- [3] Sphaier L.A., Worek W.M., Analysis of heat and mass transfer in porous sorbents used in rotary regenerators, International Journal of Heat and Mass Transfer, 2004, vol 47, pp. 3415-3430.

INVESTIGATION OF AISI 316L CARDIOVASCULAR STENT BEHAVIOUR UNDER BLOODPRESSURE AND RESTENOSIS LOADINGS

M. Benhaddou^{17*}, M. Abbadi, M. Ghammouri

1ENSA, Équipe de Mécanique et Calcul Scientifique, Université Mohamed 1er, BP 696, Oujda, Morocco

Abstract: In the present study, ABAQUS finite element modelling was used to explore the durability of cardiovascular stent made of AISI 316L. It was found that the blood pressure does not cause the fracture of the stent. This result was confirmed by the application of Dan van critical plane approach. However, when subjected to restenosis compressive loading the stent was found to experience an in-service failure. The last proved to be dependent on the stent diameter reduction, rate and location of restenosis. Since restenosis forms gradually and randomly within the artery, two distributions were considered and investigated. The eccentric restenosis turned out to be more deleterious than the concentric one. This finding is in a good agreement with that obtained by Waller[1].

Keywords: Stent; High Cycle Fatigue; Restenosis; Eccentric and concentric; ABAQUS Numerical simulation

1. Introduction

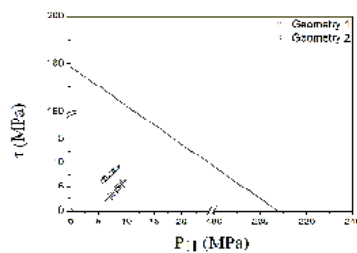
In the technical vocabulary of medicine, the term stent refers to a tiny metal mesh tube inserted into a tubular structure, such as an artery or blood vessel, to keep it wide open. The stenting procedure consists in introducing a small balloon inside the narrowed blood vessel, through a small puncture called the access site, to improve the blood flow. The stent is expanded after the balloon inside of the stent is inflated. Over 1.5 million coronary interventions, involving angioplasty with or without stenting, are performed annually worldwide. However, restenosis proved to induce some complications and remains the major limitation of such procedures. Although the concept of restenosis is common to the cardiology community, neither an appropriate definition nor an accurate origin of this affection is revealed. To avoid or at least limit clinical complications related to in-service failure, the stents are designed to endure high cycle fatigue (HCF) due to the high number of cycles caused by the blood pressure (4×10^7 cycles/year).

2. HCF life prediction

Dang van's criterion [2] Dang Van assumes that fatigue crack initiation occurs in critical stress raiser areas due to the unfavourable orientation of certain material grains with regard to the imposed loadings. The criterion is formulated as:

$$\tau(t) + \alpha p_H(t) \leq \beta \quad (1)$$

where $\tau(t)$ and $p_H(t)$ indicate the shear stress at the mesoscopic level and hydrostatic pressure, respectively, while α and β are material parameters.



^{17*} Corresponding author

E-mail address: med.benhaddou88@gmail.com

Fig. 1: Application of the Dang Van's criterion on the two geometries.

3. The effect of restenosis on the stent durability

Restenosis literally means the recurrence of stenosis. When a stent is used and restenosis occurs, this is called in-stent restenosis. Actually, the restenosis gradually forms and grows during the follow-up period of angioplasty. To investigate the effect of the restenosis rate on the resistance of the stent, the displacement responsible for the stent fracture is kept constant and the surface covered by the restenosis is gradually increased. The numerical computation shows that the stent fracture is reached around 59% (respectively, 49%) of restenosis rate for the geometry 1 (respectively, geometry 2), as displayed in Fig.2. This finding confirms the relatively good resistance of the geometry 1. This is may be explained by the low stress raiser for the U-shape as compared with the rounded shape of the stent. Moreover, the geometry 1 is found to harden very quickly and almost reach the ultimate tensile strength for a low rate of restenosis (about 16%), then this rate has practically no effect until failure. On the contrary, the von Mises stress progressively increases as a function of the restenosis rate up to failure for the geometry 2.

Conclusions

In this study, the finite element method has been used to analyse the effect of the blood pressure and restenosis on the durability of two geometries of stent made of AISI 316L. Dang van, Findley and Goodman criteria clearly show that, when subjected to the blood pressure cycle, the stent undergoes high cycle fatigue. However, it is found that the stent sometimes experiences in-service failure. The last was found to be the result of restenosis induced loading. Indeed, when the stent is totally recovered by restenosis its failure occurs at nearly 11.2% diameter reduction for geometry 1 (respectively, 10.3% for geometry 2). The effect of restenosis rate is then explored and showed that the fracture of the stent takes place when 59% (respectively, 49%) of the surface of geometry 1 (respectively, geometry 2) is covered by restenosis. Moreover, the location of restenosis proved to have a substantial effect on the stent behaviour. Indeed, an eccentric restenosis of only 14% (respectively, 13%) diameter reduction for geometry 1 (respectively, geometry 2) is responsible for the fracture of the stent. While a concentric restenosis of 26.45% (respectively, 24.85%) diameter reduction for geometry 1 (respectively, geometry 2) contributes to the stent fracture. Moreover, for the same diameter reduction, the eccentric restenosis is found to be more harmful than the concentric restenosis. This interesting result is in a good agreement with that found by Waller. Thus, the concept of the T-stress in the case of the crack stress distribution has been extended to the notch stress distribution.

References

- [1] B.F. Waller, The eccentric coronary atherosclerotic plaque: Morphologic observations and clinical relevance, *Clinical Cardiology*, 12 (1989) 14-20.
- [2] K. Dang Van, Macro-micro approach in high-cycle multiaxial fatigue. In: D.L. McDowell, R. Ellis, editors. *Advances in multi-axial fatigue*. ASTM, (1993) 120-130.

THE COLLECTOR RADIUS EFFECTS ON THE MASS FLOW RATE IN A SMALL-SCALE SOLAR CHIMNEY

M. Lebbi^{*1,2}, A. Bouabdallah², T. Chergui¹, H. Boualit¹, L. Boutina¹, M.T. Bouzaher¹, S. Laouar¹, M. Lounici³

1 Unité de Recherche Appliquée en Energies Renouvelables, URAER, Centre de Développement des Energies Renouvelables, CDER, 47133, Ghardaïa, Algeria

*Corresponding author E-mail: mlebbi2015@gmail.com

2 LTSE Université des sciences et de la technologie, USTHB, Bab Ezzouar, Algeria

3 FSI, UMBB, Avenue de l'Indépendance 35000 Boumerdes, Algeria.

Abstract: The purpose of this study is focused on the optimization of solar chimney collector area to achieve the collector aspect ratio variation, optimal point which presents the maximum mass flow rate. This methodology allows a detailed visualization of the optimal geometric effects for such devices. The main results indicated that the collector area is an important parameter for thermo-hydrodynamic flow control in a solar chimney but has an optimum value that should not be exceeded.

Keywords: Solar Chimney, Finites volume method, collector area.

1. Introduction

The basic study on the solar chimney concept was achieved by Doctor Schlaich in the 1970s. In 1981, his research team began the construction Manzanares prototype in, Spain [1]. Maia et al. [2] performed a theoretical and experimental study of the unsteady airflow inside a solar chimney. Recently Lebbi et al. [3] investigated numerically the influence of geometric parameters on the thermo-hydrodynamic control of the solar chimney. It has been shown in this work that the tower dimensions play an important role in designing of such systems.

2. Theoretical study

The governing equations presented above are discretized into algebraic equations by using the Finite Volume Method (FVM), which is widely used in computational fluid dynamics (CFD). The pressure-velocity coupling is treated by the SIMPLE algorithm.

3. Results and discussion

Fig. 1 two velocity profiles in a cross-section of the collector, for the non-dimensional radius of $r/R_t = 0.15$. This numerical result is in a good agreement with the experimental value reported by [2] for the same geometrical conditions. Fig. 2 presents the mass flow rate variation versus radii ratio at tower outlet. We note that the increase in the radii ratio produces an increase in the mass flow rate.

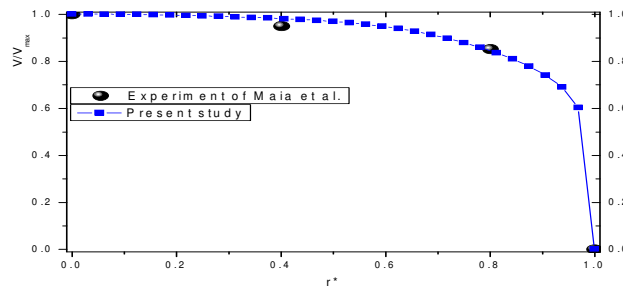


Fig. 1 Comparison between present results and experimental of ref. [2]

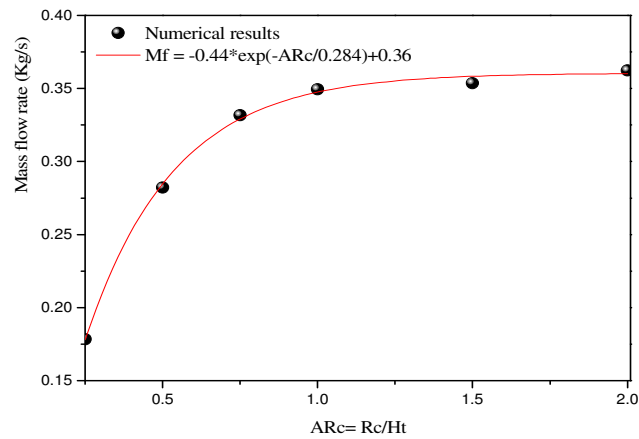


Fig. 2 Evolution of mass flow rate versus the collector aspect ratio

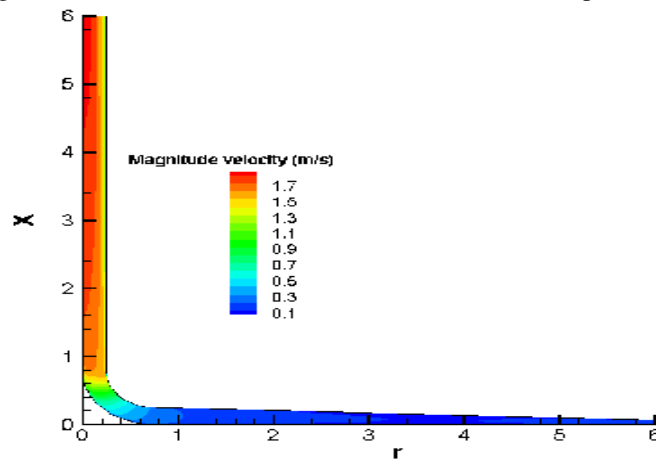


Fig. 3 magnitude velocity contours

4. Conclusion

From this study we concluded that the collector area variation is the most important factor in the SCPP system for increasing the mass flow rate and has an optimum collector area compared to their tower height that should not be exceeded.

References

- [1] W. Haaf et al, Int J Solar Energy, vol. 2, pp. 3-20, 1983
- [2] C.B. Maia et al, Comput Fluids, vol. 38, pp. 625-636, 2009
- [3] M. Lebbi et al, Int J Hydrogen Energy, vol. 39, pp. 15246-15255, 2014

EFFECT OF STRESSES INDUCED BY ION EXCHANGE IN THE CASE OF A GLASS SUBJECTED TO SOFT THERMAL SHOCK

Z. Malou^{1,2}, T. Benouioua¹, O. Gridi¹, M. Hamidouche^{1,2}, G. Fantozzi³

1 optical and mechanical precision institute, university of Setif 1, 19000 Algeria

2 Emerging materials research unit, university of Setif 1, 19000 Algeria

3Laboratory MATEIS, CNRS UMR 5510, INSA Lyon, 69621 Villeurbanne, France

Abstract: Because of its brittleness, the glass surface is very sensitive to superficial microcracks which decrease the mechanical strength. In the same time, residual stresses play a main role in the glass technology. Their amplitudes and directions must be well known and carefully controlled. In this work, a soda lime glass was submitted to chemical treatment by ion exchange in order to introduce compressive stresses in the surface. For this, we have applied an ion exchange treatment by diffusion of potassium from the bath in the place of sodium existing in the glass surface. Indentation technique is used in order to quantify the stresses introduced into the surface. The diffusion profile of the potassium is determined by microanalyse coupled with SEM. After, the specimens treated were subjected to hot-cold thermal shock technique. The cooling was made by ambient air jet on previously warmed samples. The heat transfer coefficient was about $600 \text{ W/}^\circ\text{C.m}^2$ (Biot number $\beta = 0.3$). The results show that the compressive stress profile depends on potassium ion concentration. The fracture strength is clearly improved. It passes from 95 MPa from the as received state to 320 MPa for the chemically treated state. The residual strengths of the quenched specimens were determined in a three-point bending test. The results showed that the critical temperature difference ΔT_c depends on state of the samples. The thermal shock resistance is significantly improved.

Keywords: Glass, indentation, stress, ion exchange, thermal shock, mechanical strength.

1. Introduction

The brittleness of glass is caused mainly by the presence of many surface cracks which serve as stress concentration points. [1] [2].

In order to remedy to the glass sensitivity to surface defects, a strengthening treatment by chemical tempering was used.

Strengthening by ion exchange consist to immerse heated glass in a bath of KNO_3 . Small Sodium ions (0.95 Å) present at the glass surface are replaced by larger potassium ions (1.35 Å). The result of this diffusion is to set the glass surface in a compressive state. [3], [4].

During a thermal shock, a transient temperature gradient occurs, inducing thermal stresses. The shock intensity is related to the level of temperature difference between the initial temperature and that of the environment. Thermal shock generates tensile stresses on the rapidly cooled surface. These stresses may be sufficient to activate pre-existing micro-cracks and lead to materials damage or fracture. [5], [6].

2. Results and discussion

The tensile strength of the treated samples is around of 320 MPa while it is only about 95 MPa for raw glass. Strengthening induced by ion exchange multiplies mechanical strength by a factor of 3.5.

The mechanical resistance significantly increases when the temperature and the treatment time increases, therefore the critical thermal shock temperature difference shifts to the increasingly high temperatures. The thermal shock resistance is thus greatly improved.

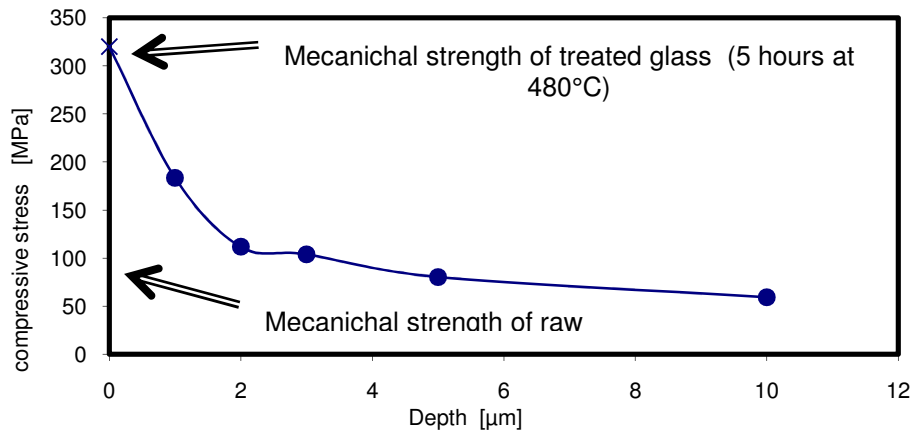


Fig.1: Compressive stressprofile induced by ion exchange

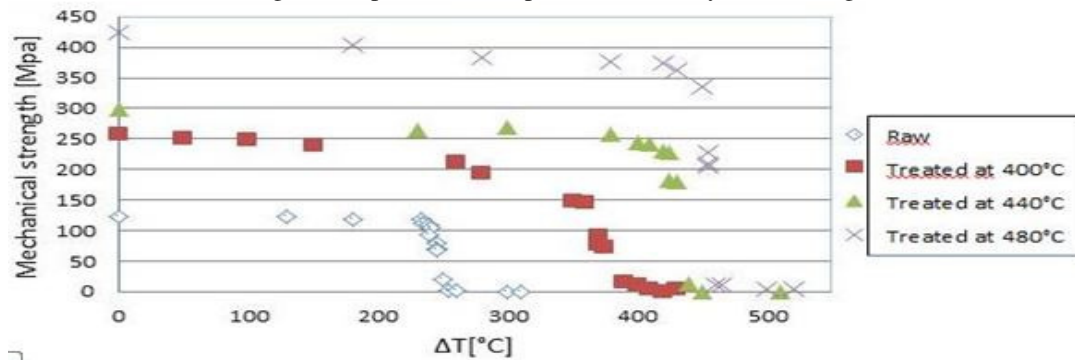


Fig.2: Mechanical strength according to ΔT for a glass treated for 50h.

References

- [1] M. Hamidouche, R. Louahdi, N. Bouaouadja, H. Osmani, The fracture of soda lime glass, *Glass Technology*, Vol. 35, N4 (1994) pp. 183-185.
- [2] Z. Malou, M. Hamidouche, M.A. Madjoubi, K. Loucif, H. Osmani, N. Bouaouadja, Interaction between indentation cracks in soda-lime glass, *Glass Technology*, 2000, 41 (2), pp.55-58
- [3] I.W. Donald, Review: Method for improving the mechanical properties of oxides glasses, *Journal of Materials Science*, Vol. 24 (1989) pp. 4177-4208
- [4] Ajit Y. Sane, A.R. Cooper, Stress buildup and relaxation during ion exchange strengthening of glass, *J. Am. Ceram. Soc.*, Vol. 70 [2] 86-89 (1987)
- [5] Z. Malou, M. Hamidouche, N. Bouaouadja, G. Fantozzi, Statistical analysis of a soda lime glass thermal shock resistance, *Ceramics – Silikáty* 55 (3) 215-221 (2011),
- [6] Z. Malou, M. Hamidouche, N. Bouaouadja, J. Chevalier, G. Fantozzi, « Thermal shock resistance of a soda lime glass », *Ceramics – Silikáty* 57 (1) 39-44 (2013).

SIMULATION OF SHUNT ACTIVE POWER FILTER CONTROLLED BY SVPWM CONNECTED TO A PHOTOVOLTAIC GENERATOR

O. Maarouf¹, I. Bouyakoub¹, B. Mazari²

¹Université Hassiba ben bou ali de Chlef

²Université USTO Oran

Abstract: In this research we are going to study "The Shunt Active Power Filter". This filter contains a voltage three-level inverter controlled by SVPWM strategy supplied by the DC bus powered by a solar array aimed at improving the quality of electric energy, eliminate harmonic currents which was generated by The Non-Linear Loads. These Harmonics were identified by the Multivariable Filter method. The objective of this study is to obtain unpolluted source into the power grid where all the simulation results are obtained by using the MATLAB environment

Keywords: Shunt Power Active Filter, Harmonic Currents, MVF, SVPWM, Three Level Inverter, GPV

I. Introduction

The Sources of Energy are divided into two categories. The Renewable sources and the Petrol and Gas energies. The Renewable are divided into many types such as: Solar, Wind and Hydraulic energies. These energies were used from the foundation of humans which means its usage was from long ages throughout history until the out-break of the industrial Revolution.

In this period of time, Petrol's prices were very sheep as a consequence, renewable sources were excluded. In contrary, during recent years and due to the increase of fuel's prices and the environmental problems caused by the use of conventional fuels we come back to use renewable sources of energy.

Renewable sources are inexhaustible, clean. These sources can be used in a decentralized way that makes it so easy to work with. It also had the additional advantage of being complimentary wherein the integration between them is favorable.

II A Studied Configuration

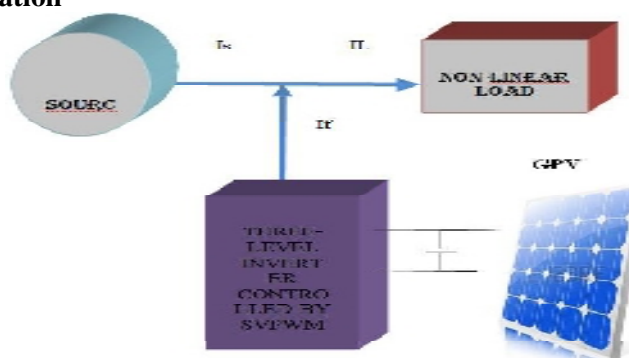


Fig1 Configurations of Photovoltaic Interactive Shunt Active Filter System

III. PV model

The Photovoltaic cell is mainly a p-n junction made in a slender plate semiconductor, a solar energy sent an electromagnetic radiation, and this radiation is converted into electricity by the photovoltaic panel when it is exposed to the Sun rays, the Photons, which have an energy higher than the Band-Gap Energy of the semiconductor, create some pairs Electron-Hole proportional to the incident rays, if we want to build a model of the PV generator, we have to start by the identification of the equivalent electrical circuit to the source. Several Mathematical models have been designed to represent their highly non-linear characteristics given by semiconductor junctions that are the most important components in PV modules. Most models of photovoltaic generators that have some numbers of concerned parameters in the compute of output voltage and current

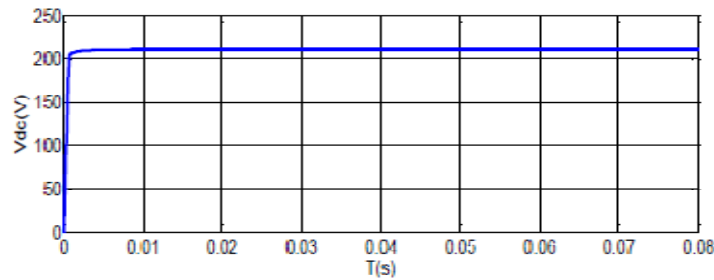


Fig.2 Evolution of a Dc bus voltage

IV. Shunt Active Filter

In power distribution network, active power filters are widely used to reduce harmonics caused by nonlinear loads. This paper describes a shunt active power filter with a control system based on the multi-level inverter (PWM). The wide spread of power electronics equipment in modern electrical systems and power converter units causes the increase of the harmonics disturbance in the AC mains currents which became a major concern due to the adverse effects on all equipment and distribution network [4].

Control Scheme

VI. Conclusion

The purpose of this article is focused on improving the power quality of the network based on the compensation of harmonic currents using a shunt active power filter.

The control of SVPWM take an essential part in improving the performance of APF and Produces good filtering quality, which has been obtained by the used of Matlab simulation environment, Show us that some self-charging current source stay close to a sinusoidal wave. Note that other techniques can also be used to enhance the system response.

The work that will be continued in this context is the development of the experimental applications of these proposed strategies, to confirm the effectiveness of the achieved Results.

References

- [1] Saleh, S. , Azizur Rahman, M., "An Introduction to Wavelet Modulated Inverters", IEEE Press, 2011.
- [2] Strandt, Rebecca, A ., " Comparison of Three Space Vector PWM Methods for a Three-Level Inverter with a Permanent Magnet Machine Load", Master's Theses (2009 -). Paper 234.
- [3] Srinivas, K., Srinivas, G., Narasihma Rao,Dr.K., "Simulation of Shunt Active Power Filter Connected to a Photovoltaic Array for ompensating Current Harmonics in Single Phase System ", International Journal of Advanced Research in Electrical,Electronics and Instrumentation Engineering Vol. 3, Issue 12, December 2014
- [4] Sandeep kumar, D.,Venu madhav, G, "power quality improvement with a shunt active power filters using matlab / simulink, international journal of innovative research in electrical, electronics, instrumentation and control engineering" ,(IJRITCC)vol. 3, issue 1, january 2015.
- [5] Djeghloud, H., Benalla ,H., " Space Vector Pulse Width Modulation Applied to the Three-Level Voltage Inverter",5th International Conference on Technology and automation, Thessaloniki,(ICTA'05) Greece, October 15-16, 2005.
- [6] Benhabib, M. C., Jacquot ,E., Saadate, S. , "An Advanced Control Approach for a Shunt Active Power Filter", International Conference on Renewable Energy and power Quality, (2003) April 9-11, Vigo, Spain.
- [7] Laib, H. , Kouara ,H., Chaghi ,A. , " A New Approach of Modular Active Power Filtering", International Journal of Advanced Science and Technology Vol. 50, January, 2013

ADSORPTION OF ANIONIC DYE BY ZEOLITE COMMERCIAL AND EQUILIBRIUM STUDY

F. LASNAMI^{1,*}, A. LABBACI¹, M. DOUANI²⁾

(1) Faculté de technologie, Département de génie des procédés, laboratoire Eau-Environnement, Université Hassiba Benbouali, B.P.151, Chlef 02000, Algérie

(2) Department of process engineering, Laboratory of Vegetal Chemistry, Water and Energy, University Hassiba Benbouali, of Chlef, Po. Box 151, Chlef, 02000, Algeria.

Abstract: This research involved the efficient adsorption of anionic dye (Acid Red 1 (AR1)) by zeolite 96096. The parameters such as contact time, initial dye concentration, initial pH. According to these experiments the maximum removal is observed after 140 min. The results showed that acid pH is favorable for the adsorption of dye and physisorption of zeolite particles seemed to play a major role in the adsorption process. The equilibrium adsorption data, obtained at 25 °C, were analyzed by Langmuir Freundlich models. The results indicate that the Langmuir model provide the best correlation of the experimental data.

Keywords: adsorbent; Acid dye; zeolite; Isotherms; Kinetics; Dye removal.

1. Introduction

There are more than 100000 types of dyes commercially available, with over 7×10⁵ tons of dyestuff produced annually, which can be classified according to their structure as anionic and cationic. In aqueous solution, anionic dyes carry a net negative charge due to the presence of sulphonate (SO⁻³) groups, while cationic dyes carry a net positive charge due to the presence of protonated amine or sulfur containing groups.

Synthetic dyes are used extensively by several industries including the textile dyeing and paper industry. It is estimated that at least 10% of the dyes are lost in the dye effluent during such dyeing processes. Several methods such as adsorption, coagulation and flocculation, biological treatment, advanced oxidation processes, photocatalytic process have been used for treatment of colored wastewater. Removal of dye from colored effluents by adsorption processes has been to be an efficient and economical. Zeolite adsorption plays a vital role in molecular purification technology. In this work, the adsorption of Acid Red 1 (figure 1) was measured on zeolite (96096), zeolite doses, and dyes concentrations.

2. Adsorption studies

The adsorption was performed by batch experiments. Kinetic experiments were carried out by stirring 100 mL of dye solution of known initial dye concentration with 4 g of zeolite for AR1 at room temperature (25 °C) at 180 rpm in different 100 mL flasks. At different time intervals, samples have been drawn out and then centrifuged at 2000 rpm for 20 min. The concentration in the supernatant solution was analyzed using a UV spectrophotometer (OPTIZEN 2010) by measuring absorbance and pH=3 for AR1. Adsorption isotherms were carried out by contacting 4 g of zeolite, with 100 mL of dye over the concentration ranging from 10 to 150 mg/L. The agitation last 180 min, which is sufficient time to reach equilibrium.

The amount of adsorption at equilibrium (q_e , mg/g) was calculated by using the following equation [1]:

$$q_e = (C_0 - C_e) \frac{V}{m} \quad (1)$$

$$E(\%) = \frac{(C_0 - C)}{C_0} \times 100 \quad (2)$$

Where C_0 and C_e (mg/ L) are the liquid-phase concentrations of dye at initial and equilibrium, respectively, V is the volume of the solution (L) and m is the mass of the adsorbent (g).

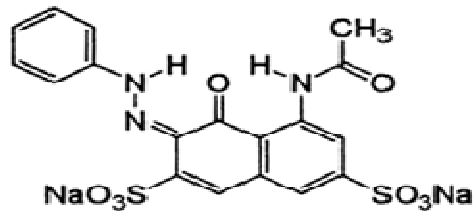


Fig.1. Chemical structure of dye (AR1).

This research involved the efficient adsorption of anionic dye (Acid Red 1(AR1)) by zeolite. The parameters such as contact time, initial dye concentration, initial pH. According to these experiments the maximum removal is observed after 140 min. The results showed that acid pH is favorable for the adsorption of dye and physisorption of zeolite particles seemed to play a major role in the adsorption process. The equilibrium adsorption data, obtained at 25 °C, were analyzed by Langmuir, Freundlich models. The results indicate that the Langmuir model provides the best correlation of the experimental data [2].

3. Conclusion

The present study showed that zeolite synthesized cannot be used as an effective adsorbent for the removal of red acid 1 dye from aqueous solution. It is observed from the experiments that about 10-8% removal is possible.

References

- [12] W.W.Huang, F.Y.Gong, F.Y., Fan, M.H., Zhai, Q., Hong, C.G.(2012). Production of light olefins by catalytic conversion of lignocellulosic biomass with HZSM-5 zeolite impregnated with 6 wt.% lanthanum. *Bioresour. Technol*, Vol.121, p.248–255.
- [13] M., Qian, C., Xu, J.,Wu, J.,Wang, G., 2009, Studies on the adsorption of dyes into clinoptilolite. *Desalination* , vol.243,p. 286-292.

AERODYNAMIC SHAPE OPTIMIZATION OF NACA0012 PROFILE USING ADJOINT SOLVER

A. E. Amor¹; R. Mdouki²; A. Bettahar¹.

1University of Chlef, LPTPM, Esalem City, 02000, Chlef, Algeria.

2University of Tébessa, Street of Constantine, 12000, Tébessa, Algeria.

Abstract: This paper presents the implementation of optimization technique that treats the design of airfoil configurations. Geometric constraints and multiple design points are described, where the design variables are handled by a module of the Adjoint Solver in ANSYS Fluent. The approach shown here is based on the use of the Adjoint solver to drive the shape modification of the considered geometry: the adjoint sensitivities are used to guide intelligent design modifications and improve the product performance. The adjoint method provides a fast and accurate way for computing the sensitivity derivatives of the objective functions (maximum lift; minimum drag maximize the lift-drag ratio of an airfoil NACA0012) with respect to the design variables. The results demonstrate that the continuous adjoint method can efficiently and significantly improve the aerodynamic performance of the design in a shape optimization problem.

Key words: Aerodynamic shape optimization, CFD, NACA 0012, Adjoint Solver, lift, drag, Ratio lift/drag, Optimum Aerodynamic Design.

1. Introduction

In numerical optimization design, the CFD and optimization processes are coupled to modify the design parameters, such as the shape of nozzles, airfoils, wings or the angle of attack (AoA), to improve the chosen cost functional subject to geometric and/or aerodynamic constraints. Among the different options available, we have chosen the Adjoint methods as the optimization tool for maximize the lift/drag ratio of an airfoil, this method rapidly determine shape modifications that improve aerodynamic performance and design safety factors. At the heart of the optimization is the computation of the objective function gradient; the sensitivity of some performance measure, such as the lift and drag functionals, to a given set of design variables that control the shape. Well-known techniques for gradient computation are the Adjoint and flow-sensitivity (or direct) methods [5; 6; 4]. An important issue in the application of Adjoints and flow-sensitivities as routine tools of aerodynamic shape optimization is the need to handle geometrically complex engineering designs. Repeated meshing of complex geometry throughout the design process creates an implicit requirement for robust, efficient, and automatic mesh generation. Finally, some illustrative numerical results of optimum design of airfoil are presented in this work.

5 Conclusions

In this work we used a procedure to perform optimization using the sensitivities obtained with the Fluent Adjoint Solver. We expect this aspect of the method to have the most impact because of the generality of the idea, the broad applicability and the opportunity to tackle robust design in a fundamental new way from an industrial perspective. In future works we will address the possibility to integrate the structural deformation of the aerodynamic components in the probabilistic design procedure and to perform multi-objective design optimization under uncertainty.

References

- [1] ANSYS FLUENT 15.0 - Theory Guide, ANSYS, Inc., Canonsburg, PA, 2012.
- [2] ANSYS FLUENT 14.5 - Adjoint Solver Module Manual, ANSYS, Inc., Canonsburg, PA, 2012.
- [3] G. Petrone, D.C. Hill and M.E. Biancolini "Optimization under Uncertainty using Adjoint Solver and RBF Morph", Conference Paper · January 2013.
- [4] Marian Nemec and Michael J. Aftosmis, "Aerodynamic Shape Optimization Using a Cartesian Adjoint Method and CAD Geometry", ELORET Corp., Moffett Field, CA 94035. NASA Ames Research Center, Moffett Field, CA 94035. July 2006.
- [5] Pironneau, O., "Optimal Shape Design for Elliptic Systems", Springer-Verlag, New York, USA, 1984.
- [6] Baysal, O. and Eleshaky, M. E., "Aerodynamic Sensitivity Analysis Methods for the Compressible Euler Equations," Journal of Fluids Engineering, Vol. 113, No. 4, 1991, pp. 681-688.

THERMAL AND DYNAMIC CHARACTERIZATION OF A TURBULENT SWIRLING JET IMPACTING PLATE PLANNE (EXPERIMENTAL AND NUMERICAL STUDY)

A. Zerrouk^{a,*}, A. Khelil^a, L. Loukarfi^a

*a Control Laboratory, Test, Measurement and Mechanical Simulation, University of Chlef, Algeria, BP 151,
02000 Chlef, Algeria, E-mail: zerroutamar@yahoo.fr*

Abstract: This work is the subject of an experimental study and a numerical swirling jet impinging a plane wall. The experimental test bench comprising a diffuser diameter D , impacting perpendicular plate, varying the impact height $H = 4D$. The swirl is obtained by a generator (swirl) of compound 12 fins arranged at 60° relative to the vertical placed just at the exit of the diffuser. The temperature of blowing swirling jets impinging the plate is raised with a portable device anemometer VELOCICALC PLUS, in different stations. The system was numerically simulated by the fluent program through the turbulence model (k- ϵ). The latter gave temperatures and rate data having profiles granted to those of the experimental results.

Keywords: turbulent swirling jet, impinging a plaque, thermal homogenization, ventilation, (k- ϵ) model.

1. Introduction

Several research papers have treated the convective transfer of free throws and confined flows, the swirling flow characteristics through an air jet impinging on flat surfaces or complex geometry, in order to improve the transfer of heat or localized mass in a portion of a system. For this it is necessary to know the structure of the impinging jet, and the parameters that influence this behavior. Many articles deal with this case, the main cited by RADY 2004 [1]. Generally the flow field of an impinging jet can be decomposed in different regions. A pseudo-free jet region, a region of impact or deflection also called stagnation region or "Impingement region», and A radial jet area parallel to the wall (wall jet or "wall-jet region»).

2-Experimental device

The realized experimental device consists of a frame of the cubic shape (5) of metal; having at its upper part the hot air blowing device, directed from the top downwards and in its lower part a diffuser (1). A particular arrangement of rods supporting temperature probes (2); the temperature field is explored through a portable anemometer device VELOCICALC more (4). The probes are supported by rods easily guided vertically and horizontally, a horizontal plate (3) Formica material, the temperature and velocity fields are measured in different stations in the axial and radial directions of flow. The ambient temperature T_a is obtained from the temperature T measures.

6. Numerical Results

6.1. Temperature field and velocity vectors

Figure (3), provides the temperature fields and field vectors for a $4D$ Impact height and inlet temperature T , calculate with (k- ϵ) model, we see that the jet appears at first as a free jet is the region of established flow from the injection port to the end of the potential cone and it is characterized by the weakening of the axis velocity and vitality hence the established flow area, then the jet is deviated from its initial direction is axial deflection region. Finally, velocity is mainly radial and where the boundary layer, whose thickness increases radially, called the wall jet region.

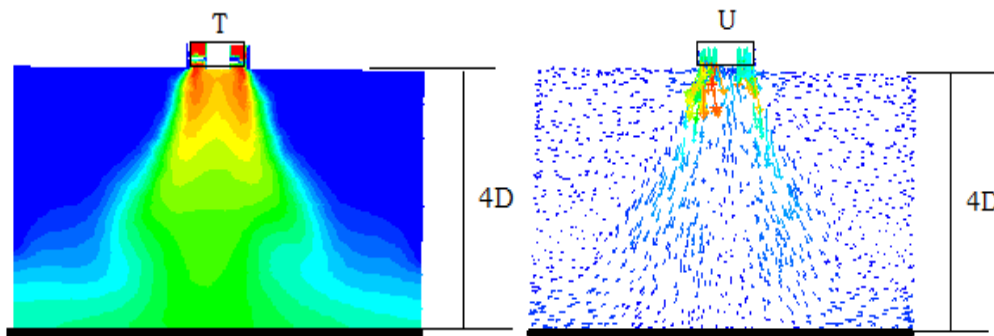


Fig.3. Temperature field and velocity vector field

7. Conclusion

The results in this study show although in the early, the jet has the same features as a free jet, close to the obstacle it undergoes a considerable deflection characterized by the weakening of speed and vitality of the jet. The swirl provides thermal homogenization with a significant spread in ensuring a uniform temperature distribution along the plate.

The presence of the plate lowers the jet temperature differences; the temperature of the plate decreases downstream of the jet gradually as one approaches the plate. The comparison between the numerical results and the experimental results presented in this study indicates that the model with two transport equations (K- ϵ) produces satisfactory results.

References

- [1]- Rady M., Arquis E., "Heat transfer enhancement of multiple impinging slat jets with symmetric exhaust ports and confinement surface protrusion", Applied Thermal Engineering, 26, 1310-1319, 2005.
- [2]- LAUNDER.B.E, SPALDING.D.B, "Mathematical Models of Turbulence", Department of Mechanical Engineering, Imperial Collogue of Science and Technology, LONDON. England 1972.
- [3] - FLUENT User's Guide, 2006.

THERMAL AND DYNAMIC CHARACTERIZATION OF AIR JET ISSUED FROM A DIFFUSER PROVIDED WITH LOBES

M. Braikia * A. Khelil, L. Loukarfi A. Bennia,

*Laboratoire de Contrôle, Essai, Mesure et Simulation Mécaniques, Université Hassiba Benbouali de Chlef,
Hay Salem, route nationale N° 19, 02000, Algérie.*

* braikia_m@yahoo.fr

Abstract: The study of the mixing process of turbulent flows to means of swirling structures is experiencing a growing interest, most of these studies focus on thermal and dynamic characteristics of the turbulent flow field. So they find their application in the design of the combustion chambers, vaporizers, dispersion of pollutants at industrial sites, injectors (for burners) and finally in the living areas, the quality of the air diffusion and therefore thermal comfort of the occupants. The first objective of this present experimental study is to search for effective ways to improve the self-induction jets for their integration in terminal units of air conditioning. The experimental setup used is basically designed to generate air jets lobed. The experiments were performed in a room of dimensions 4.0m long, 3.5m wide and 3.0m high. The installation realized is composed of a frame on which is fixed the blowing device; the latter comprises blowing hot air diffusers directed downwards. The number of diffusers may vary depending on the configuration studied. The temperatures and flow rates are measured by a multifunctional thermo-anemometer type "Veloci Calc over-8385A model," with a sensor to measure several parameters, such as temperature, velocity and flow. The probe is supported by guided rods vertically and horizontally to scan the maximum space, which allowed us to measure the temperatures and speeds axial and radial jet. A digital thermometer is placed outside the flow through the space to allow the instantaneous measurement of the ambient temperature (T_a). The lobed nozzle used consisted of 6 lobes inclined from 0° to the outside of the flow. Its hollows are inclined by 22° inwards. The nozzle is made from a 46mm circular section of tube diameter and length of 90mm. The lobe width is 6 mm and its height 10 mm, with a slightly flared opening of the lobes. The initial temperature of the air at the blowing opening is 83°C (356 K) for the jet and the initial axial velocity of the jet is 8.30 ms^{-1} . The flow takes place at Reynolds numbers ranging from 104 to 4,104. The study was carried out in uniform heat flux conditions and $Q_m \leq 56\text{ g/s}$, $r/D = 1$ to 10 and $0 \leq x/D \leq 20$. In this investigation, we examining the distribution of the axial and radial temperature and velocity profiles for a configuration of a single diffuser equipped with lobe shows the importance and role of the diffuser geometry (tilt, height and opening lobes) in the performance of the spray mixture lobed. Beyond the axial station $1d_e$ to $10d_e$ and up, there is a clear influence of the main plane on the development of temperatures along the radial axis of flow. Beyond 10 equivalent diameters of the origin and blowing up $20d_e$, profiles of temperatures and velocity are identical for the two main plans and secondaire. l'écoulement is no longer influenced by the type of plan, the effect of the lobes and the hollow diffuser disappears, the jet is as a circular jet, with a thermal and dynamic stability as well as a significant épanouissement the resultant jet.

Keywords: Thermal and dynamic characterization; lobed jet; swirling jet.

Experimental conditions

The maximum temperature at the blowing origin (T_m) is recorded for each type of configuration. The ambient temperature is measured at that time of flow temperature measurements (T_i) in different points in the flow of the jet, which is radially to several stations.

Axial and radial flow temperatures are obtained by reference to the maximum average temperature at the outlet of the blowing opening and at ambient temperature with a dimensionless expression of the form:

$$T_r = \frac{T_i - T_a}{T_{\max} - T_a}$$

The radial and axial distances are given by reference to the diameter of the blow port in dimensionless form r/R and x/D .

Experimental setup and configuration studied.

The experimental setup used is basically designed to generate air jets lobed. The experiments were performed in a room of dimensions 4.0m long, 3.5m wide and 3.0m high. The installation realized is composed of a frame on which is fixed the blowing device Figure (1), the latter comprises the blowing of hot air diffuser downwardly. The number of diffusers may vary depending on the configuration studied. The temperatures and flow rates are measured by a multifunctional thermo-anemometer type "Veloci Calc more-8385A model," with a sensor to measure several parameters, such as temperature, velocity and flow. The probe is supported by guided rods vertically and horizontally to scan the maximum space, which allowed us to measure the temperatures and velocities in axial and radial jet. A digital thermometer is placed outside of the flow through the space to allow the instantaneous measurement of the ambient temperature (T_a).

Conclusion

This experimental study of lobed jet (single diffuser initially) allowed us to draw the following conclusions:

A decrease in the axial temperature for the main direction of the station $X / D = 3$ to a station $X / D = 7$ close to the blowing diffuser, the axial temperature decreases more rapidly in the case of secondary direction beyond 7 diameters the axial velocity almost the same rate for both directions considered. more rapid reduction in axial velocity for the main direction compared to the secondary direction in all areas of the stations studied. A similarity between the respective axial profiles of temperature and velocities (identical profiles). The axial station $0,5D_e$ to $9D_e$ we clearly see the influence of the master plan on the development of temperatures along the radial axis, in this region the lobed jet has a larger induction as jet circular. A net temperature stability and speed appears when one moves away from the blowing diffuser. Beyond 9 equivalent diameters, flow is not influenced by the type of plan. The jet is as a circular jet, which is why the temperature profiles are identical, the same pace for both primary and secondary levels.

The outstanding performance of lobed jet is due to longitudinal structures made better organized and more intense by increasing the transverse shear generated by the inclination of the hollow.

We should consider studying the optimization of the geometry of this type of diffuser (value of the inclination of the lobes and troughs, height and number of lobes, many diffusers and their interaction ect ...).

ADSORPTION STUDY OF A NON-BIODEGRADABLE HERBICIDE BY NATURAL CLAY SURFACE REACTIVITY

M. Makhloufi ^a, A. Zehhaf ^a, A. Benyoucef ^a

aLaboratoire de Chimie Organique, Macromoléculaire et des Matériaux, Université de Mascara. Bp 763 Mascara 29000

Abstract: The adsorption of two herbicides used in the agriculture, namely acide 8-quinoléinecarboxylique (8QCA) and the N- (phosphonométhyl) glycine (NPGM) onto montmorillonite from Maghnia deposits (Algeria) from aqueous solutions were studied. In this view, we have characterized four Algerian montmorillonites adsorbent samples from various origin: M (purified sodium clay), M-H (sodium clay synthesized by acid activation), M-H-Org1 (sodium clay activated "M-H" and modified by ammonium acetate) and M-H-Org2 (sodium clay activated "M-H" and modified by ammonium carbamate). XRD of these samples shows an essentially montmorillonite-illite constitution of montmorillonite dominance in their clay fraction containing plus calcite and quartz. The kinetic equilibrium data show that M-H-Org1 fixes more the herbicides (8QCA and NPGM) than the M-H-Org1 > M-H-Org2 > M-H > M. The results also showed that the kinetics of adsorption is best described by a pseudo-second-order expression. Adsorption isotherms of herbicides onto M-H-Org1, M-H-Org2, M-H and M were determined and correlated with common isotherm equations such as the Langmuir and Freundlich models. The Langmuir model agrees very well with experimental data. The thermodynamic parameters obtained indicate that the adsorption of herbicides onto the four clays was a spontaneous and an exothermic process.

Keywords : Adsorption ; Clay Modification ; Cation exchange ; 8-Quinolinecarboxylic acid ; Glyphosate

NUMERICAL INVESTIGATION OF THE GEOMETRY INFLUENCE ON THE AERODYNAMIC FIELDS OF THE FREE TURBULENT JETS

Bouhamidi Y¹., khelil A^{1*}., braikia M¹., Nechad S¹., Bennia A¹ and loukarfi L¹

¹ Controls, Testing, Measurement and Simulation Mechanical laboratory, University of Chlef, Chlef, Algeria

* E-mail: khelila@yahoo.fr

Abstract: The objective of this study is to develop a numerical simulation of a flow from diffusers with different geometries. The main applications of this kind of diffuser are in forced ventilation and air conditioning. A detailed evaluation of the results, face other numerical and experimental studies in the turbulent regime was examined for a turbulent jet in free mode. The k-e turbulence model and RSM turbulence model were used in this investigation. Several flow parameters are tested such that the diffuser geometry, the number and the angle of inclination of the swirled vane located in the diffuser associated with the concept of the swirl number. The comparison of numerical results with those available in the literature was presented. Most of these comparisons are in good agreement with the experimental data. By comparing changes in the axial and radial temperature, the configuration having an inclination vane of 60 ° and a diffuser having 11 vanes is better temperature stability and large development in the radial direction with a significant decrease in the axial direction..

Keywords: : Swirling jet, Vane angle, Aerodynamic fields, Thermal homogenization, Thermal Stability.

1. Introduction

The turbulent jets are among the most studied flows both because of their general availability in nature and their use in many industrial applications. The turbulent jets are an important practical interest in the technology of ventilation, cooling and drying. The swirling jet is less known and very complex, it differs from the homogeneous turbulent jet by the existence of the tangential velocity component W. The application of the component of the tangential velocity (W) gives to the flow a component of rotation, shown by a dimensionless number (S) which is defined by the ratio of tangential flow on the axial flow:

$$S = G_{\theta} / RG_x = \int_{R_n}^{R_h} UW r^2 dr / \int_{R_n}^{R_h} R_n U^2 r dr \quad (1)$$

Details of this equation are in reference [1].

Studies show that the laws governing the real air movements are very complex, so the interest in the study of turbulent jets as a basic tool for understanding the phenomenon of air movements in free mode. The objective of the control of the turbulent flow varies depending on the Intended industrial application. We can control a turbulent flow to improve mixing using a diffuser with inclined vanes but also to direct flow and change its orientation [3, 4 and 5]. Turbulent diffusion leads to a very rapid environments homogenization. The swirling jets are particularly interesting inasmuch as they incorporate the characteristics of the rotary flow [6, 7]. The nature of the blowing system, the disposition, the number of jets, the vanes inclination and the temperature of the blown air are necessary parameters to achieve the swirling jet control [7].

Understanding the effects of turbulence, in particular the entrainment rate of the air and the stratification of the very high temperature lead to the efficiency of the air conditioning process. However, to our knowledge, the effects are barely been studied, and therefore the effect of the geometry of the swirl diffuser becomes interesting to study. Understanding the effects of the turbulence, in particular the air entrainment rate and the stratification of the temperature lead to improvement of the efficiency of the air conditioning process. However, to our knowledge, the effects are barely been studied, and therefore the effect of the geometry of the swirl diffuser becomes interesting to study. Felli et al. [8] studied experimentally the dynamics of a impinging turbulent jet generated by inclined vanes. They observed that the wall of the vanes changes the shape of the swirling jet causing it to spreading outwardly and generate a recirculation zone around the vane support, wherein the swirling takes place before breakdown against the vane surface. The effect of different parameters on the development of the flow downstream of the vanes of a swirling jet

generator in three dimensions has been widely studied numerically by the standard $k-\epsilon$ turbulence model [9]. They obtained a good agreement with experimental results. Thundil K. R. et al. [10] numerically studied the devices to generate a both weak and strong swirling. They found that the diffuser with 8 vanes inclined with an angle of 45° produces a large recirculation zone. They noted that at low turbulence, the standard $k-\epsilon$ turbulence model is sufficient, while for strong turbulence the RSM turbulence model is most appropriate. Ahmadvand et al. [11] studied experimentally and numerically the influence of the inclination of the vanes on the heat transfer and on the flow increase of the turbulent fluid. These authors have confirmed that the use of the vanes leads to a higher heat transfer compared to those obtained from smooth tubes. Georges et al. [12] conducted a systematic numerical study for single and multiple jets injection into a main flow by using the $k-\epsilon$ standard turbulence model which is available in FLUENT code. Wang and Mujumdar [13] have numerically investigated the flow and the mixing characteristics of multiple and multi-set three-dimensional confined turbulent round opposing jets in a novel in-line.

characteristics of multiple and multi-set three-dimensional confined turbulent round opposing jets in a novel in-line mixer using the standard $k-\epsilon$ turbulence model. They achieved a good agreement between the simulated and experimental results. Kucukgokoglan et al. [14] presented the performance of three different turbulence models for the prediction of turbulent flow of an oven with two burners against rotation. The numerical models used are the standard $k-\epsilon$, $k-\epsilon$ model (RNG) and the $k-\epsilon$ model. They noted that the standard $k-\epsilon$ model and the RNG model are well established in the prediction of isothermal turbulence models of vortex flows, which have been successfully compared with experimental results. Yongson et al. [15] analyzed the air conditioning system for a single room using CFD code. They studied several parameters such as temperature and velocity to determine the best position for the blower air conditioning and also the area that is suitable for occupant comfort. According to their numerical results, the authors argue that the model RSM can have an independent solution of the mesh relative to the turbulence model $k-\epsilon$ standard. Although the simulation using the RSM turbulence model takes more time compared to the $k-\epsilon$ model, the independence of the mesh solution is more important.

3. Conclusion

Optimization of parameters such as the geometry of the air blowing diffuser and the number of vanes make it possible to improve the quality of thermal homogenization characterized by a large central recirculation zone. Within this zone, the path lines move radially to widen the mean temperature distribution along the swirling jet axis.

The maximum temperature is obtained at the central recirculation zone which characterizes the mixing zone. The evolution of the radial profile of the temperatures, at a given distance from the origin of blowing, shows a more rapid thermal stability of this temperature due to a greater expansion of the jet. By comparing the evolution of the axial and radial temperature, the jet configuration having an inclination of 60° and a diffuser comprising 11 fins represents a better stability in radial temperature with a large axial decay. Of all the configurations studied, the latter quickly ensures a maximum of radial temperature stability. Overall, the results obtained with the Reynolds Constraint (RSM) turbulence model are in better agreement with the experimental data [6] than with the standard $k-\epsilon$ turbulence model. The RSM model takes into account the curvature effects of the current lines and the rapid changes in the strain rate in a more rigorous manner than the standard $k-\epsilon$ model.

References

- [1] Huang, Y., and Yang, V., Dynamics and stability of lean-premixed swirl-stabilized combustion, *Progress in Energy and Combustion Science*, 35, pp. 293-364, (2009).
- [2] PRATTE, B.D., KEFFER, J.R., The swirling turbulent jet, *Jl. of Engineering transactions of the J.S.M.E*, PP, 739-748(1972):
- [3] Davis, M.R, Variable control of jet decay, *AIAA Journal*, 20, pp.606-609, (1982).
- [4] Roudane, M., Loukarfi, L., Khelil, A., and Hemis, M., Numerical investigation of thermal characteristics of confined rotating multi-jet, *Mechanics & Industry*, 14 , 04 , pp. 317-324, (2013).

